EIGENSTRUCTURE ASSIGNMENT TECHNIQUES APPLIED TO HELICOPTER FLIGHT CONTROL LAW DESIGN

Gail Hughes
Department of Electronics and Electrical Engineering
University of Glasgow

A thesis submitted for the degree
of Doctor of Philosophy
of the University of Glasgow.

October 1994

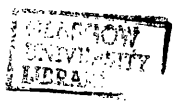

ABSTRACT

This thesis is concerned with the application of eigenstructure assignment methods to helicopter flight control law design.

Helicopters are inherently multivariable dynamic systems and, in some cases, can be unstable. Pilot workload is increased by the effects of the cross-coupled helicopter dynamics. As well as providing stability and reducing pilot workload the controller has to produce satisfactory handling qualities and ride quality over a range of flight conditions.

Eigenstructure assignment methods are reviewed and previous results from the use of these methods are discussed. The need to adopt a modified approach is established by considering the complex nature of the helicopter control problem in that the controller should decouple the helicopter's dynamics, track pilot inputs and meet helicopter handling requirements.

A multivariable control law design method which cancels zeros and zero directions and also creates a decoupled tracking system is presented. The effect of output selection on system zero positions is tabulated. Control law design is performed on an 8th order linear model of the helicopter's rigid body dynamics. An inner/outer loop structure is adopted. The inner loop contains a scheduled controller which provides stability and a decoupled response across a range of flight conditions while the outer loop involves a proportional plus integral controller to augment performance. The resulting controlled system meets helicopter handling qualities requirements. Actuator and rotor dynamics that were not included at the design stage are added to the model to test for robustness. The controller is then tested on helicopter models for flight conditions other than that at which the design was produced and it is shown to be robust to the changes. The linear helicopter model is then replaced by a non-linear representation. It is shown that the controller continues to give good performance with the non-linear model. The non-linear controlled system is then tested for disturbance rejection by adding turbulence to the simulation. The ability of the system to filter out sensor noise is also investigated. The results show that the controller maintains stable

behaviour across the range of flight conditions for which the inner loop controller was scheduled, responses which are decoupled are achieved and handling quality requirements are met.

CONTENTS

ACKNOWLEDGEMENTS

This research has been carried out in the department of Electronics and Electrical Engineering as the University of Glasgow. The author would like to thank Professor David J. Murray-Smith of Glasgow University for his support and supervision.

The support of Dr. Philip Smith of Defence Research Agency, Bedford is also gratefully acknowledged as is the assistance of Miss Anne McKinnon, Mr. Stephen Gallacher and Mr. Dugald Campbell of the Department of Electronics and Electrical Engineering, University of Glasgow. The author would also like to thank Dr. Michael A. Manness for his assistance.

The author gratefully acknowledges the support of the Science and Engineering Research Council and the Defence Research Agency (Aerospace Division) at Bedford.

List of Figures

Tables

* Hoh, R H, Mitchell, D G & Aponso, B L
Proposed Specification for Handling Qualities of Military Rotorcraft vol. 1 - Requirements.
NASA Technical Memorandum, USAAVSCOM Technical Report 87-A-4
May 1988.

CHAPTER 1 INTRODUCTION

A helicopter is a rotorcraft which, in its commonest form, derives lift from a power-driven main rotor rotating about an axis which is vertical, or nearly so when the helicopter is in horizontal flight, with an additional tail rotor to counteract the effect of torque on the main rotor and to provide directional control. The main rotor must provide propulsion, lift and manoeuvrability and it is this aspect that particularly sets the helicopter apart from fixed wing aircraft.

In order to become air-borne, sufficient lift must be generated by the main rotor. When air strikes a blade it divides into flows over the upper and lower surfaces of the blade's aerofoil section. Because of the angle of attack of the blade and the differences in the amount of upper and lower surface camber, the velocity of the air flow over the upper surface is greater than that over the lower surface. Since the air pressure decreases as the velocity increases, the pressure acting on both surfaces of the blade will be less than the surrounding atmosphere. However the camber of the upper surface will result in the upper surface having less pressure acting on it than the lower surface. It is the net difference in these two pressures which produces lift.

If we assume that a helicopter is hovering in a no-wind situation, the velocity of the airflow at the blade tips is the same throughout the tip path plane and decreases at points closer to the rotor hub. When the helicopter moves into forward flight the airflow velocity becomes a combination of the rotor rotational velocity and the forward velocity of the helicopter. The resultant velocity of the advancing blade is the combination of these two velocities whereas the resultant velocity of the retreating blade is the difference of the two velocities. Hence during forward flight the lift over the advancing half of the rotor will be greater than that over the retreating half of the rotor. This is obviously not acceptable as it would cause the helicopter to roll. To

equalise the rotor blade lift the blades are allowed to flap about special hinges. Blade pitch angles can therefore change cyclically relative to the air flowing over them.

The pilot has four inceptors with which to fly the helicopter: collective, longitudinal cyclic, lateral cyclic and yaw. The collective pitch lever changes the pitch on all the blades collectively. By increasing the angle of attack of the blades, more air is drawn through the rotor producing an increase in lift if the rotor is maintained at the same speed. If the cyclic pitch stick is in a central position, the rotor tip path plane is flat. This means that the total rotor thrust acts vertically as lift. By moving the cyclic stick forward, the tip path plane is tilted forward which has the effect of angling some of the rotor thrust backwards. With some of the rotor thrust acting backwards, lift is reduced. To restore the lift, the blade angle of attack is increased using collective.

The turning of the main rotor produces a torque which causes the fuselage to rotate in the opposite direction. The tail rotor produces a counteracting moment to prevent counter-rotation of the fuselage. The yaw pedals control the pitch of the tail rotor blades in a collective fashion and this also provides lateral directional control capabilities.

Helicopters can present difficulties in terms of manual control due to effects such as slow response to pilot demands, inherent instability of the uncontrolled vehicle, non-linearities and cross-coupling. These factors can result in a high pilot workload and can make it difficult to make full use of the capabilities of the vehicle in certain types of mission tasks.

Flight control systems aim to provide an improvement in the handling qualities of a helicopter. This, in turn, benefits the pilot by reducing the workload during flight and

allowing more account to be taken of other stimuli (thus improving safety and mission effectiveness). However, even with a flight control system in use, the flight envelope which is considered usable in present-day helicopters is still considerably smaller than that which is within the capabilities of many modern rotorcraft such as the Lynx helicopter. This margin is introduced in the interests of safety, but by constraining the usable flight envelope in this way the performance that can be demanded from the helicopter is limited and much of the helicopter's potential is unused.

Ideally, what is required is a flight control system which incorporates control laws able to cope with the complex cross-couplings within helicopter dynamics and able to extend the boundaries of the usable flight envelope to exploit the full potential of the helicopter without compromising safety.

Handling qualities criteria are necessary to assist control system designers in producing controllers which give improved closed loop system performance. The opinion of the pilot as to which controllers give good or bad handling can often be translated into criteria to be met which will result in improved performance or at least interpreted in such a way as to give the designer guidelines to be used in subsequent designs of controllers. Over the years much information has been gathered covering different types of aircraft, different types of tasks and different operational environments. From this information it has been possible to define some measurable quantities which can give an indication of the quality of handling that can be expected from the controlled helicopter. However, the handling qualities criteria, as they exist at present, are not sufficient to guarantee that the controller will give high performance even if the criteria have been complied with.

The helicopter is a highly coupled, non-linear multivariable system and for the purposes of analysis and control system design we require a mathematical model. In

general terms a model is a structure which has certain properties in common with the system under investigation. By its very nature a model is not a perfect replica of the real system as it is intended to simplify the problem in hand. What is important therefore is the degree of similarity between the model and the system. A diagram is shown (fig. 1.1) of a method of developing a control system for a helicopter by varying the complexity of the model. The diagram begins with the real helicopter system. The helicopter is then described by a set of equations to give a full non-linear model. The non-linear model is then linearised around the point in the flight envelope about which the design is to be carried out. The non-linear model used here was Helisim and the linear model was obtained from Helistab. (Padfield, 1981) Both the Helisim and Helistab models originated at the Royal Aerospace Establishment (Bedford).

In the approach adopted in this work the linearised actuator and rotor dynamics are removed for the initial stages of the work to leave a linearised model of the rigid body dynamics which incorporates a quasi steady state description of the main and tail rotors. It is on this model that the control law design is performed. The reason for removing the actuator and rotor dynamics is that significant uncertainties exist in the rotor description in the version of the model used in this work. It was considered undesirable to make the control system design too dependent upon the rotor description since the imprecision could cause robustness problems. Only when a controller which gives a satisfactory closed loop performance in conjunction with the linear rigid body model and quasi-steady rotor description is achieved does the development move on. Because subsequent stages of development involve the reinstatement of rotor and actuator dynamics in the model, the control law design method has to be robust to the addition of unmodelled dynamics especially in the upper part of the frequency range of significance.(Ray & Stengel, 1992) The performance of the controller and model is then tested and if necessary the controller can be retuned. The controller is then

implemented on the non-linear model and if it works sufficiently well at this stage, it can then be tested for insensitivity to noise and for disturbance rejection. The development process continues in this way, in an iterative fashion, the helicopter model becoming more complex as it approaches the original system.

There are many methods of developing control laws for multivariable systems such as the helicopter. Examples include proportional and integral, LQR/LQG (linear quadratic regulator/linear quadratic gaussian), singular perturbation methods, H^{∞} and eigenstructure assignment methods.(Gribble et al., 1992 & Manness et al., 1990) Each of these has different properties which may or may not make them suitable for the helicopter application.

A multivariable proportional and integral controller has been used to improve the performance of an Apache YAH-64 helicopter (Enns, 1987). The inner loop provided stability augmentation, decoupled responses and gust attenuation. The resulting control laws were successfully flight-tested.

One particular form of singular perturbation method (Porter & Bradshaw, 1981) developed at the University of Salford can be used to design high gain error-actuated controllers for linear tracking systems. These controllers take the form of multivariable proportional and integral controllers. This method assumes that the dynamics of the system to be controlled can be separated into two distinct groups: one of low frequency and the other of high frequency. The lower frequency dynamics are considered quasi-static when compared with the higher frequency dynamics. In order to select an appropriate controller matrix, feedback from the fast states is required. In the case of the helicopter these fast states are associated with the rotor and actuator and with some rigid body modes. In order to apply the Salford Singular Perturbation Method information must be available concerning the blade angles of each of the

actuators but this is not currently a routinely measured variable on helicopters. This means that it is necessary to make extra measurements either by using observers in the controller or to install sensors in the main rotor hub.

By using the H^{∞} method (Francis, Helton & Zames, 1981), bounds on system performance can be guaranteed by information gathered from singular values. The H^{∞} norm of a transfer matrix is defined as the maximum of its largest singular value over all frequencies and it can be used to place an upper bound on the uncertainty level in a system (e.g. from unmodelled dynamics, changes in flight condition and non-linearities). Controllers devised by this method can be of very high order and therefore require more computation time. Problems may be encountered due to a lack of processor speed. H^{∞} methods have been used to develop helicopter flight controllers that provide decoupling and stability augmentation (Yue & Postlethwaite, 1990). The frequency and time responses of the controlled helicopter were evaluated and stability robustness was assessed using singular value techniques. The controller had 39 states initially but these were reduced to 18 by using approximations that did not result in a significant deterioration of the controller's performance.The controller was used in simulation tests and then in piloted trials. The performance was found to be generally good. Another approach to helicopter flight controller design (Walker & Postlethwaite, 1990) involves using a design structure consisting of an inner loop to provide stability and an outer loop containing a dynamic controller designed by H^{∞} optimisation. By using this inner/outer loop technique the order of the H^{∞} controller can be reduced.

LQR can be used to derive an optimal, stabilising feedback law which gives desirable closed loop system properties. However, the method involves choosing values for weighting functions. The relationship between these weightings and their effect on closed loop system performance is not always clear which tends to make selection of

weightings a difficult task.

Eigenstructure assignment can offer a straightforward method of achieving static compensators that satisfy time response specifications but does not offer guaranteed stability margins like some LQR methods (Innocenti & Stanziola, 1990). The good stability margins achieved by LQR are, however, only achieved by trial and error in the selection of performance index weighting matrices. High gains are usually required to improve stability margins and this can result in closed loop poles moving toward transmission zeros. In order to prevent this occurring we can define upper bounds on gains. It has been shown that the eigenstructure of the plant is related to the selection of weighting matrices (Harvey & Stein, 1978) - the implication being that eigenstructure plays an important role where robustness issues are of concern. On this premise, Innocenti and Stanziola outlined a method applied to a rotorcraft problem which showed that eigenstructure assignment was a viable alternative in terms of robustness, performance and dimension of compensator dynamics (Innocenti & Stanziola, 1990). There was also a reduction in gain associated with the method.

The objective of this research is to investigate eigenstructure methods. Eigenstructure assignment techniques have a significant advantage over other methods of synthesising control laws in that there is a level of visibility attached to the design process which facilitates the understanding of the relationship between the helicopter dynamics and the controller structure.

Given the following linear, time-invariant system with m inputs ($m < n$)

$$\dot{x} = Ax + Bu \qquad (1.1)$$

$$y = Cx + Du \qquad (1.2)$$

where A is the nxn system matrix

B is the nxm input matrix

C is the mxn output matrix

D is the mxm direct coupling matrix

it has been shown that n eigenvalues and m elements of the n corresponding eigenvectors can be arbitrarily assigned using full state feedback. (Moore, 1976)

The behaviour of the system is governed by the eigenvalues of the A matrix. Eigenvalues define the rate of decay (negative eigenvalues) or growth (positive eigenvalues) of the response. Each eigenvalue has an eigenvector associated with it. In order to tailor the dynamics of the system to meet given system specifications (such as those defined by handling qualities requirements) the position of these eigenvalues must be modified. There is both an eigenvalue and an an eigenvector associated with each mode. When one mode of the system is excited, the other modes of the system should not be excited due to cross-coupling effects.

In terms of eigenstructure, the cross-coupling can be seen by inspecting the eigenvectors of the system. The eigenvectors are distributed over six modes (three lateral modes and three longitudinal modes) or, if heading is included, over seven modes in such a way that each mode has associated with it an eigenvector or an eigenvector subspace. A linearised state space representation of a Lynx can be generated by the Helistab package.(Smith, 1984) The eigenstructure of the system matrix (A) at a flight condition of 80 knots is shown in Table 1

Table 1 Eigenstructure of a Lynx Helicopter at 80 knots

Mode		Fast Pitch	Slow Pitch	Phugoid
Eigenvalue		-3.1988	-0.4055	0.1338 ± 0.3766i
Eigenvector	u	0.0398	-0.7209	1.0000 ± 0.0000i
	w	1.0000	1.0000	0.3244 ∓ 0.6149i
	q	-0.0576	0.0101	0.0134 ∓ 0.0114i
	θ	0.0178	-0.0238	-0.0159 ∓ 0.0405i
	v	0.2918	0.0878	0.1336 ∓ 0.1887i
	p	0.0401	0.0227	-0.0010 ∓ 0.0084i
	φ	-0.0127	-0.0554	-0.0209 ∓ 0.0043i
	r	0.0194	-0.0125	-0.0076 ∓ 0.0011i
	ψ	-0.0031	0.0090	-0.0026 ∓ 0.0052i

Mode		Roll	Spiral	Dutch Roll	Heading
Eigenvalue		-10.5525	-0.0305	-0.6531 ± 2.2543	0
Eigenvector	u	0.0124	-0.4314	-0.0002 ∓ 0.0046i	0
	w	0.2700	-0.0064	-0.0110 ∓ 0.0168i	0
	q	-0.0519	-0.0036	0.0011 ∓ 0.0007i	0
	θ	0.0043	0.0001	-0.0012 ∓ 0.0003i	0
	v	0.7965	1.0000	1.0000 ± 0.0000i	0
	p	1.0000	-0.0164	-0.0162 ± 0.0050i	0
	φ	-0.0951	0.4623	0.0035 ± 0.0061i	0
	r	0.1855	0.1079	0.0127 ∓ 0.0539i	0
	ψ	-0.0020	-0.6213	-0.0011 ∓ 0.0002i	1

From Table 1 we see that all the modes are fully coupled except heading. The decoupled situation with respect to heading arises because the dynamics of the helicopter are not dependent on the direction in which the helicopter is flying. The longitudinal modes consist of two stable pitching modes and an unstable phugoid mode. From the eigenvectors we see that the fast pitch and phugoid modes appear in the lateral velocity state, v, even though they are described as longitudinal modes. The lateral modes are roll, spiral, dutch roll and phugoid. There is more evidence of the high degree of coupling in that the roll mode eigenvector shows that it appears in the vertical velocity state, w. It is also worth noting that the dutch roll damping ratio is poor. This will result in lateral directional oscillations in long term responses.

Heading will not be included in the initial design. The eigenvector components are therefore as shown below:

$$\begin{bmatrix} u \\ w \\ q \\ \theta \\ v \\ p \\ \varphi \\ r \end{bmatrix} \quad \begin{matrix} \text{forward velocity} \\ \text{vertical velocity} \\ \text{pitch rate} \\ \text{pitch attitude} \\ \text{lateral velocity} \\ \text{roll rate} \\ \text{roll attitude} \\ \text{yaw rate} \end{matrix}$$

To design a controller which will improve the helicopter's performance, for each mode we choose which of the above states are to be active and attempt to make all other states in that eigenvector zero. When this mode is excited we should have contributions from the chosen states only.

With regard to the positioning of assignable eigenvalues - we would obviously want them to be in the left half plane to ensure stability. There is a relationship between the position of the eigenvalue and the bandwidth: the more negative the eigenvalue becomes, the larger the bandwidth. Some bandwidth requirements (e.g. from Handling Qualities Specification) will also give an indication as to how far into the left half plane the eigenvalues must be and, together with damping requirements, time constants etc., areas of the left half plane can be determined within which each eigenvalue must lie.

However, as we would expect, the eigenvalues of the actuators of a helicopter and those due to the rotor are at somewhat higher frequencies than those of the rigid body dynamics of the fuselage. Therefore a trade-off exists between how far we move the eigenvalues in order to create a higher bandwidth and how far left we can move them without involving these higher frequency dynamics.

The handling qualities requirements give a set of design criteria. These can be used

in eigenstructure assignment methods to choose sets of eigenvalue/eigenvector pairs which give adequate performance. There are three categories of performance, a good performance rating Level 1 and a poor performance Level 3. Further details of the definition of these performance levels are included in Chapter 3. Although we may achieve a Level 1 performance with respect to handling qualities at the design condition, we must also evaluate the robustness of the controlled system.(Osder & Caldwell, 1992) It must be robust both to the addition of higher frequency dynamics and to changes in flight condition. Insensitivity to external disturbances and noise rejection must also be achieved and the overall system must not be oversensitive to sensor noise.

The eigenvalues and eigenvectors occurring naturally in the uncontrolled system can be altered to a more desirable condition by applying feedback laws to the system. For instance, by applying u = r - Fy as shown in Figure 1.2

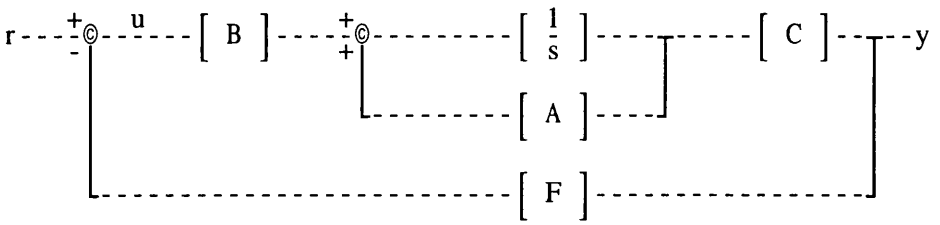

Figure 1.2 Block diagram of system with output feedback

the closed loop system is represented by $\dot{x} = (A - BFC)x + Br$

For each eigenvalue/eigenvector pair we have

$$(A - BFC)v_i = \lambda_i v_i \qquad (1.3)$$

Therefore

$$v_i = (A - \lambda_i I)^{-1} BFCv_i \qquad (1.4)$$

A full state feedback matrix, F, of dimension (m x n) does not allow complete freedom to assign eigenvectors. The assignable eigenvectors must lie in a subspace spanned by the columns of Γ,

$$\Gamma = \left[\lambda_i I - A \right]^{-1} B \qquad (1.5)$$

where λ_i is the desired eigenvalue for this mode.

The purpose of the feedback controller, F, is to produce the achievable set of closed loop eigenvalues and eigenvectors which is as near the desired set as possible. The desired eigenvalues and eigenvectors are chosen according to handling qualities requirements.

Once suitable eigenvalue/eigenvector pairs have been chosen, the desired eigenvector can be projected onto the subspace Γ in order to find the achievable eigenvector which is closest to the desired eigenvector.

From $(A - BFC)V = V\Lambda$ (1.6)

where V is a matrix of eigenvectors

and Λ is a matrix of eigenvalues

we have $(AV - V\Lambda) = BFCV$ (1.7)

Therefore $F = B^{+} (AV - V\Lambda) (CV)^{-1}$ (1.8)

where B^{+} is the pseudoinverse of B

By creating a closed loop system which incorporates this feedback matrix, F, the eigenstructure of the system will be derived from the matrix A - BFC rather than the A matrix (as in the open loop case). In this way the eigenstructure of the system can be altered.

In the subsequent chapters three different eigenstructure assignment methods will be used to design controllers for a helicopter.

References

Enns, D F

Multivariable Flight Control for an Attack Helicopter

IEEE Control Systems Magazine, 1987, 7, pp 34 - 38

Francis, B A, Helton, J W & Zames, G

H^{∞} - Optimal Feedback Controllers for Linear Multivariable Systems

IEEE Trans. Auto Control, vol. AC - 26, pp 4 - 16, 1981.

Gribble, J J, Manness, M A & Murray-Smith, D J

Helicopter Flight Control Design: Multivariable Methods and Design Issues

Dept. of Electronics & Electrical Engineering

University of Glasgow

Harvey, G A & Stein, G

Generalized Quadratic Weights for Asymptotic Regulator Properties

IEEE TR-AC-23, June 1978, pp 378 - 387

Innocenti, M & Stanziola, C

Performance-Robustness Trade-off of Eigenstructure Assignment Applied to Rotorcraft

Aeronautical Journal, 1990, 94, pp 124 - 131

Manness, M A, Gribble, J J & Murray-Smith, D J

Multivariable Methods for Helicopter Flight Control Law Design

Proceedings 16th European Rotorcraft Forum, Glasgow, UK

18 - 21 September 1990

Moore, B C

On the Flexibility Offered by State Feedback in Multivariable Systems beyond Closed-Loop Eigenvalue Assignment

IEEE Trans. Auto Control, vol. 21, pp689 - 692, 1976

Osder, S & Caldwell, D

Design and Robustness Issues for Highly Augmented Helicopter Controls

Journal of Guidance, Control & Dynamics

vol. 15, no. 6, pp 1375 - 1380

November - December 1992

Padfield, G D

A Theoretical Model of Helicopter Flight Dynamics for Application to Piloted Simulation

RAE

Technical Report 81048

April, 1981

Porter, B & Bradshaw, A

Singular Perturbation Methods in the Design of Tracking Systems Incorporating High-Gain Error-Actuated Controllers.

International Journal of Systems Science, vol.12, no.10, pp 1169 - 1179 1981.

Ray, L R & Stengel, R F

Stochastic Measures of Performance Robustness in Aircraft Control Systems

Journal of Guidance, Control & Dynamics

vol. 15, no. 6, pp 1381 - 1387

November - December 1992

Smith, J

An Analysis of Helicopter Flight Mechanics part 1 -

User's Guide to the Software Package Helistab

RAE (Bedford)

Technical Memo FS(B) 569

October 1984

Walker, D & Postlethwaite, I

Full Authority Active Control System Design for a High Performance Helicopter

Proceedings 16th European Rotorcraft Forum, Glasgow, UK

18 - 21 September, 1990

Yue, A & Postlethwaite, I

Improvement of Helicopter Handling Qualities using H^{∞} Optimization

IEE Proc. D., 1990, 137, pp 115 - 129

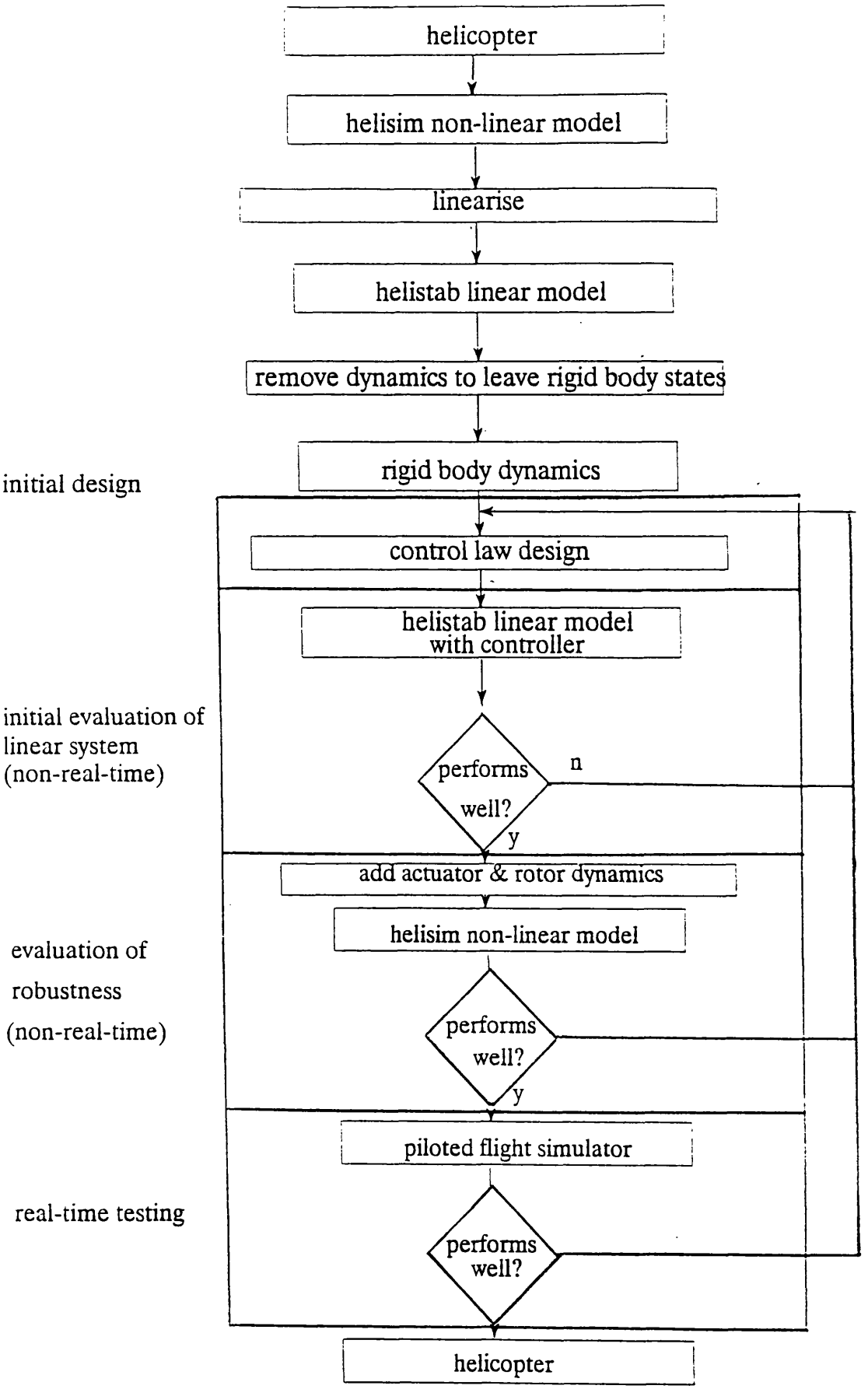

Figure 1.1 A Method of Developing a Controller for a Helicopter

CHAPTER 2 HELICOPTER MODELS

A mathematical model of a helicopter provides opportunities for design investigations, eg. control system design, handling qualities studies and rotor load investigations, without the risks involved with using the helicopter itself. For the conclusions drawn from these investigations to be valid, the model must be a reliable representation in terms of the aspects of the system under investigation. The model is not an exact replica of the helicopter's dynamics, instead certain properties are selected for inclusion in the model while others are approximated or neglected completely. This is done in such a way that the characteristics which are judged important for the intended application are retained. The model can be validated by comparing the helicopter responses to those of the model for cases which relate directly to the type of application intended. A high degree of similarity between the helicopter and the model behaviour means that the model can be used to predict flight behaviour. A trade-off also exists between model accuracy and computational speed.

Fundamentals of Flight Mechanics

A helicopter in flight is assumed to be a rigid body. The distance between any two points in the body is fixed and forces acting between mass elements are ignored. This means that the motion of the helicopter body can be described by a translation and rotation about the centre of mass. Using earth-fixed axes, equations for the forces and moments acting on the helicopter can be obtained. However because these axes are non-rotating, the moments and products of inertia will vary as the helicopter rotates. This can be avoided by fixing the frame of reference with respect to the helicopter to provide a body-fixed set of axes. One result of having body-fixed axes is that they move with the helicopter and so the moments and products of inertia become constants. The derivatives of vectors with respect to a rotating frame of reference now need to be found but this is simpler than dealing with variable inertia coefficients. The force and moment equations referred to the body-fixed

axes can be shown to be (Prouty)

$$F = m \frac{\delta v_c}{\delta t} + m\omega \times v_c \qquad (2.1)$$

$$G = \frac{\delta h}{\delta t} + \omega \times h \qquad (2.2)$$

where F resultant force

G resultant moment

m mass of helicopter

v_c velocity of centre of mass

ω angular velocity

h angular momentum

The scalar components of these equations are as follows:

$$X = F_x = m(\dot{u} + qw - rv) \qquad (2.3)$$

$$Y = F_y = m(\dot{v} + ru - pw) \qquad (2.4)$$

$$Z = F_z = m(\dot{w} + pv - qu) \qquad (2.5)$$

$$L = G_x = \dot{h}_x + qh_z - rh_y \qquad (2.6)$$

$$M = G_y = \dot{h}_y + rh_x - ph_z \qquad (2.7)$$

$$N = G_z = \dot{h}_z + ph_y - qh_x \qquad (2.8)$$

where X,Y,Z are components of resultant aerodynamic force (drag, sideforce, lift)

L,M,N are rolling, pitching, yawing moments

u,v,w are components of velocity at centre of mass

p,q,r are rolling, pitching, yawing velocity

Since the origin is the centre of mass all the products of inertia are zero ($I_{xy} = I_{yz} = I_{xz} = 0$). The equations reduce to

$$L = I_x\dot{p} + (I_z - I_y)\, rq \qquad (2.9)$$

$$M = I_y\dot{q} + (I_x - I_z)\, pr \qquad (2.10)$$

$$N = I_z\dot{r} + (I_y - I_x)\, pq \qquad (2.11)$$

Equations 2.3, 2.4, 2.5, 2.9, 2.10 & 2.11 are known as Euler's equations of motion. They relate the forces and moments acting in body-fixed axes to those in earth-fixed axes. Figure 2.1 shows the relationship between earth-fixed and body-fixed axes. We begin with axes in positions C x1 y1 z1. Three rotations are then applied. The first rotation, ψ, about C z1 takes the axes to C x2 y2 z2. The second rotation, θ, about C y2 takes axes to C x3 y3 z3 and the final rotation, φ, about C x3 takes the axes to C x y z. θ, φ & ψ are known as euler angles.

The Euler transformation matrix allows transformation between earth and body axes. It is shown below

$$\begin{bmatrix} a_{11} & a_{12} & a_{13} \\ a_{21} & a_{22} & a_{23} \\ a_{31} & a_{32} & a_{33} \end{bmatrix} \qquad (2.12)$$

where $a_{11} = \cos\theta \cos\psi$

$a_{12} = \cos\theta \sin\psi$

$a_{13} = -\sin\theta$

$a_{21} = \sin\varphi \sin\theta \cos\psi - \cos\varphi \sin\psi$

$a_{22} = \sin\varphi \sin\theta \sin\psi + \cos\varphi \cos\psi$

$a_{23} = \sin\varphi \cos\theta$

$a_{31} = \cos\varphi \sin\theta \sin\psi + \sin\varphi \sin\psi$

$a_{32} = \cos\varphi \sin\theta \sin\psi - \sin\varphi \cos\psi$

$a_{33} = \cos\varphi \cos\theta$

$$\dot{\varphi} = p + q \sin\varphi \tan\theta + r \cos\varphi \tan\theta \qquad (2.13)$$

$$\dot{\theta} = q \cos\varphi - r \sin\varphi \qquad (2.14)$$

$$\dot{\psi} = q \sin\varphi \sec\theta + r \cos\varphi \sec\theta \qquad (2.15)$$

It can be assumed that all the variables consist of a steady state (trimmed) component and a perturbation component.

$$X_p = X_e + X \qquad (2.16)$$

where X_p is the perturbed state

X_e is the trimmed state

X is the perturbation

The equations can be linearised by subtracting the trimmed state from the perturbed state to leave only the perturbation component.

All products of perturbations are assumed to be small and are therefore ignored. Small angle assumptions are also made. This gives

$$\dot{u} = -(w_e q - v_e r) - g\theta \cos\theta_e + X/M \qquad (2.17)$$

$$\dot{v} = -(u_e r - w_e p) + g(\varphi \cos\theta_e \sin\varphi_e - \theta \sin\theta_e \sin\varphi_e) + Y/M$$

$$\dot{w} = -(v_e p - u_e q) - g(\theta \sin\theta_e \cos\varphi_e + \varphi \sin\varphi_e \cos\theta_e) + Z/M$$

$$I_{xx}\dot{p} = I_{xz}\dot{r} + L \qquad (2.20)$$

$$I_{yy}\dot{q} = M \qquad (2.21)$$

$$I_{zz}\dot{r} = I_{xz}\dot{p} + N \qquad (2.22)$$

$$\dot{\theta} = q \cos\varphi_e - r \sin\varphi_e \qquad (2.23)$$

$$\dot{\varphi} = p + q \sin\varphi_e \tan\theta_e + r \cos\varphi_e \tan\theta_e \qquad (2.24)$$

$$\dot{\psi} = r \cos\varphi_e \sec\theta_e + q \sin\varphi_e \sec\theta_e \qquad (2.25)$$

Using an expansion based on the Taylor series,

$$X = X_e + \delta X/\delta u\ u + \delta X/\delta v\ v + \delta X/\delta w\ w + \ldots + \delta X/\delta\theta_{otr}\ \theta_{otr}$$

The equations of motion can now be substituted in. In the case of the first translational equation this gives

$$\begin{aligned} M\dot{u} = {} & -M(w_e q - v_e r) - Mg\theta \cos\theta_e + \delta X/\delta u\ u + \delta X/\delta v\ v + \\ & \delta X/\delta w\ w + \delta X/\delta p\ p + \delta X/\delta q\ q + \delta X/\delta r\ r + \delta X/\delta\theta\ \theta + \\ & \delta X/\delta\varphi\ \varphi + \delta X/\delta\theta_o\ \theta_o + \delta X/\delta\theta_{ls}\ \theta_{ls} + \delta X/\delta\theta_{lc}\ \theta_{lc} + \\ & \delta X/\delta\theta_{otr}\ \theta_{otr} \end{aligned} \qquad (2.26)$$

where θ_o collective

θ_{ls} longitudinal cyclic

θ_{lc} lateral cyclic

θ_{otr} collective of tail rotor

By applying the same process to each of the equations of motion, a model is produced in state space form

$$\dot{x} = Ax + Bu$$

where $x = [u, v, w, p, q\ r, \theta, \varphi]^t$

$u = [\theta_o, \theta_{ls}, \theta_{lc}, \theta_{otr}]^t$

In this research the components of the state vector are given in a different order

$$x = [u, w, q, \theta, v, p, \varphi, r] \qquad (2.28)$$

This gives an A matrix which is partitioned in terms of longitudinal and lateral dynamics.

longitudinal dynamics	cross-coupling lateral to longitudinal
cross-coupling longitudinal to lateral	lateral dynamics

This eight state model describes the rigid body motion of the helicopter. The rotor coning angle and the longitudinal and lateral flapping angles are determined through algebraic relationships. If the coning angle, longitudinal and lateral flapping angles are added as state variables the model becomes eleventh order. The model becomes fourteenth order when the rates of change of these three angles are added as states.

The linearised equations are valid for small perturbations about a trim condition. A change in angle of 15 degrees or a change in velocity of 5 ms^{-1} is considered to be the limit for a linear model. This is a generalisation and in fact the limits should be assessed according to the flight condition and type of manoeuvre.

Helicopter Model System Analysis and Simulation

Using a VAX-VMS computing environment, MATLAB and TSIM (Anon., 1988)were used for analysis and simulation.(Murray-Smith et al., 1991) These packages were used because they were standard at RAE. As stated in the introductory chapter, experiments were performed on both linear & non-linear models of a helicopter. The linear model was represented in state space form within MATLAB (Moler et al., 1987). MATLAB is a collection of functions for linear algebra, matrix computation and numerical analysis. A collection of algorithms in the MATLAB Control System Toolbox (Moler et al., 1987) allows implementation of common control system design, analysis and modelling techniques.

The HELISTAB software package provides a choice of system order for the linear helicopter model. The eighth order model provides rigid body states only, whereas the eleventh order model includes coning angle, β_0, longitudinal flapping angle, β_{1c}, and lateral flapping angle, β_{1s}, to model main rotor dynamics. The fourteenth order model also includes β_0, β_{1s} & β_{1c}.

The state space matrices for each flight condition were obtained from the HELISTAB program. Another software package called HELISIM was used to obtain a non-linear model. Both the Helistab and Helisim programs are based upon the work of Padfield. (Padfield, 1981)

The linear model (including only rigid body dynamics) will be used to design a flight control system and then actuator and rotor dynamics will be added to the linear model. The non-linear model is used to investigate noise and disturbance rejection as well as robustness to changes in flight condition and response during large maneouvres. The performance obtained in each experiment is compared with the handling qualities specification outlined in Mil-spec 8501. (Anon, 1961)

Helistab

Helistab was created within RAE (Bedford).(Smith, 1984) The Helistab package provides a theoretical model of the flight mechanics of a helicopter. It contains a non-linear model and can be used to derive reduced order linear models. Helistab can be used to compute time responses and to plot these responses.

The user can choose a model of a Lynx or a Puma. In this research the Lynx configuration was used. The user must also define the flight condition.

When an aircraft is put in a state of equilibrium by the action of the pilot adjusting the controls, it is said to be trimmed. The body attitudes and control angles which are necessary to achieve and maintain equilibrium are computed by a trim algorithm in Helistab. The forces and moments acting on the trimmed helicopter are then calculated. The equations used are outlined in Appendix 1.

In order to calculate stability and control derivatives of the helicopter model states are perturbed in a positive sense and in a negative sense. Force and moment calculations are performed for each of these two perturbed states. The states are then returned to their equilibrium values. The derivatives are computed by assuming a linear force/state relationship.

The user can define the control input by selecting the input type (step, ramp, doublet,etc.), its size and duration. This information is used to produce the time response.

The Helistab model has been validated through comparison with flight data.(Padfield & Duval, 1991) It is thought that, within the normal flight envelope, characteristics can in some cases be predicted to within 20% of flight values.(Smith, 1984) An approximation which is relevant to this research is that the blade dynamics modelling is taken to be quasi-steady flapping motion (i.e. the rotor disc takes up a new position as an instantaneous

function of the fuselage state). In a multi-blade coordinate system the lowest frequency rotor mode is the regressing flap mode which responds below 1 Hertz. This should be noted as it can couple into control system modes and produce misleading results.(Hanson, 1982)

Helisim

Helisim is a TSIM implementation of Helistab. It is used for a non-linear simulation of the helicopter and controller and provides a route to piloted simulation. Helisim uses the same equations as Helistab to calculate forces and moments. One difference between Helisim and Helistab is that the centre of gravity position along the x axis is of opposite sign. Helisim uses the convention of positive aft of the rotor centre whereas Helistab uses positive forward of rotor centre.

A block diagram of the Helisim software structure is shown in Figure 2.2.

The file SESAME calls CONTROLS, TOTF and TOTM.

CONTROLS calls all the control subroutines which perform the control functions such as actuators. It also gathers the information needed by the model, e.g. blade angles and rotor speeds.

CIN picks up the pilot or VDU inputs and applies a shaping function to each input. Thus control inputs can be dead-banded, non-linear and bounded by variables.

FCS provides the model with a basic autostab.

ENG calculates engine torque, engine power and tail rotorspeed.

CMX collects pilot inputs and applies control mixing (usually done mechanically in the helicopter). It is not called when active controls are on.

ATR equates active control outputs to the actuator outputs.

The file TOTF calls the model subroutines and sums the forces generated to produce information required by SESAME.

TOTM sums the moments generated in the model subroutines and passes the information to

SESAME.

PAR calculates the reference forces and moments for the model.

RTR calculates the main rotor forces and moments.

TRT calculates the tail rotor forces and moments.

FSG calculates the fuselage forces and moments.

FIN calculates the fin forces and moments.

TLP calculates the tailplane forces and moments.

UCR calculates the undercarriage forces and moments.

TWIND controls the generation of turbulence.

USERCMI sets up the user input to the model, e.g. autostab setting, active controls and TSIM switches. It also initialises forward speed and height.

USERCMO communicates any user information back from the model to TSIM, e.g. engine power, and it also contains all the externals.

ACTLAW contains the active control law defined by the user. The control law simulated by this file is discussed in Chapter 5.

More information on the software functions is contained in Appendix 5.

References

Anon.

General Requirements for

Helicopter Flying and Ground Handling Qualities

Mil-H-8501A (1961)

Anon.

TSIM Non-linear Dynamic Simulation Package

User's Guide

Cambridge Control Ltd., 1988

Hanson, R A

Towards a Better Understanding of Helicopter Stability Derivatives

Proc. 8th European Rotorcraft Forum

Aix-en–provence

France, 1982

Moler, C, Little, J & Bangert, S

PRO-MATLAB for VAX/VMS Computers

User's Guide

The MathWorks Inc.

South Natick MA

Murray-Smith, D J, Hughes, G & Manness, M A

An Integrated Environment for the Design and Analysis of Robust Control Systems

IMACS/IFAC Symposium on Modelling and Control Of Technological Systems

Lille, 1991

Padfield, G D

A Theoretical Model of Helicopter Flight Mechanaics for Application to Piloted Simulation

RAE Technical Report 81048

April 1981

Padfield, G D & Duval, R W

Application Areas for Rotorcraft System Identification:Simulation Model Validation

AGARD LS-178 pp 12.1 - 12.39

AGARD, Neuilly-sur–Seine, France, 1991

Prouty, R W

Helicopter Aerodynamics

Smith, J

An Analysis of Helicopter Flight Mechanics part 1 -

User's Guide to the Software Package Helistab

RAE (Bedford)

Technical Memo FS(B) 569

October 1984

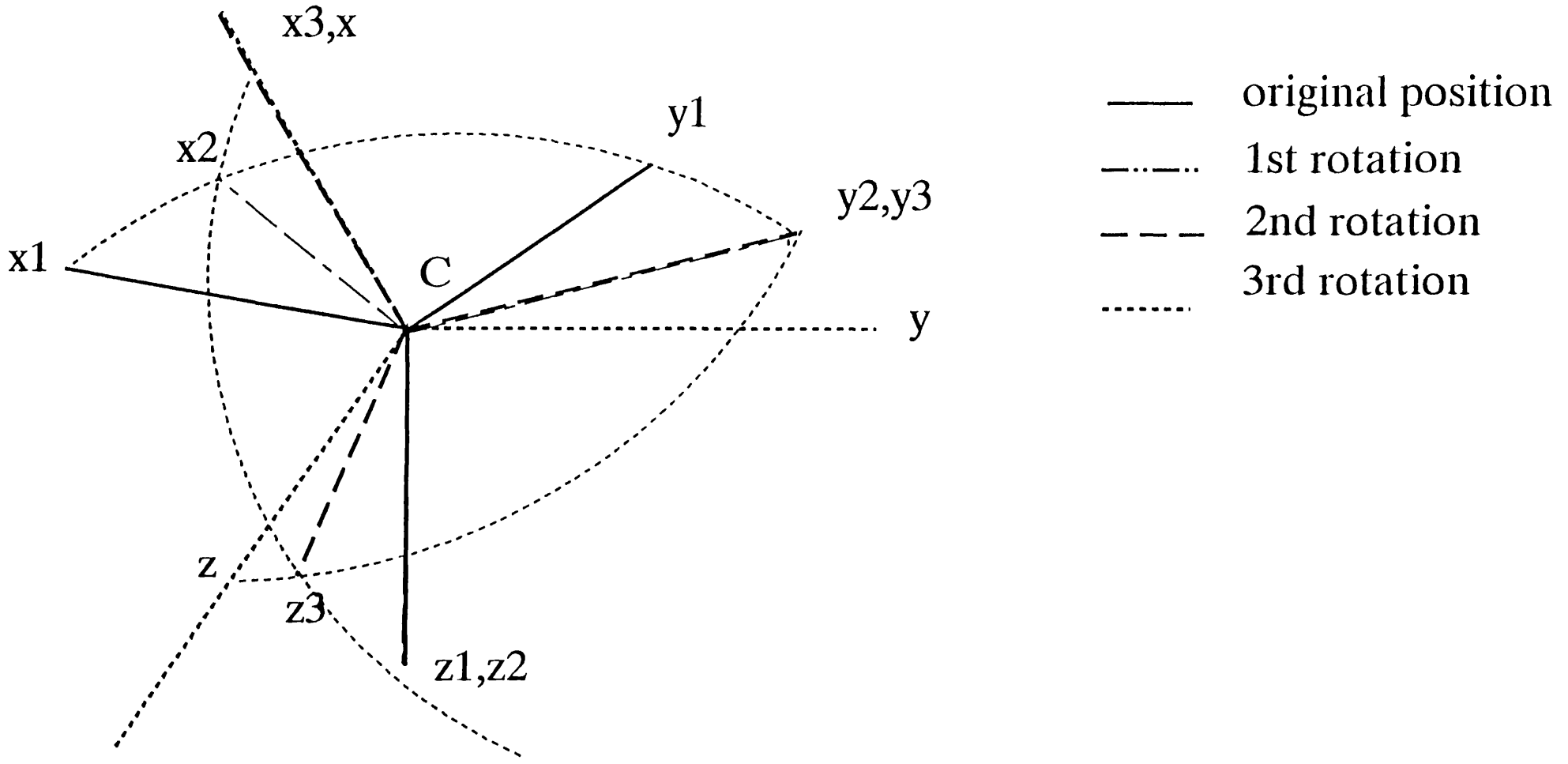

Figure 2.1 Axes system

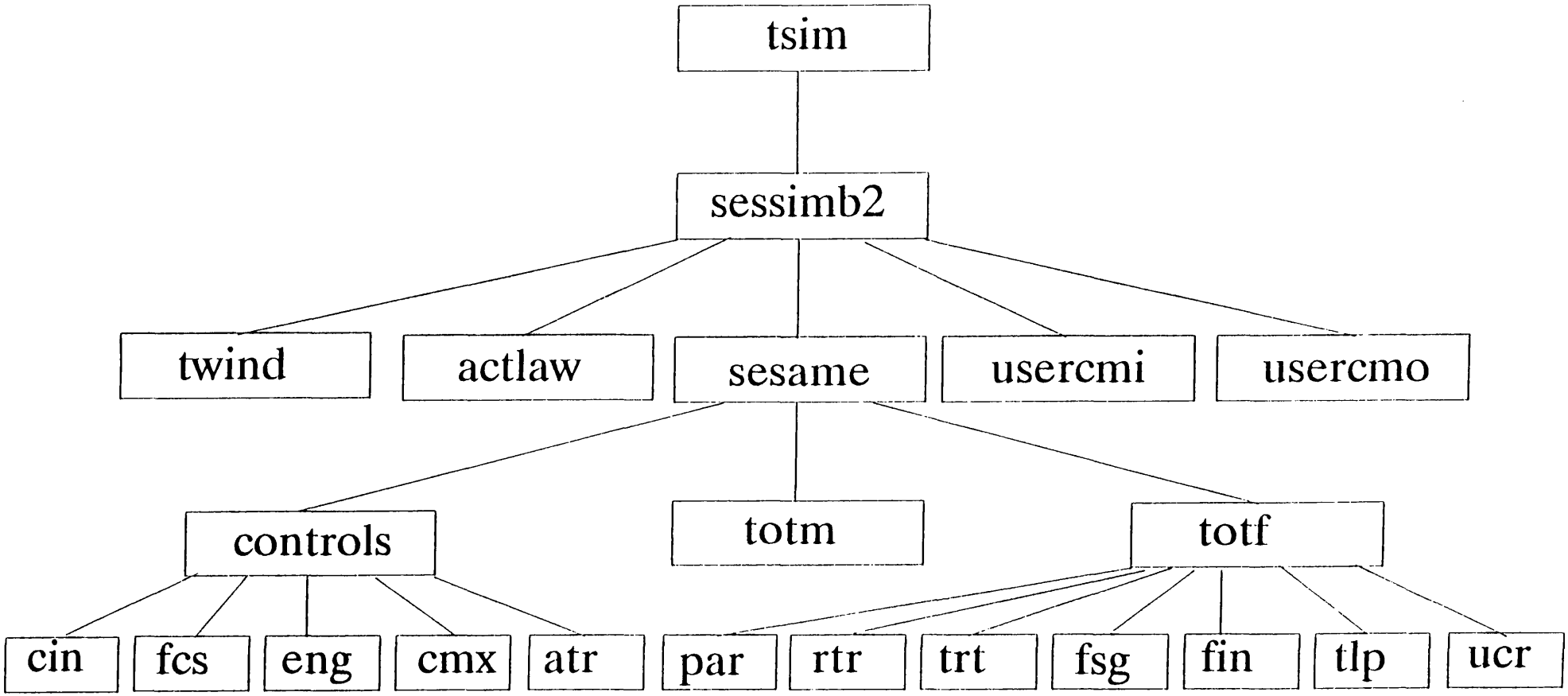

Figure 2.2 Block Diagram of Helisim Software Structure

CHAPTER 3 HELICOPTER HANDLING QUALITIES

The purpose of designing a flight control system for a helicopter is to provide improved safety, to improve the performance of the vehicle in terms of agility and manoeuvrability and to reduce the pilot's workload. In order to assess the improvement in performance created by the addition of a controller, a set of design objectives is required. In the past these design criteria were provided by MIL-H-8501A. (Anon, 1961) The current standards are contained within an updated draft version of MIL-H-8501A.(Hoh, 1988) This handling qualities document contains specifications relating to system bandwidth, damping and levels of coupling for many different types of flight condition and types of manoeuvre. These parameters have been identified as those to which a pilot is sensitive and acceptable parameter ranges have been subsequently defined by monitoring pilot reactions to changes in helicopter transfer functions within a piloted flight simulation. It also defines handling qualities specifications in terms of response types and operational environment. The response types can be defined as follows:

Attitude Rate - Attitude diverges away from trim for at least 4 seconds following a step change applied at the inceptor.

Attitude Command (AC) - Constant cockpit control force input must produce proportional angular displacement in terms of vehicle attitude. A separate trim control must be supplied.

Attitude Hold (AH) - Attitude must return to within 10% of peak within 20 seconds following a pulse cockpit controller input, or input directly into the control surface actuator. This is illustrated in figure 3.3. (Hoh, 1988)

Translational Rate Command with Position Hold (TRCPH) - Constant controller force input must result in constant translational rate. The rotorcraft must hold position if the force on the cockpit controller is zero.

The response type is a classification based upon the operational requirements of the helicopter. If the Bode plot of a response type is considered it can be seen that the

positions of the dominant poles and zeros are restricted.(Hoh, 1988) This means, therefore, that the required response type affects the design of the flight control system.

It should also be noted that since different response types may be suited to different forward velocities, the required response type may change with flight condition. The character of the controller may have to change as a consequence of the different requirements.

During initial testing stage of flight control system development in terms of the flow chart of figure 1.1, only the handling qualities requirements for small amplitude responses may be used due to the limits imposed on model validity by the linear model.

Many of the handling quality requirements refer to the response of the helicopter to pilot inputs. A representative set of tasks is defined within the handling qualities documentation. These are known as mission task elements (MTE) and are defined because different tasks require different handling qualities. The dynamic response requirements are divided into two categories: low speed/hover (< 45 knots) and forward flight. In this study the initial tests have been performed on a model of a Lynx at 80 knots. This means that the Low Speed/ Hover requirements for dynamic response are not needed. Of the forward flight requirements (Section 3.4), the most stringent requirements are those for Air Combat. It is assumed that these are to be used to assess performance. The performance of the controller can be assigned to one of three categories:

Level 1 - Flying qualities are completely adequate for the MTE being considered.

Level 2 - Flying qualities are adequate for the MTE being considered but there is a loss of effectiveness of the mission or an increase in workload is imposed on the pilot to achieve the mission.

Level 3 - Flying qualities are such that the helicopter can be controlled but either mission effectiveness is severly impaired or the pilot workload is so great that it approaches the

limit of the pilot's capacity.

It is desirable that all Mission Task Elements should have Level 1 handling qualities. Bandwidth criteria will be used to assess the performance of the controller initially. The bandwidth is a measure of the maximum closed loop frequency that a pilot can achieve without threatening stability. Bandwidth is a function of the gain or phase margin of the open loop frequency response of the attitude response to cockpit inputs and is defined in figure 3.1.(Hoh, 1988) Actual bandwidth criteria are given in figure 3.2.(Hoh, 1988)

Phase delay is a measure of how quickly the phase lag increases at frequencies beyond that which has a phase shift of 180 degrees. The phase delay parameter is sensitive to lags and delays in the flight control system. It can be seen from figure 3.2 that as the phase delay, τ_p, increases the required bandwidth increases. This is because it is thought that an aircraft with rapid rate of change of phase will be more sensitive in terms of closed loop performance than one with a smaller rate of change of phase. A good system will have a bandwidth that is higher than the maximum input frequency that it is designed to track. Systems can be PIO prone (pilot induced oscillation - approximately 1 Hz) if the gain margin bandwidth is low. This is because small changes in pilot gain cause a large reduction in phase margin. The higher bandwidth is therefore required to provide a larger margin. Analysis of the frequency response of the pitch, roll and yaw channels will provide measurements of bandwidths and phase delays.

As shown in Figure 1.1 piloted simulation using a flight simulator would be the final step in assessing the control system prior to implementation in the real vehicle and subsequent flight test. At this stage the controller can be tested by large scale manoeuvres with a non-linear model. The pilot rates the handling qualities of the controlled helicopter according to the Cooper-Harper scale.(Harper, 1986) These ratings relate to the handling qualities ratings outlined above as follows:

Cooper-Harper Handling Qualities

1 - 3.5 $\Rightarrow$ Level 1

3.5 - 6.5 $\Rightarrow$ Level 2

6.5 - 10 $\Rightarrow$ Level 3

A decision can then be made as to whether to continue testing the controller by an inflight demonstration. From the inflight demonstration pilots return handling qualities ratings for various tasks. These ratings give an indication of whether the controller is performing satisfactorily.

Software for Handling Qualities Analysis

The Helicopter Handling Qualities Toolbox (Howitt) was written for the PRO-MATLAB package. This allows the designer to utilitise not only the handling qualities toolbox but also the other toolboxes available in MATLAB.

The handling qualities toolbox performs analysis relating to the criteria from the Mil. Spec. MIL-H-8501A update. It contains three types of functions: analysis, plotting and data functions. Analysis functions define the handling qualities parameters from the responses of the system, the plotting functions plot the parameters which are calculated by the analysis functions and the data functions contain data pertaining to handling qualities boundaries and text.

Frequency responses can be generated for each of the axes (pitch, roll & yaw) from linear simulation in MATLAB. These are used as the basis for analysis.

The analysis function DEF–SHORT–TERM is used to define the effective bandwidth and phase delay from the small amplitude, short term frequency response. PLOT–SHORT–TERM then plots the parameters calculated for each body axis, pitch, roll & yaw. The plots displayed allow the designer to relate the performance of the controlled system to the handling qualities boundaries. The designer can use this information to produce a satisfactory design.

Other functions deal with mid-term response. The handling qualities toolbox can also be used in conjunction with a non-linear model.

This toolbox will be used to present results in subsequent chapters.

Choice of Outputs for Handling Qualities

It has been shown that some combinations of outputs for control purposes are more compatible with handling qualities specifications than others.(Buckingham & Padfield, 1986) The choice of outputs available were as follows:

output1:	h	height rate
	γ	flight path angle
	wb	vertical velocity
output2:	θ	pitch attitude
	q	pitch rate
	vt	total velocity
	ub	longitudinal velocity
output3:	Ω	turn rate
	φ	bank angle
	p	roll rate
	vb	lateral velocity
output 4:	β	sideslip
	r	yaw rate
	vb	lateral velocity

The four outputs to be controlled were chosen by selecting one variable from each of the above sections. Obviously, there are 144 combinations. However, 12 of these can be eliminated because they have vb in both the third and fourth outputs. Also some other combinations would not be desirable from a handling qualities point of view.(Buckingham & Padfield, 1986) In Chapter 5 the remaining 132 combinations are inspected. The outcomes of the investigations are tabulated in Appendix 2.

References

Anon.

General Requirements for Helicopter Flying

and Ground Handling Qualities

MIL-H-8501A, 1961

Buckingham S L & Padfield, G D

Piloted Simulations to Explore Helicopter Advanced Control Systems

RAE Technical Report 86022 April 1986

Harper, R P & Cooper, G E

Handling Qualities and Pilot Evaluation

J. Guidance and Control

vol. 9 N0. 5

pp 515 - 529, 1986

Hoh, R H

Dynamic Requirements in the New Handling Qualities Specification for US Military Rotorcraft

Proc. of the Helicopter Handling Qualities and Control Conference

London

paper no. 4, 15 - 17 November 1988

Hoh, R H, Mitchell, D G, Aponso, B L, Key, D L & Blanken, CL

Proposed Specification for Handling Qualities of Military Rotorcraft,

Volume 1 - Requirements

Draft, NASA Tech. Memo.

US Army AVSCOM Tech.

Report 87-A-4

May, 1988

Howitt, J

A Software Toolbox for Handling Qualities Analysis of Combat Helicopters

RAE (Bedford)

hase Delay:

$$\tau_p = \frac{\Delta\Phi 2\omega_{180}}{57.3(2\omega_{180})}$$

s: *1) if phase is nonlinear between ω_{180} and $2\omega_{180}$, τ_e shall be determined from a linear least squares fit to phase curve between ω_{180} and $2\omega_{180}$*

CAUTION:
For ACAH, if $\omega_{BW_{gain}} < \omega_{BW_{phase}}$, or if $\omega_{BW_{gain}}$ is indeterminate, the rotorcraft may be PIO prone for super-precision tasks or aggressive pilot technique.

Rate Response-Types:

ω_{BW} is lesser of $\omega_{BW_{gain}}$ and $\omega_{BW_{phase}}$

Attitude Command/Attitude Hold Response-Types (ACAH):

$\omega_{BW} \equiv \omega_{BW_{phase}}$

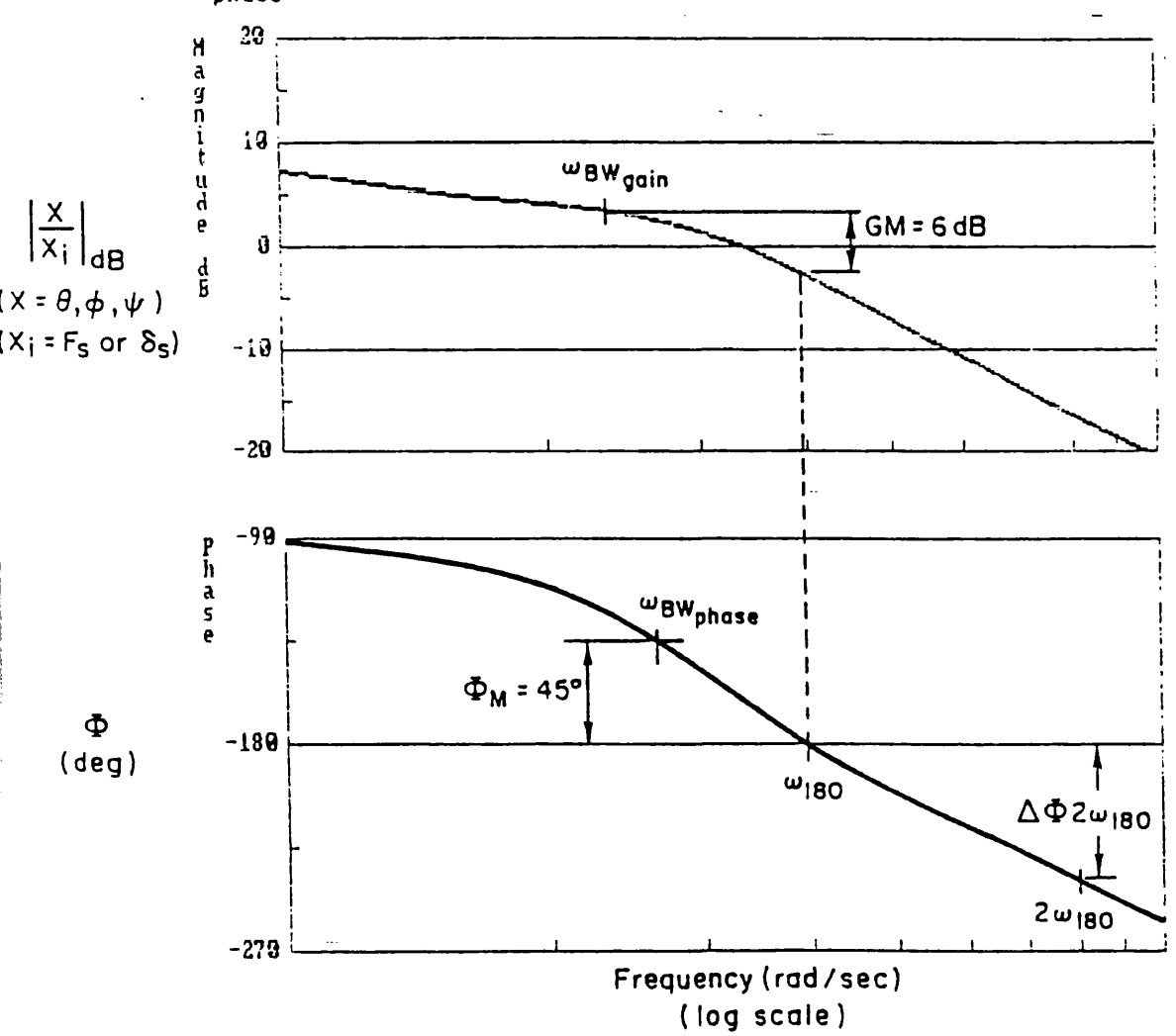

Figure 3.1 Definitions of Bandwidth and Phase Delay

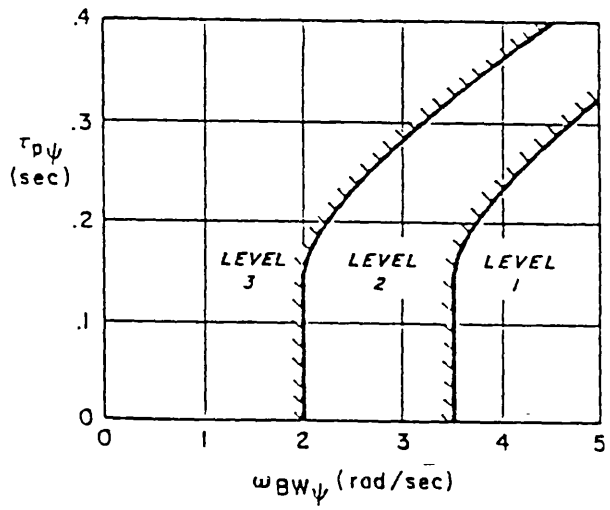

a) Target Acquisition and Tracking

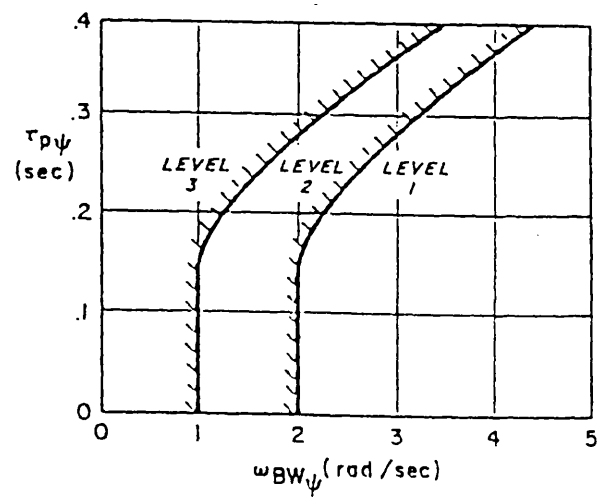

b) All Other MTEs

Figure 3.2 Bandwidth and Phase Delay Requirements for Handling Qualities

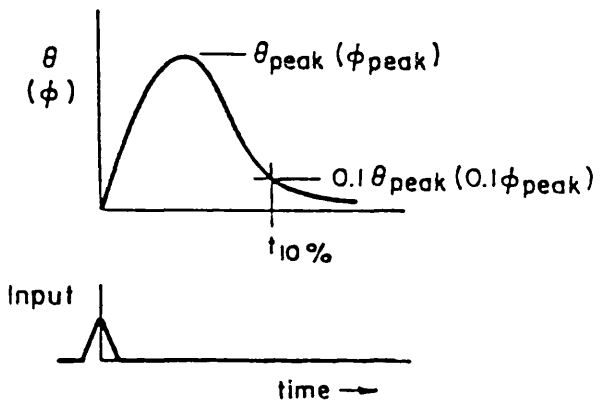

Figure 3.3 Illustration of Pulse Response Required for Attitude Hold Response-Types

CHAPTER 4 CONTROLLERS DESIGNED BY TWO DIFFERENT EIGENSTRUCTURE ASSIGNMENT TECHNIQUES

4.1 Eigenstructure Assignment Method with Eigenvector Specification

There are many methods of assigning eigenstructure. One method (Andry, Shapiro & Chung, 1983) allows the desired eigenvalue positions to be achieved and also permits some control over the eigenvectors. This method is outlined below.

We consider the linear, time-invariant system described by

$$\dot{x} = Ax + Bu \qquad (4.1)$$

$$y = Cx \qquad (4.2)$$

where x is state vector, u is input vector & y is output vector.

Given a self-conjugate set of scalars, $\{\lambda_i^d\}$ i=1..n, and a corresponding self-conjugate set of n vectors, $\{v_i^d\}$ i=1..n, find a real (mxn) matrix F such that the eigenvalues of (A + BF) are precisely those of the self-conjugate set of scalars $\{\lambda_i^d\}$ with corresponding eigenvectors the self-conjugate set $\{v_i^d\}$.

If we define

$$S = [\ \lambda I - A \ \vdots\ B\ ] \qquad (4.3)$$

and a compatibly partitioned matrix

$$R_\lambda = \begin{bmatrix} N_\lambda \\ M_\lambda \end{bmatrix} \qquad (4.4)$$

where the columns of R_λ form a basis for the null space of S_λ.

For rank(B)=m, columns of N_λ are linearly dependent and $N_\lambda^* = N_{\lambda^*}$. If we let $\{\lambda_i\}$ i=1..n be a self-conjugate set of distinct complex numbers, there exists a real (mxn) matrix F such that

$$(A + BF)v_i = \lambda_i v_i \quad i=1..n \qquad (4.5)$$

if and only if

(i) $\{v_i\}$ i=1..n are a linearly independent set in $\mathbb{C}^n$, the space of complex n vectors.

(ii) $v_i = v_j^*$ when $\lambda_i = \lambda_j^*$

(iii)v_i = span $\{N_{\lambda i}\}$

$$(\lambda_i I - A)v_i = BFv_i \tag{4.6}$$

$$[\lambda_i I - A \quad B]\begin{bmatrix} v_i \\ -Fv_i \end{bmatrix} = 0 \tag{4.7}$$

Since the columns of $R_{\lambda i}$ form a basis for the null space of $S_{\lambda i}$, it follows that

$$v_i \in \text{span}\{N_{\lambda i}\} \tag{4.8}$$

If we assume the set $\{v_i\}$ i=1..n satisfies (i), (ii) & (iii) then there exists a vector z_i (real or complex) such that

$$v_i = N_{\lambda i} z_i \tag{4.9}$$

$$(\lambda I - A)N_{\lambda i} + BM_{\lambda i} = 0 \tag{4.10}$$

$$(\lambda I - A)N_{\lambda i} z_i + BM_{\lambda i} z_i = 0 \tag{4.11}$$

$$(\lambda I - A)v_i + BM_{\lambda i} z_i = 0 \tag{4.12}$$

If an F can be chosen so that

$$-M_{\lambda i} z_i = Fv_i \tag{4.13}$$

then

$$[\lambda I - (A + BF)]v_i = 0 \tag{4.14}$$

If such an F exists it satisfies

$$F[v_1, \ldots, v_n] = [-M_{\lambda 1} z_1, \ldots, -M_{\lambda n} z_n] \tag{4.15}$$

If each λ_i is real and the matrix of eigenvectors is non-singular,

$$F = [-M_{\lambda 1} z_1, \ldots, -M_{\lambda n} z_n]\,[v_1, \ldots, v_n]^{-1}$$

If desired eigenvalues are complex, a slight alteration of the above equation is required

Assume that $\lambda_1 = \lambda_2^*$

From (ii) $v_1 = v_2^*$ which implies $z_1 = z_2^*$. Thus assuming all other eigenvalues are real, F must satisfy

$$F[v_{1R} + jv_{1I} \; v_{1R} - jv_{1I} \; v_3 \ldots v_n] = [w_{1R} + jw_{1I} \; w_{1R} - jw_{1I} \; w_3 \ldots w_n]$$

where $w_i = -M_{\lambda i} z_i$ (4.16)

Multiplication on both sides of the equation by non-singular matrix

$$\begin{bmatrix} 1/2 & -j/2 & 0 \\ 1/2 & j/2 & 0 \\ 0 & 1 & \end{bmatrix} \tag{4.17}$$

results in

$$[\tfrac{1}{2}(w_{1R}+jw_{1I})+\tfrac{1}{2}(w_{1R}-jw_{1I}) \quad -\tfrac{1}{2}j(w_{1R}+jw_{1I})+\tfrac{1}{2}j(w_{1R}-w_{1I}) \quad w_3 \ \cdots \ w_n]$$

$$= [\tfrac{1}{2}(w_{1R}+jw_{1I}+w_{1R}-jw_{1I}) \quad \tfrac{1}{2}(-jw_{1R}+w_{1I}+jw_{1R}+w_{1I}) \quad w_3 \ \cdots \ w_n]$$

$$= [w_{1R} \ w_{1I} \ w_3 \ \cdots \ w_n] \qquad (4.18)$$

Therefore

$$F[v_{1R} \ v_{1I} \ v_3 \ \cdots \ v_n] = [\ w_{1R} \ w_{1I} \ w_3 \ \cdots \ w_n]$$

Since the set $\{v_i\}$ is independent, the matrix $[v_{1R} \ v_{1I} \ v_3 \ \ldots \ v_n]$ is non-singular and F can be calculated.

It has been shown that (Andry et al., 1983)

(1) n eigenvalues and a maximum of nxm eigenvector entries can be arbitrarily specified.

(2) no more than m entries of any one eigenvector can be chosen arbitrarily.

Given the controllable and observable system and assuming B & C are full rank, then max(m,r) closed loop eigenvalues can be assigned and max(m,r) eigenvectors can be partially assigned with min(m,r) entries in each eigenvector arbitrarily chosen using gain output feedback.

1. Total Specification Of v_i^d

Consider the closed loop system

$$\dot{x}(t) = (A + BF)x(t) \qquad (4.19)$$

Assume we are given $\{\lambda_i\}$ i=1..r as the desired closed loop eigenvalues where v_i is the closed loop eigenvector corresponding to λ_i. So for the eigenvalue/eigenvector pair we have

$$(A + BFC)v_i = \lambda_i v_i \qquad (4.20)$$

$$v_i = (\lambda_i I - A)^{-1}BFCv_i \qquad (4.21)$$

It is assumed that none of λ_i^d match the existing eigenvalues of A so that $(\lambda I - A)^{-1}$ exists.

$$m_i = FCv_i \qquad (4.22)$$

$$v_i = (\lambda_i I - A)^{-1}Bm_i \qquad (4.23)$$

This implies the eigenvector v_i must be in the subspace spanned by the columns of $(\lambda_i I - A)^{-1}B$ of dimension m (equal to rank(B) or the number of independent variables).

Therefore the dimension of the subspace is determined by A, B & λ_i.

Therefore, if we choose an eigenvector which lies in this subspace, it will be achieved exactly.

2. Best Possible v_i^d

In general the chosen eigenvector will not lie within the subspace and therefore cannot be exactly achieved. We must develop a method to achieve the "best possible" choice of eigenvector which will lie in the subspace.

Define

$$L_i = (\lambda_i I - A)^{-1}B \qquad (4.24)$$

$$v_i^A = L_i z_i \quad z \epsilon \mathbf{R} \qquad (4.25)$$

where v_i^A is the achievable eigenvector (the projection of v_i^d onto the subspace).

In order to find this projection, we choose to minimise

$$J = \|v_i^d - v_i^A\|^2 = \|v_i^d - L_i z_i\|^2 \qquad (4.26)$$

$$\frac{dJ}{dz_i} = 2L_i^T (L_i z_i - v_i^d) \qquad (4.27)$$

$$\frac{dJ}{dz_i} = 0 \quad \text{implies} \qquad (4.28)$$

$$z_i = (L_i^T L_i)^{-1} L_i^T v_i \qquad (4.29)$$

$$v_i^A = L_i (L_i^T L_i)^{-1} L_i^T v_i^d \qquad (4.30)$$

3. Partial Specification Of v_i^d

Assume v_i^d has the following structure

$$v_i^d = \begin{bmatrix} v_{i1} \\ v_{ij} \\ v_{in} \end{bmatrix} \qquad (4.31)$$

where v_{ij} are components specified by the designer and other components are unspecified.

Reordering,

$$\{v_i^d\} = \begin{bmatrix} l_i \\ d_i \end{bmatrix} \tag{4.32}$$

l_i vector of specified components

d_i vector of unspecified components of v_i^d

$$(\lambda I - A)^{-1}B = \begin{bmatrix} L_i \\ D_i \end{bmatrix} \tag{4.33}$$
$$\tag{4.34}$$

$$z_i = (L_i^T L_i)^{-1} L_i^T l_i \tag{4.35}$$

$$v_i^A = L_i (L_i^T L_i)^{-1} L_i^T l_i \tag{4.36}$$

4. Feedback Gain Computation

Hereafter eigenvector refers to assignable eigenvector.

Transform the B matrix to form

$$B \rightarrow \begin{bmatrix} I_m \\ 0 \end{bmatrix} \tag{4.37}$$

$$T \rightarrow [B \; P] \tag{4.38}$$

where P is any matrix such that rank(T) = n

$$\tilde{A} = T^{-1}AT \tag{4.39}$$

$$\tilde{B} = T^{-1}B = \begin{bmatrix} I_m \\ 0 \end{bmatrix} \tag{4.40}$$

$$\tilde{C} = CT \tag{4.41}$$

$$\dot{\tilde{x}}(t) = \tilde{A}\tilde{x}(t) + \tilde{B}u(t) \tag{4.42}$$

$$y(t) = C\tilde{x}(t) \tag{4.43}$$

Under this transformation the eigenvalues of the system are unaffected and the eigenvectors are related by

$$T^{-1}v_i = \tilde{v}_i \tag{4.44}$$

The closed loop eigenvalue/eigenvector equation is

$$(\lambda I - A)v_i = BFCv_i \qquad (4.45)$$

We partition this conformally

$$\begin{bmatrix} \lambda I_m - A_{11} & -A_{12} \\ -A_{21} & \lambda I_{n-m} - A_{22} \end{bmatrix} \begin{bmatrix} z_i \\ w_i \end{bmatrix} = \begin{bmatrix} I_m \\ 0 \end{bmatrix} FC \begin{bmatrix} z_i \\ w_i \end{bmatrix} \qquad (4.46)$$

where

$$v_i = \begin{bmatrix} z_i \\ w_i \end{bmatrix} \qquad (4.47)$$

$$A = \begin{bmatrix} A_{11} & A_{12} \\ A_{21} & A_{22} \end{bmatrix} \qquad (4.48)$$

$$[\lambda_i I_m - A_{11} \quad -A_{12}] \begin{bmatrix} z_i \\ w_i \end{bmatrix} = FC \begin{bmatrix} z_i \\ w_i \end{bmatrix} \qquad (4.49)$$

Multiplying out

$$(\lambda_i I_m - A_{11})z_i - A_{12}w_i = FCv_i \qquad (4.50)$$

$$\lambda_i I_m z_i - (A_{11}z_i + A_{12}w_i) = FCv_i \qquad (4.51)$$

$$\lambda_i z_i - A_1 v_i = FCv_i \qquad \text{where } A_1 = [A_{11} \; A_{12}]$$

$$(A_1 + FC)v_i = \lambda_i z_i \qquad (4.52)$$

$$(A_1 + FC)V = Z \qquad (4.53)$$

$$F = (Z - A_1 V)(CV)^{-1} \qquad (4.54)$$

where $V = [\, v_1 \; v_2 \; \ldots \; v_r \,]$

$Z = [\, \lambda_1 z_1 \; \lambda_2 z_2 \; \ldots \; \lambda_r z_r \,]$

Results From The Above Method

The above method was applied to the helicopter control problem. Using the Helistab model of the helicopter's rigid body dynamics at 80 knots and in forward level flight, 8 eigenvalues were assigned (and 8 eigenvectors partially assigned) to create a feedback controller which would give better performance. Although this method was found to give accurate eigenvalue placement and a best fit to the desired eigenvector structure at the design condition, at flight conditions away from the design flight condition the eigenstructure of the controlled system changed to such an extent (fig. 4.4) that it produced a significant deterioration in performance.

4.2 Eigenstructure Assignment Method with Condition Number

During flight the helicopter will stray from the design condition and the natural eigenstructure of the helicopter will change. The ability of a controller to cope with such a change is referred to as robustness. It would be useful if some parameter could

be calculated from the controlled system which would reflect to what extent the assigned eigenstructure of the system would change from that at the design condition. The following method (Kautsky, Nichols & Van Dooren, 1975) does this. It allows eigenvalues to be assigned and also gives a condition number to indicate how robust the solution is. (When perfectly conditioned, the condition number is 1.) This method is outlined below.

Consider the time–invariant, linear, multivariable system

$$\dot{x}(t) = Ax(t) + Bu(t) \qquad (4.55)$$

Given the real matrix pair (A, B) and eigenvalue set Œ, our objective is to choose eigenvectors, given by X, satisfying

$$(A + BF)X = X\Lambda \quad \text{where } \Lambda = \text{diag}\{\lambda_1 \ldots \lambda_n\}$$

and such that the conditioning of the eigenproblem is minimised.

If X is non-singular, there exists F, a solution to

$$(A + BF)X = X\Lambda \qquad (4.56)$$

if and only if

$$U_1^T(AX - X\Lambda)=0 \qquad (4.57)$$

where

$$B = [\, U_0 \; U_1 \,] \begin{bmatrix} Z \\ 0 \end{bmatrix} \text{ by QR decomposition}$$

Therefore F is given by

$$F = Z^{-1}U_0^T(X\Lambda X^{-1} - A) \qquad (4.58)$$

Proof

$$(A + BF)X = X\Lambda \qquad (4.59)$$

$$BF = X\Lambda X^{-1} - A \qquad (4.60)$$

premultiplying by U^T gives

$$ZF = U_0^T(X\Lambda X^{-1} - A) \qquad (4.61)$$

$$0 = U_1^T(X\Lambda X^{-1} - A) \qquad (4.62)$$

(4.58) implies that F exists if and only if

$$R\{X\Lambda X^{-1} - A\} \subset R\{B\} \equiv R\{U_0\} \qquad (4.63)$$

R denotes range and N denotes null space.

Therefore $R\{X\Lambda X^{-1} - A\}$ is orthogonal to $N\{B\} \equiv R\{U_1\}$

The feedback matrix is calculated in three steps:

Step 1

The QR decomposition of B gives U_0, U_1 & Z.

This allows us to construct orthonormal bases s_j and s_j for the space $\hat{\eta}_j$ in which each eigenvector lies

$$\eta_j = N\{U_1^T(A - \lambda_j I)\} \qquad (4.64)$$

$$(U_1^T(A - \lambda_j I))^T = [\hat{S}_j \; S_j] \begin{bmatrix} R_j \\ 0 \end{bmatrix} \qquad (4.65)$$

Step 2

The objective is to choose vectors $x_j \in \eta_j$ $j = 1 \ldots n$ such that each vector is as orthogonal as possible to the space spanned by the remaining vectors, i.e. the angle between x_j and the space $X_j = \langle x_i \; i \neq j \rangle$ is maximised for all j. Or we choose x_j to minimise the angle between x_j and the normalised vector y_j orthogonal to the space x_j $\forall$ j.

Each vector x_j is taken in turn and replaced by a new vector with maximum angle to the current space X_j.

We obtain y_j by QR decomposition of

$$X_j = [x_1 \; x_2 \; \ldots \; x_{j-1} \; x_{j+1} \; \ldots \; x_n] \qquad (4.66)$$

$$= [Q_j \; y_j] \begin{bmatrix} R_j \\ 0 \end{bmatrix}$$

The projection of y_j into η_j is given by

$$x_j = S_j w_j = \frac{S_j \, S_j^T \, y_j}{\| S_j \, y_j \|^2} \qquad (4.67)$$

which gives the vector x_j which has minimum angle to y_j.

Step 3

$$M = A + BF \tag{4.68}$$

$$M = X\Lambda X^{-1} \tag{4.69}$$

M is calculated by solving for M^T in

$$X^T M^T = (X\Lambda)^T \tag{4.70}$$

$$F = Z^{-1} U_0^T (M-A) \tag{4.71}$$

The condition number of the eigenvector matrix X gives an indication of how robust we can expect the solution to be. $K_{2(X)} = 1$ is perfectly conditioned.

Results From The Above Method

Using a flight condition of 80 knots forward flight and a rigid body model, this second method was used to design feedback controllers for 3 different eigenvalue sets. Higher order dynamics were then added to the rigid body model and the flight condition was changed from 80 knots to between 60 and 100 knots in steps of 5 knots.

This was to test for robustness to changes in the coefficients of the system matrices with changes in flight condition and also to the addition of high frequency dynamics unmodelled at the design condition. The migration of the eigenvalues at each flight condition was plotted. From the graphs we see that the condition number does indeed give an indication of the extent to which the eigenvalues move. The system with the condition number of 30 (fig. 4.2) has shown very little eigenvalue movement compared with the system with condition number 185 (fig. 4.1). We can conclude that $k_2(X)$ gives a reliable indication of robustness in terms of the unwillingness of the eigenvalues of the closed loop system to move when higher frequency dynamics are added to the model and the flight condition is changed.

Taking the middle case with condition number 66 (fig. 4.3), the same eigenvalue set was used with the first eigenstructure assignment (Andry) method to obtain a feedback

controller. In order to obtain a comparison of the two methods, the same changes were made to the model dynamics and flight condition. Fig. 4.4 shows the results from the Andry method. The moderate and low frequency eigenvalues show greater movement in the Kautsky method than in the Andry method but the higher frequency eigenvalues move more in the Andry method than in the Kautsky approach.

It is generally true to say that the controller developed by the first method gives a more robust performance in terms of the lack of movement of the eigenvalues and may therefore be better suited to the helicopter application where there is a large range of dynamic change than the other method.

References

Andry, A N, Shapiro, E Y & Chung, J C

Eigenstructure Assignment for Linear Systems

IEEE Trans. Aerospace & Electronic Systems

vol. AES-19 no. 5, September 1983 pp 711 - 714

Kautsky, J, Nichols, N K & Van Dooren, P

Robust Pole Assignment in Linear State Feedback

Int. Journal Control

vol. 41, no. 5, 1975 pp 1129 - 1155

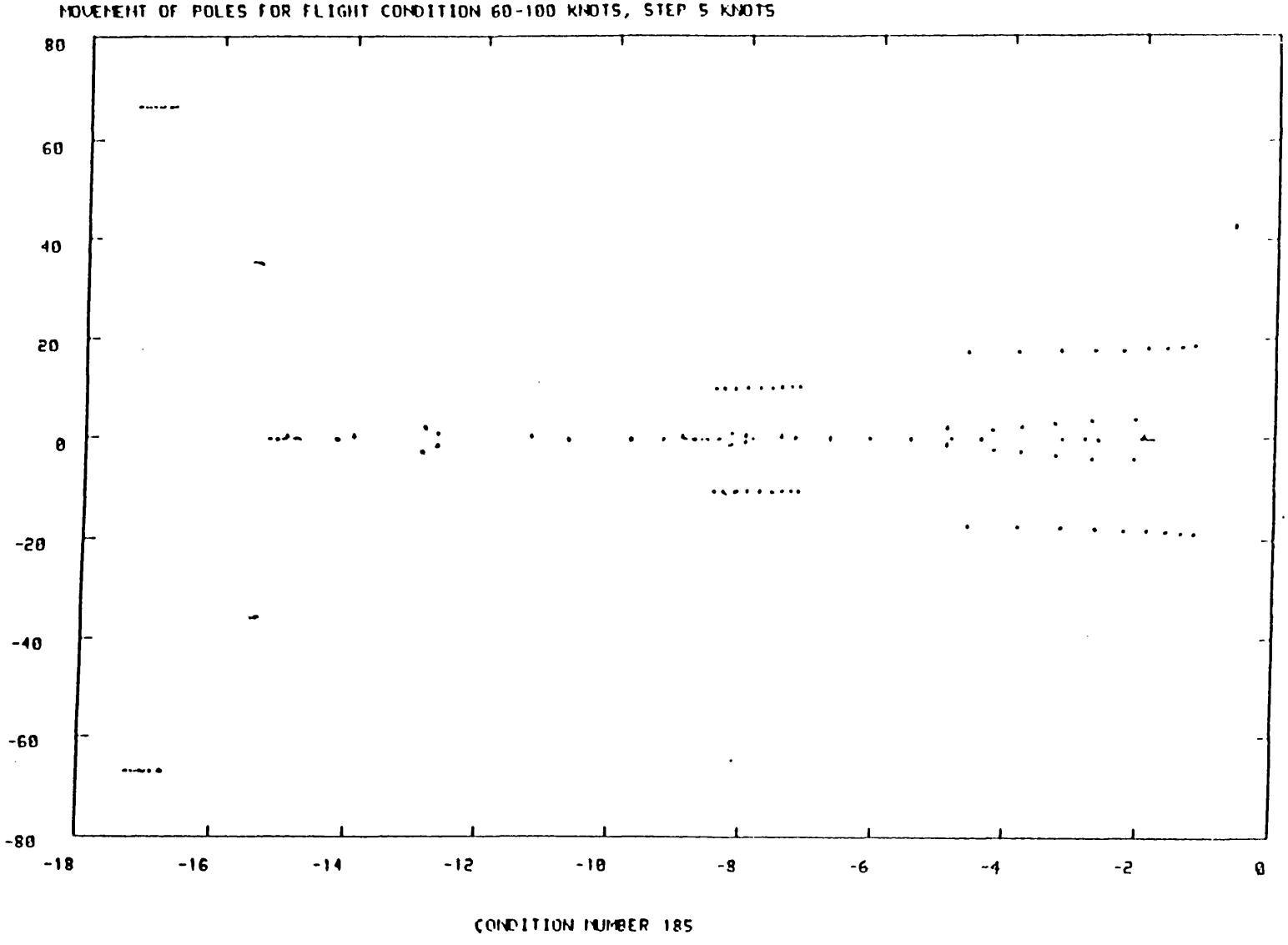

Figure 4.1 Migration of Eigenvalues of Closed-loop System With Change in Flight Condition

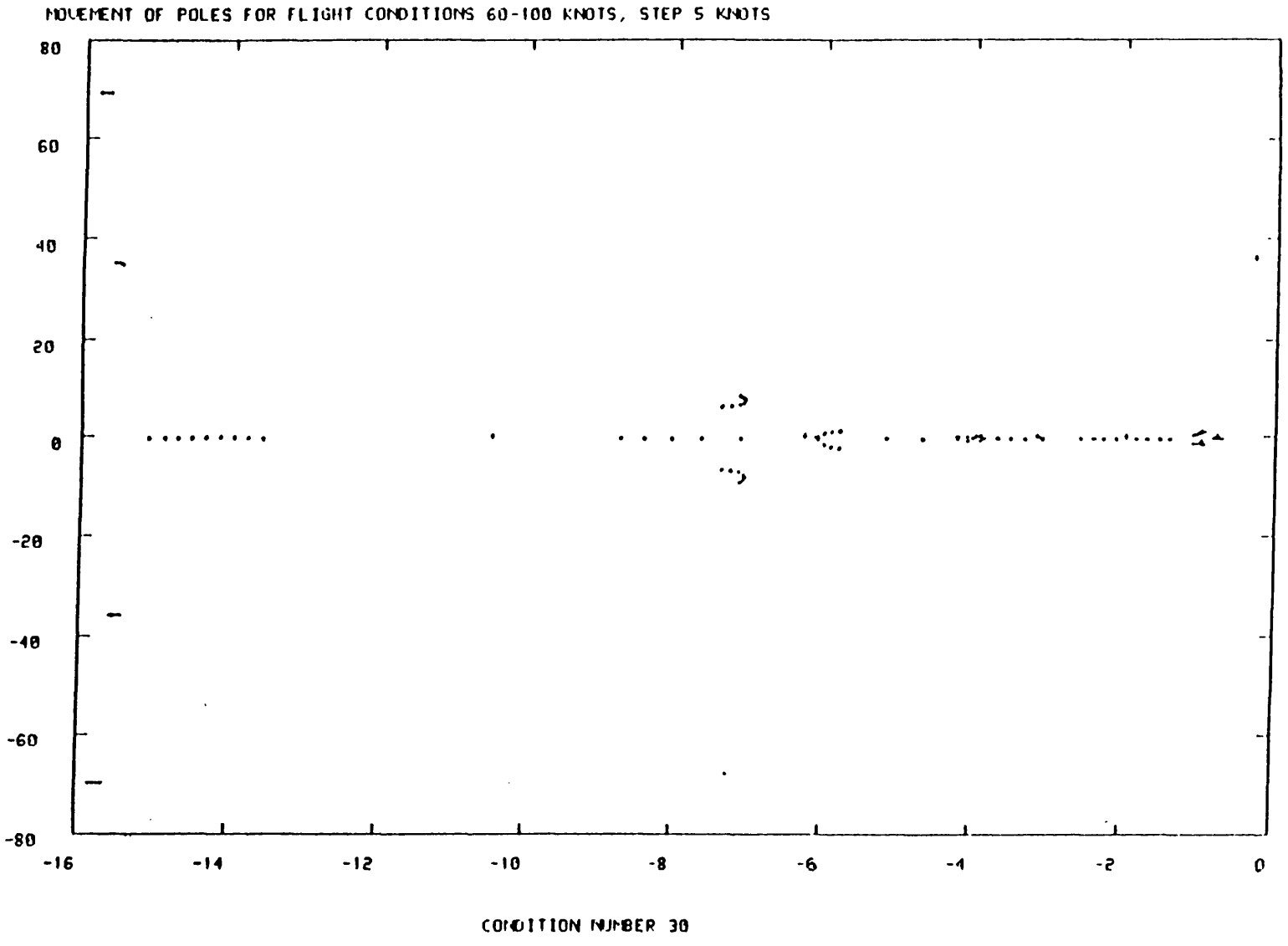

Figure 4.2 Migration of Eigenvalues of Closed-loop System With Change in Flight Condition

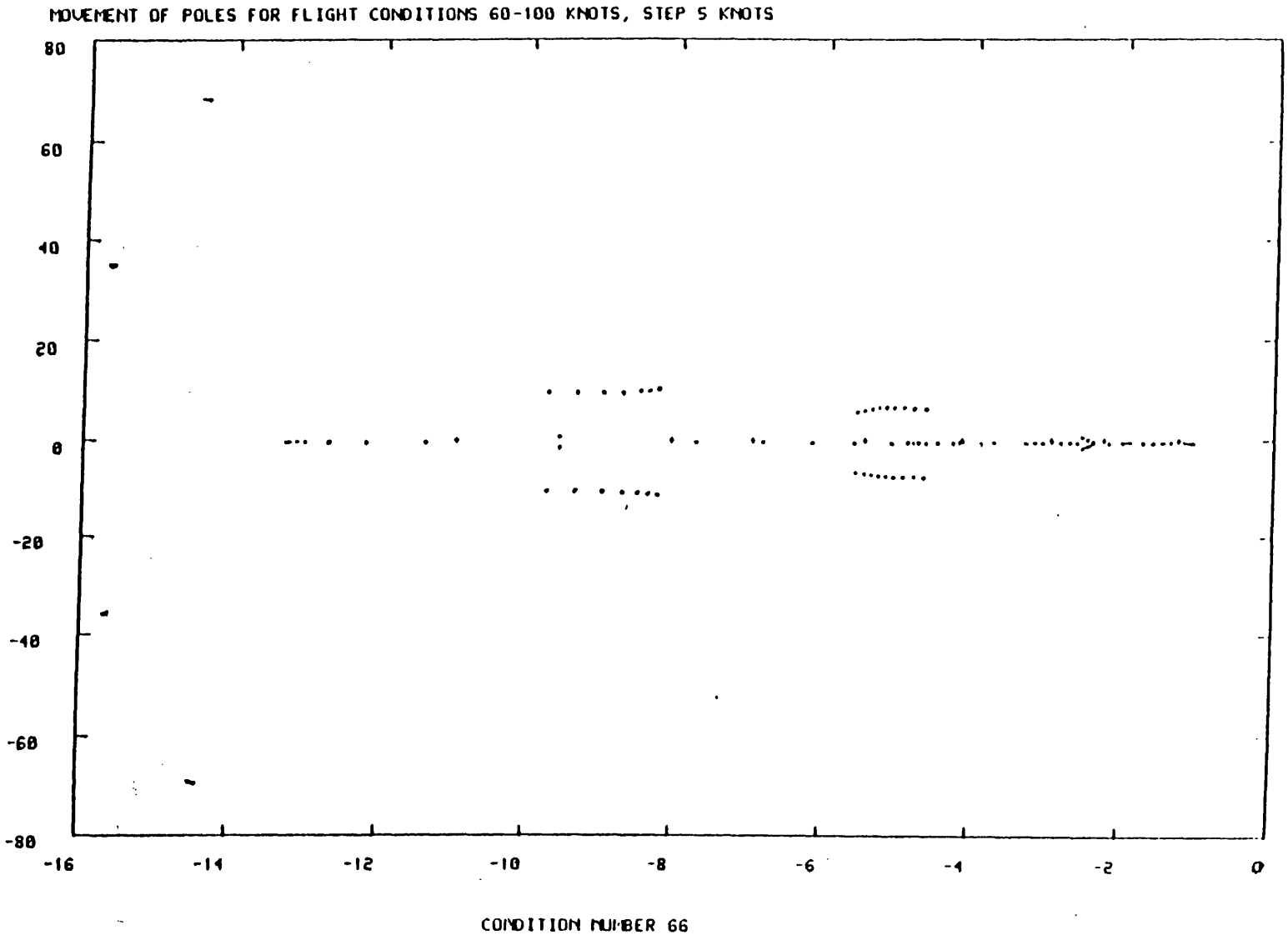

Figure 4.3 Migration of Eigenvalues of Closed-loop System With Change in Flight Condition

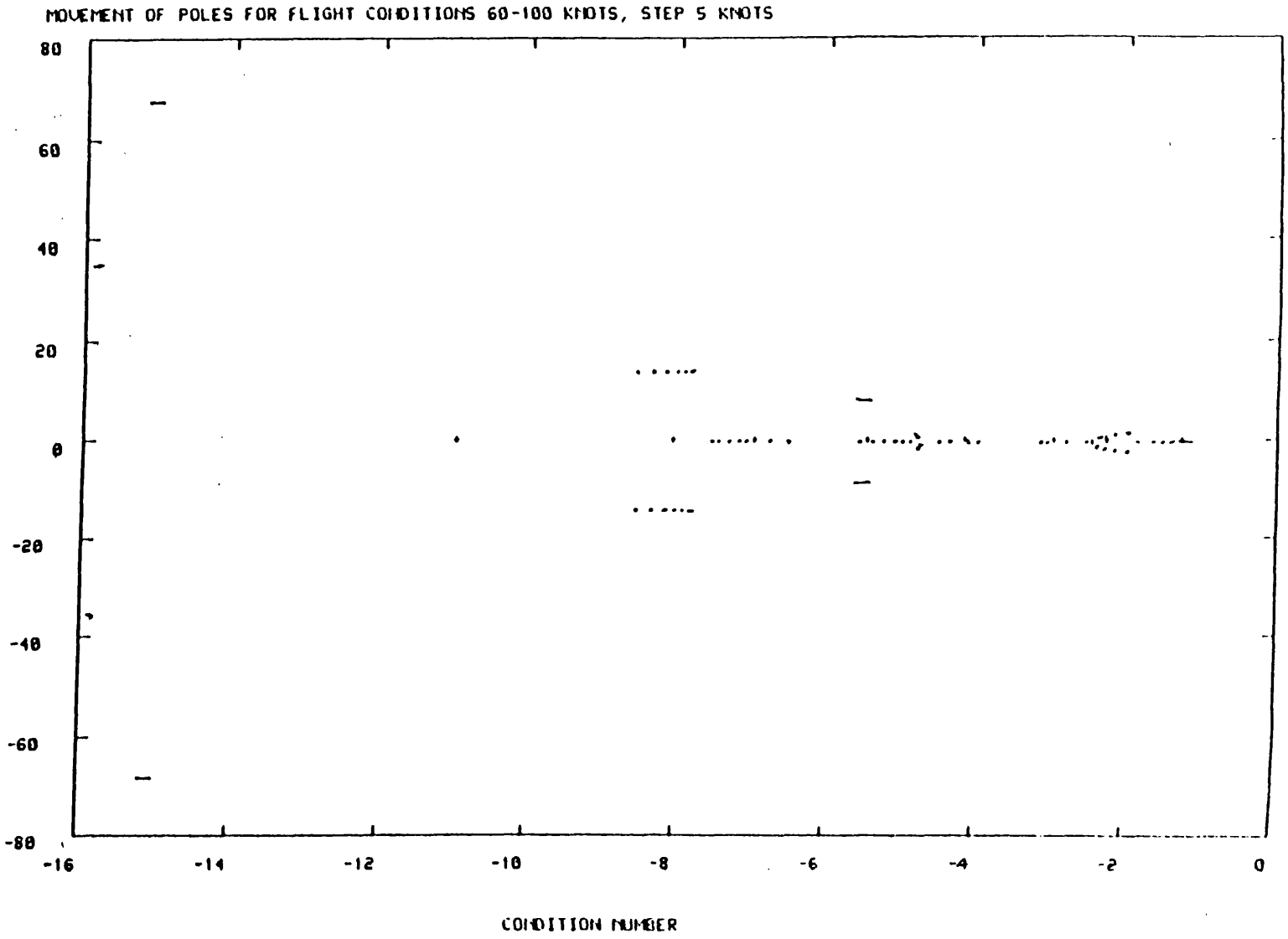

Figure 4.4 Migration of Eigenvalues of Closed-loop System With Change in Flight Condition

CHAPTER 5 EIGENSTRUCTURE ASSIGNMENT METHOD FOR DECOUPLED TRACKING

5.1 Method for Eigenstructure Assignment

The third eigenstructure assignment method is based upon a control system structure of the type shown in the Figure 5.1a

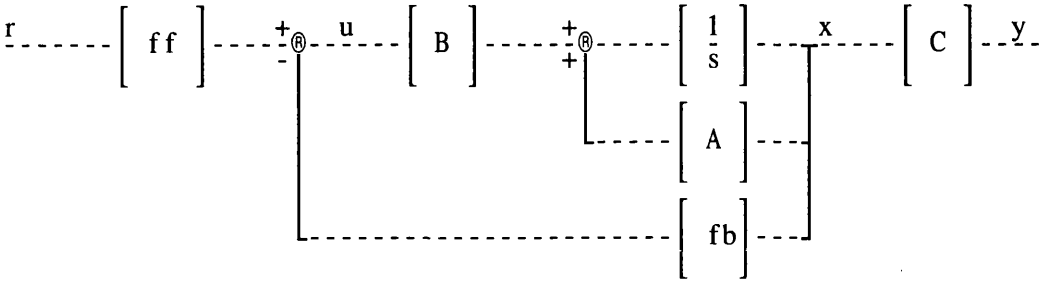

Figure 5.1a Block diagram of controller configuration

Two of the objectives in designing a control law are to create a well-decoupled tracking system (each input being tracked by one output) and to decrease the pilot workload. It was felt that one approach to decreasing pilot workload could involve simplifying the transfer function of the closed loop system so that, from the pilot's point of view, more predictable characteristics could be obtained and so make flying the helicopter an easier task.

To simplify the system from the pilot's point of view, the effective system order should be decreased over the frequency range of relevance. This can be achieved by using an extension of pole-zero cancellation in SISO systems to the multivariable case. (Hughes et al., 1990)

It is well known that poles can be identified in relation to linear dynamic systems, however, it is less well known that such systems also have zeros associated with them. The poles occur at characteristic frequencies of the system. The zeros give information about how the dynamics of the system are coupled to the external environment. Zeros of

G(s) are called transmission zeros (MacFarlane & Karcanias, 1976) and zeros of P(s) are called invariant zeros. The invariant zeros of a multivariable system are those frequencies at which transmission through the system is blocked. The invariant zeros of a state space representation are those values of s for which the matrix P(s) is singular (i.e. det(P(s))=0).

The matrix P(s) is considered rather than the transfer function matrix, G(s), because G(s) represents only the controllable and observable parts of the system defined by the state space equations, and so more information is available from P(s). If the system is completely controllable and observable then the zeros obtained from G(s) and P(s) will be the same.

$$P(s) = \begin{bmatrix} sI - A & -B \\ C & D \end{bmatrix} \qquad (5.1)$$

There are also system zeros and decoupling zeros. The definition for each type is as follows:

(i) Transmission zeros are defined by the Smith-Macmillan form of the transmittance matrix G(s). They are associated with the transmission-blocking properties of the system.

(ii) Invariant zeros are defined by the system matrix P(s) and are associated with the zero output behaviour of the system.

(iii) Decoupling zeros are defined by the Smith form of

$$\begin{bmatrix} sI-A & -B \end{bmatrix} \quad \text{and} \quad \begin{bmatrix} sI-A \\ C \end{bmatrix}$$

and are associated with the existence of uncoupled modes for systems which are not completely observable or completely controllable.

(iv) System zeros contain both transmission and decoupling zeros.

The transfer function matrix is a representation of how information is transmitted through the system and can be divided into two parts:

1. the coupling into and out of the internal energetic processes of the system (represented by the zeros)
2. the action of these internal energetic processes (represented by the poles)

Therefore, zero positions can be altered by changing the way in which power is coupled into the system or by altering the way in which information is extracted from it. In the

case of the helicopter, we are limited to four pilot inputs but can choose different combinations of outputs to create different output spaces. Each output space will contain different zero positions as mentioned in chapter 3.

Invariant zeros also have associated with them invariant zero directions.
In the multivariable system, available assignable modes can be used to cancel invariant zeros of the system (effectively reducing the order of the system). Not only must some of the assignable eigenvalues be used to cancel the zeros exactly but also the corresponding eigenvectors must match the zero directions. The remaining assignable modes can then be placed to give optimum performance. Once this has been done, the controlled system at the design condition will respond to pilot inputs in a similar fashion as a system which has only the remaining assigned modes (and no zeros). It is possible that the controller will not be robust and as the eigenstructure of the helicopter changes with flight condition, the assigned eigenstructure due to the controller may no longer cancel zeros and zero directions. Consequently, we may find that the eigenvalues and eigenvectors which cancelled zeros and zero directions initially, now add undesirable components into the response characteristics of the controlled system and also that we now have the effects of the cancelled zeros too. On the other hand, the controller may prove to be robust and so, as the eigenstructure of the helicopter moves with changes in flight condition, the assigned eigenstructure moves in such a way that the zeros and directions remain cancelled and adequate performance is maintained.

Obviously, we wish only to assign modes to the left half plane in order to retain stability. Also, even if we could avoid assigning eigenvalues to cancel zeros in the right half plane zeros which lie in the right half plane can cause problems when gain is increased and poles migrate towards them. Therefore the invariant zero structure for each set of outputs chosen must be inspected to ensure that only left half plane zeros are present. Also this method cannot, for reasons which will be explained later, deal with those cases which have a zero at the origin.

In Chapter 3 it was mentioned that some combinations of outputs are more compatible with handling qualities specifications than others. Of the 144 possible combinations, some were

eliminated to leave 132. The zero structures of the remaining 132 combinations were inspected (the flight condition chosen was 80 knots forward, level flight). The 43 cases with a zero at the origin were also unsuitable because the design method adopted cannot include such systems. (If the zero at the origin were to be cancelled, this would introduce a pole at the origin making the state space A matrix impossible to invert. If the zero at the origin was not cancelled, as the feedback increased there would be the possibility of a pole migrating toward it and perhaps finally crossing into the right half plane creating instability in the system.) Some configurations gave left half plane zeros at very high frequencies and these had also to be discounted because a controller which had poles positioned at such high frequencies would not be realisable. Those combinations of outputs which resulted in right half plane zeros had to be discounted as the following method would assign eigenvalues to positions in the right half plane in order to cancel the right half plane zeros. This left only 29 different output sets which involved satisfactory zero positions. The outcomes of all of the zero investigations are tabulated in Appendix 2.

5.2 Description of Method for Decoupled Tracking

The eigenstructure assignment method outlined below attempts to cancel the effects of the zeros by using some of the assignable modes. This also effectively reduces the order of the system.

The first task is to find the positions of the zeros in the left half plane and their associated directions. We then assign modes to cancel these zeros and their directions. The zero and cancelling eigenvalue must be in the same position within the s-plane. Therefore, we have the desired position of the cancelling eigenvalue, λ. Together with the A and B matrices (from the state space description of the helicopter model) we can define the subspace, spanned by the columns of Γ, in which each eigenvector must lie. (Wilkinson, 1965)

$$\Gamma = (A - \lambda I)^{-1} B \qquad (5.2)$$

We also know that the desired eigenvector must match the zero direction. The desired eigenvector will be known as Q1. The next step is to attain the achievable eigenvector

which is as close as possible to the desired eigenvector given the subspace in which it must lie, Γ. This is done as follows:

Firstly, a set of orthogonal vectors is formed from Γ.

$$Q_2 = orth(\Gamma) \tag{5.3}$$

$$M = Q_2' * Q_1 \tag{5.4}$$

where Q_1 contains the zero directions

Then a singular value decomposition is performed on M to find the principal angles

$$[U, S, V] = SVD(M) \tag{5.5}$$

Therefore the assigned eigenvalue, λ_0, is in the same place as the zero being cancelled and the assigned eigenvector is given by

$$[v_0 \; h_0] = Q_2 * U \tag{5.6}$$

Having assigned available modes to cancel zeros and directions, the remaining modes must then be assigned to decouple the control channels. If the number of remaining assignable modes, number of inputs and number of outputs are all equal, then each input should excite only one mode which should be present on only one output. (In cases where there are more remaining modes than outputs, then more than one mode may be assigned to an output channel.)

By considering the null space of the output matrix, C, we can achieve this. If a mode (λ_i, v_i) is to be present on the first control channel, then the output space description of the mode, μ_i, is given by

$$\mu_i = C \; v_i \tag{5.7}$$

and should have the form

$$\mu_i = [\; 1 \; 0 \; \ldots \; 0 \;]^T \tag{5.8}$$

Therefore the eigenvector must lie in the null space of the matrix C_{n1} where

$$C_{n1} = \begin{bmatrix} C_2 \\ \vdots \\ C_m \end{bmatrix} \tag{5.9}$$

where C_i are the ith rows of the matrix C.

Once the positions of the eigenvalues and eigenvectors have been determined, we can calculate the feedback matrix, fb, as follows:

$$fb = B^+ (A V - V \Lambda) V^{-1} \tag{5.10}$$

where B^+ is the pseudo-inverse of B

V is the matrix of eigenvectors

Λ is the matrix of eigenvalues

5.3 Broussard Command Generator Tracking

The block diagram shown in Figure 5.1 has not only a feedback matrix but also a matrix in the forward path. This provides Broussard Command Generator Tracking. The Broussard Command Generator is a linear feedforward controller which maps the transfer function of the controlled system onto a reference model which in this case is an identity matrix. This produces a system whose inputs are tracked by its outputs.

The method by which this feedforward matrix is derived is outlined below. (O'Brien & Broussard, 1978).

Assume the helicopter is represented by

$$\dot{x} = Ax + Bu \qquad (5.11)$$

$$y = Cx \qquad (5.12)$$

If we want a subset of the helicopter's outputs to track the pilot's inputs, then we have

$$y_t = Hx \qquad (5.13)$$

where y_t contains the tracking outputs.

It is assumed that the number of inceptors available match the number of control actuators. The objective is to create a feedforward controller which has effect in such a way as to make the helicopter behave in the same way as a model defined as

$$\dot{x}_M = A_M x_M + B_M u_M \qquad (5.14)$$

$$y_M = C_M x_M + D_M u_M \qquad (5.15)$$

If we assume that the tracking outputs, y_t, are identical to the model outputs, y_M, at time t_0, and we let the input which maintains this condition be u^*, then

$$y_t u_M^* = y_t^* = y_M \quad \text{for } t > t_0 \qquad (5.16)$$

The equations describing the helicopter model are now

$$\dot{x}^* = Ax^* + Bu^* \qquad (5.17)$$

$$y^* = Cx^* \qquad (5.18)$$

$$y_t{}^* = Hx^* \qquad (5.19)$$

Expressions for the ideal helicopter state, x^*, and the ideal helicopter input, u^*, can be given in terms of the helicopter states and inputs of the reference model. (Sobel & Shapiro, 1985)

$$x^* = S_{11}x_M + S_{12}u_M + HOD(u_M) \qquad (5.20)$$

$$u^* = S_{21}x_M + S_{22}u_M + HOD(u_M) \qquad (5.21)$$

where HOD indicates higher order derivatives.

When the model inputs, u_M, are restricted to step functions applied at $t=t_0$, we have

$$\begin{bmatrix} x^* \\ u^* \end{bmatrix} = \begin{bmatrix} S_{11} & S_{12} \\ S_{21} & S_{22} \end{bmatrix} \begin{bmatrix} x_M \\ u_M \end{bmatrix} \qquad (5.22)$$

Equation (5.22) related the ideal states and inputs to the model states and inputs by means of a transformation matrix. The elements of the transformation matrix are as follows

$$S_{11} = \Omega_{11}S_{11}A_M + \Omega_{12}C_M \qquad (5.23)$$

$$S_{12} = \Omega_{11}S_{11}B_M + \Omega_{12}D_M$$

$$S_{21} = \Omega_{21}S_{11}A_M + \Omega_{22}C_M$$

$$S_{22} = \Omega_{21}S_{11}B_M + \Omega_{22}D_M$$

where

$$\begin{bmatrix} \Omega_{11} & \Omega_{12} \\ \Omega_{21} & \Omega_{22} \end{bmatrix} = \begin{bmatrix} A & B \\ H & 0 \end{bmatrix}^{-1} \qquad (5.24)$$

From equations 5.14 & 5.15 we get

$$\begin{bmatrix} \dot{x}_M \\ y_M \end{bmatrix} = \begin{bmatrix} A_M & B_M \\ C_M & D_M \end{bmatrix} \begin{bmatrix} x_M \\ u_M \end{bmatrix} \qquad (5.25)$$

And from equations (5.17), (5.18) & (5.19) we get

$$\begin{bmatrix} \dot{x}^* \\ y_t{}^* \end{bmatrix} = \begin{bmatrix} A & B \\ H & 0 \end{bmatrix} \begin{bmatrix} x^* \\ u^* \end{bmatrix} \qquad (5.26)$$

By differentiating equation (5.20) and using equation (5.16) we get

$$\begin{bmatrix} \dot{x}^* \\ y_t^* \end{bmatrix} = \begin{bmatrix} S_{11} & 0 \\ 0 & I \end{bmatrix} \begin{bmatrix} \dot{x}_M \\ y_M \end{bmatrix} \qquad (5.27)$$

From equations (5.22), (5.26)

$$\begin{bmatrix} S_{11} & S_{12} \\ S_{21} & S_{22} \end{bmatrix} \begin{bmatrix} x_M \\ u_M \end{bmatrix} = \begin{bmatrix} A & B \\ H & 0 \end{bmatrix}^{-1} \begin{bmatrix} \dot{x}^* \\ y_t^* \end{bmatrix} \qquad (5.28)$$

Then using equations (5.25) & (5.27)

$$\begin{bmatrix} S_{11} & S_{12} \\ S_{21} & S_{22} \end{bmatrix} \begin{bmatrix} x_M \\ u_M \end{bmatrix} = \begin{bmatrix} A & B \\ H & 0 \end{bmatrix}^{-1} \begin{bmatrix} S_{11} & 0 \\ 0 & I \end{bmatrix} \begin{bmatrix} A_M & B_M \\ C_M & D_M \end{bmatrix} \begin{bmatrix} x_M \\ u_M \end{bmatrix}$$

If the model input, u_M, is tracked by the model output, y_M, then

$$y_M = u_M \qquad (5.29)$$

The reference model matrices will be

$$A_M = 0 \qquad (5.30)$$

$$B_M = 0$$

$$C_M = 0$$

$$D_M = I$$

This allows us to simplify equations (5.27)

$$S_{11} = 0 \qquad (5.31)$$

$$S_{12} = \Omega_{12}$$

$$S_{21} = 0$$

$$S_{22} = \Omega_{22}$$

Therefore from equation (5.22) the ideal state and input are given by

$$u^* = \Omega_{22} u_M \qquad (5.32)$$

$$x^* = \Omega_{12} u_M \qquad (5.33)$$

Computation of Ω_{12} & Ω_{22} depends upon A, B & H being composed of elements which are constant. As this cannot be relied upon, we can introduce some feedback to protect the performance should changes in the elements occur.

If we have a regulating feedback law

$$u_r = Fy \qquad (5.34)$$

then any non-zero output, y, will cause the control law to act until the output is zeroed. Because we are concerned with a tracking system, we expect the output to vary with the input, and so we wish the difference between the output, y, and the output demanded by the pilot, y^*, to be zero rather than the output itself. The feedback law is therefore

$$u_f = F [y - y^*] \qquad (5.35)$$

By taking into account the need for command following (by using the ideal input) and protection from changes in the coefficients of the system matrices (by using feedback), the necessary control law has to be

$$u = u_f + u^* \qquad (5.36)$$

By using equations (5.18), (5.32), (5.33) & (5.35)

$$u = F [y - y^*] + \Omega_{22} u_M \qquad (5.37)$$

$$u = F [y - Cx^*] + \Omega_{22} u_M \qquad (5.38)$$

$$u = F [y - C\Omega_{12} u_M] + \Omega_{22} u_M \qquad (5.39)$$

which results in

$$u = [\Omega_{22} - FC\Omega_{12}] u_M + Fy \qquad (5.40)$$

Another method of creating a compensator which causes the outputs to exactly track the inputs has been developed (O'Brien & Broussard, 1979). A constraint of this method was that only systems which had no transmission zeros at the origin were considered because it was necessary to ensure that the matrix Ω existed.

The method outlined above forms the third eigenstructure assignment method which will be used to form a controller design to improve the performance of the helicopter.

5.4 Design Example

The state space matrices A, B, C and D were generated from Helistab to give an 8th order rigid body model of a Lynx helicopter flying at 80 knots in straight and level flight. Heading, ψ, was not included as a state in the model used at the design condition. This is often the case because heading is not fully coupled with the other states and introduces an eigenvalue at the origin (making the A matrix singular). There may be effects on the stability of the controlled system if a controller is developed without heading and also

handling qualities define heading hold functions, therefore heading will be included in subsequent stages of development.

The pilot has four inceptors and we have chosen four output variables to be controlled. The outputs to be controlled were chosen as height rate, pitch attitude, roll attitude and yaw rate (h θ φ r). This combination may be seen from Appendix 2 to be one of the 29 acceptable sets. Due to the choice of output variables the system will be of an ACAH type. For the purpose of creating a decoupled tracking system each output is assigned to track one input (h to the first inceptor, θ to the second, φ to the third and r to the fourth) so that, for example, some input applied to the first inceptor will be tracked by h but there will be no coupling into the other three outputs θ, φ and r.

It was discovered that this choice of outputs gives two left half plane zeros at very low frequencies. Therefore of the eight assignable modes, two were assigned to cancel these zeros leaving six to be distributed over the four outputs.

The auto–eig subroutine listed in appendix 3 was used to calculate two control matrices, fb & ff, for different distributions of the modes across the outputs. Refer to figure 5.1a.

Using classical methods it was found that the best distribution (with respect to bandwidth and phase delay of closed loop system) was as follows:

output number	output controlled	number of modes	pole positions
1	h	1	-4.0
2	θ	2	-2.5 -4.5
3	φ	2	-5.5 -7.0
4	r	1	-5.0

5.5 Results at Design Condition

The gains of the controller matrices, fb & ff (fig. 5.2), are small and the specified

eigenstructure (fig. 5.3) has been achieved (with the eigenvalues at -0.0237 & -0.1080 and their eigenvectors cancelling the zeros & their directions).

A unit step function was applied to each input (fig. 5.4). Obviously, to apply a step demand of 1 radian is not realistic but as we are working with a linear model, the responses could easily be scaled down to a realistic value.
In each case the input is well tracked by the corresponding output and there is very little cross coupling into the other outputs. Any activity in other inputs (although in all cases the behaviour is stable, returning to steady state value) can be thought of as negligible as it is so small.

Tests involving step inputs applied to the controlled system (fig. 5.4) have shown that the outputs track the inputs well and there is very little coupling into other channels.

Input and Output Coupling

By normalising the columns of C*v and the rows of inv(v)*B, we have a numerical indication of the amount of coupling we can expect in the system fig. 5.5. (Smith, 1990).

From the first row of rownorm1 we see that the first mode, corresponding to eigenvalue of -0.0237, is predominantly coupled to the 2nd input. From the second row we see that the second mode, corresponding to eigenvalue of -0.1080, is coupled mainly to the 4th input but there is also a significant amount of coupling to the 3rd input. The other six modes have been assigned to the specified channels and perfectly decoupled from the others.

Similarly, by looking at the first column of colnorm1 we see that the first mode is mainly coupled to the 1st output but has a significant amount of coupling into the 4th output and some into the 3rd. The second mode, however, is coupled into the 1st output and fairly well decoupled from the others. Again, the other six modes have been assigned to the specified channels.

The information contained within colnorm1 & rownorm1 indicates that any cross-coupling

between inputs and outputs will be due to the first two modes, i.e. those assigned to cancel the zeros. For example, we would expect an input to the 2nd input to excite the modes with eigenvalues -0.0237, -2.5 & -4.5. These modes would result in responses in output2, but also, due to the coupling, in output1 and maybe a little in output3.

5.6 Additional Dynamics

The actuators of the main & tail rotors can be modelled as first order lags with time constants of 80 ms for the three main rotor actuators and 40 ms for the tail rotor actuator. These actuators can prevent us achieving a desired bandwidth because of the introduction of the lag which becomes an effective delay. Also, controller gains must be kept small in order to avoid exceeding actuator limits as this would decrease the degrees of freedom in the pilot's control inputs. Actuators were not included at the initial design stage because the actuator states are unobservable and full state feedback would therefore be impossible to implement.

5.7 Results including Actuator Dynamics and Heading,ψ

Using the same controller matrices, fb & ff, but having added heading and actuator dynamics to the model, inputs were applied in the same way as at the design condition.

Table 5.1 Bandwidth & Phase Delay Measurements

Including Actuator Dynamics and Heading

	Pitch	Roll	Yaw	
Bandwidth	5.5	7.3	4.17	rad/s
Phase Delay	0.041	0.028	0.025	seconds

Bandwidth and phase delay measurements were made by using a software toolbox from RAE (Howitt, 1991). The results are shown in Table 5.1. By comparing these bandwidth and phase delay measurements with handling qualities (fig. A4.11) we see that Level 1 performance would be obtained.

It is easily seen from the eigenstructure of this system that the addition of these dynamics has caused the position of the eigenvalues to move (fig. 5.6) and has also increased the coupling between the eigenvectors.

The time responses (fig. 5.7) now show that there is an increased level of coupling within the controlled system. The level of coupling has increased but the responses due to the coupling into the outputs still return to a steady state value. Although the step input on the third inceptor causes the third output to overshoot slightly, the inputs are still generally well tracked by the outputs.

Numerical Indication of Coupling

Even from a superficial look at rownorm2 & colnorm2 (fig. 5.8) it is clear that the coupling in the system has increased significantly. For instance, an input applied to the fourth input would excite the first, second and last modes (eigenvalues 0, -20.4 & -0.150). The mode at the origin is not coupled to any output. The mode at -20.4 is coupled to the fourth output with very little into each of the others. However, it can be seen from the last column of colnorm2 that the mode at -0.150 couples mainly into output 1 but also has a significant amount of coupling into output 4 and some into both 3 and 2. All of this information together would indicate that the cross-coupling in the controlled system has increased with the addition of heading and actuators to the model in such a way that an input to the 4th inceptor would cause some response, in varying degrees, to all of the outputs. Other inputs applied to other inceptors would be similarly affected by the increased level of coupling.

5.8 Results Including Actuator Dynamics, Heading & Rotor Dynamics

Six additional rotor states can be incorporated into the model to allow for second order rotor flapping dynamics. The addition of rotor dynamics causes an increase in coupling and can further restrict the bandwidth achieved.

Again, inputs were applied in the same manner as at the design condition but to the

system with heading, actuator and rotor dynamics added.

Table 5.2 Bandwidth & Phase Delay Measurements

Including Actuator Dynamics, Heading & Rotor Dynamics

	Pitch	Roll	Yaw	
Bandwidth	3	2	2	rad/s
Phase Delay	0.11	0.09	0.17	seconds

By comparing the bandwidth and phase delay measurements shown in Table 5.2 with handling qualities specifications (figs. 3.6 & 3.7) we see that Level 1 performance has been obtained.

The time responses (fig. 5.9) show another increase in the level of coupling between channels.

The effect of the additional dynamics can be seen in the extent of change of the eigenvalue positions of the system (fig. 5.10). With regard to changes in time responses, the character of the responses to step inputs is similar to the previous case. However, the transients due to cross coupling are slightly larger when inputs are applied to the first and second inceptors, but inputs are still well tracked by the corresponding output.

Numerical Indication of Coupling

By comparing rownorm3 and colnorm3 (fig. 5.11) to rownorm2 and colnorm2 (fig. 5.8), the changes in coupling due to the addition of rotors can be seen.

5.9 Additional Control Loop

In order to augment the performance of the inner loop containing the matrices fb and ff which were determined by this method, an outer loop was added which contained a proportional and integral controller as shown below.

Proportional and integral controllers can be useful in reducing steady state error and improving transient responses. They can also provide robust performance over a wide range of operating conditions such as we find in the helicopter. Figure 5.1b shows the structure of the control system modified to include an outer loop which incorporates proportional and integral control. This configuration introduces an extra control state, cont–x.

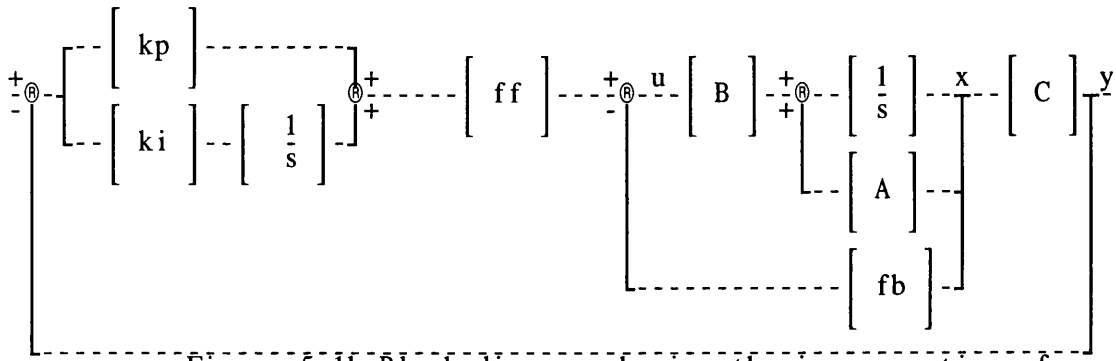

Figure 5.1b Block diagram showing the incorporation of proportional & integral control

The equations corresponding to Figure 5.1b are as follows:

$$\begin{aligned} \text{cont–x} &= ki(r - y) \\ &= ki(r - Cx) \\ &= kir - kiCx \end{aligned} \qquad (5.41)$$

$$\begin{aligned} x &= Ax + B(fft - fbx) \\ &= Ax + Bfft - Bfbx \\ &= Ax - Bfbx + Bff(kpPIINP + cont–x) \\ &= (A - Bfb)x + Bffcont–x + Bffkp(r - Cx) \\ &= (A - Bfb - BffkpC)x + Bffcont–x + Bffkpr \end{aligned} \qquad (5.42)$$

$$\begin{bmatrix} \dot{x} \\ \dot{cont–x} \end{bmatrix} = \begin{bmatrix} A-Bfb-BffkpC & Bff \\ -kiC & 0 \end{bmatrix} \begin{bmatrix} x \\ cont–x \end{bmatrix} + \begin{bmatrix} Bffkp \\ ki \end{bmatrix} r \qquad (5.43)$$

The diagonal coefficients in the kp and ki matrices were generated by classical methods.

$$ki = \begin{bmatrix} 1.8 & 0 & 0 & 0 \\ 0 & 0.8 & 0 & 0 \\ 0 & 0 & 1.5 & 0 \\ 0 & 0 & 0 & 2.8 \end{bmatrix} \qquad kp = \begin{bmatrix} 0.2 & 0 & 0 & 0 \\ 0 & 0.2 & 0 & 0 \\ 0 & 0 & 0.1 & 0 \\ 0 & 0 & 0 & 0.3 \end{bmatrix}$$

5.10 Results Including Heading, Actuator & Rotor Dynamics With P+I Control

The usual inputs were applied to the model with heading, actuator and rotor dynamics added to the system. In this case there were four controller matrices, fb, ff, kp & ki, as shown in Figure 5.1b.

Table 5.3 Bandwidth & Phase Delay Measurements

Including Heading, Actuator & Rotor Dynamics With P + I Control

	Pitch	Roll	Yaw	
Bandwidth	3	2	2	rad/s
Phase Delay	0.1	0.09	0.18	seconds

By comparing the bandwidth and phase delay results shown in Table 5.3 with handling qualities specifications we see that Level 1 performance has been maintained.

Numerical Indication Of Coupling

The new positions of the eigenvalues can be seen in fig. 5.12.

By comparing colnorm6 & rownorm6 with colnorm3 & rownorm3 we see the changes in the coupling between inputs and outputs.

It can be seen from the time responses (fig. 5.14) that many of the transients caused by cross coupling have been reduced. However, although the addition of P+I control has reduced it from around 11 degrees per sec, a step input applied to φ still gives a yawrate (r) of about 5 degrees per sec. In an attempt to reduce this transient, the off diagonal elements were used. kp(4,3) was set to 0.13. This resulted in the reduction of that transient. It is easily seen however that the addition of the proportional and integral controller has made the response more sluggish.

5.11 Performance of Controller With Change in Flight Condition

Having investigated the robustness of the controller to the addition of higher order dynamics we must now look at its robustness to changes in flight condition. Initially time responses were taken for the system with state space matrices at 50 knots (fig. 5.15) and then at 120

knots fig. 5.16 (heading, actuators and rotors were included) but the controller matrices (kp, ki, fb & ff) remained those designed for the 80 knots case. The character of the responses was shown to have changed quite considerably, particularly h. The inner loop matrices, fb & ff, were then scheduled at sixteen points across the range 50-120 knots forward level flight. The number of points at which the design must be performed across a range depends on the robustness of the design method. The resulting time responses (figs. 5.17 & 5.18) show a marked improvement and a return to the general character of those responses obtained at 80 knots.

A more thorough investigation of the changes within the system to change in flight condition was undertaken. Using the controller matrices fb & ff only, designed at the 80 knots flight condition,and replacing the 8th order, 80 knots helicopter model by 8th order models for forward flight conditions between hover and 160 knots at intervals of 5 knots, the position of the closed loop eigenvalues were plotted across the range (fig. 5.19).
This was repeated for the case where not only ff & fb were used but also ki & kp in the outer loop (fig. 5.20). The invariant zero positions of each model were found and were also plotted across the range (fig. 5.21). The movement of the eigenvalues which were designed to cancel these zeros was also plotted (figs. 5.22 & 5.23).

It can be seen from these results (figs. 5.21,22,23) that in the case with the outer loop containing the P+I controller, the poles assigned to cancel the zeros follow the movement of the zeros much more closely than in the case with only the inner loop containing ff & fb. It can also be seen by inspecting the numerical eigenstructure that the eigenvectors are closer to the zero directions when the outer loop is present.

In order to establish whether the addition of an outer control loop improved performance, another set of outputs was chosen to give a different zero configuration. This set was selected to give faster zeros and also states within the zero direction which were more evenly spread. This output set was [h θ Ω β] giving zeros at -0.0237 and -3.4295 $\pm$ 8.0075i.

Fig. 5.26 shows the movement of zeros associated with this set of outputs. Figs. 5.24 & 5.25 show the movement of the eigenvalues across the same range of flight conditions. In both cases (in keeping with the zeros shown in fig. 5.26) we see movement of eigenvalues into the right half plane. However, where the system has been augmented by the outer loop, the system remains stable across a larger range of flight conditions before crosssing into the right half plane and does not penetrate as far right as the system without the P+I control loop.

Also, by close inspection of the eigenstructure of the cancelling eigenvalues, it can be seen that again in the case of the two loop structure, the eigenstructure cancels the zerostructure much more effectively.

These results (figs. 5.24,25,26) also indicate that the system remains stable for longer and that the zeros are cancelled more effectively.
In case this property was specific to matrices designed at the flight condition of 80 knots, exactly the same procedure was followed for controller matrices designed at flight conditions of 40 knots forward, level flight and at hover for the output set [h θ φ r]. These demonstrated the same properties.

5.12 Investigations with the Non-linear Model

Having obtained a satisfactory reponse from the controlled linear system, the same scheduled controller was used with a non-linear helicopter model, Helisim. The model was trimmed at 80 knots. For small inputs the results were found to be similar to those obtained from the linear model.

A doublet (of amplitude 7.5 degrees) was applied to θ so that the speed, VTKT, would vary across the range of the scheduled controller (50-120 knots). The results are in fig. 5.27.

The shape of the height rate response is in keeping with that of the linear model (fig.

5.14) but the transient is far greater (reaching 3.5 ft/sec). The effect of the doublet switching between different states is clearly seen in the height rate response. The φ response is trimmed at 1.1 degrees and has maximum transient of 3 degrees. The r response has maximum transient of 2.3 degrees/sec. All responses are stable and return to a steady state condition.

It can be concluded from these results that the controller which gave good performance with the linear helicopter model, has also performed well with the non-linear model and that it has done so over the full range for which the inner loop controller was scheduled.

References

Howitt, J

A Software "Toolbox" for Handling Qualities Analysis of Combat Helicopters

RAE (Bedford) 1991.

Hughes, G, Manness, M A & Murray-Smith, D J

Eigenstructure Assignment for Handling Qualities in Helicopter Flight Control Law Design

16th European Rotorcraft Forum

paper III.10.2, 1990

MacFarlane, A G J & Karcanias, N

Poles and Zeros of Linear Multivariable Systems: A Survey of the Algebraic, Geometric and Complex-variable Theory

Int Journal Control, vol. 24, no. 1, pp 33 - 74, 1976.

O'Brien, M J & Broussard J R

Feedforward Control To Track the Output of a Forced Model

Proc. 17th IEEE Conference on Decision & Control, San Diego,1978

pp 1149 - 1155.

Smith, P R

Input/Output Coupling in Eigenstructure Assignment

RAE (Bedford), UK

HMSO, London, 1990.

Sobel, K M & Shapiro, E Y

A Design Methodology for Pitch Pointing Flight Control Systems

J. Guidance, Control & Dynamics

Vol. 8 N0.2

pp 181 - 187, 1985

TSIM

Non-Linear Simulation Package

Cambridge Control Ltd, Cambridge.

Wilkinson, J H

The Algebraic Eigenvalue Problem

Oxford University Press, Oxford, 1965.

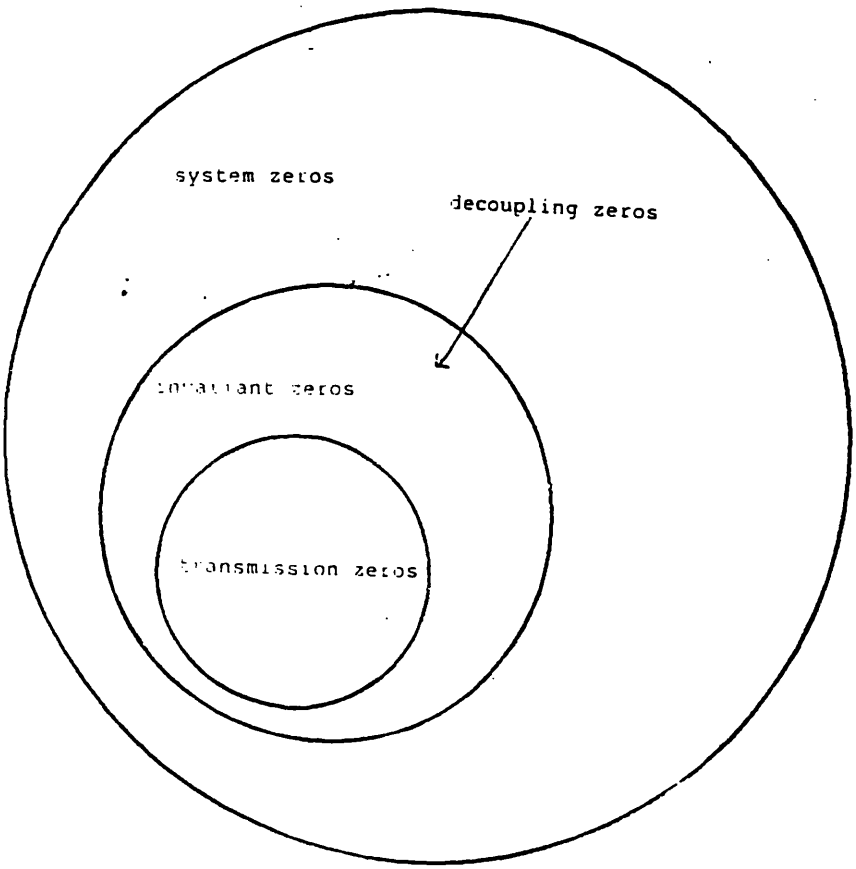

Figure 5.1 Relationship Between Different Types of Zeros

Results Of Design

Feedback Matrix,fb

fb =

0.0006	-0.0307	-0.0453	1.4632
0.0007	0.0141	0.1804	-0.2572
0.0003	-0.0101	-0.0255	0.3420
0.0013	-0.0134	-0.0313	0.7067
0.0012	0.0006	0.0120	-0.0002
0.0000	0.0109	-0.0558	0.0028
0.0014	-0.0155	-0.2430	0.0021
-0.0067	0.1191	0.3382	-0.2063

Feedforward matrix,ff

ff =

0.0382	-0.1100	0.0131	0.0020
-0.0167	0.4297	-0.0563	-0.0058
0.0106	-0.0925	-0.2427	0.0045
0.0193	-0.0893	0.3888	-0.2799

Figure 5.2 Components of Gain in Controller Matrices

Eigenvalues Of Controlled System At The Design Condition

-0.0237
-0.1080
-4.0000
-7.0000
-5.0000
-2.5000
-5.5000
-4.5000

Eigenvectors Of The Controlled System At The Design Condition

0.9998	-0.0017	0.0759	0.0003
0.0214	-0.0329	-0.9969	-0.0106
0.0000	0.0000	0.0000	0.0000
0.0000	0.0000	0.0000	0.0000
-0.0043	-0.9995	0.0199	-0.1997
0.0000	0.0000	0.0000	-0.9700
0.0000	0.0000	0.0000	0.1386
0.0000	0.0000	0.0000	0.0000
0.0007	0.0959	0.0003	0.0681
0.0326	0.9931	-0.0143	0.9914
-0.0041	-0.0601	0.0000	-0.1081
0.0000	0.0240	0.0000	0.0240
0.9918	0.0176	-0.2813	0.0131
-0.0027	0.0000	-0.9440	-0.0001
0.0000	0.0000	0.1716	0.0000
0.1235	0.0000	0.0000	0.0000

Figure 5.3 Eigenstructure of Controlled System At Design Condition

Time Responses To A Step Input On Each Inceptor

At Design Condition Using fb & ff With The 8th Order Helistab Model

Step Applied To First Inceptor

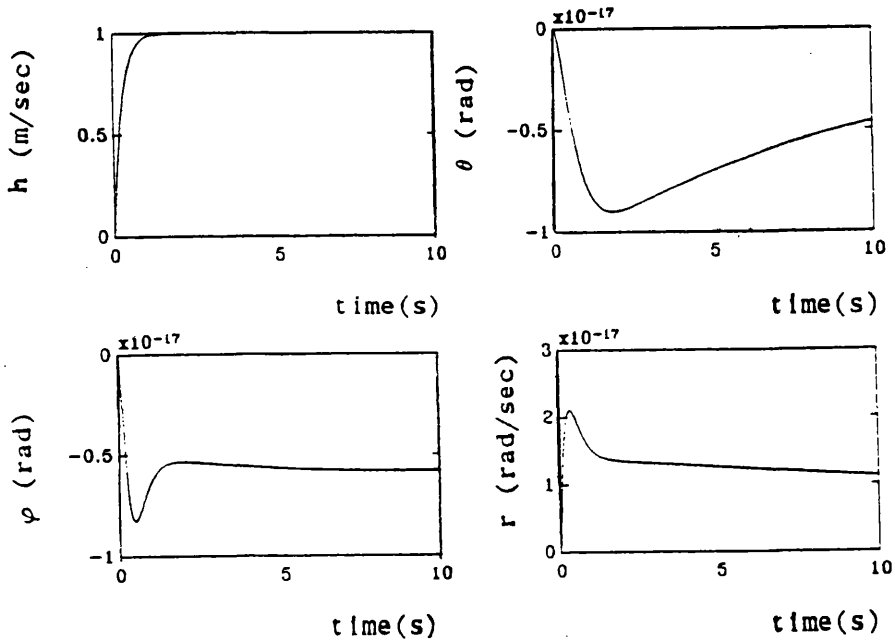

Step Applied To Second Inceptor

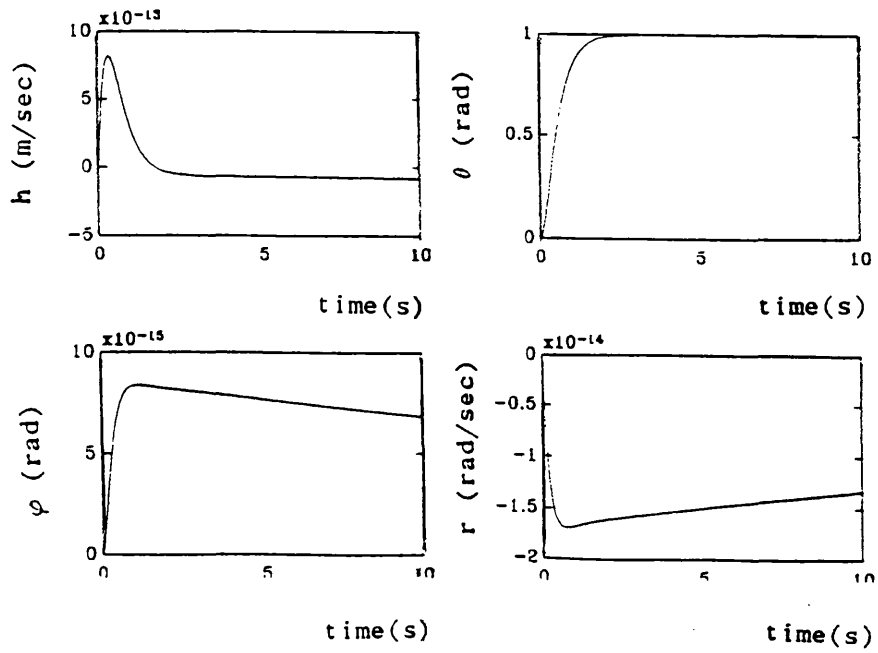

Figure 5.4

Step Applied To Third Inceptor

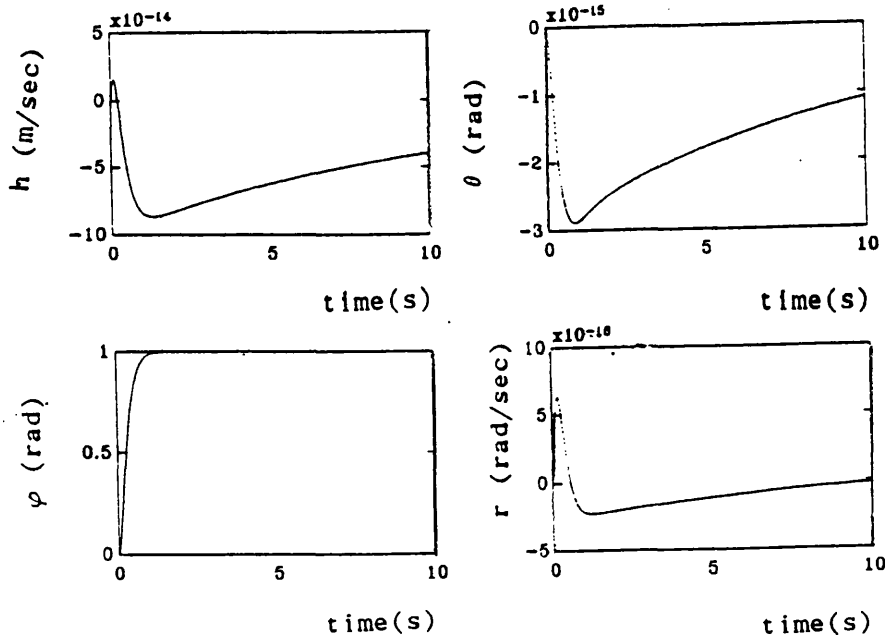

Step Applied To Fourth Inceptor

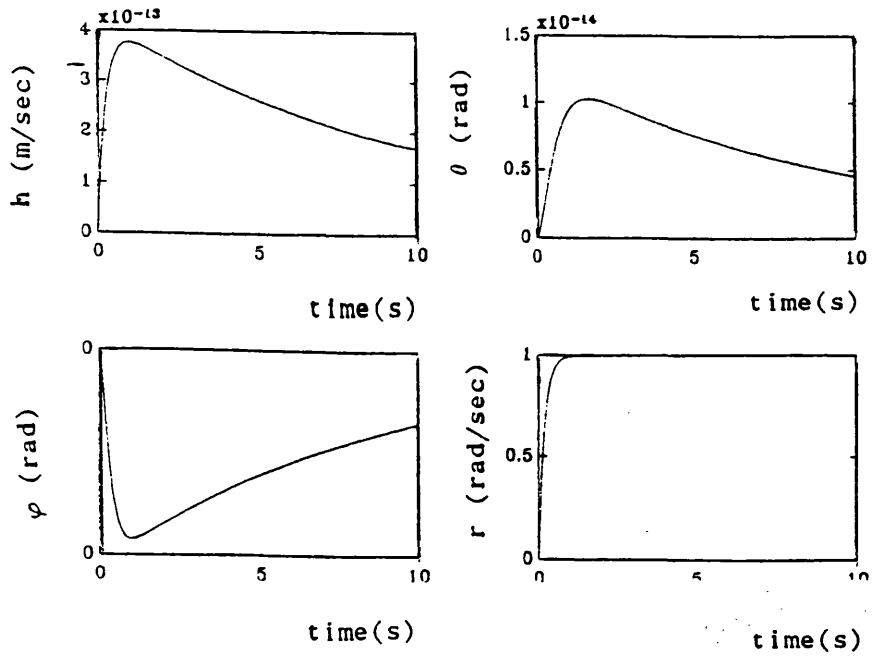

Input And Output Coupling

rownorm1 =

-0.0010	1.0000	0.0015	-0.0100
-0.0008	0.0392	-0.2392	1.0000
1.0000	0.0000	0.0000	0.0000
0.0000	0.0000	1.0000	0.0000
0.0000	0.0000	0.0000	1.0000
0.0000	1.0000	0.0000	0.0000
0.0000	0.0000	1.0000	0.0000
0.0000	1.0000	0.0000	0.0000

colnorm1 =

1.0000	1.0000	1.0000	0.0000
-0.0081	0.0283	0.0000	0.0000
0.1255	-0.0119	0.0000	1.0000
-0.2404	0.0038	0.0000	0.0000
0.0000	0.0000	0.0000	0.0000
0.0000	1.0000	0.0000	1.0000
0.0000	0.0000	1.0000	0.0000
1.0000	0.0000	0.0000	0.0000

Figure 5.5 Input & Output Coupling of Controlled System at the Design Condition

Eigenvalues Of System Controlled By ff & fb

(heading & actuator dynamics included

```
         0
-20.3834
-13.2791
  -6.3405 + 3.8391i
  -6.3405 - 3.8391i
  -4.1622 + 4.0262i
  -4.1622 - 4.0262i
  -6.7079 + 1.6879i
  -6.7079 - 1.6879i
  -7.1443
  -0.0236
  -2.6054
  -0.1050
```

Figure 5.6

Response Of System (including heading & actuator dynamics)When Controlled By ff & fb

Time Responses To A Step Input On Each Inceptor

Step Applied To First Inceptor

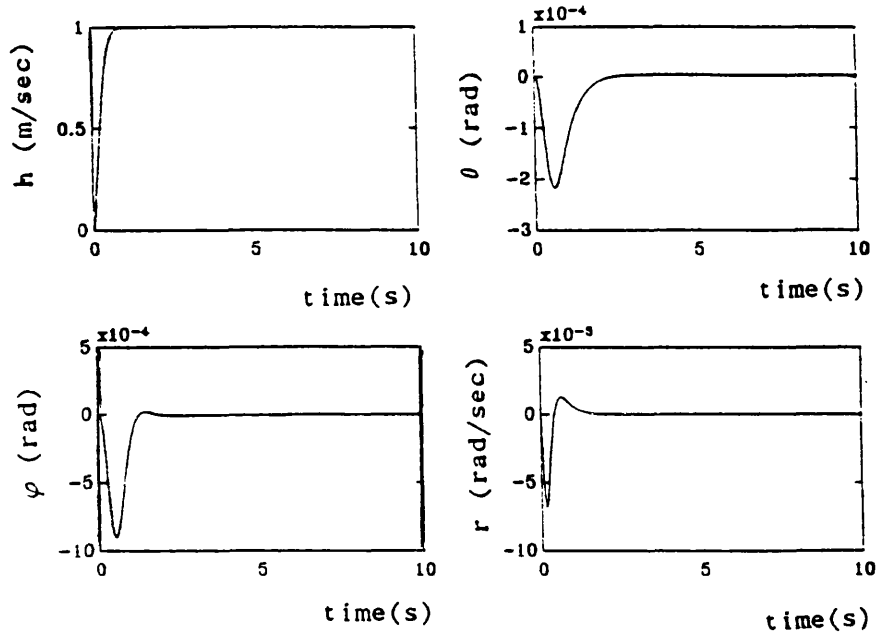

Step Applied To Second Inceptor

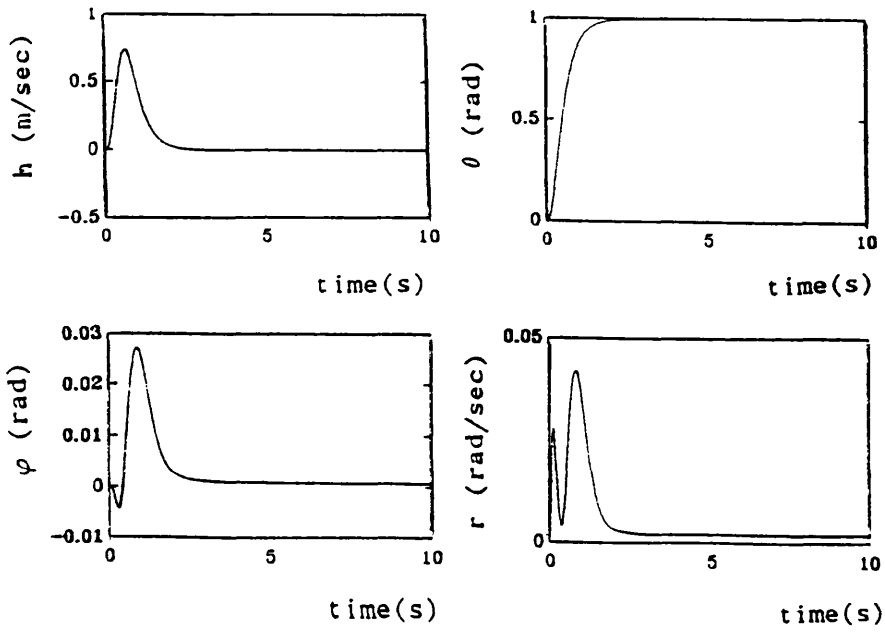

Figure 5.7

Step Applied To Third Inceptor

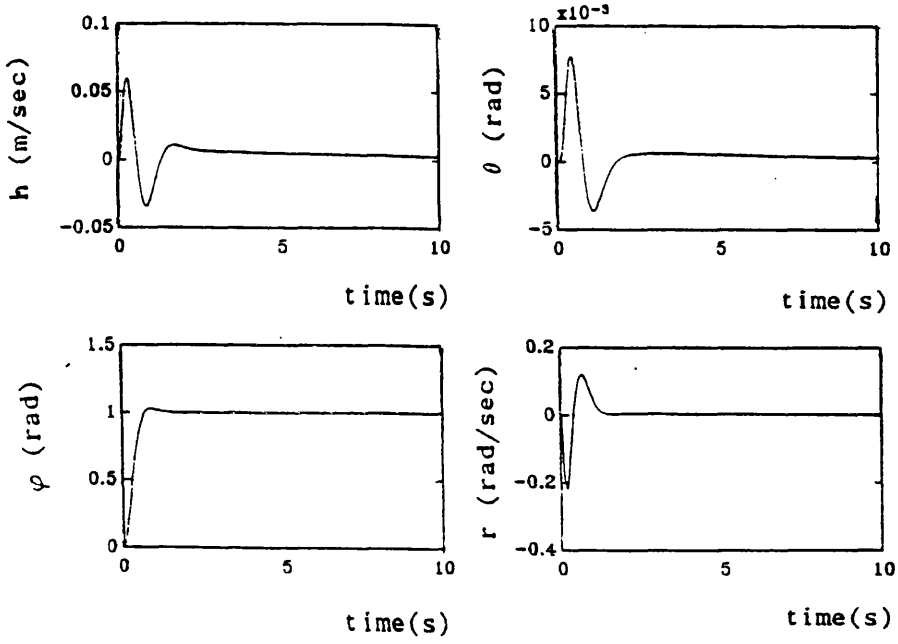

Step Applied To Fourth Inceptor

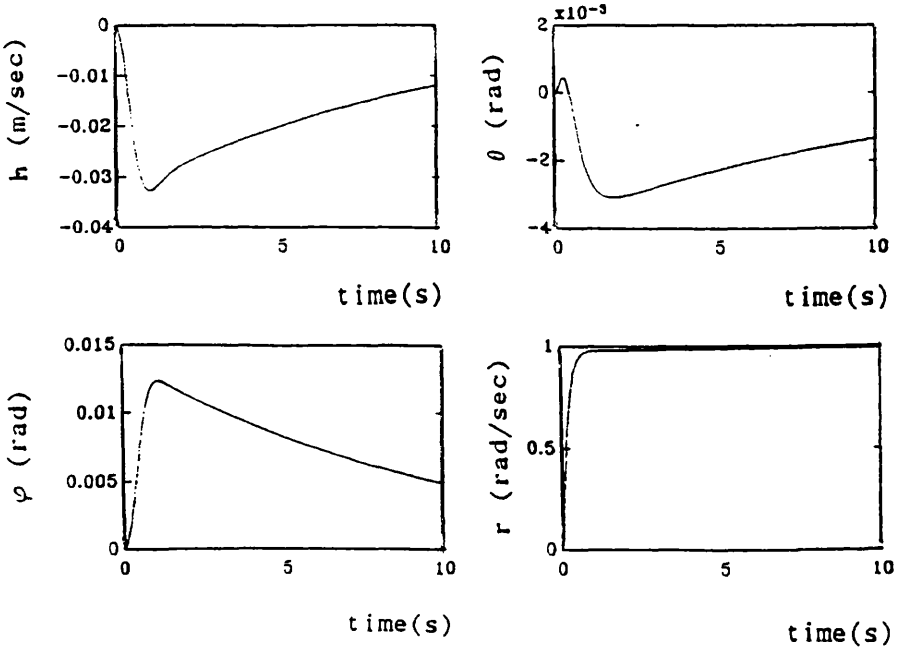

ut And Output Coupling

wnorm2 =

0.0000 - 0.0000i	0.0000 - 0.0000i	0.0000 - 0.0000i	1.0000
-0.0702 - 0.0000i	0.3542 + 0.0000i	-0.0465 + 0.0000i	1.0000
0.0145 - 0.0000i	0.1758 - 0.0000i	1.0000	-0.0793 + 0.0000i
-0.0168 + 0.0052i	1.0000	0.4841 - 0.0900i	-0.0206 - 0.0061i
-0.0168 - 0.0052i	1.0000	0.4841 + 0.0900i	-0.0206 + 0.0061i
-0.0061 - 0.0045i	0.0579 - 0.4319i	1.0000	0.0046 - 0.0188i
-0.0061 + 0.0045i	0.0579 + 0.4319i	1.0000	0.0046 + 0.0188i
0.0639 - 0.0117i	1.0000	0.5179 - 0.0978i	-0.0301 - 0.0207i
0.0639 + 0.0117i	1.0000	0.5179 + 0.0978i	-0.0301 + 0.0207i
0.0777 - 0.0000i	1.0000	0.9251 - 0.0000i	-0.1736 + 0.0000i
-0.0010 - 0.0000i	1.0000	0.0013 - 0.0000i	-0.0090 + 0.0000i
0.0012 - 0.0000i	1.0000	0.0427 + 0.0000i	-0.0061 - 0.0000i
-0.0007 - 0.0000i	0.0391 - 0.0000i	-0.2392 - 0.0000i	1.0000

norm2 =

0	-0.0312	0.4898	1.0000
0	-0.0007	-0.0240	0.0350 - 0.0103i
0	-0.0154	0.2214	-0.0277 + 0.0049i
0	1.0000	1.0000	0.0681 + 0.0166i

1.0000	1.0000	1.0000	1.0000
0.0350 + 0.0103i	0.0524 + 0.0614i	0.0524 - 0.0614i	-0.0099 + 0.0039i
-0.0277 - 0.0049i	-0.3084 + 0.3417i	-0.3084 - 0.3417i	0.0246 - 0.0125i
0.0681 - 0.0166i	-0.0534 + 0.6272i	-0.0534 - 0.6272i	0.1223 - 0.2027i

1.0000	0.6835	1.0000	1.0000
-0.0099 - 0.0039i	-0.0183	0.3766	-0.2580
0.0246 + 0.0125i	0.0715	-0.1246	0.0505
0.1223 + 0.2027i	1.0000	-0.5217	0.0371

1.0000
0.1137
-0.4098
0.7269

Figure 5.8 Input & Output Coupling of Controlled System with Heading & Actuators

When Controlled By ff & fb

Time Responses To A Step Input On Each Inceptor

Step Applied To First Inceptor

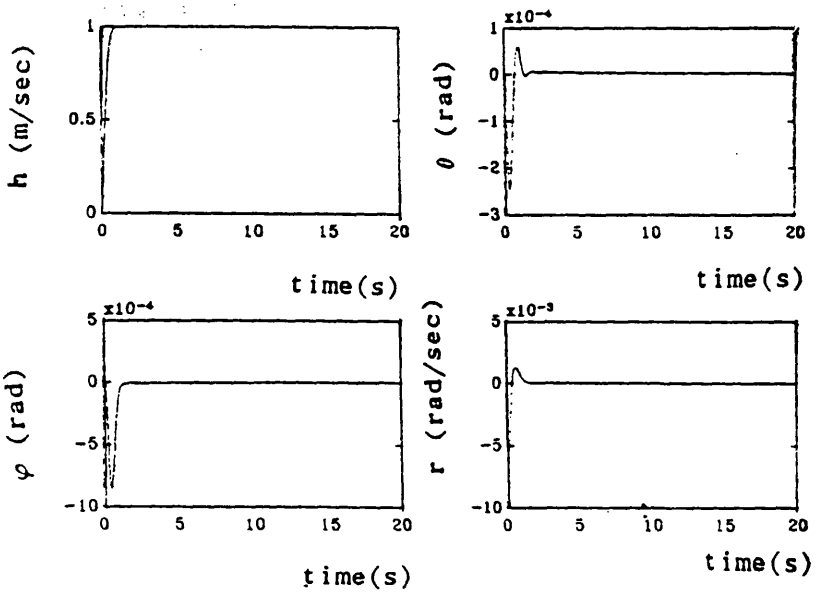

Step Applied To Second Inceptor

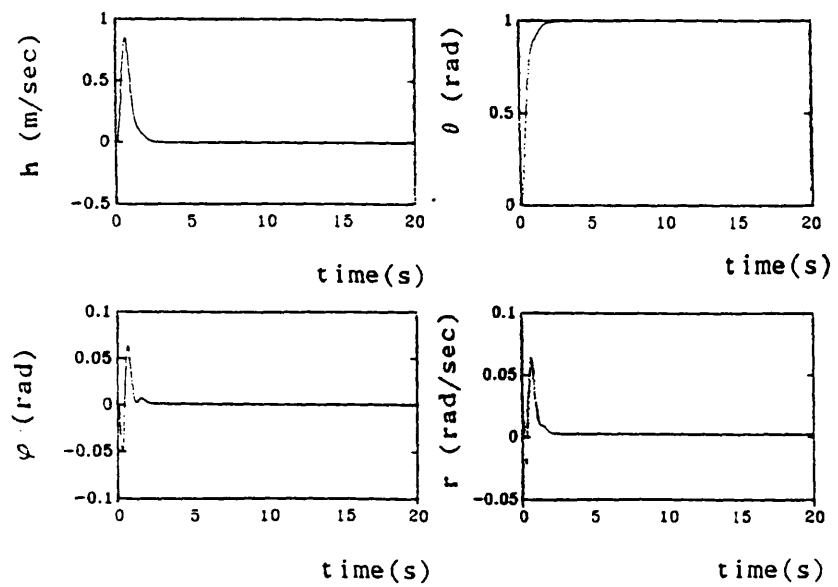

Figure 5.9

Step Applied To Third Inceptor

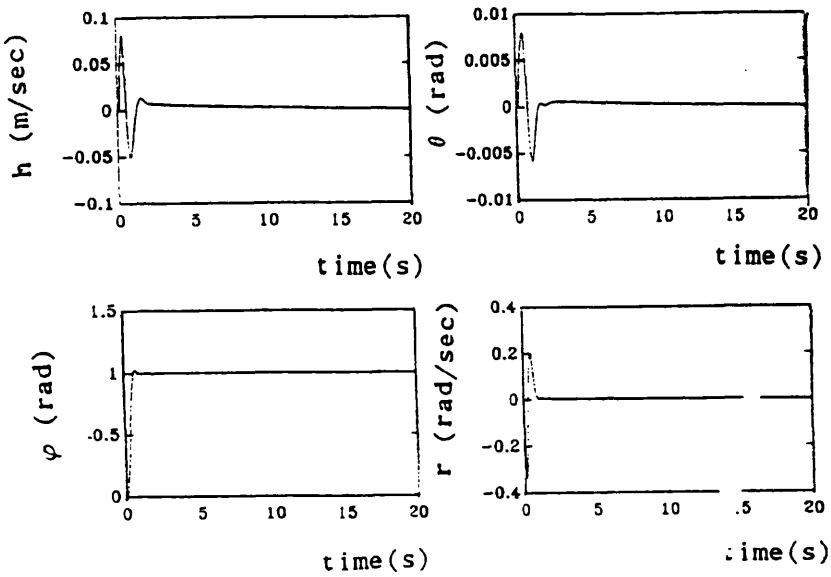

Step Applied To Fourth Inceptor

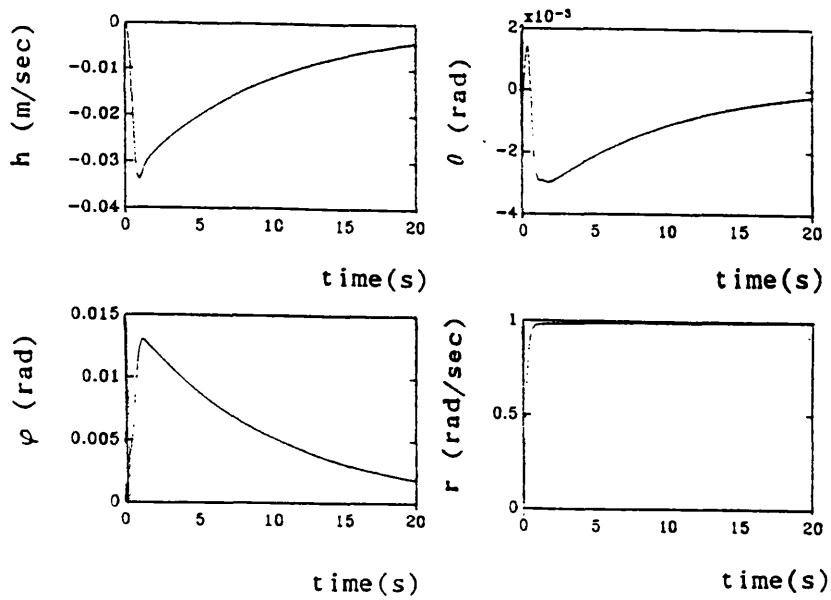

Eigenvalues Of System Controlled By ff & fb

(heading,actuator & 2nd order rotor dynamics included)

```
         0
-15.5976 +69.6525i
-15.5976 -69.6525i
-15.8487 +35.3651i
-15.8487 -35.3651i
-19.6813 + 0.1328i
-19.6813 - 0.1328i
-11.2648
 -5.5107 + 7.6320i
 -5.5107 - 7.6320i
 -3.2217 + 6.2652i
 -3.2217 - 6.2652i
 -7.0592 + 3.0618i
 -7.0592 - 3.0618i
 -6.5251 + 1.3654i
 -6.5251 - 1.3654i
 -0.0236
 -2.3251
 -0.1051
```

Figure 5.10

vnorm3 =

0.0000 - 0.0000i	0.0017 - 0.0000i	0.0000 - 0.0000i	1.0000
-0.0077 - 0.0086i	1.0000	0.0135 + 0.6289i	-0.0163 - 0.0086i
-0.0077 + 0.0086i	1.0000	0.0135 - 0.6289i	-0.0163 + 0.0086i
1.0000	0.1502 - 0.3925i	0.6281 + 0.3888i	0.0041 + 0.0006i
1.0000	0.1502 + 0.3925i	0.6281 - 0.3888i	0.0041 - 0.0006i
0.0135 + 0.0119i	1.0000	0.5219 + 0.3888i	-0.1330 - 0.1559i
0.0135 - 0.0119i	1.0000	0.5219 - 0.3888i	-0.1330 + 0.1559i
0.0208 + 0.0000i	0.1901 + 0.0000i	1.0000	-0.0797 + 0.0000i
-0.0038 + 0.0033i	-0.0598 - 0.2714i	1.0000	-0.0208 - 0.0095i
-0.0038 - 0.0033i	-0.0598 + 0.2714i	1.0000	-0.0208 + 0.0095i
0.0015 - 0.0019i	1.0000	-0.0296 + 0.2496i	-0.0073 + 0.0054i
0.0015 + 0.0019i	1.0000	-0.0296 - 0.2496i	-0.0073 - 0.0054i
-0.0475 + 0.0502i	-0.1337 + 0.0244i	1.0000	-0.0474 - 0.0573i
-0.0475 - 0.0502i	-0.1337 - 0.0244i	1.0000	-0.0474 + 0.0573i
0.0708 + 0.0135i	0.3174 + 0.0285i	1.0000	-0.0507 - 0.1268i
0.0708 - 0.0135i	0.3174 - 0.0285i	1.0000	-0.0507 + 0.1268i
-0.0010 - 0.0000i	1.0000	0.0012 - 0.0000i	-0.0086 - 0.0000i
0.0000 - 0.0000i	1.0000	0.0287 - 0.0000i	-0.0048 - 0.0000i
-0.0008 - 0.0000i	0.0391 - 0.0000i	-0.2392 - 0.0000i	1.0000

olnorm3 =

0	0.0163 + 0.0492i	0.0163 - 0.0492i	-0.0329 + 0.0687i
0	0.0135 + 0.0014i	0.0135 - 0.0014i	-0.0267 + 0.0221i
0	-0.0075 + 0.0796i	-0.0075 - 0.0796i	-0.0989 + 0.1652i
0	1.0000	1.0000	1.0000

-0.0329 - 0.0687i	-0.0280 - 0.0245i	-0.0280 + 0.0245i	0.8400
-0.0267 - 0.0221i	0.0028 + 0.0073i	0.0028 - 0.0073i	-0.0288
-0.0989 - 0.1652i	0.0031 - 0.0002i	0.0031 + 0.0002i	0.2617
1.0000	1.0000	1.0000	1.0000

0.1975 - 0.7293i	0.1975 + 0.7293i	1.0000	1.0000
-0.0578 - 0.0197i	-0.0578 + 0.0197i	0.2294 + 0.0030i	0.2294 - 0.0030i
0.6079 + 0.5589i	0.6079 - 0.5589i	0.0693 - 0.1889i	0.0693 + 0.1889i
1.0000	1.0000	-0.0152 - 0.0884i	-0.0152 + 0.0884i

1.0000	1.0000	1.0000	1.0000
0.0029 - 0.0076i	0.0029 + 0.0076i	-0.0074 + 0.0057i	-0.0074 - 0.0057i
-0.0265 + 0.0833i	-0.0265 - 0.0833i	0.0874 - 0.0609i	0.0874 + 0.0609i
0.1534 + 0.1153i	0.1534 - 0.1153i	0.0575 - 0.4714i	0.0575 + 0.4714i

1.0000	1.0000	1.0000
0.3803	-0.3205	0.1194
0.0969	0.0359	-0.4334
0.1934	0.0401	0.6906

Figure 5.11 Input & Output Coupling of Controlled System with Heading, Actuators & Rotors

Eigenvalues Of System Controlled By ff,fb,kp & ki

(heading, actuator & rotor dynamics included)

```
        0
-15.5966 +69.6528i
-15.5966 -69.6528i
-15.8485 +35.3652i
-15.8485 -35.3652i
-19.7014
-17.7778
-12.2252
 -6.6759 + 7.1727i
 -6.6759 - 7.1727i
 -3.0206 + 6.0067i
 -3.0206 - 6.0067i
 -3.7764 + 2.9954i
 -3.7764 - 2.9954i
 -4.6013 + 1.8446i
 -4.6013 - 1.8446i
 -3.2862
 -2.8868 + 1.1647i
 -2.8868 - 1.1647i
 -1.3363 + 0.5029i
 -1.3363 - 0.5029i
 -0.0237
 -0.1081
```

Figure 5.12

```
)rm6 =

 .0000 + 0.0000i   0.0000 + 0.0000i   0.0000 + 0.0000i   1.0000
 .0082 - 0.0080i   1.0000             0.0445 + 0.2991i  -0.0253 - 0.0110i
 .0082 + 0.0080i   1.0000             0.0445 - 0.2991i  -0.0253 + 0.0110i
 .0000             0.2090 - 0.3782i   0.3357 + 0.1393i   0.0061 + 0.0008i
 .0000             0.2090 + 0.3782i   0.3357 - 0.1393i   0.0061 - 0.0008i
 .0032 + 0.0000i   1.0000             0.0222 + 0.0000i  -0.0168 - 0.0000i
 .0583 + 0.0000i  -0.6994 - 0.0000i   0.5836 - 0.0000i   1.0000
 .0270 - 0.0000i  -0.7658 - 0.0000i   1.0000             0.1914 + 0.0000i
 .0088 + 0.0058i   0.2551 - 0.1073i   1.0000            -0.0501 - 0.0685i
 .0088 - 0.0058i   0.2551 + 0.1073i   1.0000            -0.0501 + 0.0685i
 .0004 - 0.0042i   1.0000             0.3155 + 0.1429i  -0.0155 + 0.0182i
 .0004 + 0.0042i   1.0000             0.3155 - 0.1429i  -0.0155 - 0.0182i
 .0038 - 0.0237i   0.0681 + 0.0623i   1.0000             0.1314 - 0.1302i
 .0038 + 0.0237i   0.0681 - 0.0623i   1.0000             0.1314 + 0.1302i
 .0035 - 0.2402i   0.4949 + 0.1371i   1.0000            -0.0358 - 0.3846i
 .0035 + 0.2402i   0.4949 - 0.1371i   1.0000            -0.0358 + 0.3846i
 .3943 - 0.0000i  -0.3293 + 0.0000i   1.0000            -0.4041 - 0.0000i
 .0220 + 0.0054i   0.0245 + 0.0901i   1.0000            -0.0619 + 0.1479i
 .0220 - 0.0054i   0.0245 - 0.0901i   1.0000            -0.0619 - 0.1479i
 .0003 + 0.0001i   1.0000            -0.0020 + 0.0337i   0.0131 - 0.0123i
 .0003 - 0.0001i   1.0000            -0.0020 - 0.0337i   0.0131 + 0.0123i
 .0010 + 0.0000i   1.0000             0.0015 - 0.0000i  -0.0098 + 0.0000i
 .0008 + 0.0000i   0.0414 + 0.0000i  -0.2437 + 0.0000i   1.0000

norm6 =

    0
    0                0.0162 + 0.0489i   0.0162 - 0.0489i  -0.0319 + 0.0675i
    0                0.0134 + 0.0014i   0.0134 - 0.0014i  -0.0258 + 0.0218i
    0               -0.0073 + 0.0790i  -0.0073 - 0.0790i  -0.0946 + 0.1621i
    0                1.0000             1.0000             1.0000

 .0319 - 0.0675i   -0.3281             -0.0003             0.4511
 .0258 - 0.0218i    0.0953             -0.0037            -0.0222
 .0946 - 0.1621i    0.0027              0.0099             0.1780
 .0000              1.0000              1.0000             1.0000

 .4992 - 0.6203i   0.4992 + 0.6203i    1.0000             1.0000
 .0372 - 0.0238i  -0.0372 + 0.0238i    0.1702 + 0.0238i   0.1702 - 0.0238i
 .3978 + 0.4169i   0.3978 - 0.4169i    0.1527 - 0.0900i   0.1527 + 0.0900i
 .0000             1.0000              0.0878 - 0.1524i   0.0878 + 0.1524i

 .0000             1.0000             1.0000
 .0155 + 0.0126i   0.0155 - 0.0126i   0.0034 + 0.0021i   1.0000
 .1593 - 0.1162i  -0.1593 + 0.1162i  -0.0328 - 0.0178i   0.0034 - 0.0021i
 .2271 + 0.5089i  -0.2271 - 0.5089i  -0.0832 + 0.0111i  -0.0328 + 0.0178i
                                                        -0.0832 - 0.0111i

 .0000             1.0000             1.0000
 .0025            -0.0132 - 0.0095i   -0.0132 + 0.0095i  1.0000
 .0286             0.2302 - 0.2340i    0.2302 - 0.2340i  0.1787 - 0.4485i
 .0325            -0.4339 + 0.4860i   -0.4339 - 0.4860i  0.0366 - 0.0013i
                                                        0.0275 + 0.0021i

 .0000             1.0000             1.0000
 .1787 + 0.4485i   0.8595             0.2814
 .0366 + 0.0013i   0.1141            -0.5149
 .0275 - 0.0021i  -0.1222             0.4293
```

Figure 5.13 Input & Output Coupling of Controlled System (including P + I Controller)

Response Of System (including heading, actuator & rotor dynamics)

When Controlled By ff, fb, kp & ki

Time Responses To A Step Input On Each Inceptor

Step Applied To First Inceptor

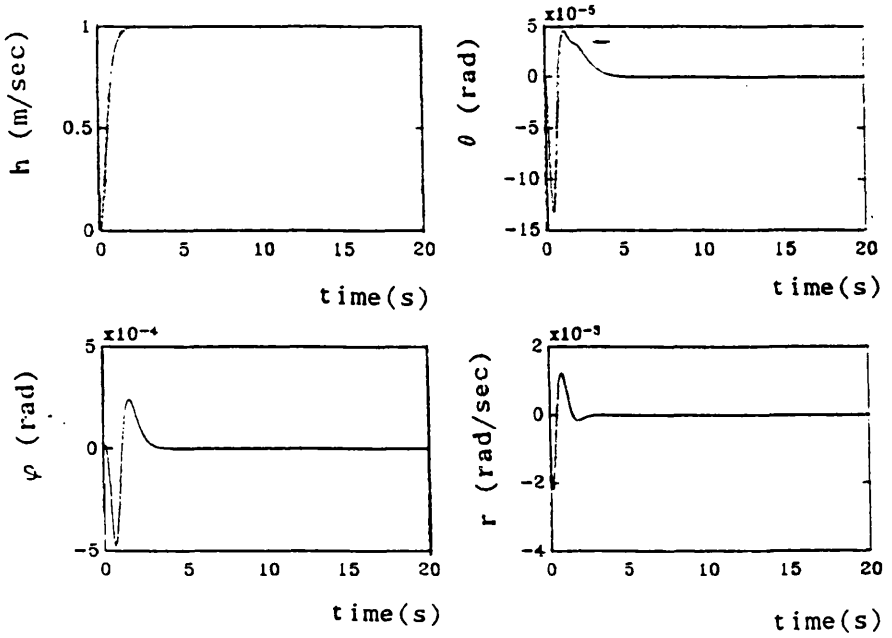

Step Applied To Second Inceptor

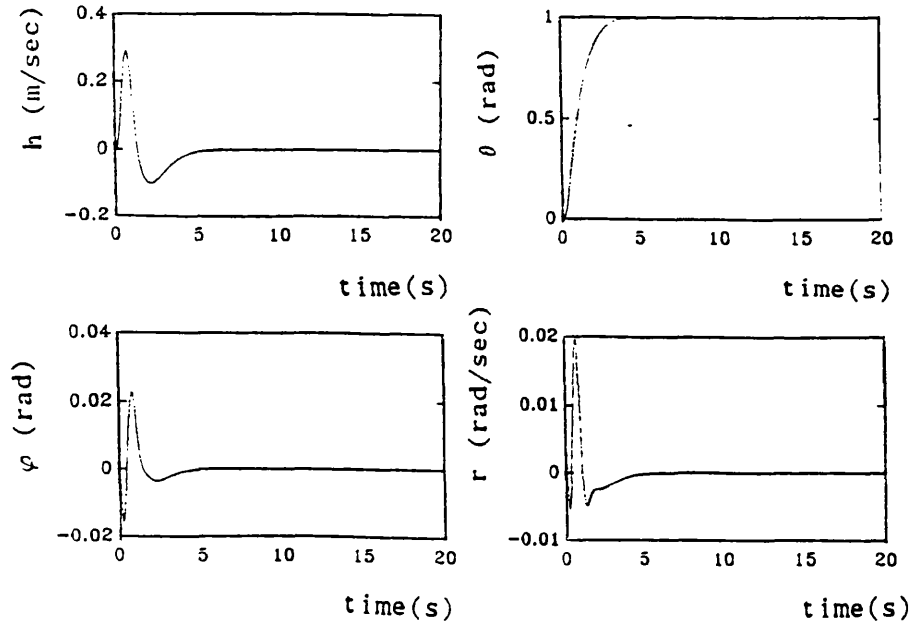

Figure 5.14

Step Applied To Third Inceptor

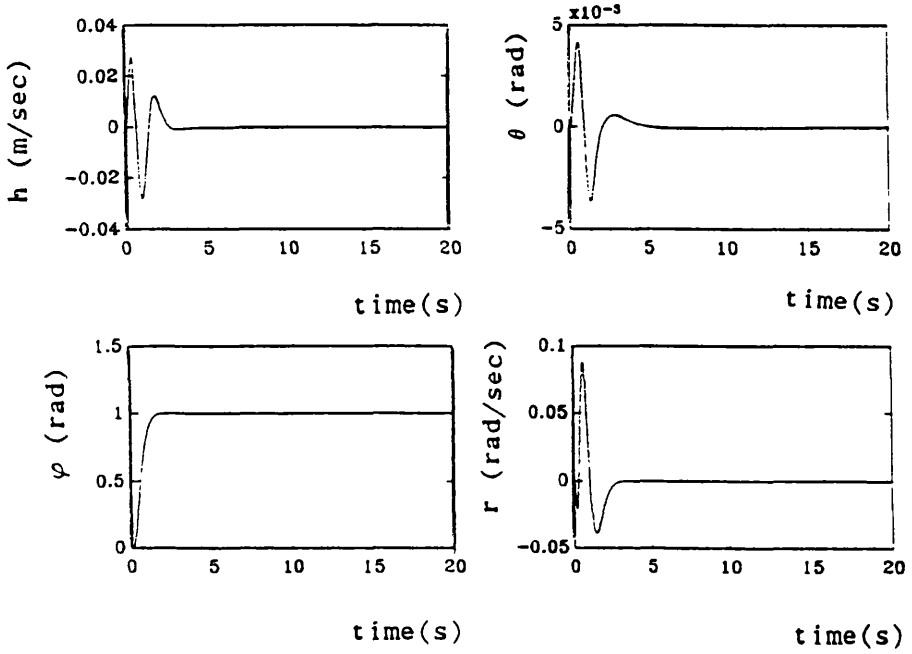

Step Applied To Fourth Inceptor

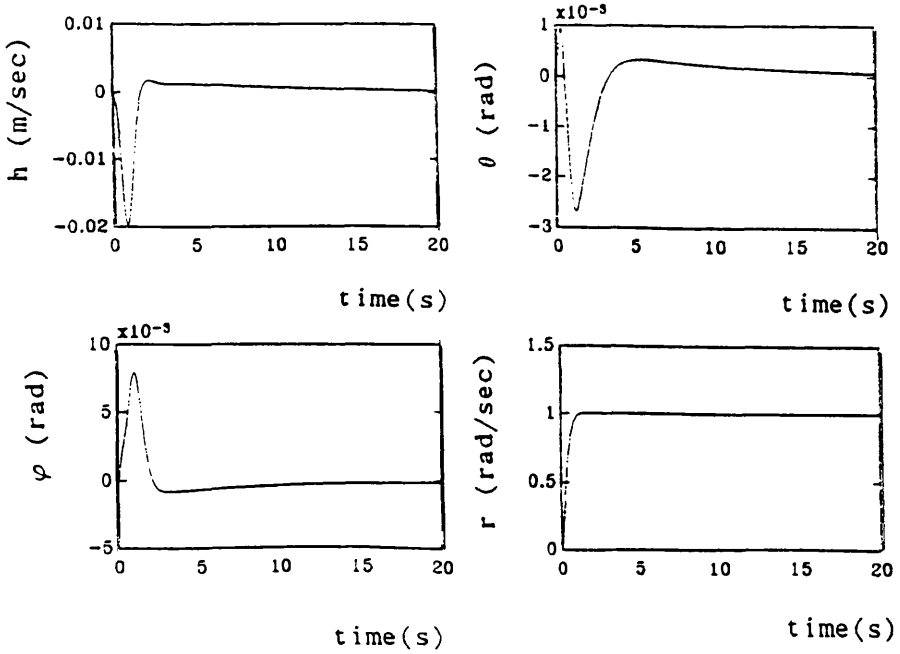

Response Of 50 knots System (including heading, actuator & rotor dynamics) When Controlled by ff,fb,kp & ki Designed At 80 knots Flight Condition

Time Responses To A Step Input On Each Inceptor

Step Applied To First Inceptor

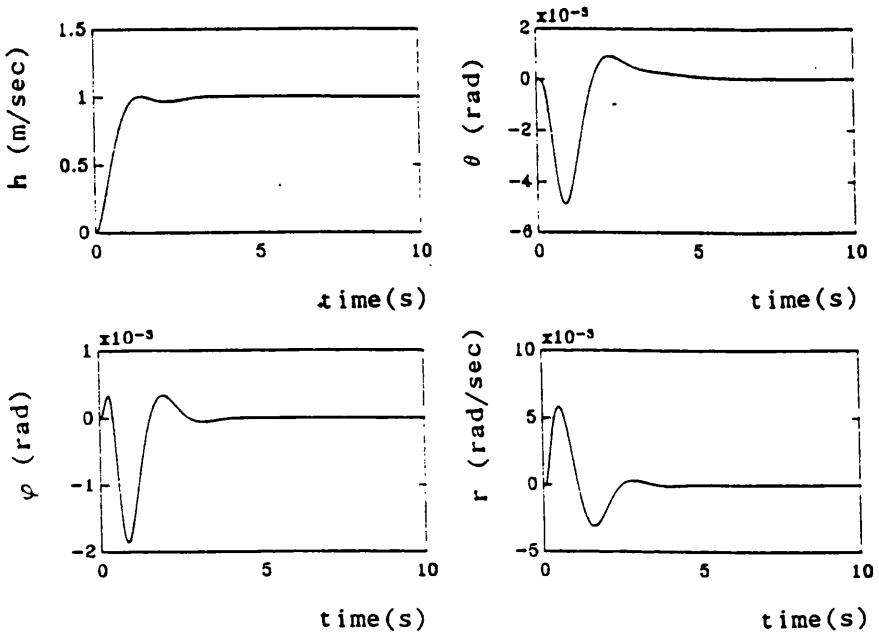

Step Applied To Second Inceptor

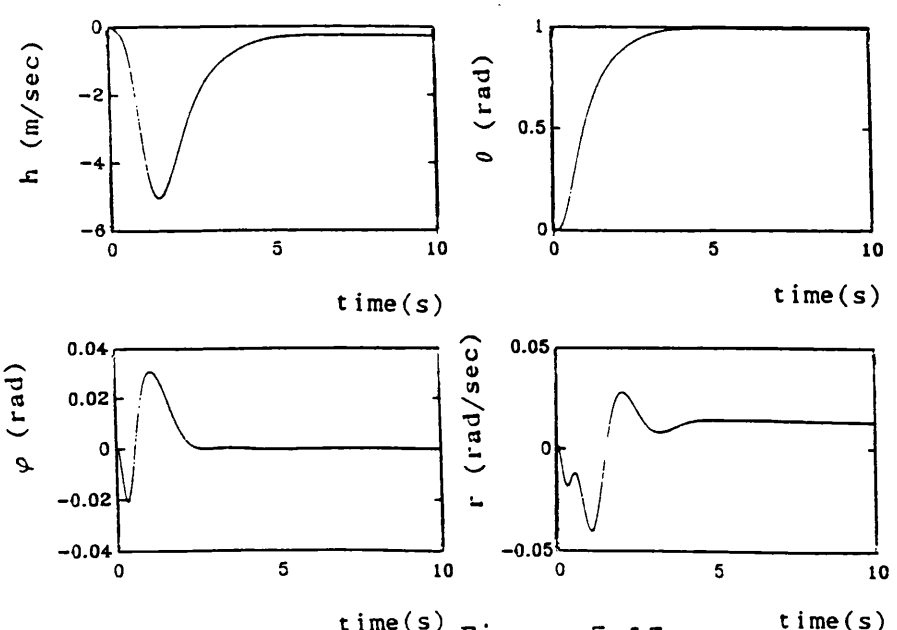

Figure 5.15

Step Applied To Third Inceptor

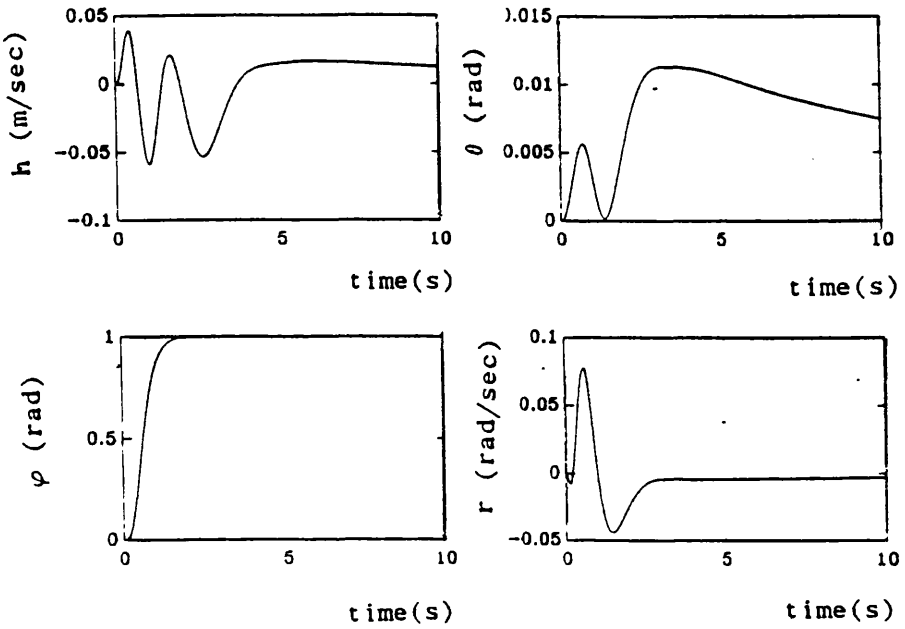

Step Applied To Fourth Inceptor

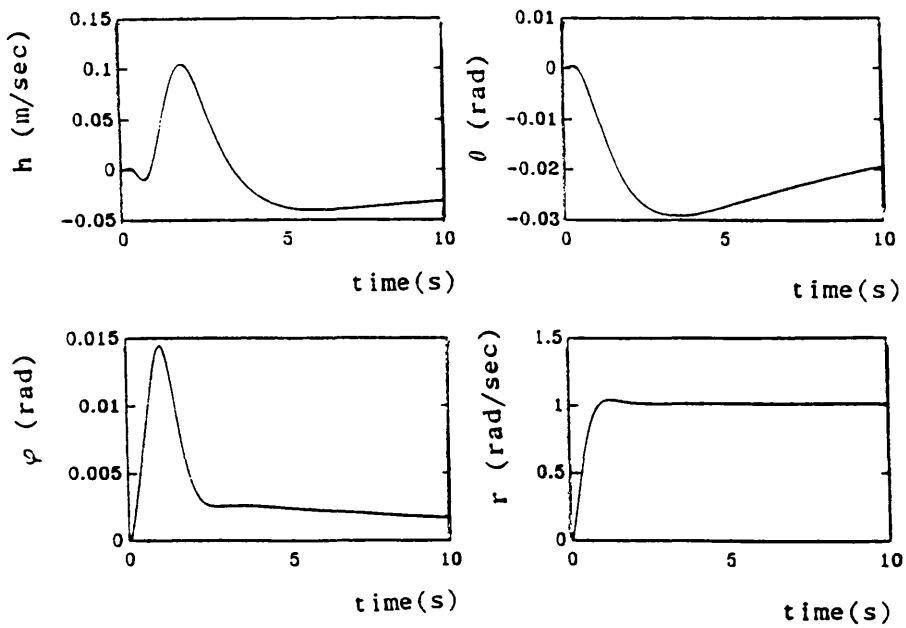

Response Of 120 knots System (including heading,actuator & rotor dynamics) When Controlled By ff,fb,kp & ki Designed At 80 knots Flight Condition

Time Responses To A Step Input On Each Inceptor

Step Applied To First Inceptor

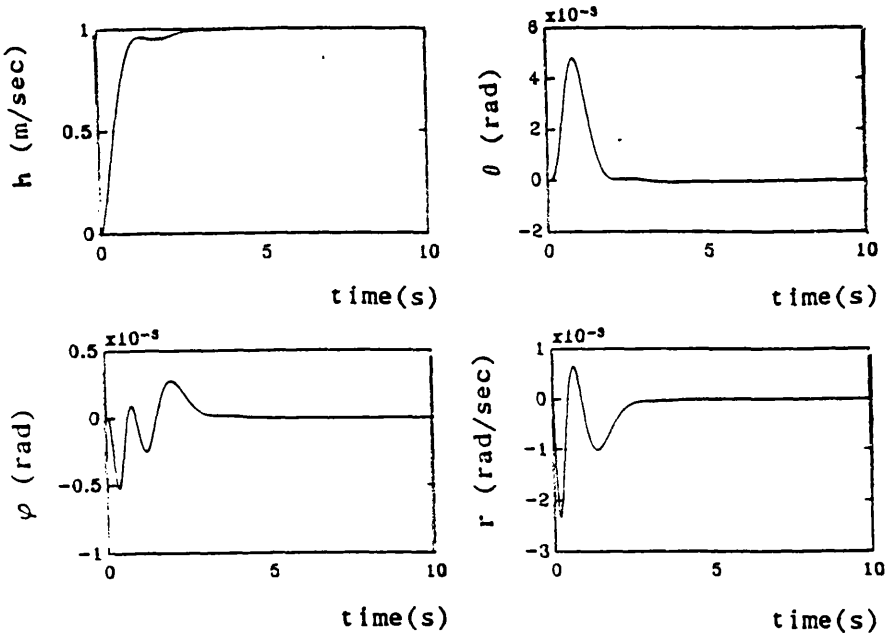

Step Applied To Second Inceptor

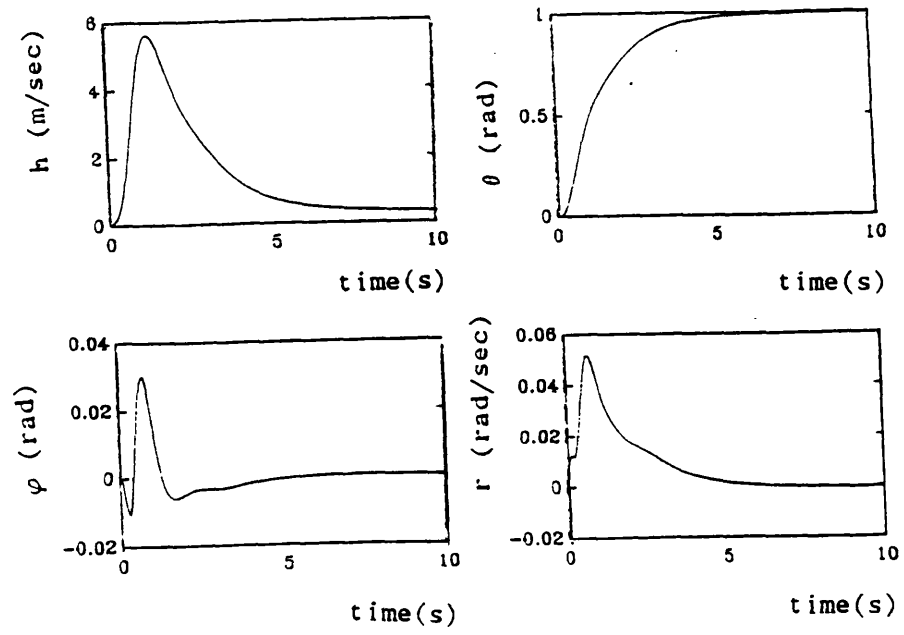

Figure 5.16

Step Applied To Third Inceptor

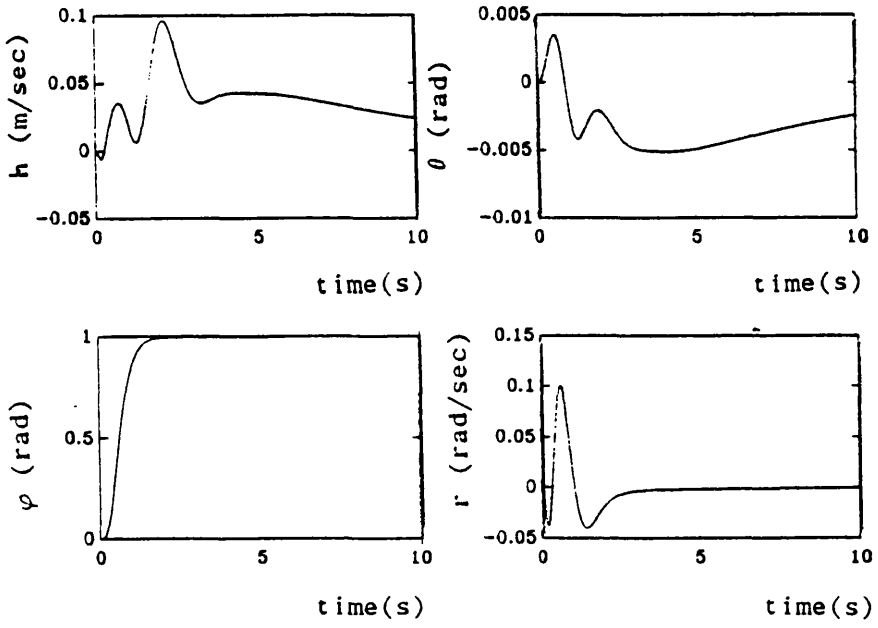

Step Applied To Fourth Inceptor

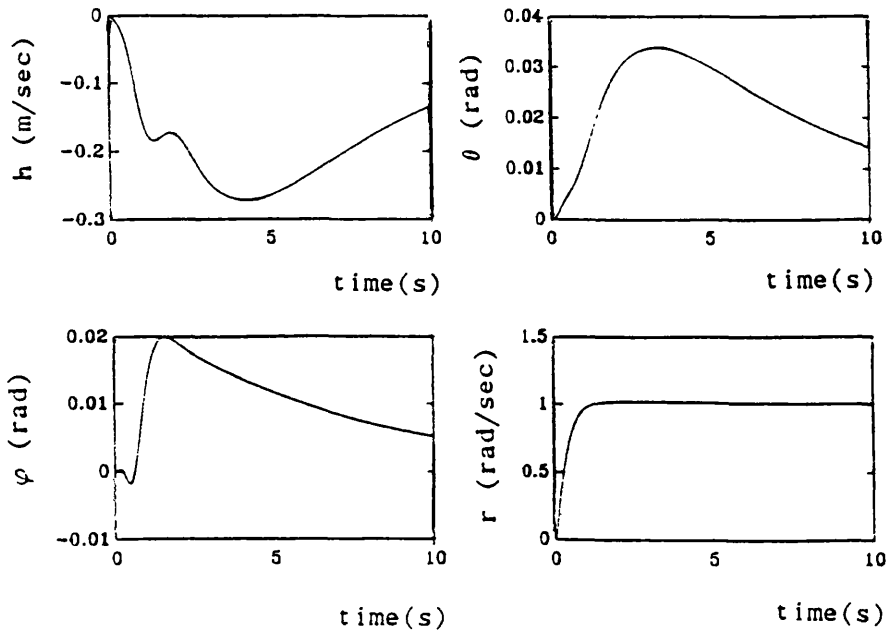

Response Of 50 knots System (including heading, actuator & rotor dynamics) Using A Scheduled Controller In The Inner Loop

Time Responses To A Step Input On Each Inceptor

Step Applied To First Inceptor

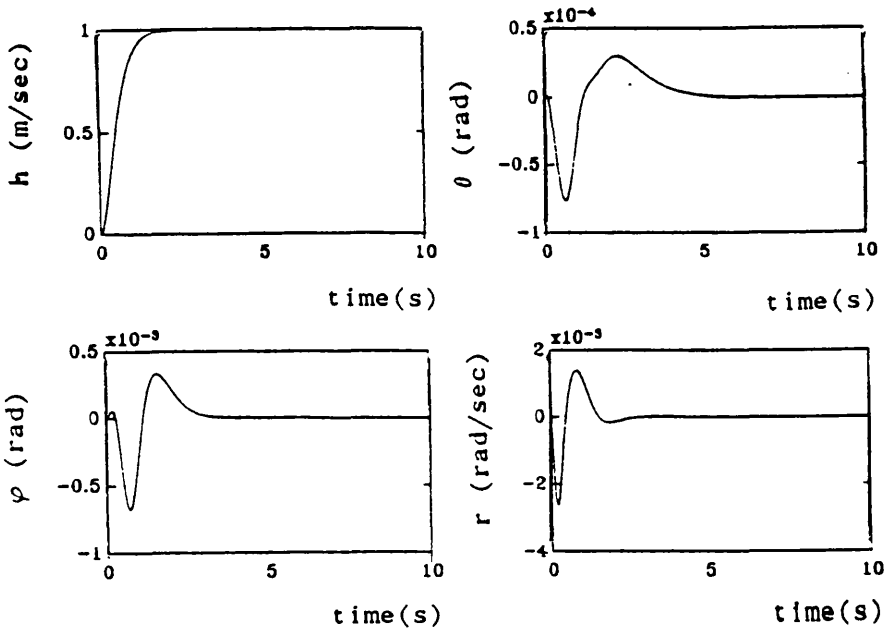

Step Applied To Second Inceptor

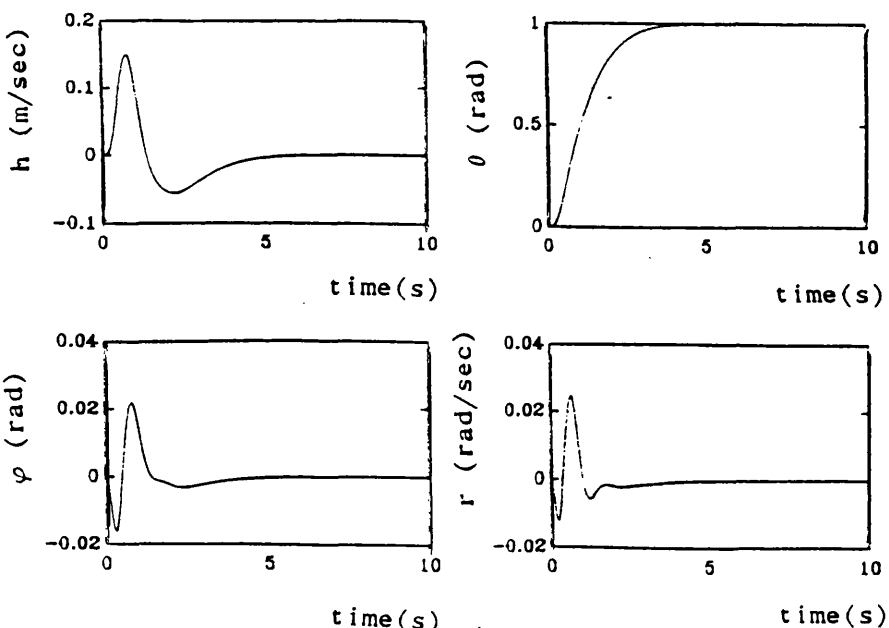

Figure 5.17

Step Applied To Third Inceptor

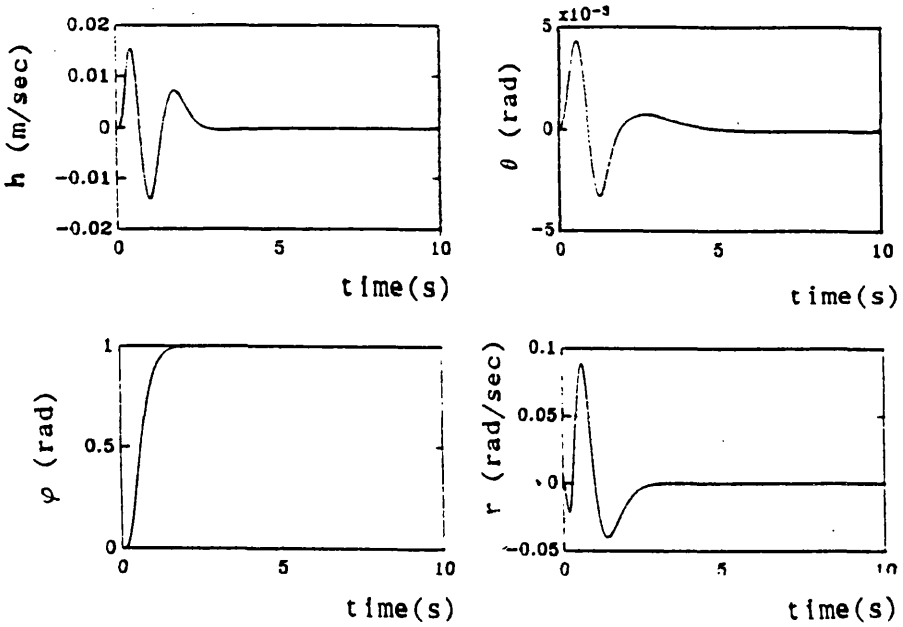

Step Applied To Fourth Inceptor

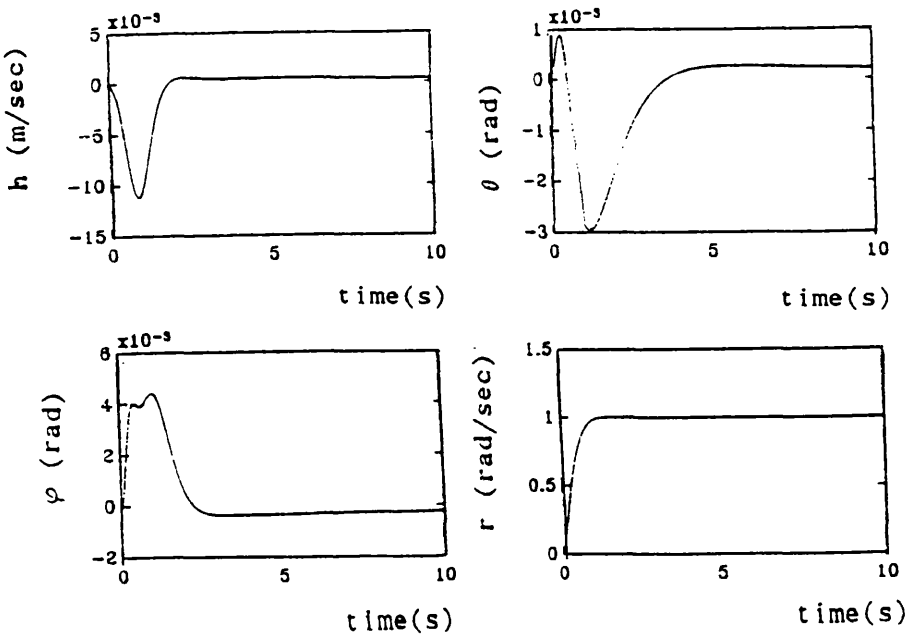

Response Of 120 knots System (including heading, actuator & rotor dynamics) Using A Scheduled Controller In The Inner Loop

Time Responses To A Step Input On Each Inceptor

Step Applied To First Inceptor

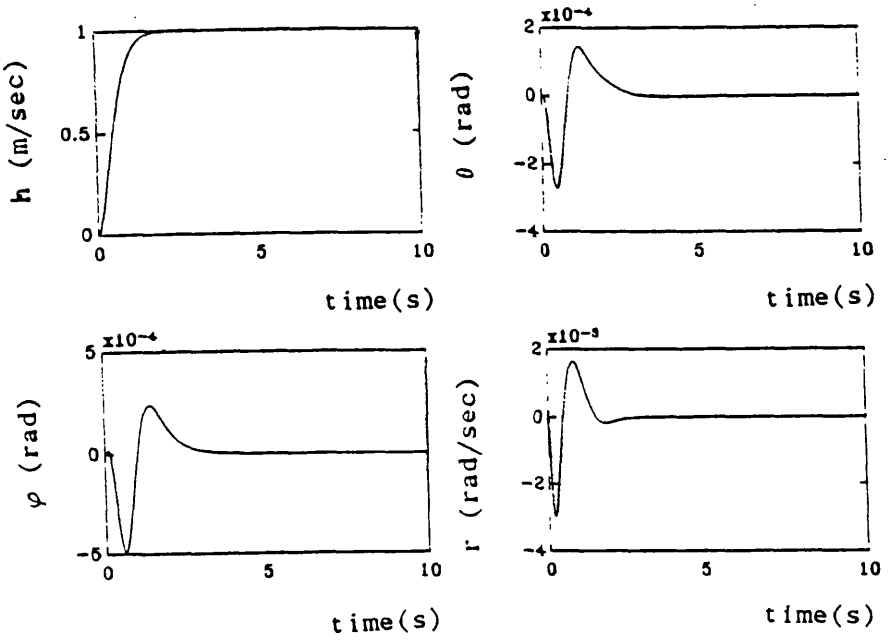

Step Applied To Second Inceptor

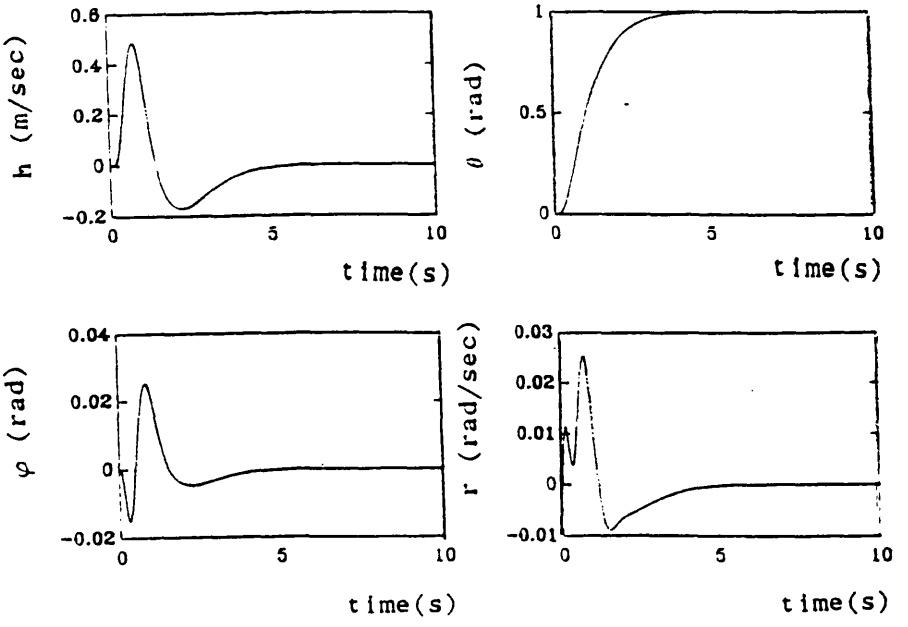

Figure 5.18

Step Applied To Third Inceptor

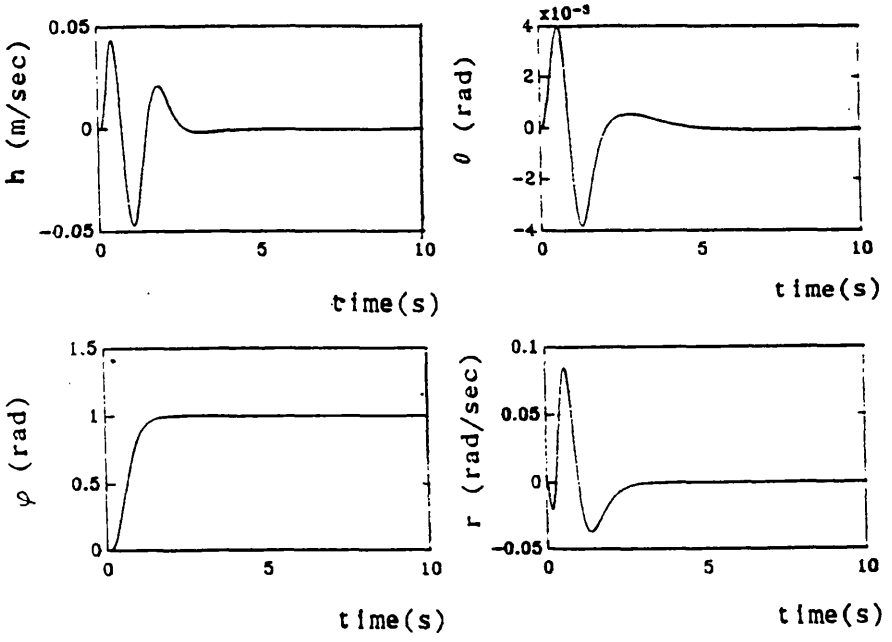

Step Applied To Fourth Inceptor

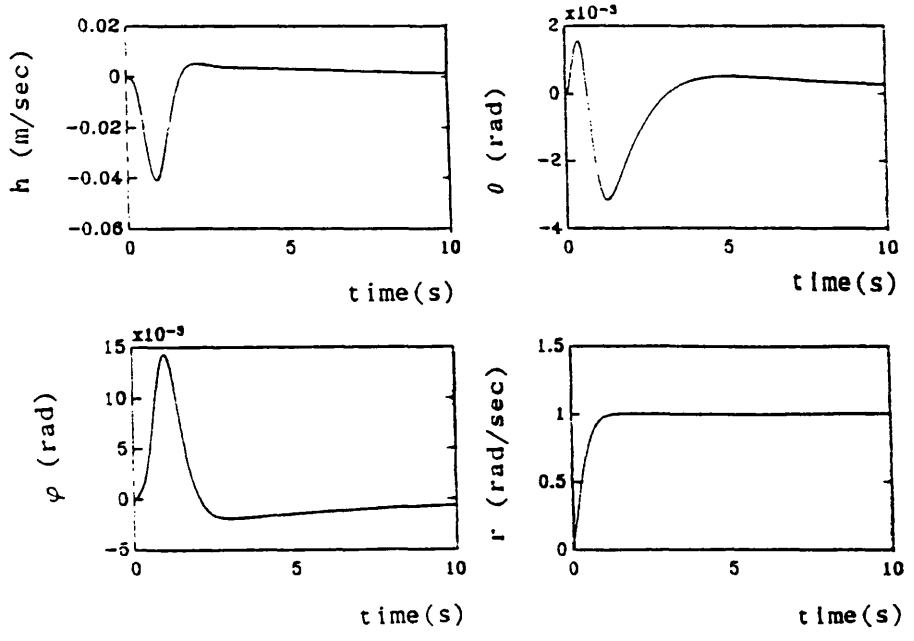

Movement Of Closed Loop Poles Across A Range Of Flight Conditions 0 - 160 knots Forward Flight (controlled by ff & fb from 80 knots design)

[h θ φ r]

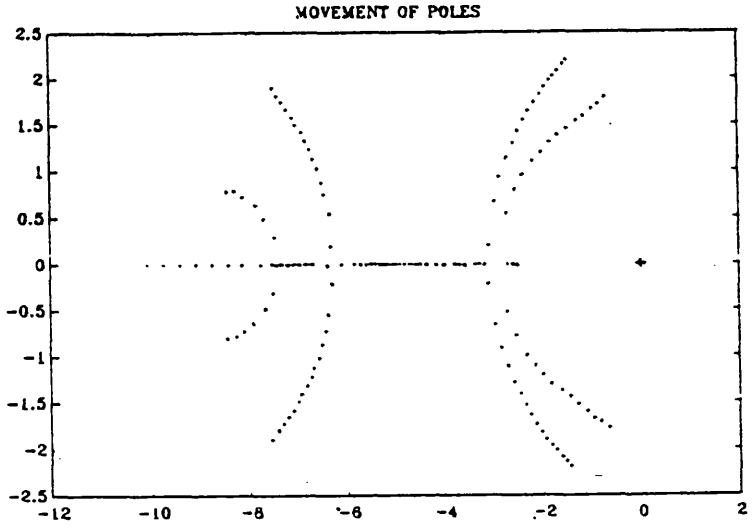

Figure 5.19

Movement Of Closed Loop Poles Across Range Of Flight Conditions 0 - 160 knots Forward Flight (controlled by ff, fb, kp & ki from 80 knots design

[h θ φ r]

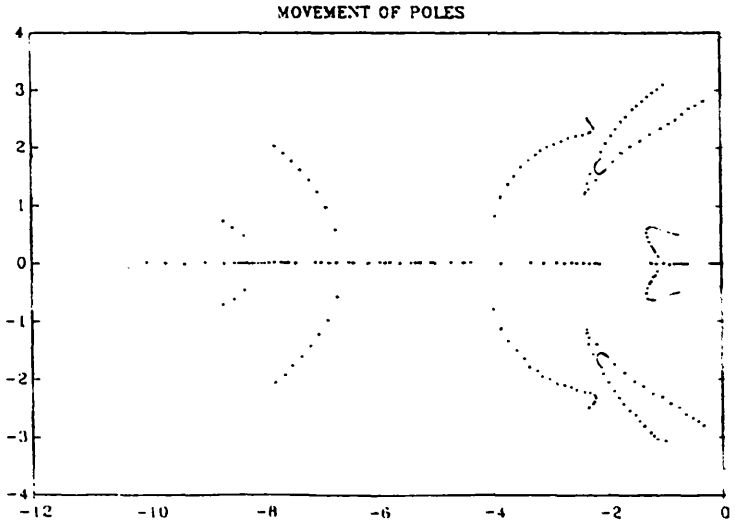

Figure 5.20

Movement Of Zeros Across A Range Of Flight Conditions

0 - 160 knots Forward Flight

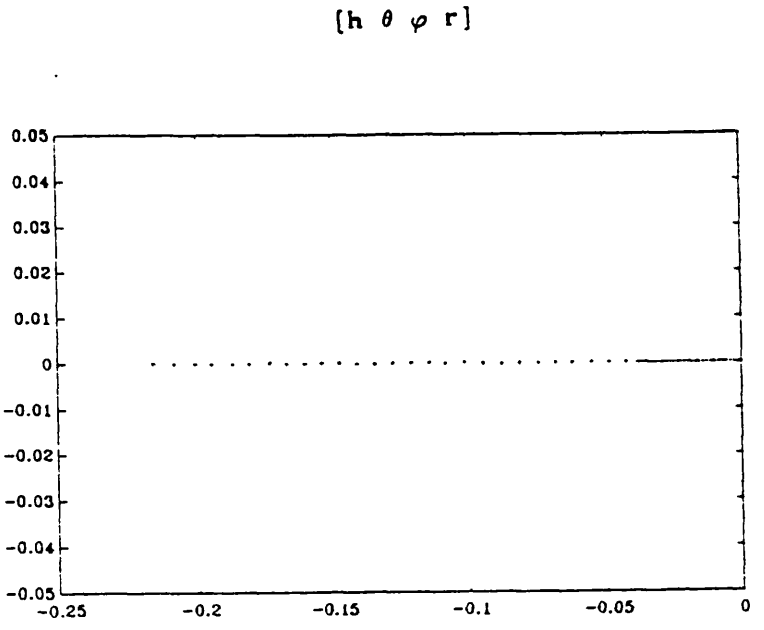

Figure 5.21

Movement Of The Cancelling Poles Across A Range Of Flight Conditions 0 - 160 knots forward flight (controlled by ff & fb from 80 knots design)

[h θ φ r]

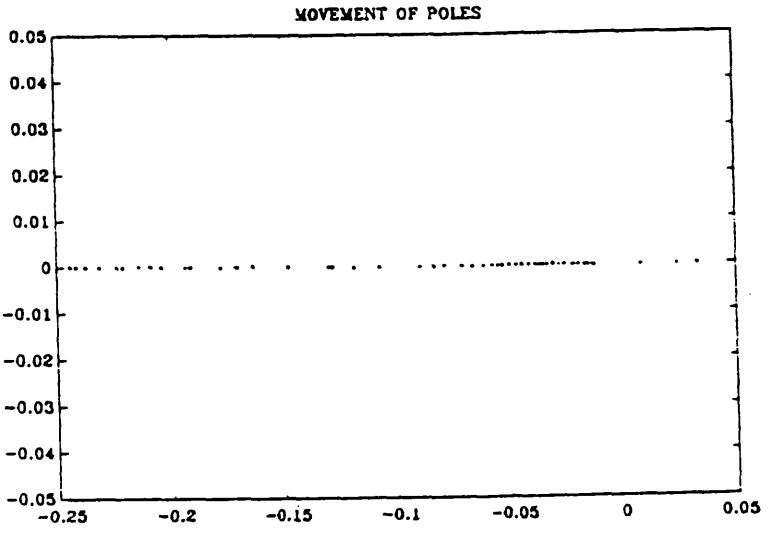

Figure 5.22

Movement Of The Cancelling Poles Across A Range Of Flight Conditions 0 - 160 knots forward flight (controlled by ff, fb, kp & ki from 80 knots design

[h θ φ r]

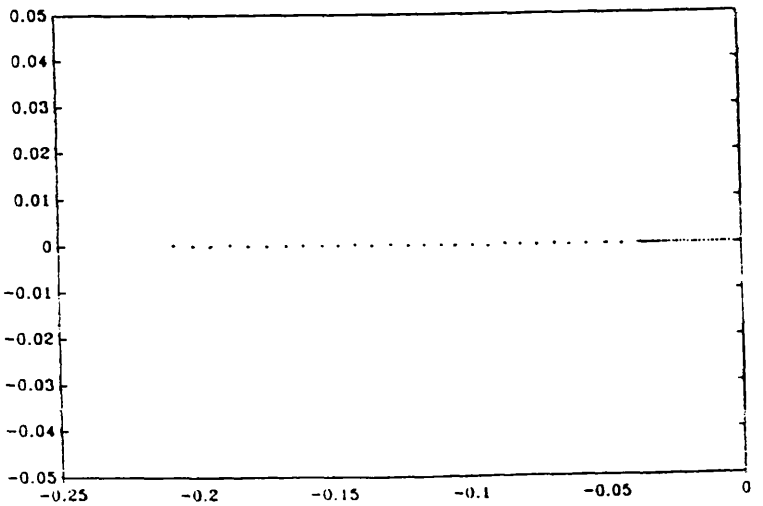

Figure 5.23

Movement Of Closed Loop Poles Across A Range Of Flight Conditions 0 - 160 knots Forward Flight (controlled by ff & fb from 80 knots design)

[h θ Ω β]

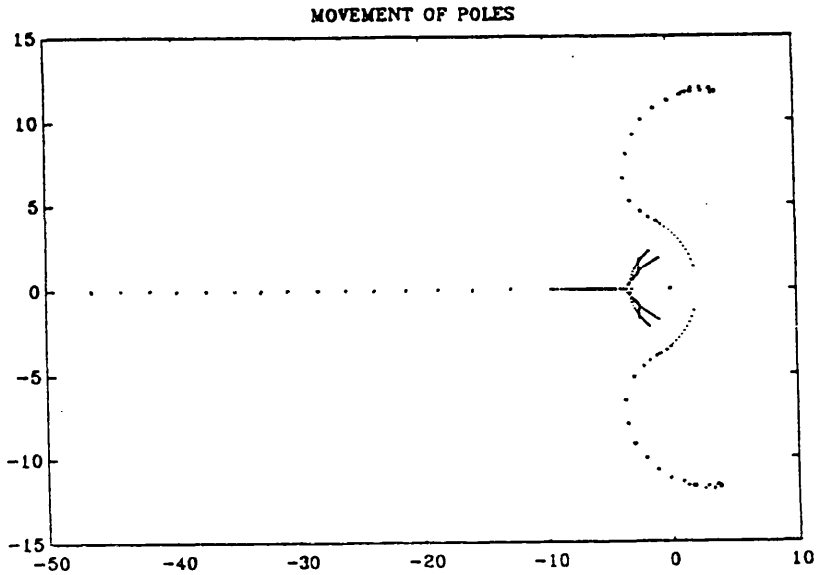

Figure 5.24

Movement Of Closed Loop Poles Across Range Of Flight Co. 0 - 160 knots Forward Flight (controlled by ff, fb, kp & ki from 80 knots design

[h θ Ω β]

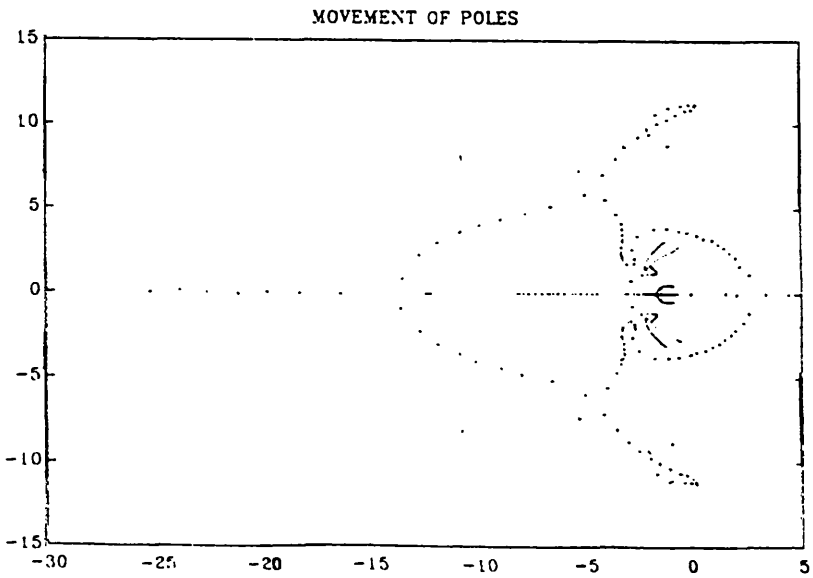

Figure 5.25

Movement Of Zeros Across A Range Of Flight Conditions

0 - 160 knots Forward Flight

[h θ Ω β]

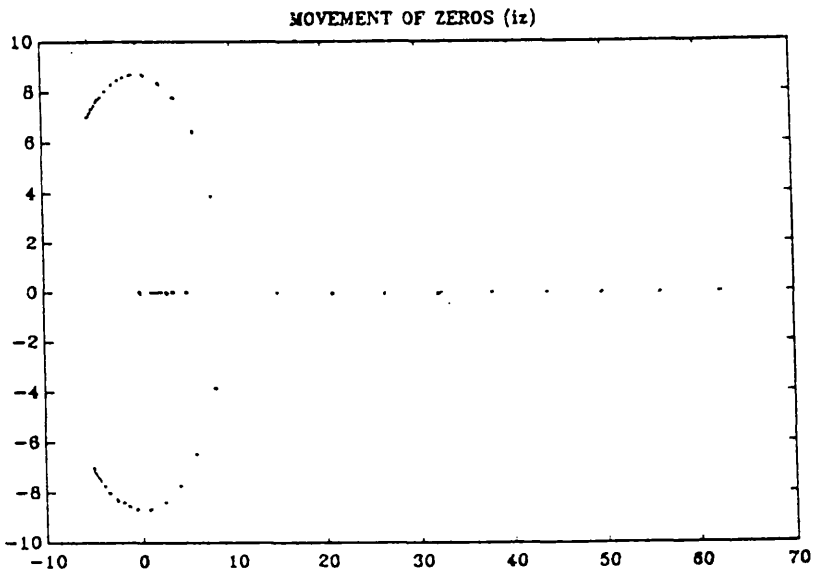

Figure 5.26

Response Of Non-Linear Helisim Model Controlled By kp,ki and fb & ff Scheduled In Inner Loop

(Doublet applied to pitch in order to vary vtkt between 50 & 120 knots - the range over which the controller was scheduled.)

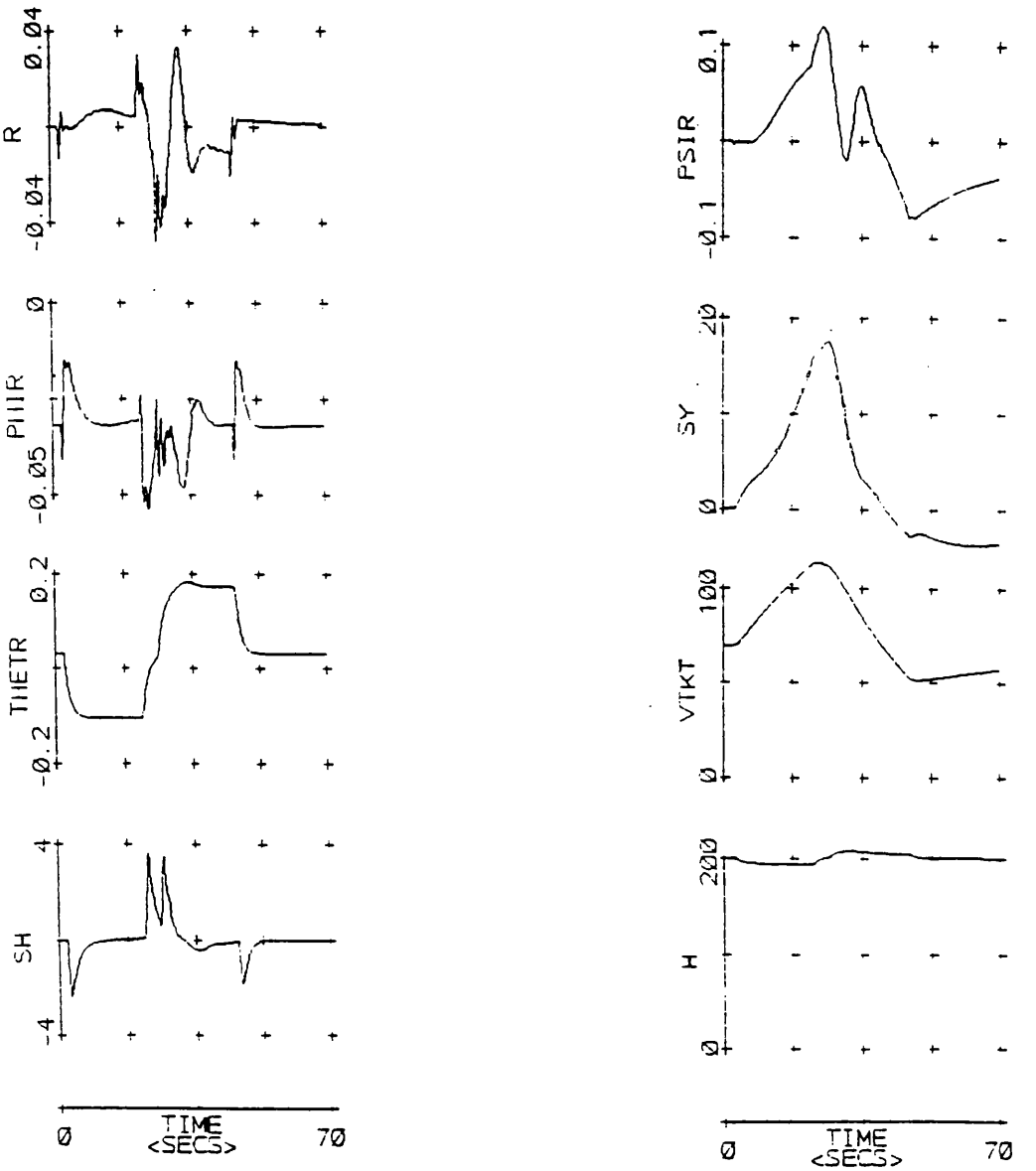

Figure 5.27

CHAPTER 6 EFFECTS OF TURBULENCE & NOISE ON CONTROLLER PERFORMANCE

6.1 Insensitivity to Atmospheric Disturbances

The controller must be capable of overcoming the effects of atmospheric disturbances and give an acceptable level of ride quality. In this case the actuators are expected to compensate for the disturbances because the disturbances are active in the same frequency range as the pilot's inputs. (The amount of control effort required is also of interest.) Turbulence was added to the Helisim model to determine the level of disturbance rejection achieved by the controller.

Results From Experiments With Turbulence

In the case of the controlled non-linear model without turbulence, a satisfactory trim was obtained (fig.6.1). The fluctuations in ψ, p, q, r & h are negligible and the residuals appearing in the plots can be attributed to numerical error. Also, because the trim is good, the activity of the actuators negligible.

When turbulence was added (in the form of states uturb, vturb & wturb which were calculated in body axes) to this model in the trimmed condition (fig.6.8) there was an increase in the activity of the actuator states for collective, longitudinal cyclic, lateral cyclic and tail rotor (TH0D, THSAD,THCAD & TH0TRD) because the control system is acting as a regulator and the actuators are moving to counter the effects of the disturbances. The effect of these external disturbances can be seen in the change in the responses of the states UB,VB & WB (forward, lateral & vertical velocity) which are no longer in a steady trimmed condition following the introduction of the turbulence. The variables which have been chosen to be controlled are SH, THETR, PHIR & R (height rate, pitch attitude, roll and yaw rate). With turbulence added to the system, these 4 variables deviate from the trim values but are centred around the original trim values from fig 6.1.

A step input of amplitude -1.0 is applied to the first inceptor at time=1 sec (fig. 6.9). By comparing with the same turbulence but without input (fig. 6.8), the effect of the step input can be seen in the response of SH. Except for a slight increase in the response of R, there appears to be very little cross coupling into other variables. This is in keeping with the results of the same input condition without turbulence (fig. 6.2).

A step input of amplitude -0.1 was applied to the second inceptor at time=1 sec (fig. 6.11). The effect of this input is clearly seen in the THETR response, indicating good tracking properties have been preserved from the similar case without turbulence (fig. 6.3). In fig. 6.3 it can be seen that at the time of the input being applied, SH and, to a lesser extent, PHIR show a rapid decrease in value. This same reaction can be seen in these two states by comparing this input condition including turbulence (fig. 6.11) with the no input condition with the same turbulence (fig. 6.8). The character of the response of VB has changed with the addition of turbulence, but the character of the responses of the other variables has been retained.

A step input of amplitude -0.1 was applied to the third inceptor (fig. 6.12). The response of PHIR shows that the input has been well tracked. The SH & R responses are almost identical to those from the case with no input and same turbulence (fig. 6.8) indicating a low level of coupling between these states and inputs to the third inceptor. Looking at the graphs from the experiment with the same input but no turbulence (fig. 6.4), we see that for P there is a sudden excursion away from and back to trim value when the input is applied. This can also be seen by comparing P in fig. 6.12 (input and turbulence) with P in fig. 6.8 (no input and turbulence). Also in fig. 6.4 can be seen a large increase in PSIR and a large decrease in VB, both of which can be seen in fig. 6.12. However, by far the worst response in fig. 6.12 is VB although it does recover slightly from its

largest excursion from the trim value. By comparing fig. 6.12 (input & turbulence) with fig. 6.8 (turbulence but no input) we see that the SH response is almost identical. This indicates that there is very little coupling between SH and the third inceptor. There is some indication of coupling into THETR & R however not a large amount.

A step input of amplitude +0.1 was applied to the fourth inceptor at time=1 sec (fig. 6.14). When a similar experiment was performed without turbulence (fig. 6.5) it was noted that R initially overshot the amplitude of the step input but returned to a steady state value which was close to 0.1. This behaviour can also be seen when turbulence is added (fig. 6.14). In both figs. 6.5 & 6.14 there is very little coupling into SH and the general character of the initial responses of the variables in fig. 6.5 can also be seen in the same variables in fig. 6.14. In the latter part of some responses in fig. 6.14 there is some oscillatory behaviour which was not present when there was no turbulence. This is, once again, attributable to the sensitivity of PSIR to inputs to the fourth inceptor. Because of the large PSIR response, the experiment was repeated with a smaller step amplitude of +0.06 (fig. 6.15) and then smaller again with an amplitude of +0.03 (fig. 6.13). Fig. 6.15 shows that the reduction in step size to 0.06 does not cause the oscillatory behaviour of fig. 6.14 and returns most of the responses to conditions which are comparable to those obtained for the same input without the turbulence (fig. 6.6). The reduction in input size also significantly decreased the range of activity of the actuator states THSAD & THCAD.

6.2 Noise Rejection

Signals generated by the sensors and airframe vibrations may contain components at frequencies higher than that of the closed loop bandwidth of the controlled helicopter. Noise rejection is the ability of the controller to attenuate such high frequency components by low pass transmittances in the controller design or

actuators and so cause little or no additional activity in actuator states. (High frequency activity in the actuators will not be more effective in controlling the helicopter and will cause wear.) In order to test the performance of the controller for noise rejection, the non-linear Helisim model was used together with inner and outer loop controller matrices and noise was added to each of the feedback states.

Results Of Experiments With Noise

Fig. 6.16 shows the responses of the controlled system with noise but no input applied. In comparison with no noise and no input (fig. 6.1), the responses of the variables are much more noisy but all values remain close to trim. The actuator states show some increase in activity due to the addition of the noise but much of the noise has been attenuated. With no inputs applied the system has remained stable.

A step input of amplitude -1.0 was applied to the first inceptor at time=1 sec (fig. 6.18). It can be seen that the input step is well tracked by SH. Comparing fig. 6.18 with the no noise response for the same step (fig. 6.2) although most of the responses are noisier the general shapes and sizes of most of the responses are very similar. The only exceptions to this are PSIR and VB. This is again attributable to the sensitivity of these states to changes in R.

A step input of amplitude -0.1 was applied to the second inceptor at time=1sec (fig. 6.21). The response of THETR shows good tracking of the input. The effects of the addition of noise can be seen by comparing with the no noise responses for the same input (fig. 6.3). The SH & THETR responses are very alike but the PHIR & R responses have deteriorated. The states PSIR and VB, sensitive to changes in R, have changed accordingly and the responses of the actuator states THSAD & TH0TRD have also been altered.

A step input of amplitude -0.1 was applied to the third inceptor at time=1 sec

(fig. 6.22)(noise with a step input applied to the third inceptor). When this is compared with fig. 6.4 (no noise, step input applied to the third inceptor), it can be seen that there is a deterioration in tracking properties. The PSIR response has changed and the VB response is poorer. However, the system remains stable.

A step input of amplitude +0.06 was applied to the fourth inceptor at time=1 sec (fig. 6.25). As in the case without noise (fig. 6.6), R overshoots the amplitude of the input step but returns to a similar value. With the addition of noise far more coupling into SH and PHIR is evident which has resulted mainly in an increase in WB.

6.3 Effect on Controlled Non-linear System when both Turbulence and Noise are added

Results From Experiments With Both Turbulence & Noise

Both turbulence and noise were added to the controlled system but no input was applied. The results can be seen in fig. 6.17. Comparing these results with those from the case with turbulence but no noise and no input (fig. 6.8) it was found that the responses were generally more noisy but were of same general shape and size of response. The exception to this being the slight increase in R which causes a greater response in VB. This is as expected from the results of fig. 6.16 which indicated that by adding noise alone to the system, the responses became noisy but, other than a deterioration in R, were not greatly affected when no input was applied.

A step input of amplitude -1.0 was applied to the first inceptor at time=1 sec (fig. 6.19). By comparison with the no input case with noise & turbulence (fig. 6.17) the effect of the tracking of the input can be seen in the SH response. There appears to be little additional coupling into the other three variables to be

controlled (PHIR , THETR & R). Compared with the case with the same input but with turbulence and without noise (fig. 6.9), the response of R is slightly larger which causes to become larger but otherwise responses are similar.

A step input of amplitude -0.1 was applied to the second inceptor at time=1 sec. (fig. 6.20).The PHIR & R responses (and consequently PSIR,VB & WB) of fig. 6.20 ,although noisy, are much closer in nature to those of fig. 6.21 (same input with noise but no turbulence) than those of fig. 6.11 (same input no noise but turbulence) suggesting that for response to inputs applied to the second inceptor, noise has a greater effect on PHIR & R performances than turbulence.

A step input of amplitude -0.1 was applied to the third inceptor at time=1 sec (fig. 6.23). Comparing this with fig. 6.12 (same input with turbulence but no noise) we see that tracking is not quite so good but generally the character of the respones, though showing some turbulence, is retained. By comparing fig. 6.23 with fig. 6.22 (same input with noise but no turbulence) we see again that the tracking properties are not as good and the VB response of fig. 6.23 is better than in fig. 6.22 and again stability is retained.

A step input of amplitude +0.06 was applied to the fourth inceptor at time=1sec. (fig. 6.24). By comparing fig. 6.24 with fig. 6.15 (the same input with turbulence but without noise) it can be seen that the most of the responses are similar with the exception of PHIR (which will also affect WB response). The PHIR response is similar to that in fig. 6.25 (same input without turbulence with noise) suggesting that the PHIR response to inputs applied to the fourth inceptor is affected more by noise than turbulence. R (& PSIR & VB) have also been affected in this way.
It can be concluded from these results that the controller is able to withstand the effects of turbulence and noise in the sense that stability is maintained. Actuator rate and authority limits are at no point exceeded. There is some deterioration in

the ability of the controller to track inputs in some cases, but performance is generally good.

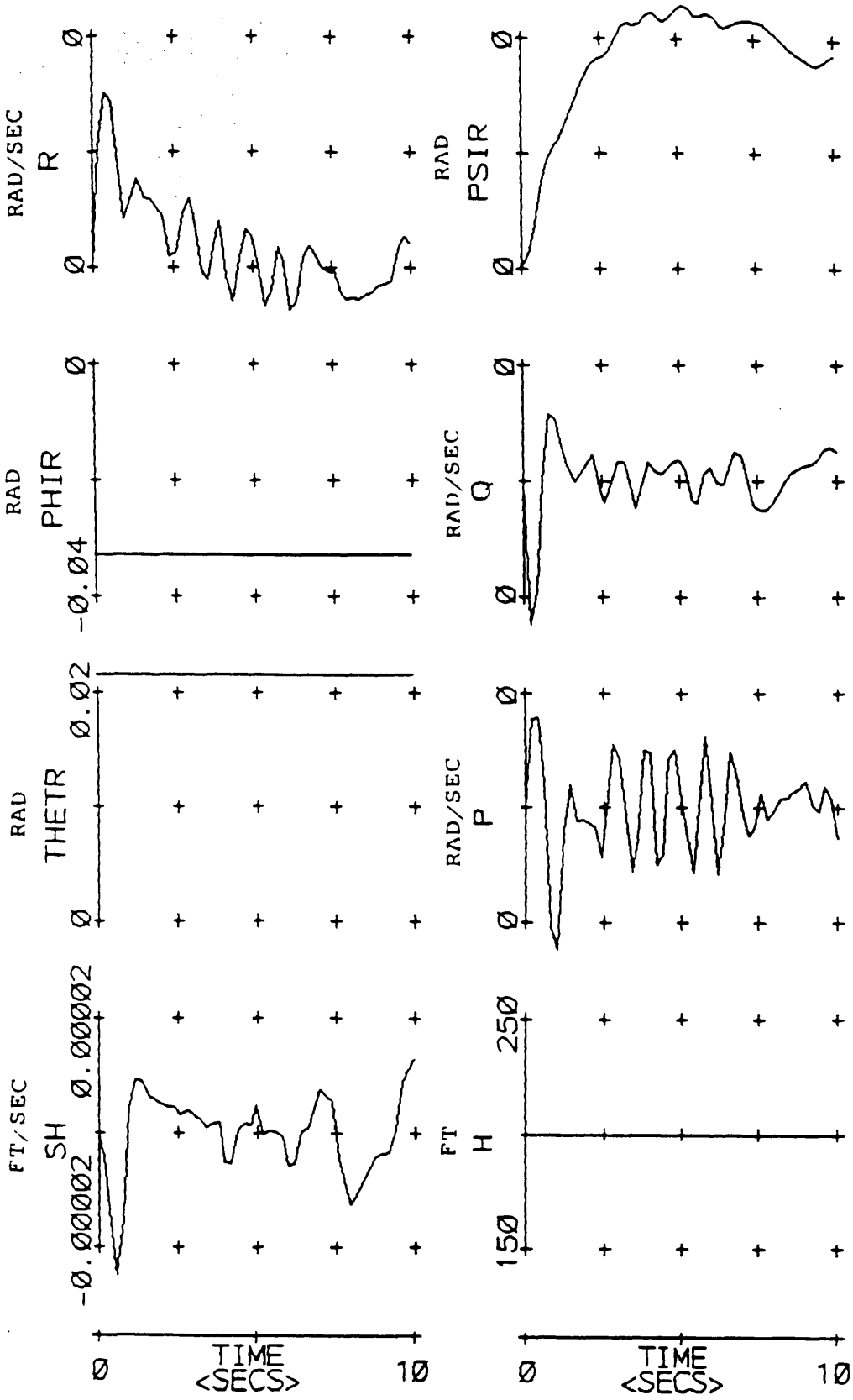

Figure 6.1 Helisim model without turbulence and without noise

Trim condition

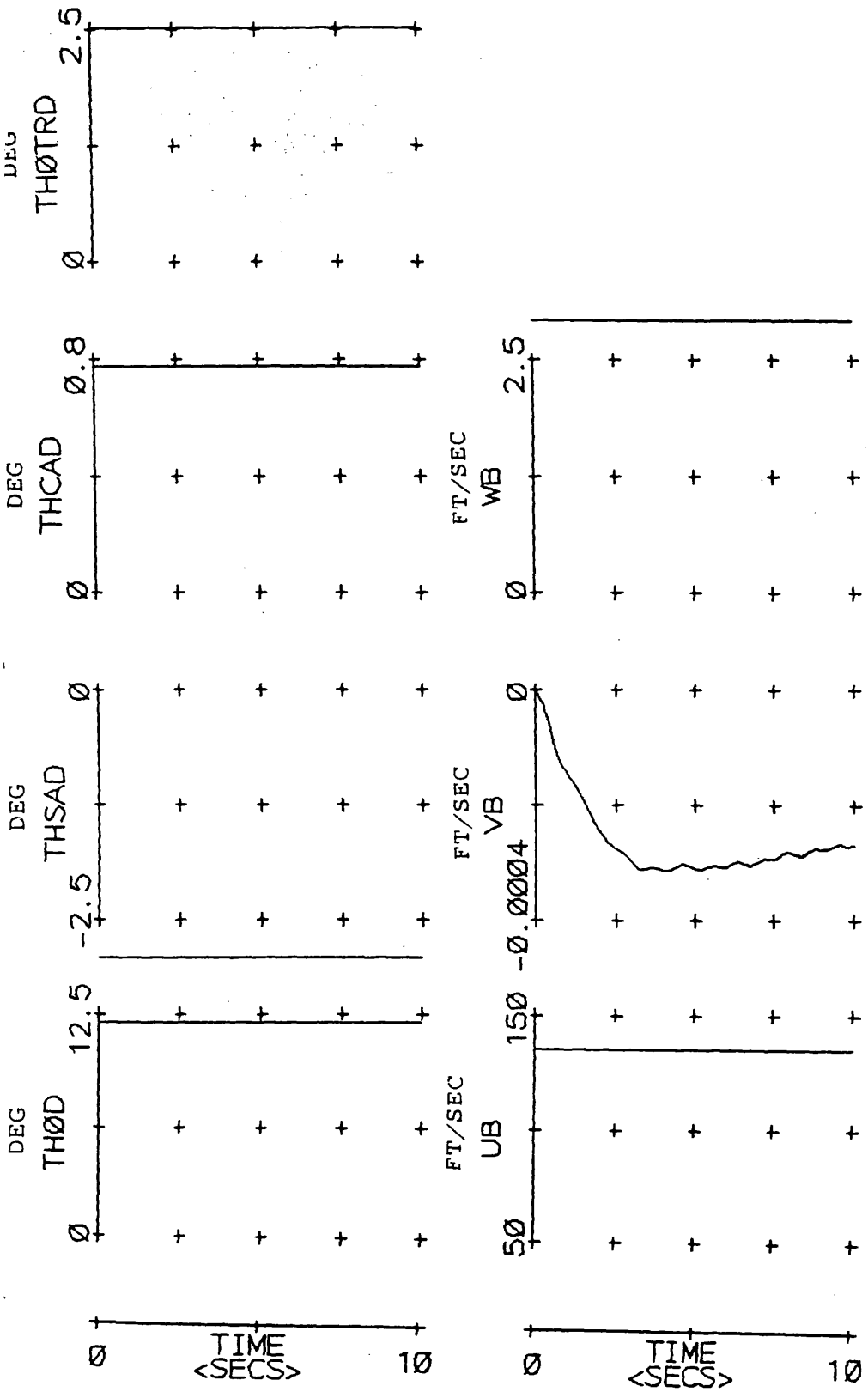
DEG
THØTRD
2.5
Ø
DEG
THCAD
Ø.8
Ø
FT/SEC
WB
2.5
Ø
DEG
THSAD
Ø
-2.5
FT/SEC
VB
Ø
-Ø.ØØØ4
DEG
THØD
12.5
Ø
FT/SEC
UB
15Ø
5Ø
Ø
TIME
<SECS>
10
Ø
TIME
<SECS>
10

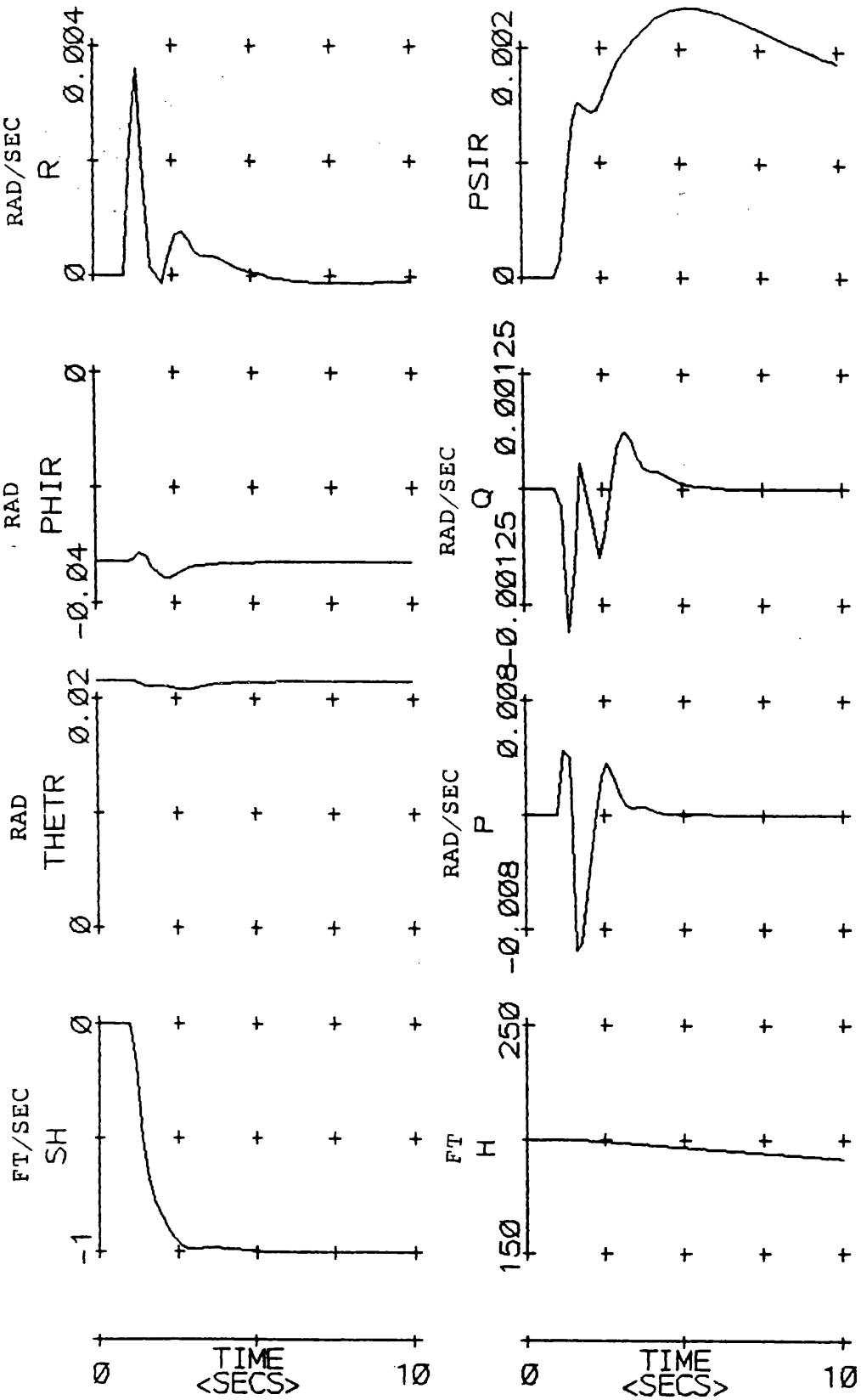

Figure 6.2 Helisim Model Without Turbulence And Without Noise

Step Input Of Amplitude -1.0 Applied To First Inceptor

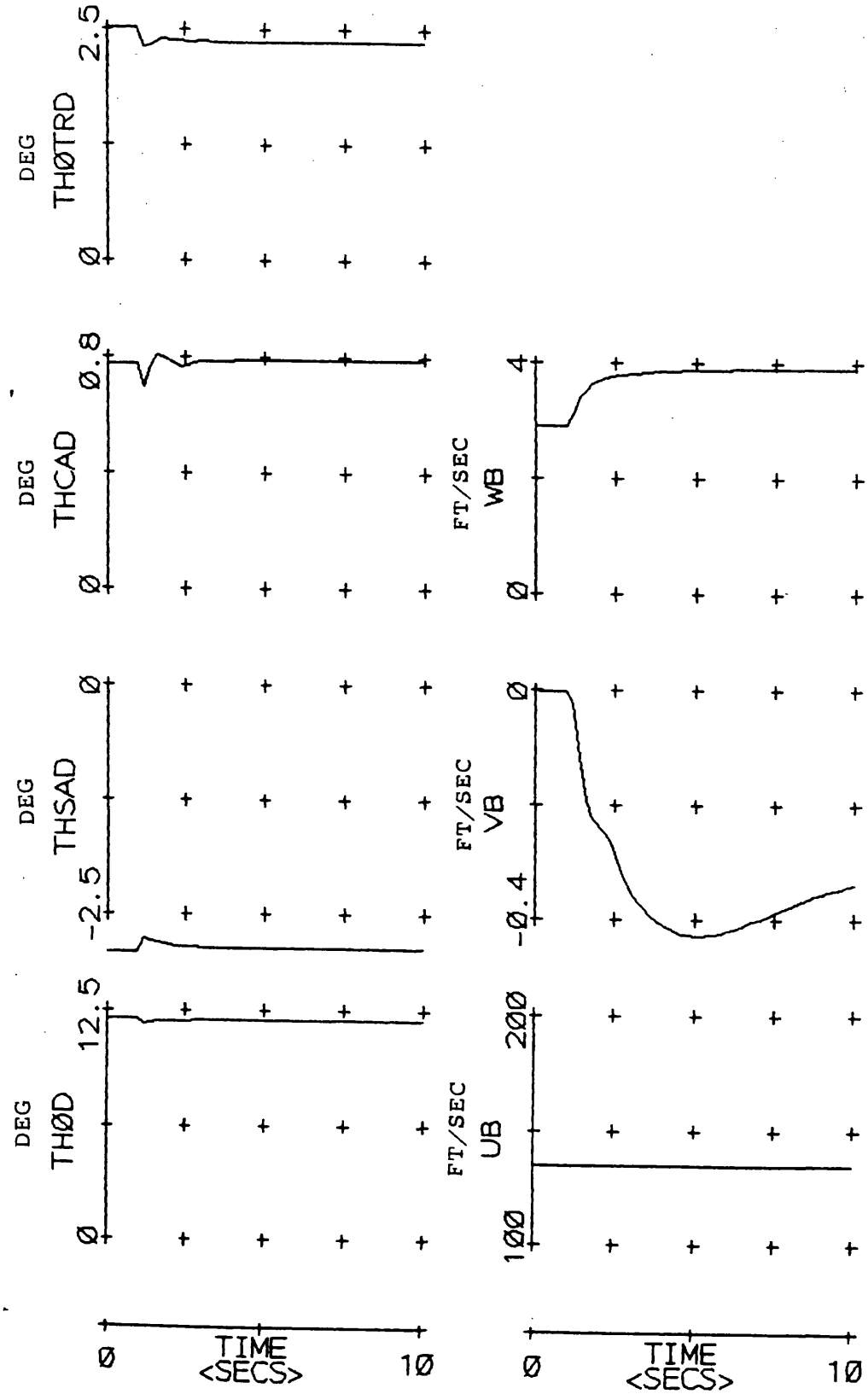
DEG
THØTRD
2.5
Ø
DEG
THCAD
Ø.8
Ø
FT/SEC
WB
4
Ø
DEG
THSAD
Ø
-2.5
FT/SEC
VB
Ø
-Ø.4
DEG
THØD
12.5
Ø
FT/SEC
UB
2ØØ
1ØØ
Ø
TIME
<SECS>
1Ø
Ø
TIME
<SECS>
1Ø

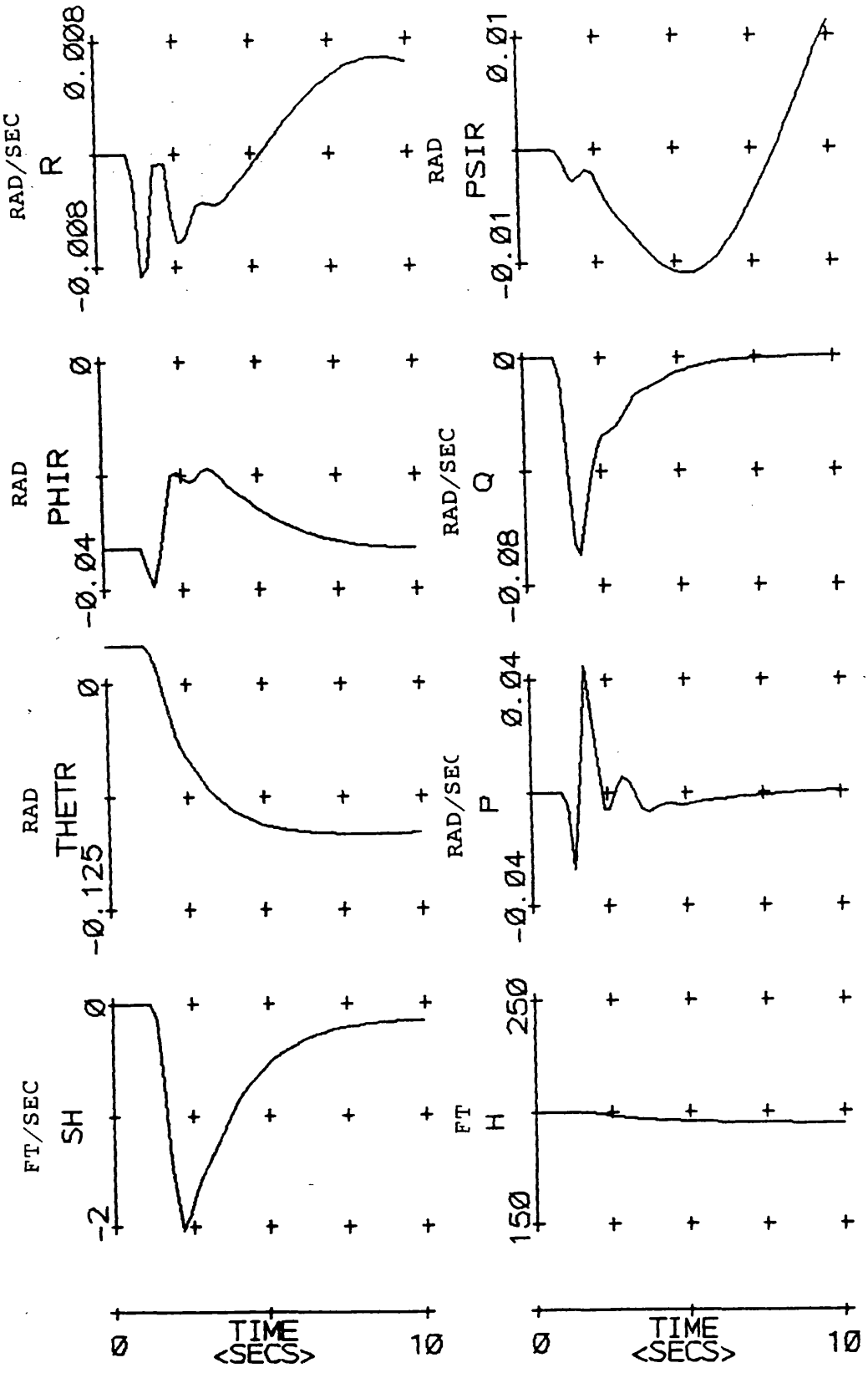

Figure 6.3 Helisim Model Without Turbulence And Without Noise Step Input Of Amplitude -0.1 Applied To Second Inceptor

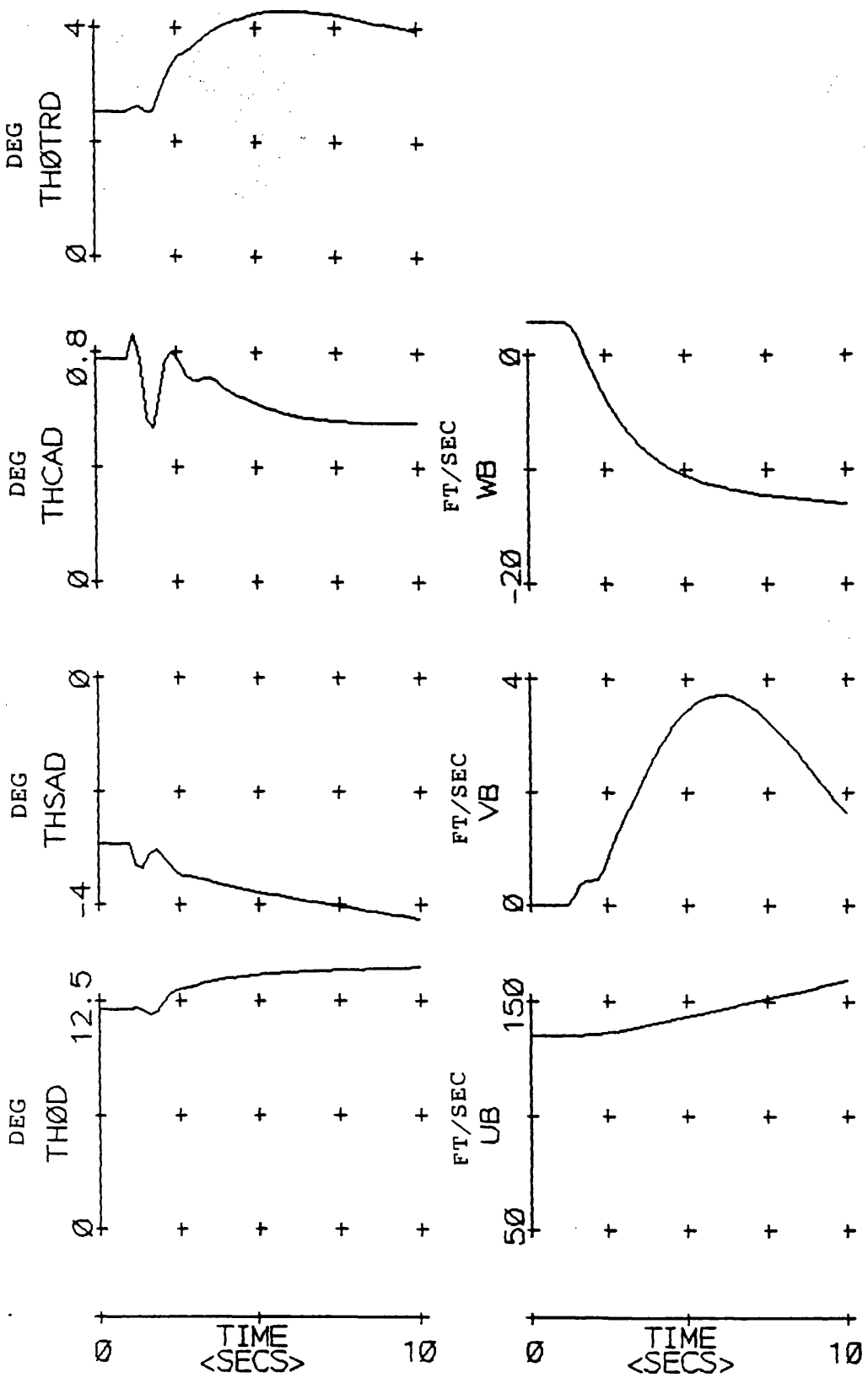
DEG
THØTRD
4
Ø
DEG
THCAD
Ø.8
Ø
FT/SEC
WB
Ø
-2Ø
DEG
THSAD
Ø
-4
FT/SEC
VB
4
Ø
DEG
THØD
12.5
Ø
FT/SEC
UB
15Ø
5Ø
Ø
TIME
<SECS>
1Ø
Ø
TIME
<SECS>
1Ø

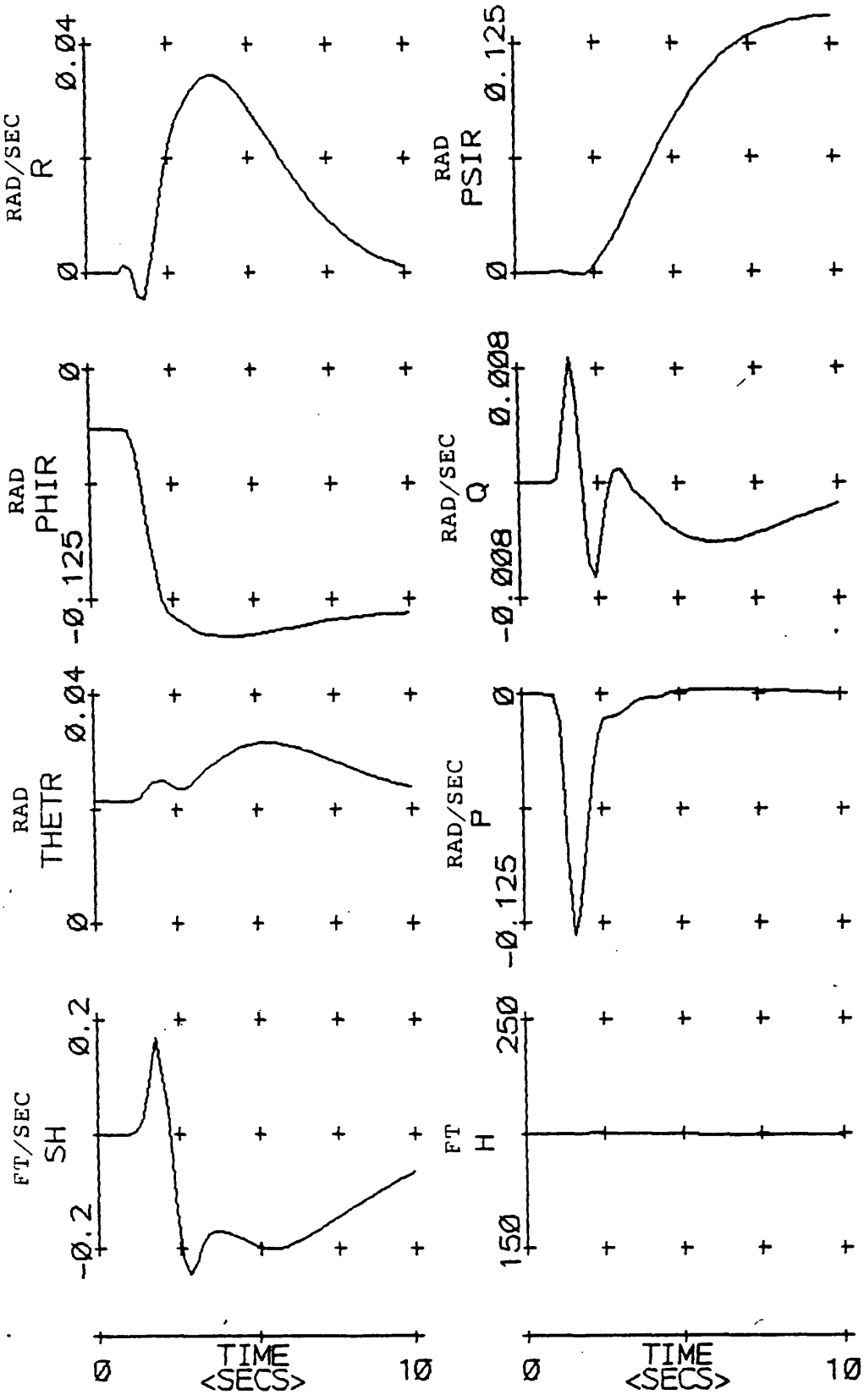

Figure 6.4 Helisim Model Without Turbulence And Without Noise Step Input Of Amplitude -0.1 Applied To Third Inceptor

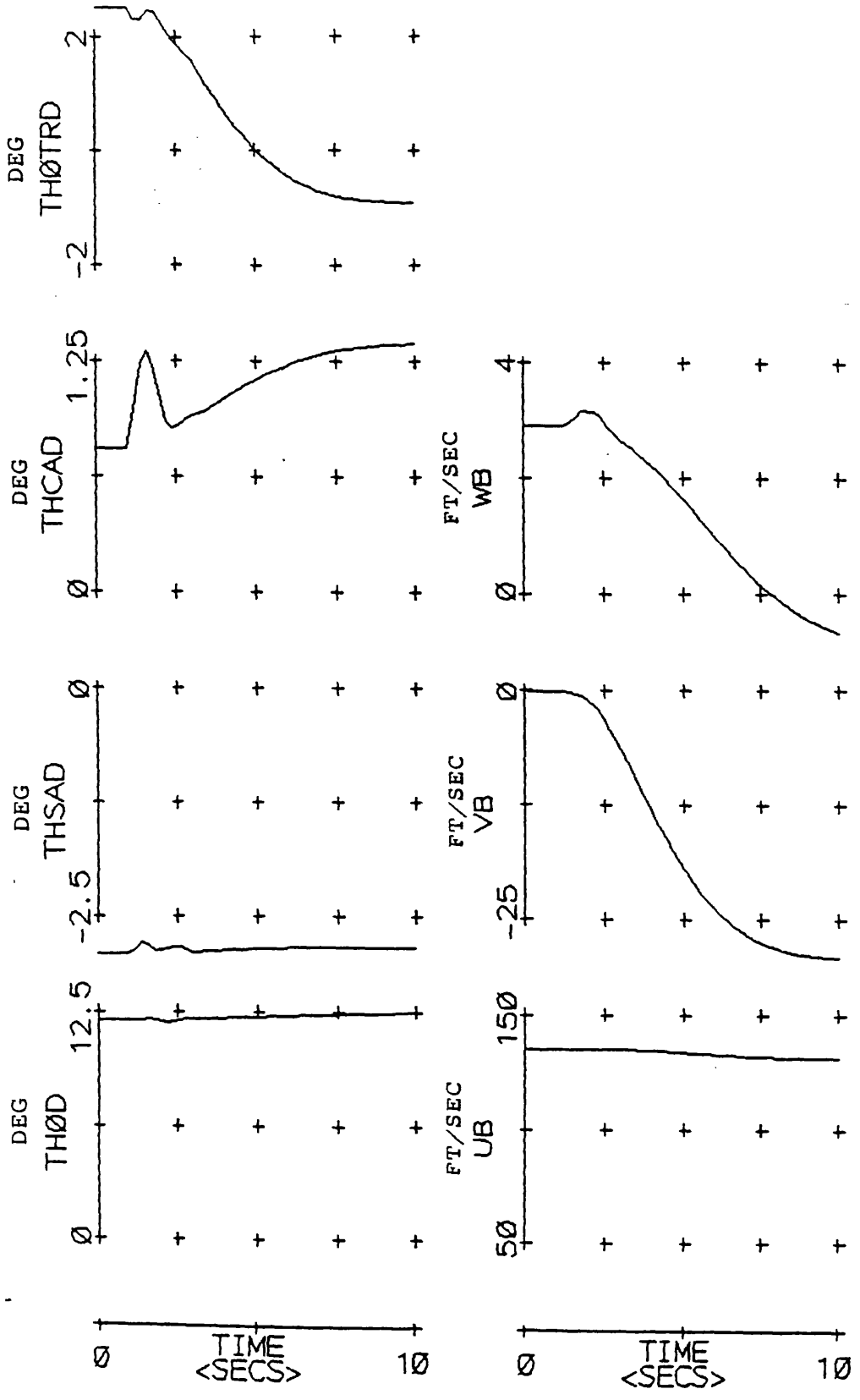
DEG
THØTRD
2
-2
DEG
THCAD
1.25
Ø
FT/SEC
WB
4
Ø
DEG
THSAD
Ø
-2.5
FT/SEC
VB
Ø
-25
DEG
THØD
12.5
Ø
FT/SEC
UB
150
50
Ø
TIME
<SECS>
10
Ø
TIME
<SECS>
10

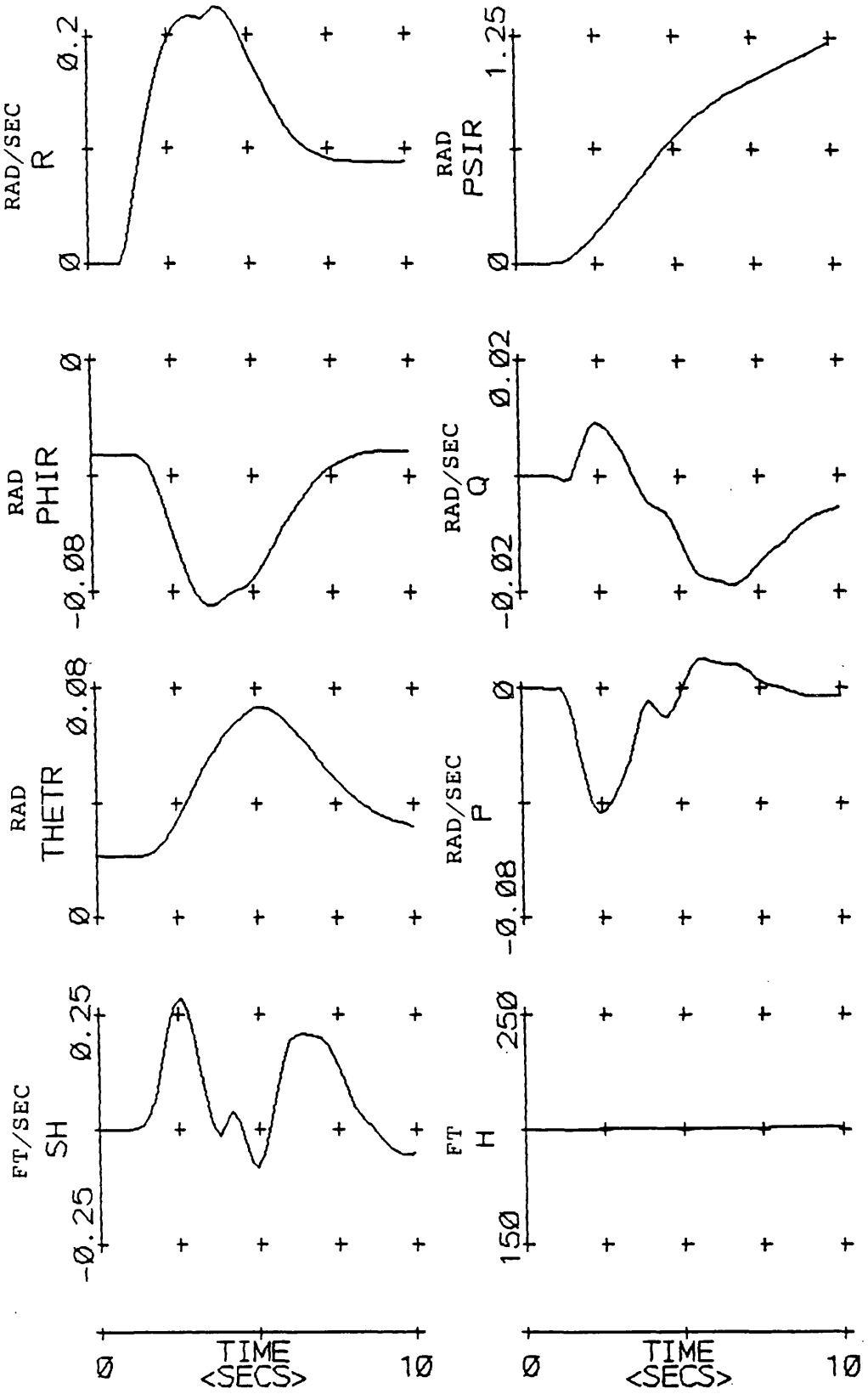

Figure 6.5 Helisim Model Without Turbulence And Without Noise Step Input Of Amplitude 0.1 Applied To Fourth Inceptor

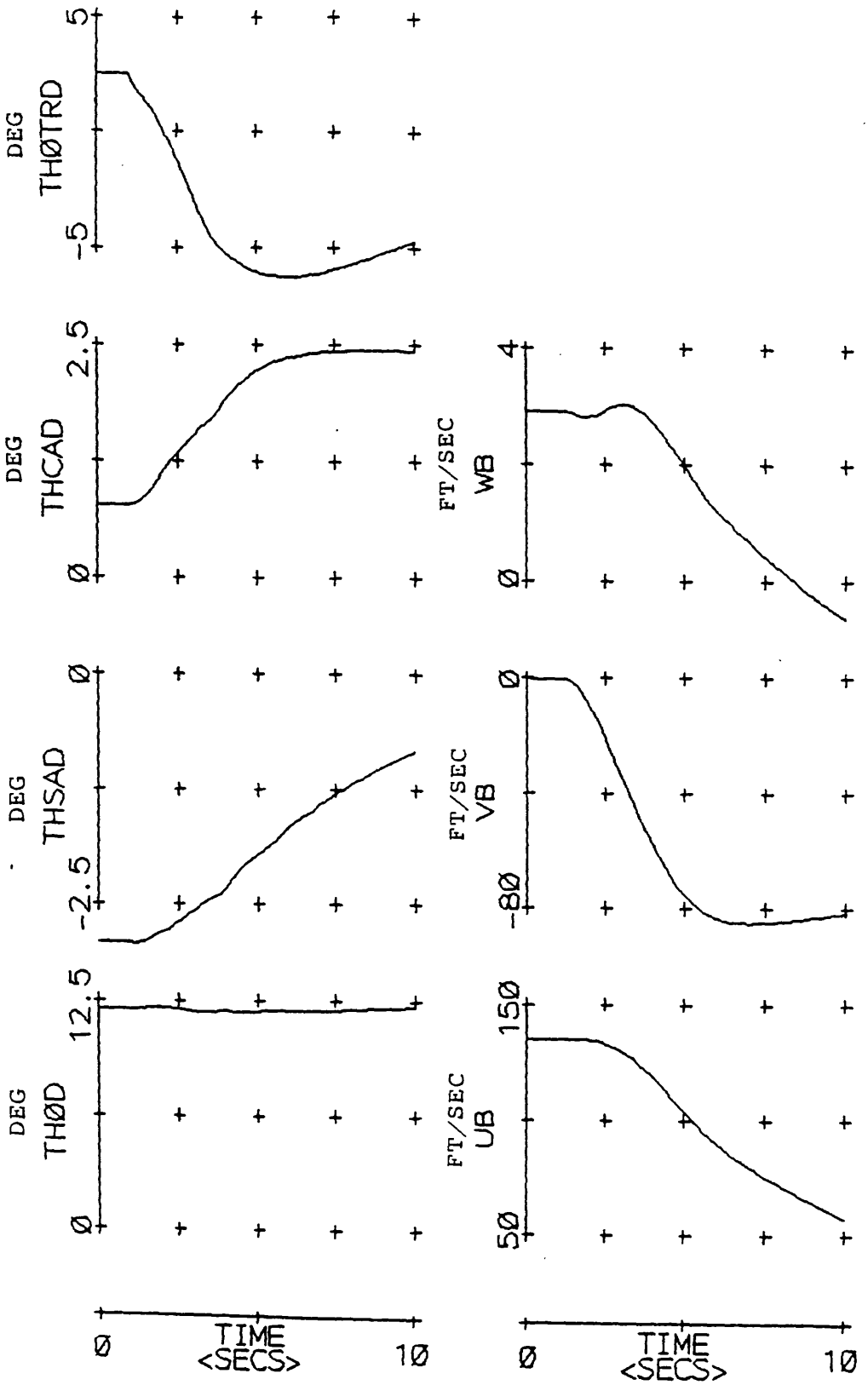
DEG
THØTRD
5
-5
DEG
THCAD
2.5
Ø
FT/SEC
WB
4
Ø
DEG
THSAD
Ø
-2.5
FT/SEC
VB
Ø
-8Ø
DEG
THØD
12.5
Ø
FT/SEC
UB
15Ø
5Ø
Ø
TIME
<SECS>
10
Ø
TIME
<SECS>
10

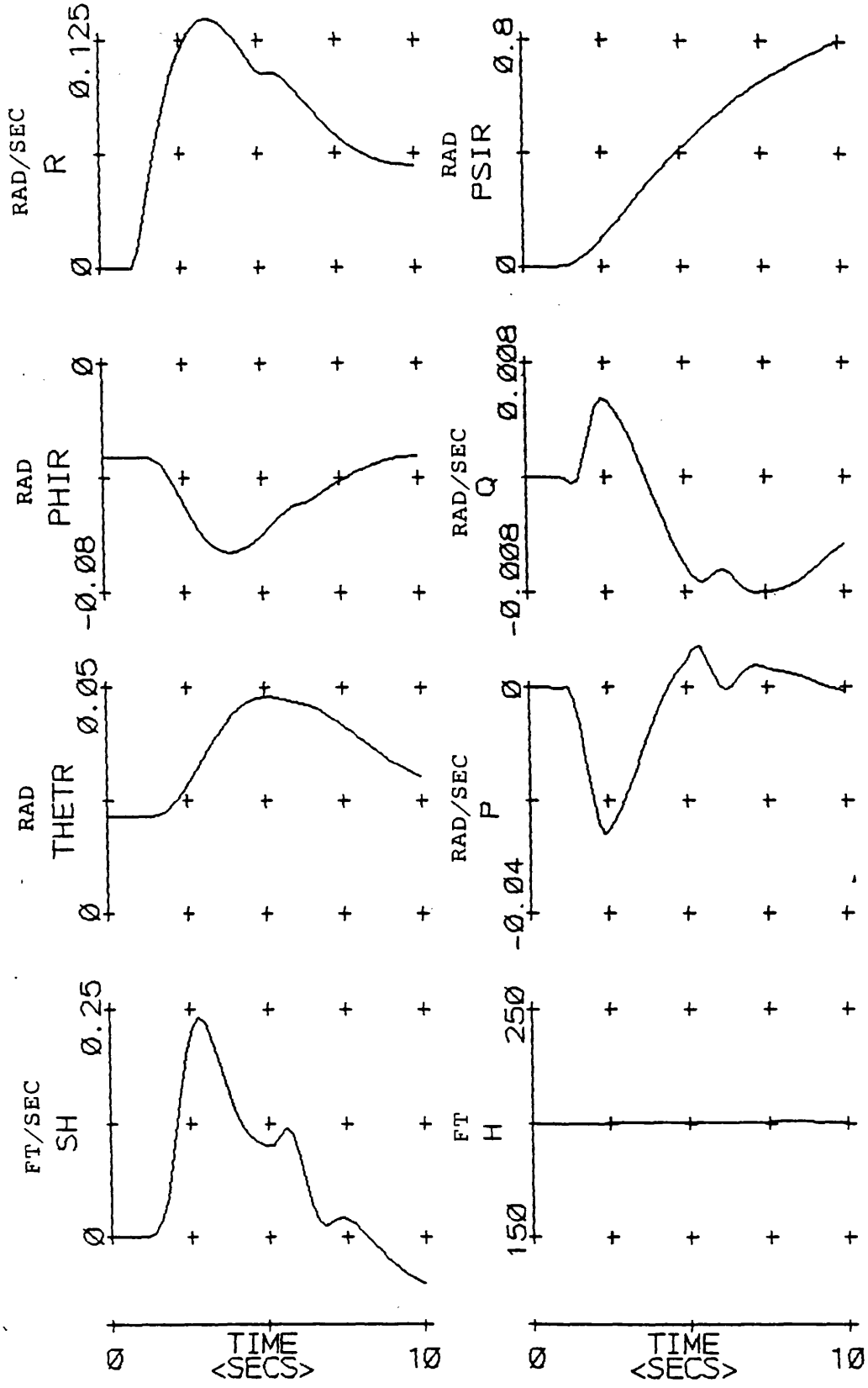

Figure 6.6 Helisim Model Without Turbulence And Without Noise

Step Input Of Amplitude 0.06 Applied To Fourth Inceptor

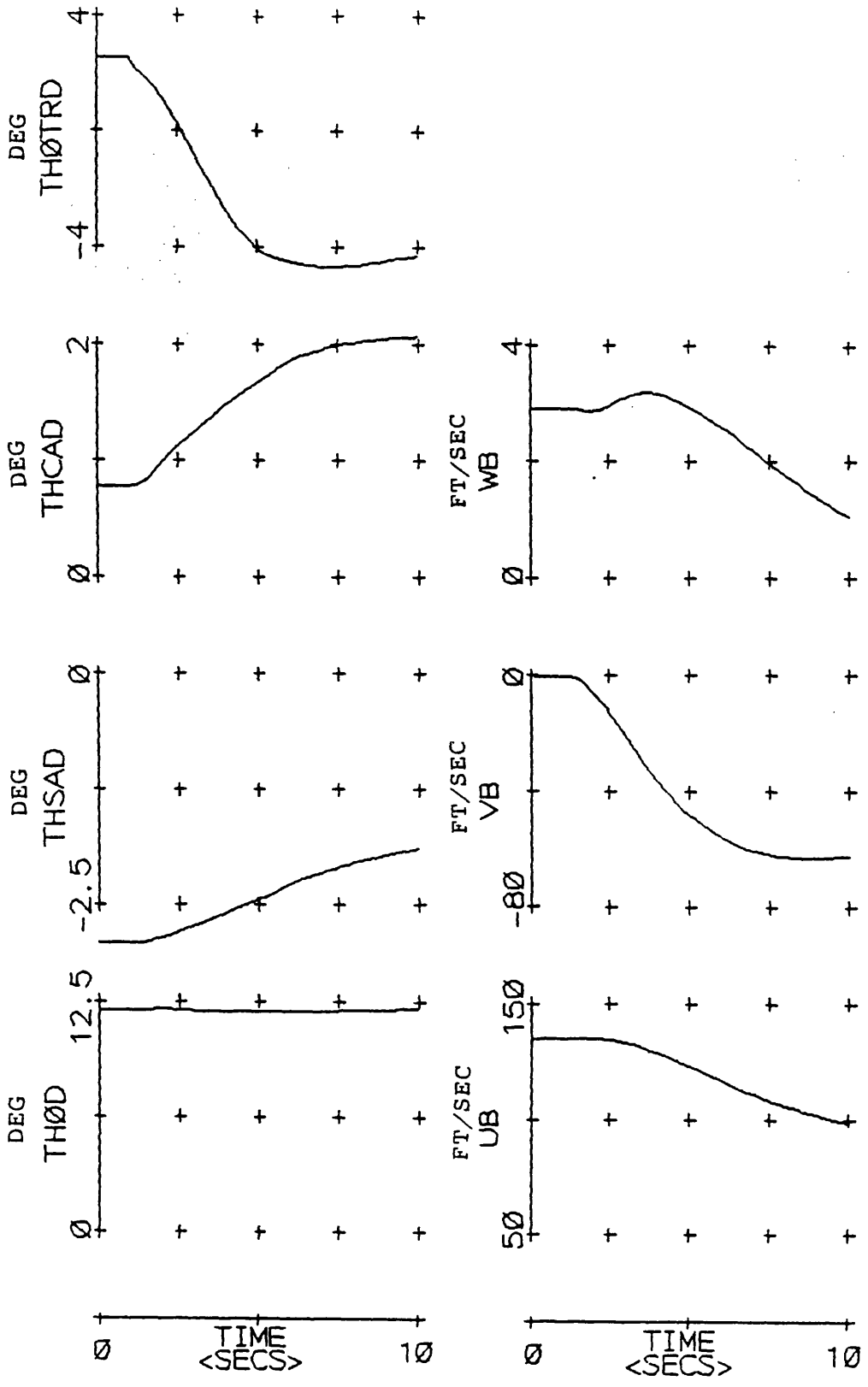
DEG
THØTRD
4
-4
DEG
THCAD
2
Ø
FT/SEC
WB
4
Ø
DEG
THSAD
Ø
-2.5
FT/SEC
VB
Ø
-8Ø
DEG
THØD
12.5
Ø
FT/SEC
UB
15Ø
5Ø
Ø
TIME
<SECS>
1Ø
Ø
TIME
<SECS>
1Ø

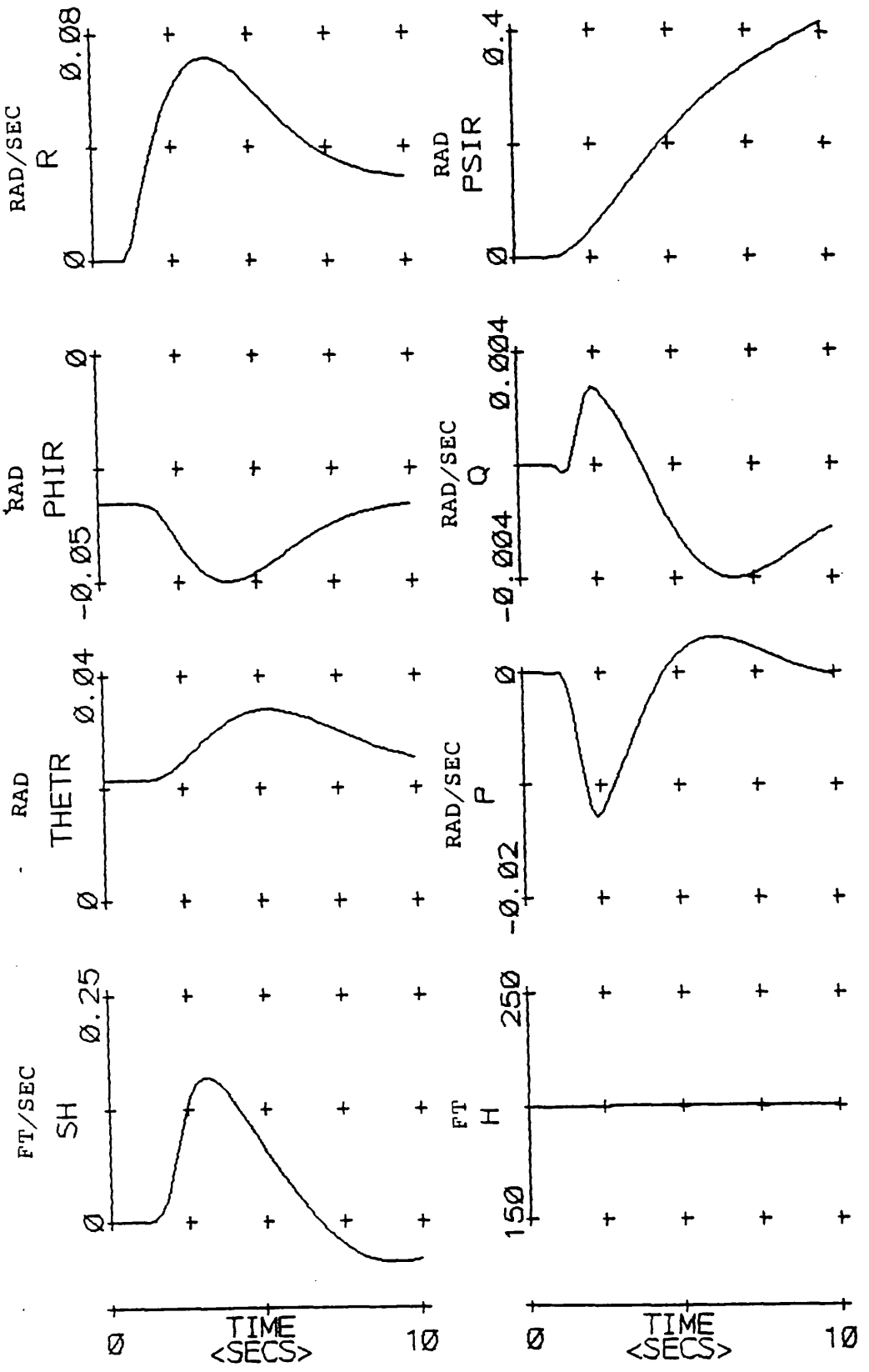

Figure 6.7 Helisim Model Without Turbulence And Without Noise

Step Input Of Amplitude 0.03 Applied To Fourth Inceptor

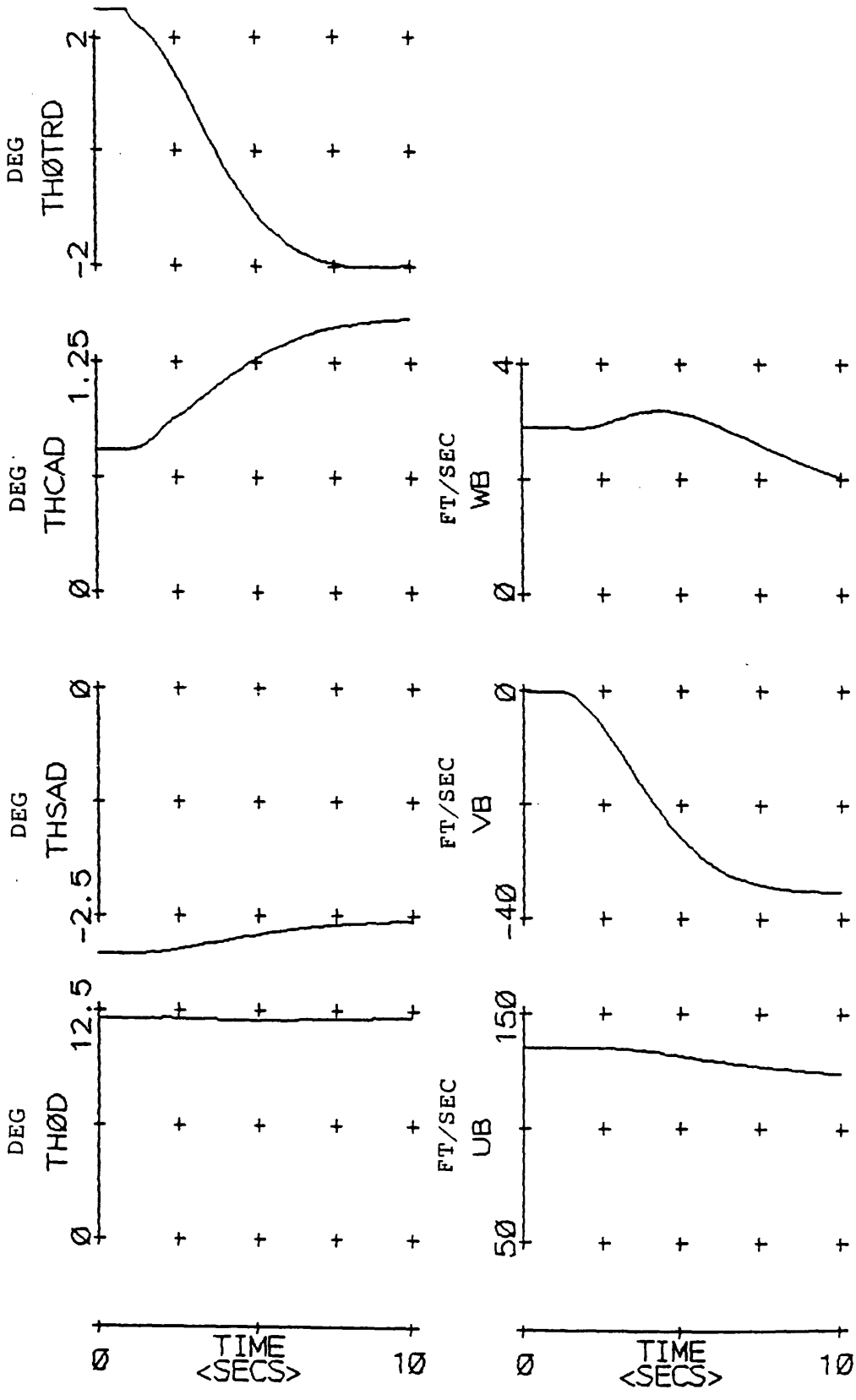
DEG
THØTRD
2
-2
DEG
THCAD
1.25
Ø
DEG
THSAD
Ø
-2.5
DEG
THØD
12.5
Ø
TIME
<SECS>
Ø
1Ø
FT/SEC
WB
4
Ø
FT/SEC
VB
Ø
-4Ø
FT/SEC
UB
15Ø
5Ø
TIME
<SECS>
Ø
1Ø

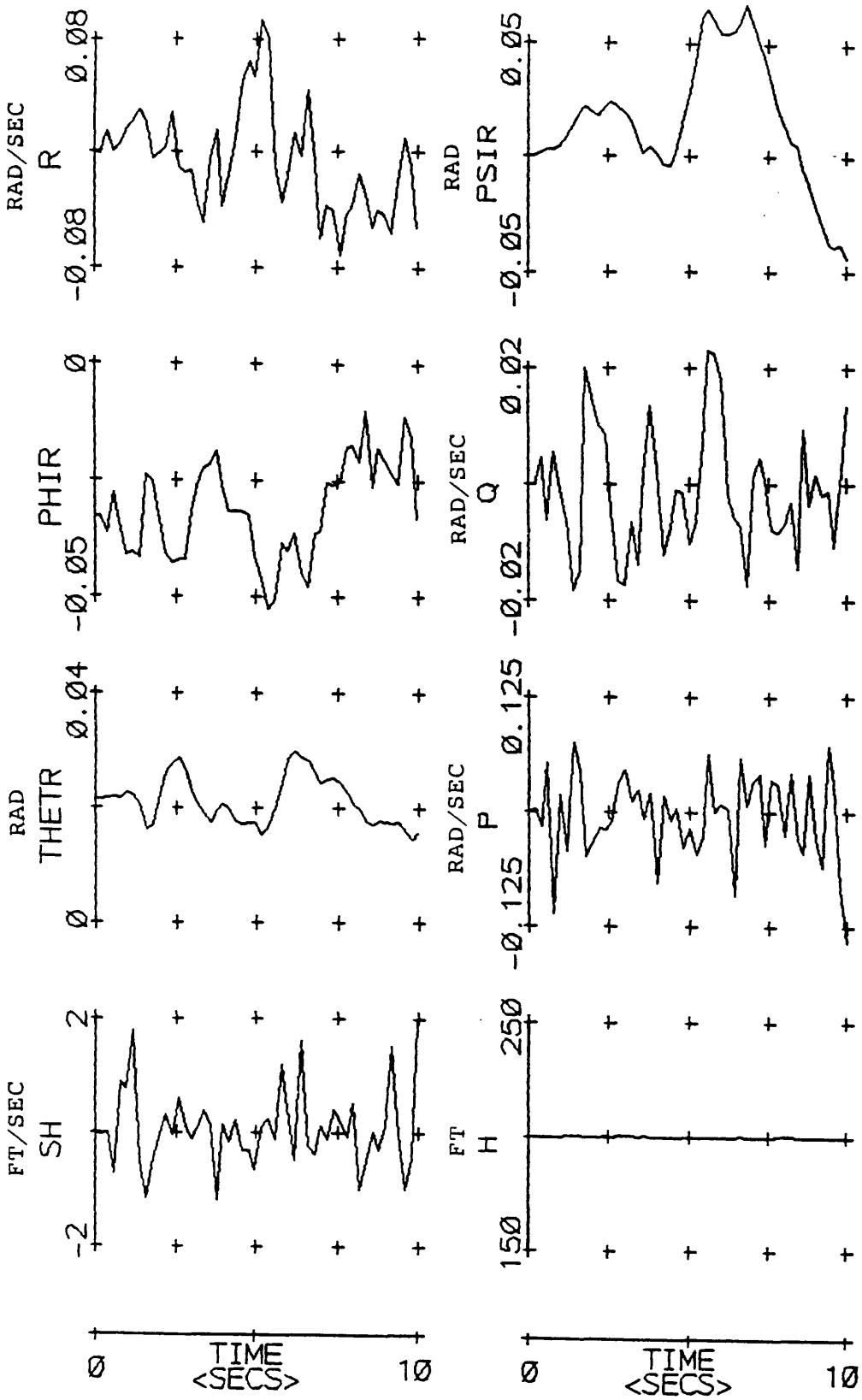

Figure 6.8 Helisim Model With Turbulence But Without Noise

Trim Condition

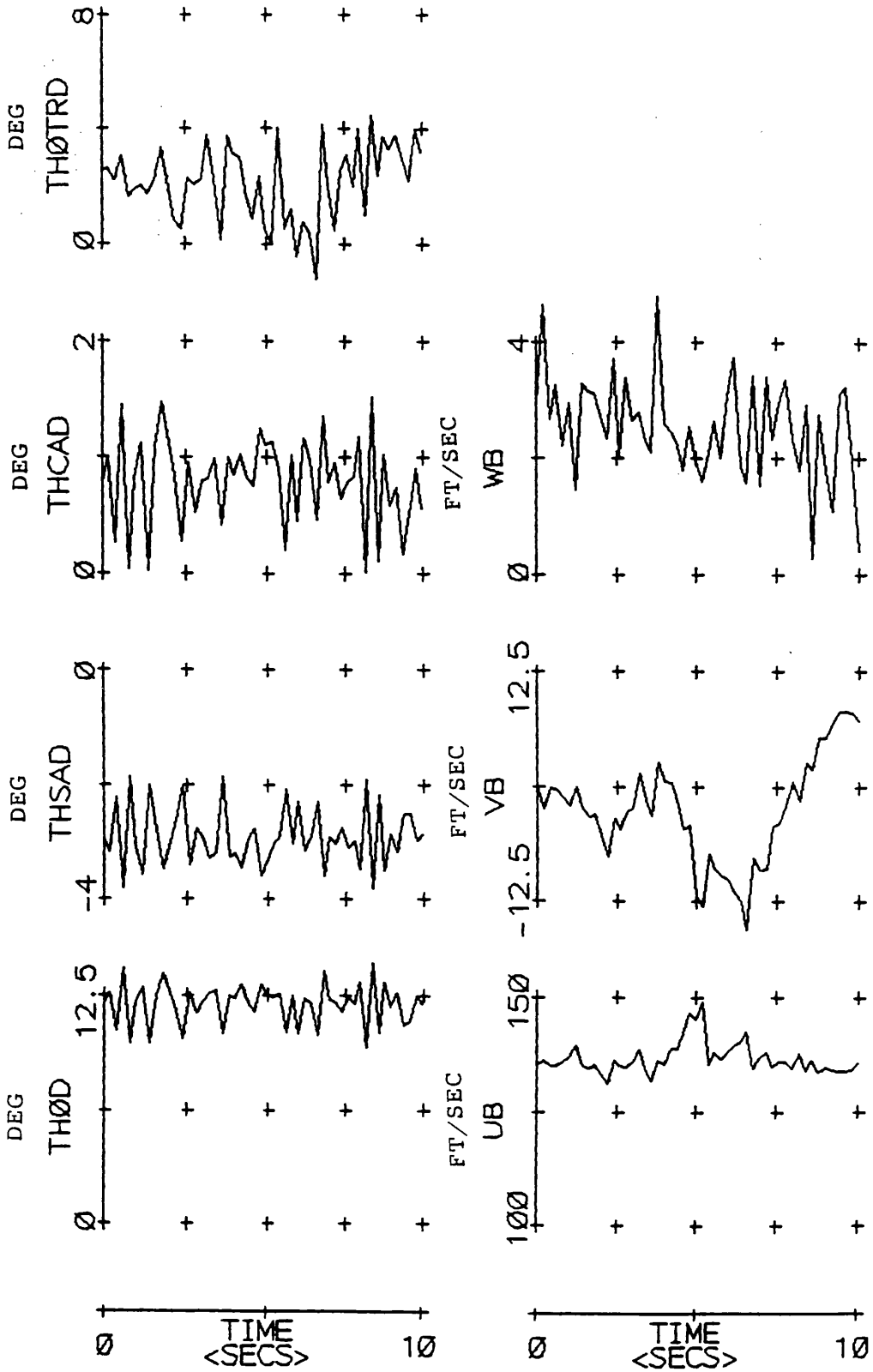
DEG
THØTRD
8
Ø
DEG
THCAD
2
Ø
FT/SEC
WB
4
Ø
DEG
THSAD
Ø
-4
FT/SEC
VB
12.5
-12.5
DEG
THØD
12.5
Ø
FT/SEC
UB
15Ø
1ØØ
Ø
TIME
<SECS>
1Ø
Ø
TIME
<SECS>
1Ø

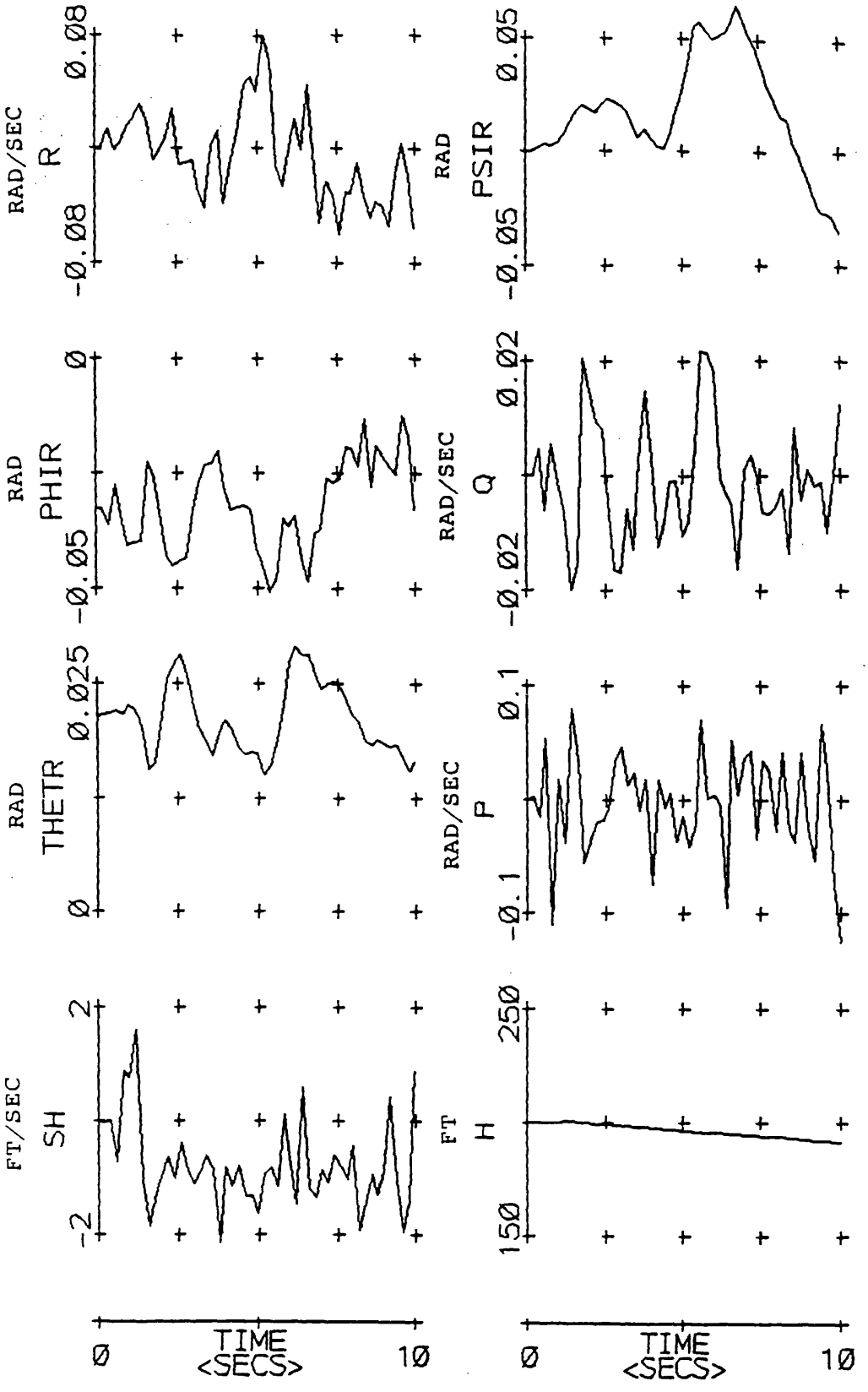

Figure 6.9 Helisim Model With Turbulence But Without Noise

Step Input Of Amplitude -1.0 Applied To First Inceptor

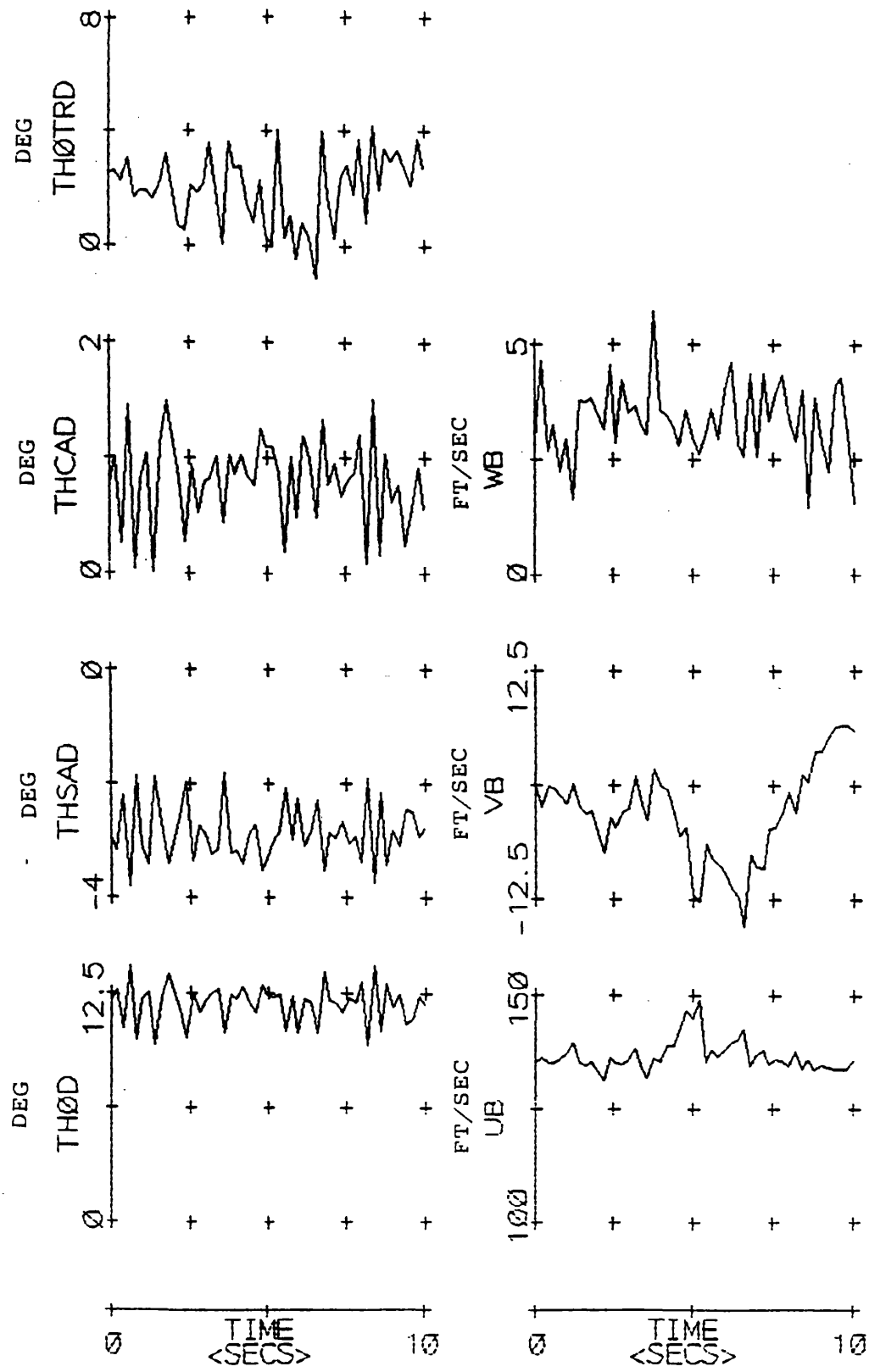
DEG
THØTRD
8
Ø
DEG
THCAD
2
Ø
FT/SEC
WB
5
Ø
DEG
THSAD
Ø
-4
FT/SEC
VB
12.5
-12.5
DEG
THØD
12.5
Ø
FT/SEC
UB
15Ø
1ØØ
TIME
<SECS>
Ø
1Ø
TIME
<SECS>
Ø
1Ø

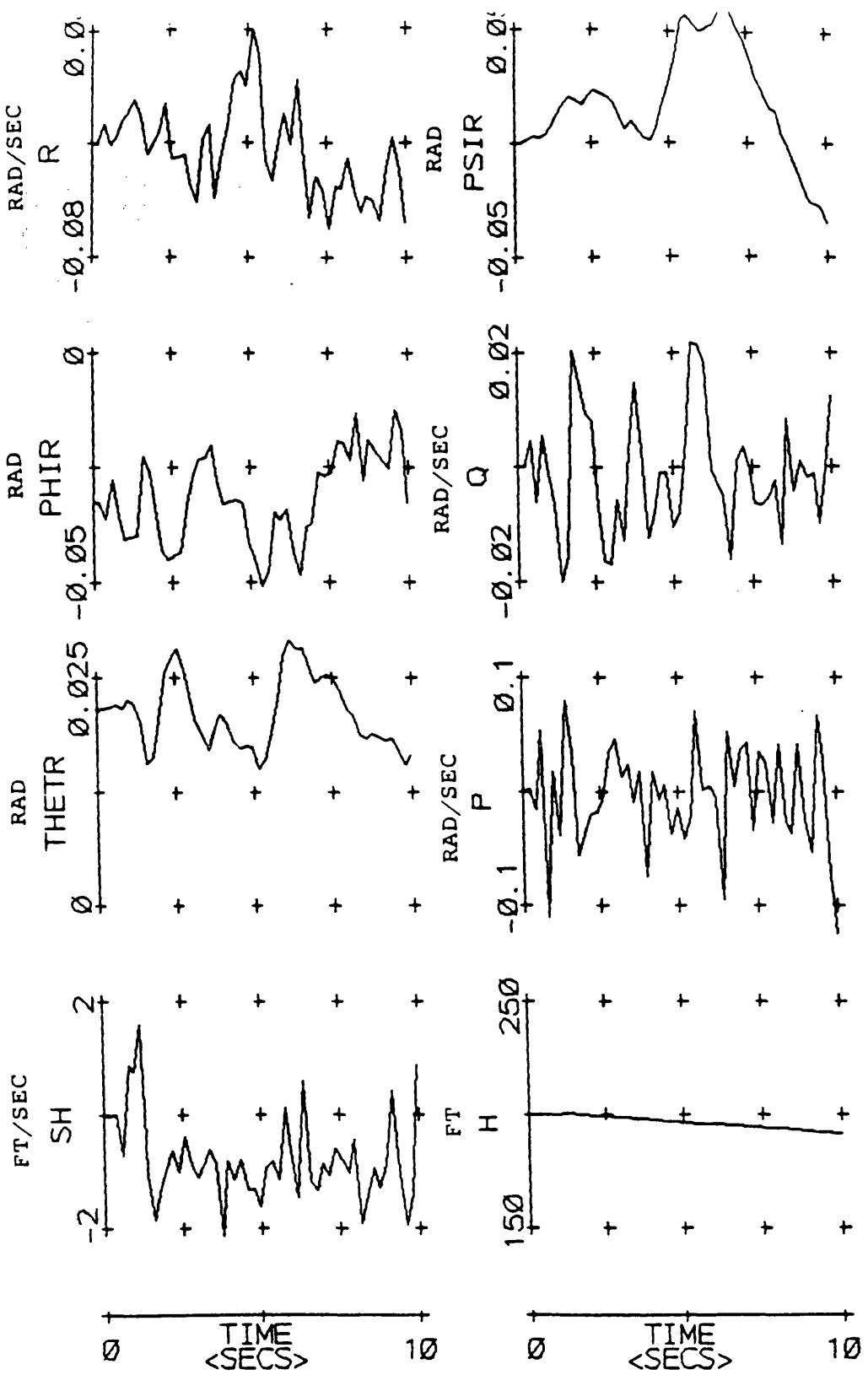

Figure 6.10 Helisim Model With Turbulence But Without Noise

Step Input Of Amplitude -1.05 Applied To First Inceptor

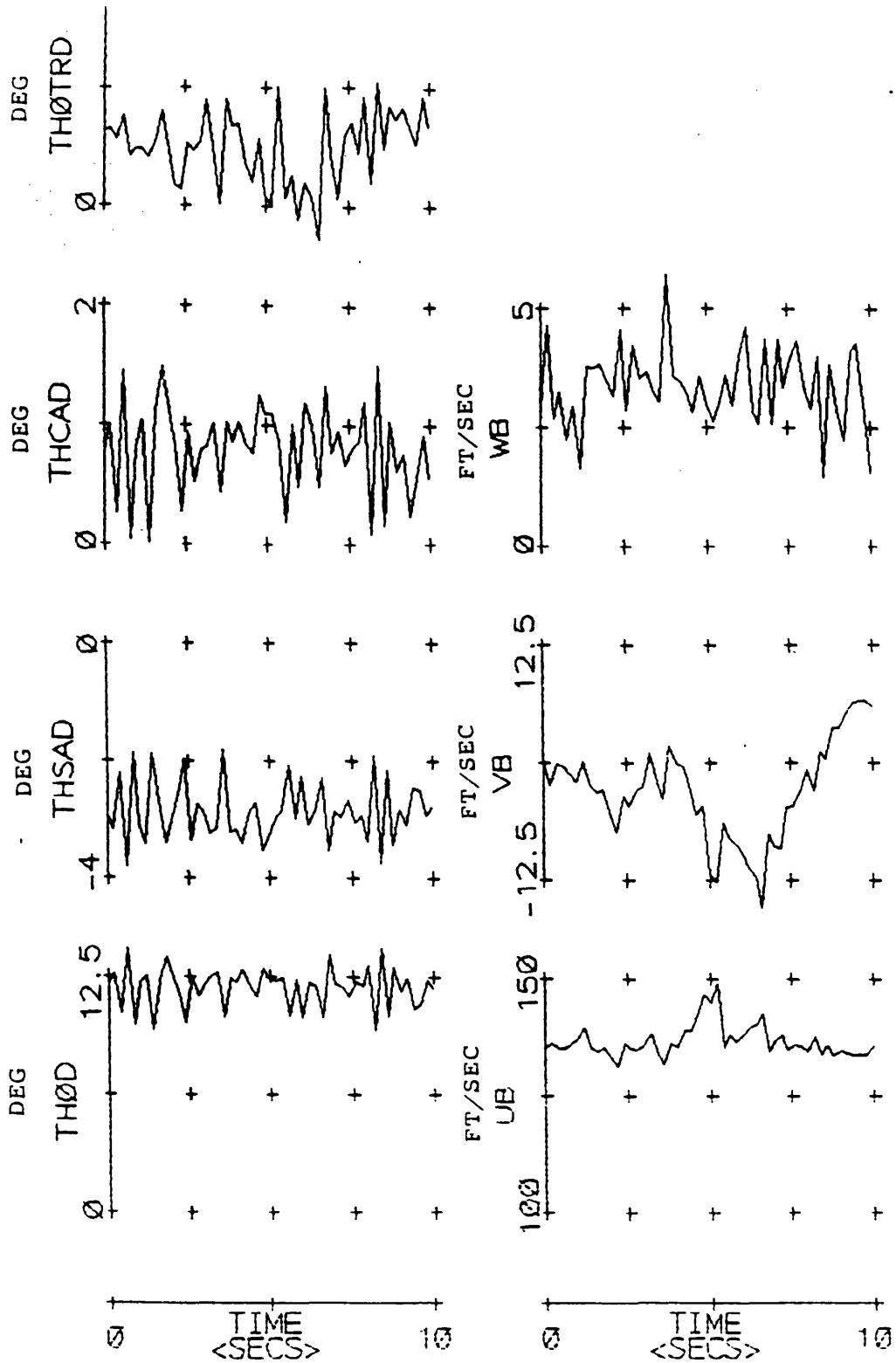
DEG
THØTRD
Ø
DEG
THCAD
2
Ø
FT/SEC
WB
5
Ø
DEG
THSAD
Ø
-4
FT/SEC
VB
12.5
-12.5
DEG
THØD
12.5
Ø
FT/SEC
UB
150
100
Ø
TIME
<SECS>
10
Ø
TIME
<SECS>
10

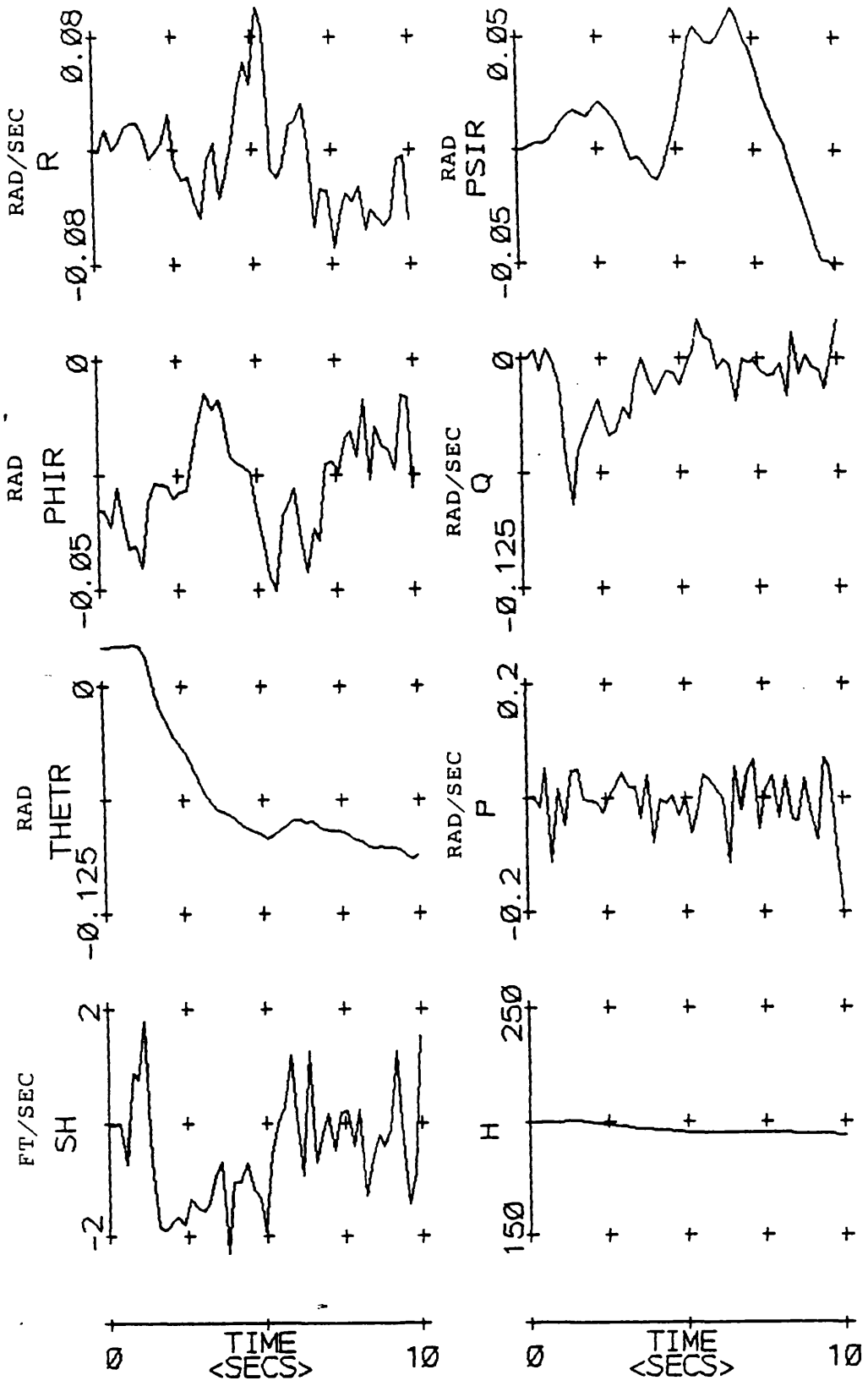

Figure 6.11 Helisim Model With Turbulence But Without Noise

Step Input Of Amplitude -0.1 Applied To Second Inceptor

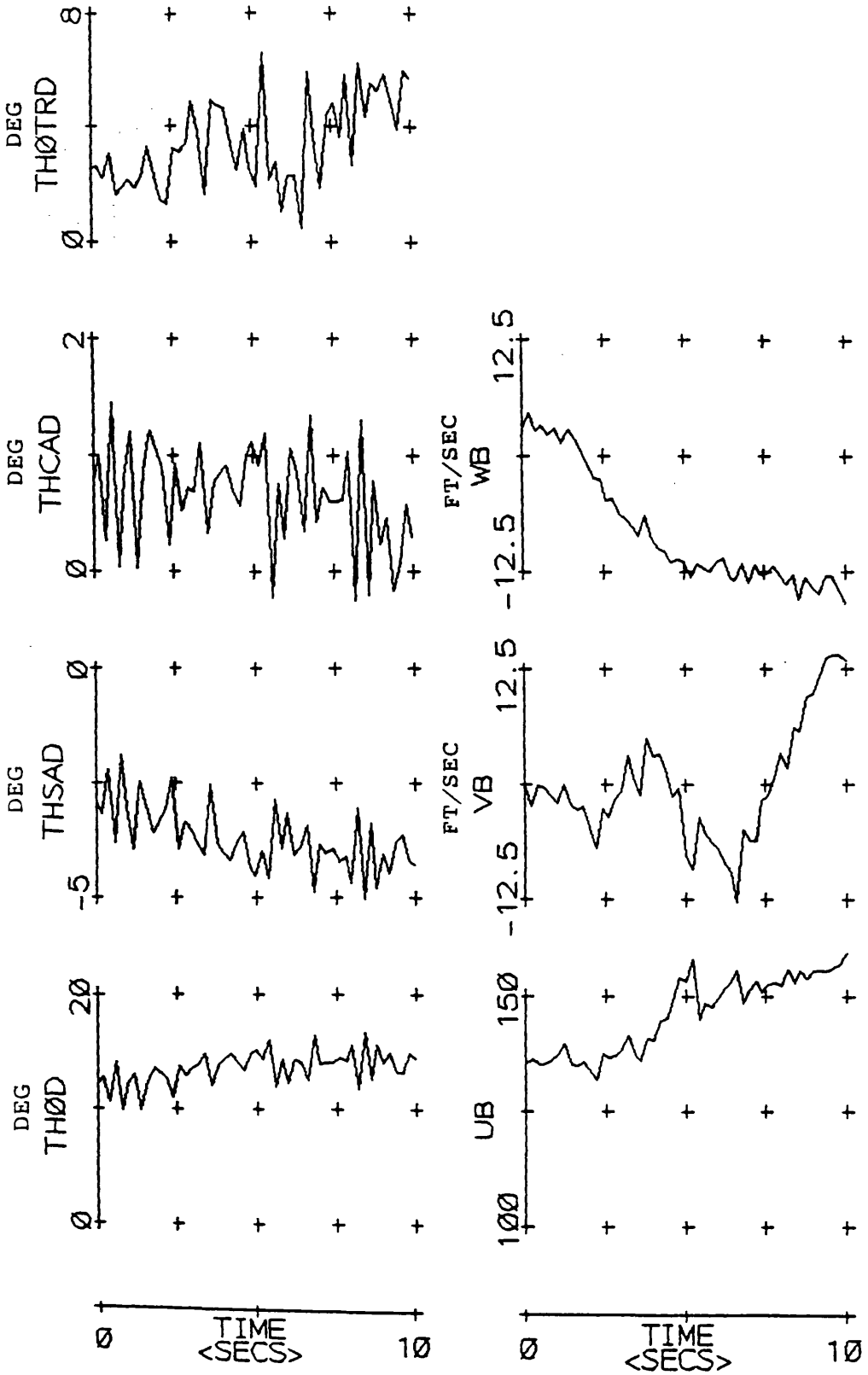
DEG
THØTRD
8
Ø
DEG
THCAD
2
Ø
DEG
THSAD
Ø
-5
DEG
THØD
2Ø
Ø
Ø
TIME
<SECS>
1Ø
FT/SEC
WB
12.5
-12.5
FT/SEC
VB
12.5
-12.5
UB
15Ø
1ØØ
Ø
TIME
<SECS>
1Ø

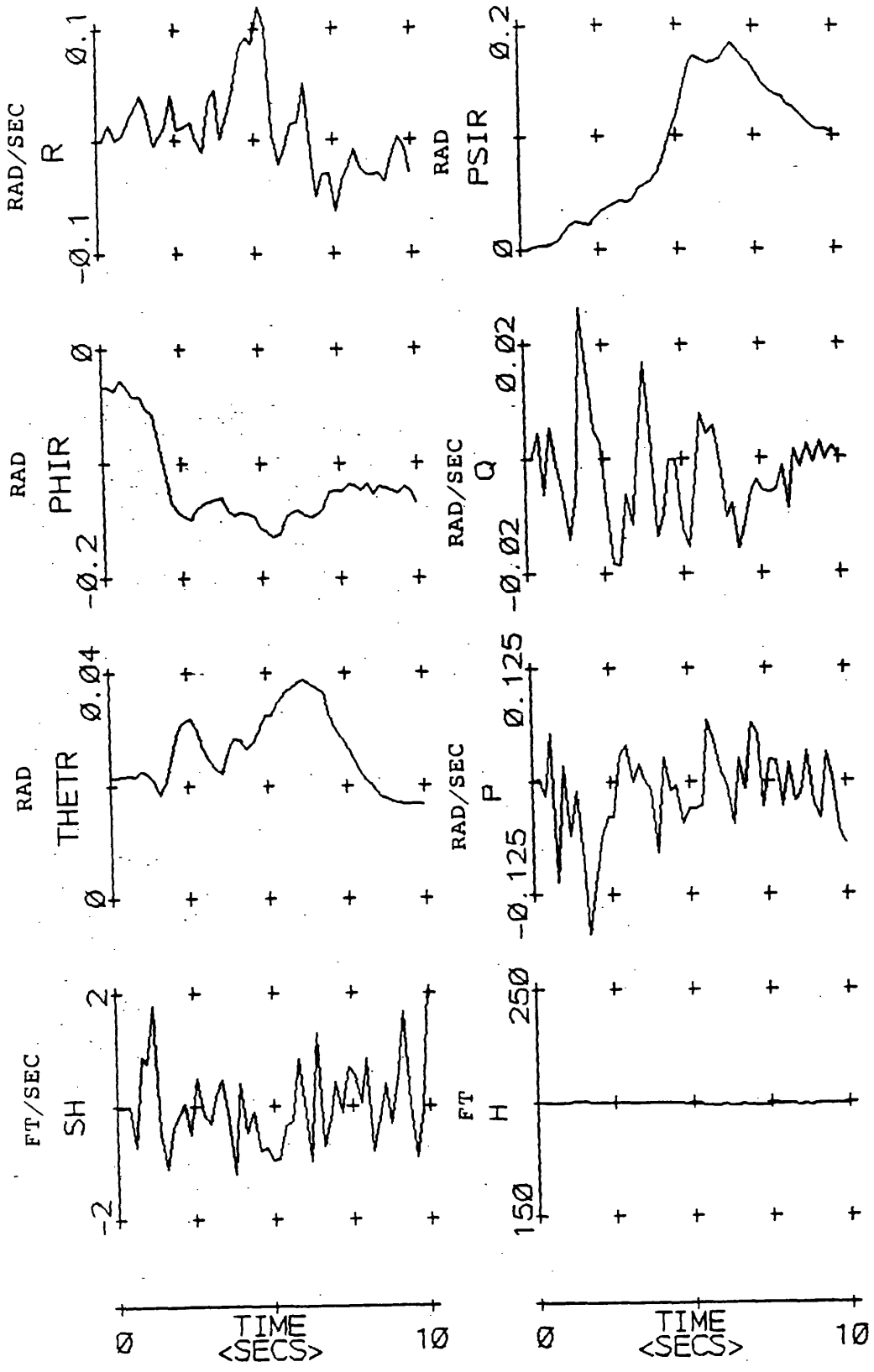

Figure 6.12 Helisim Model With Turbulence But Without Noise

Step Input Of Amplitude -0.1 Applied To Third Inceptor

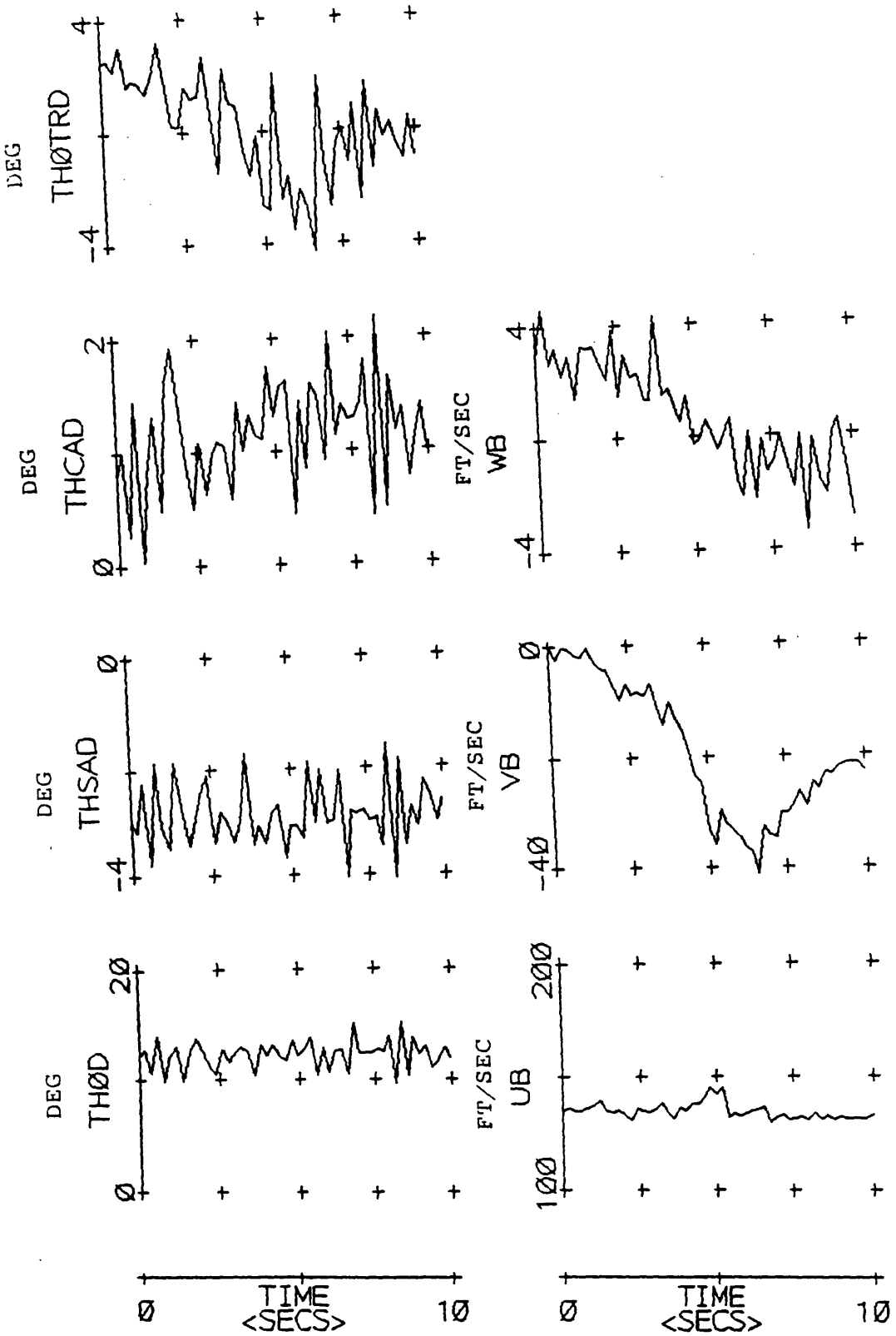
DEG
THØTRD
4
-4
DEG
THCAD
2
Ø
FT/SEC
WB
4
-4
DEG
THSAD
Ø
-4
FT/SEC
VB
Ø
-4Ø
DEG
THØD
2Ø
Ø
FT/SEC
UB
2ØØ
1ØØ
Ø
TIME
<SECS>
1Ø
Ø
TIME
<SECS>
1Ø

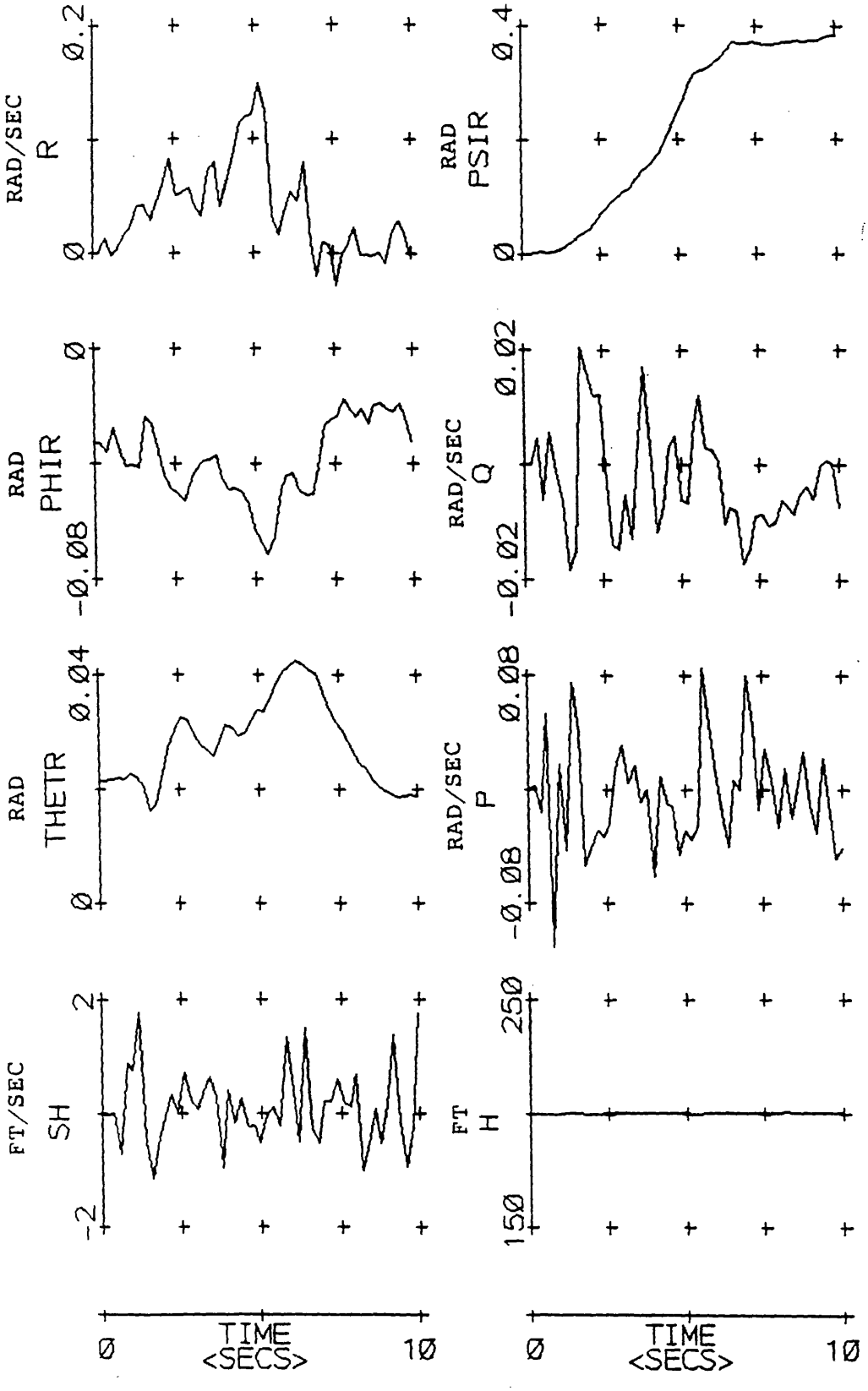

Figure 6.13 Helisim Model With Turbulence But Without Noise

Step Input Of Amplitude 0.03 Applied To Fourth Inceptor

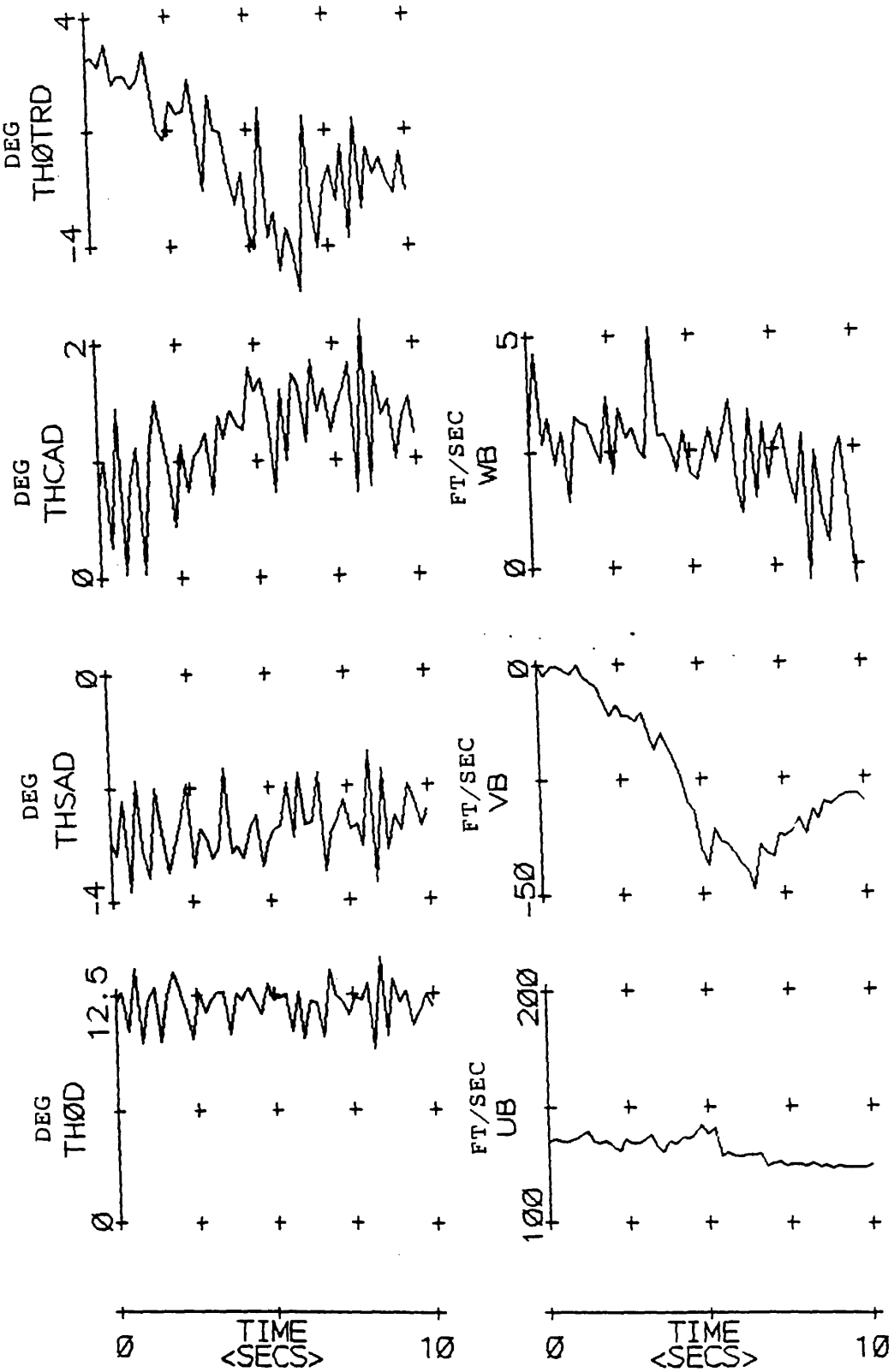
DEG
THØTRD
4
-4
DEG
THCAD
2
Ø
FT/SEC
WB
5
Ø
DEG
THSAD
Ø
-4
FT/SEC
VB
Ø
-5Ø
DEG
THØD
12.5
Ø
FT/SEC
UB
2ØØ
1ØØ
Ø
TIME
<SECS>
1Ø
Ø
TIME
<SECS>
1Ø

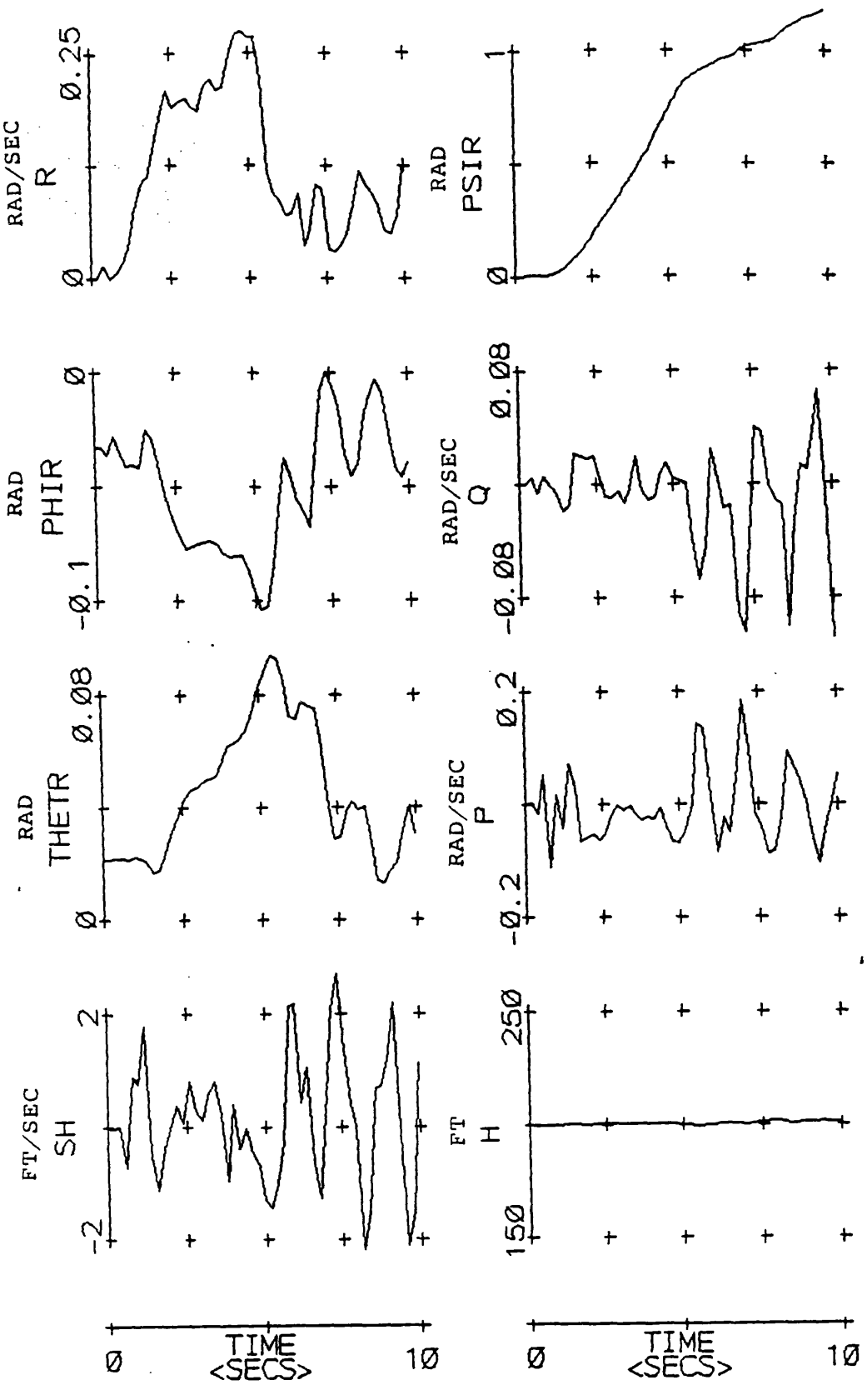

Figure 6.14 Helisim Model With Turbulence But Without Noise

Step Input Of Amplitude 0.1 Applied To Fourth Inceptor

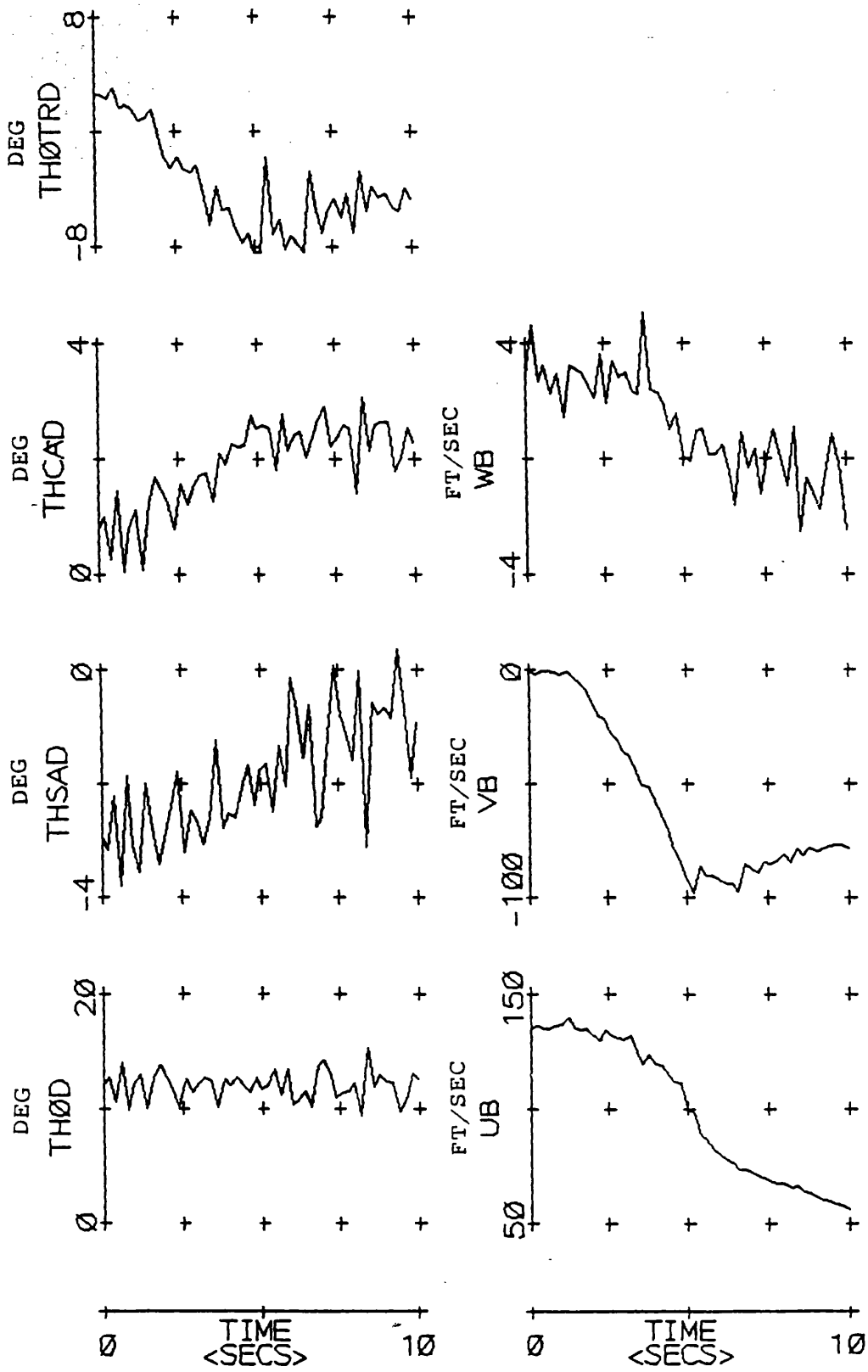
DEG
THØTRD
8
-8
DEG
THCAD
4
Ø
FT/SEC
WB
4
-4
DEG
THSAD
Ø
-4
FT/SEC
VB
Ø
-1ØØ
DEG
THØD
2Ø
Ø
FT/SEC
UB
15Ø
5Ø
Ø
TIME
<SECS>
1Ø
Ø
TIME
<SECS>
1Ø

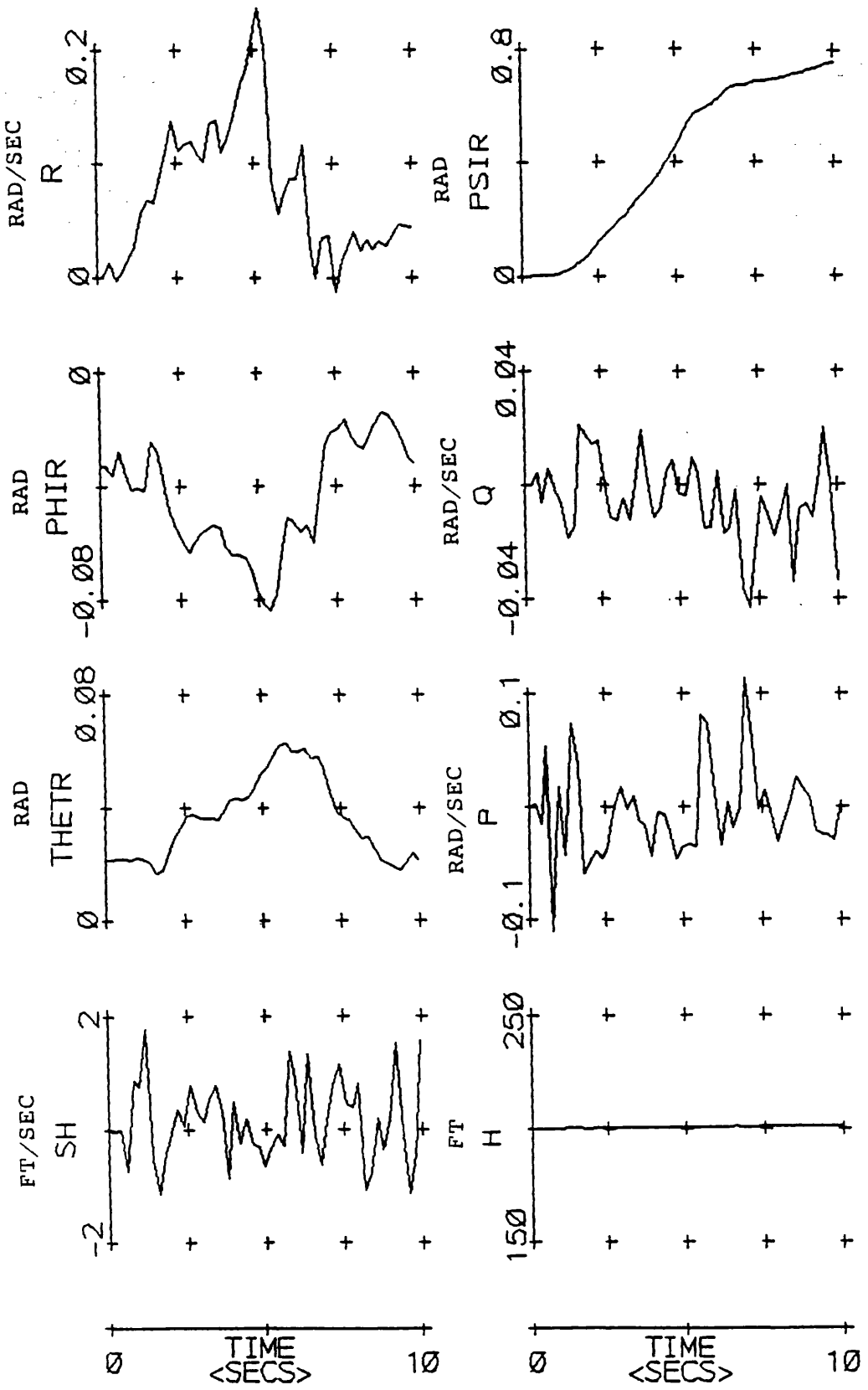

Figure 6.15 Helisim Model With Turbulence But Without Noise

Step Input Of Amplitude 0.06 Applied To Fourth Inceptor

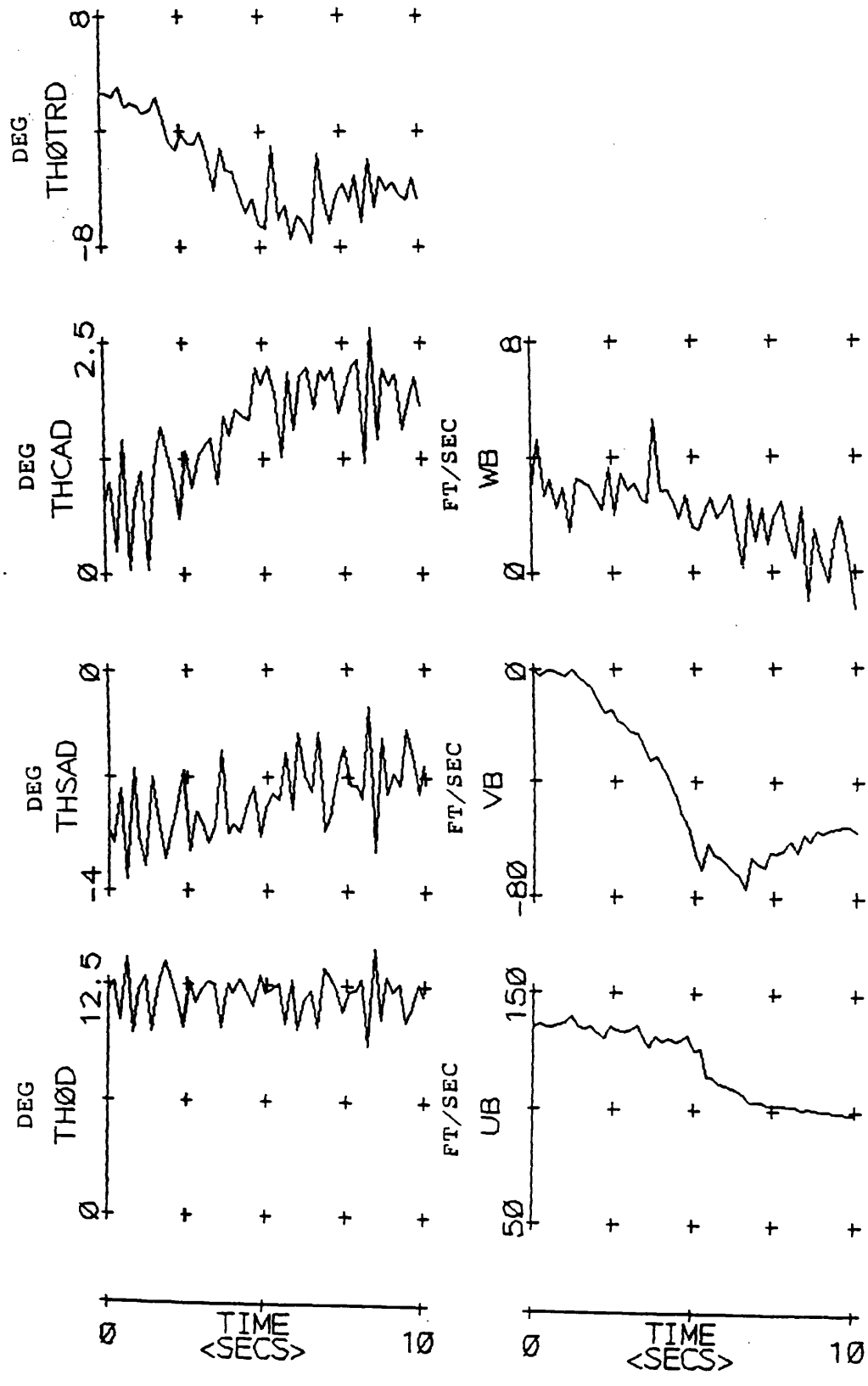
DEG
THØTRD
8
-8
DEG
THCAD
2.5
Ø
FT/SEC
WB
8
Ø
DEG
THSAD
Ø
-4
FT/SEC
VB
Ø
-8Ø
DEG
THØD
12.5
Ø
FT/SEC
UB
15Ø
5Ø
Ø
TIME
<SECS>
1Ø
Ø
TIME
<SECS>
1Ø

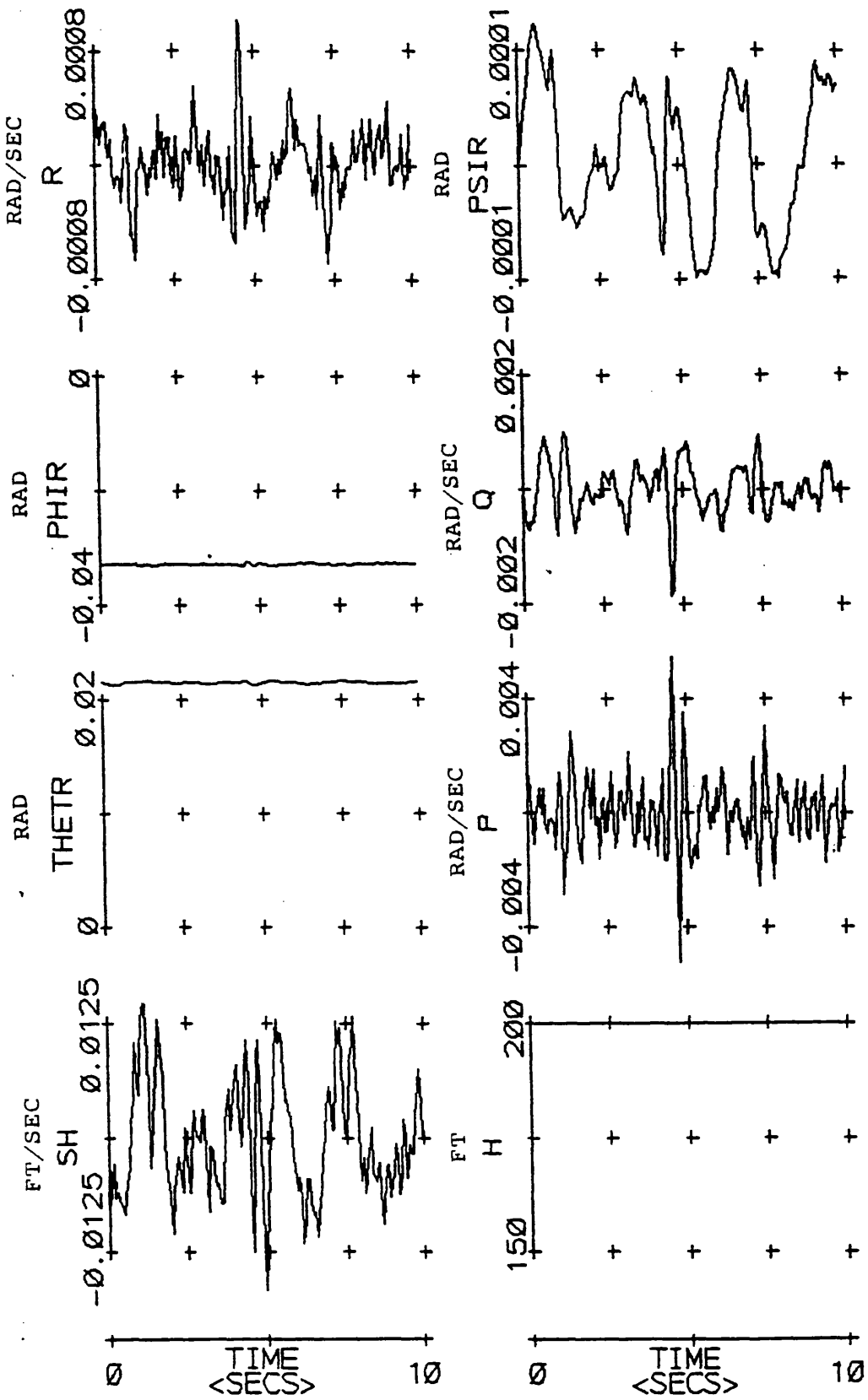

Figure 6.16 Helisim Model Without Turbulence But With Noise Trim Condition

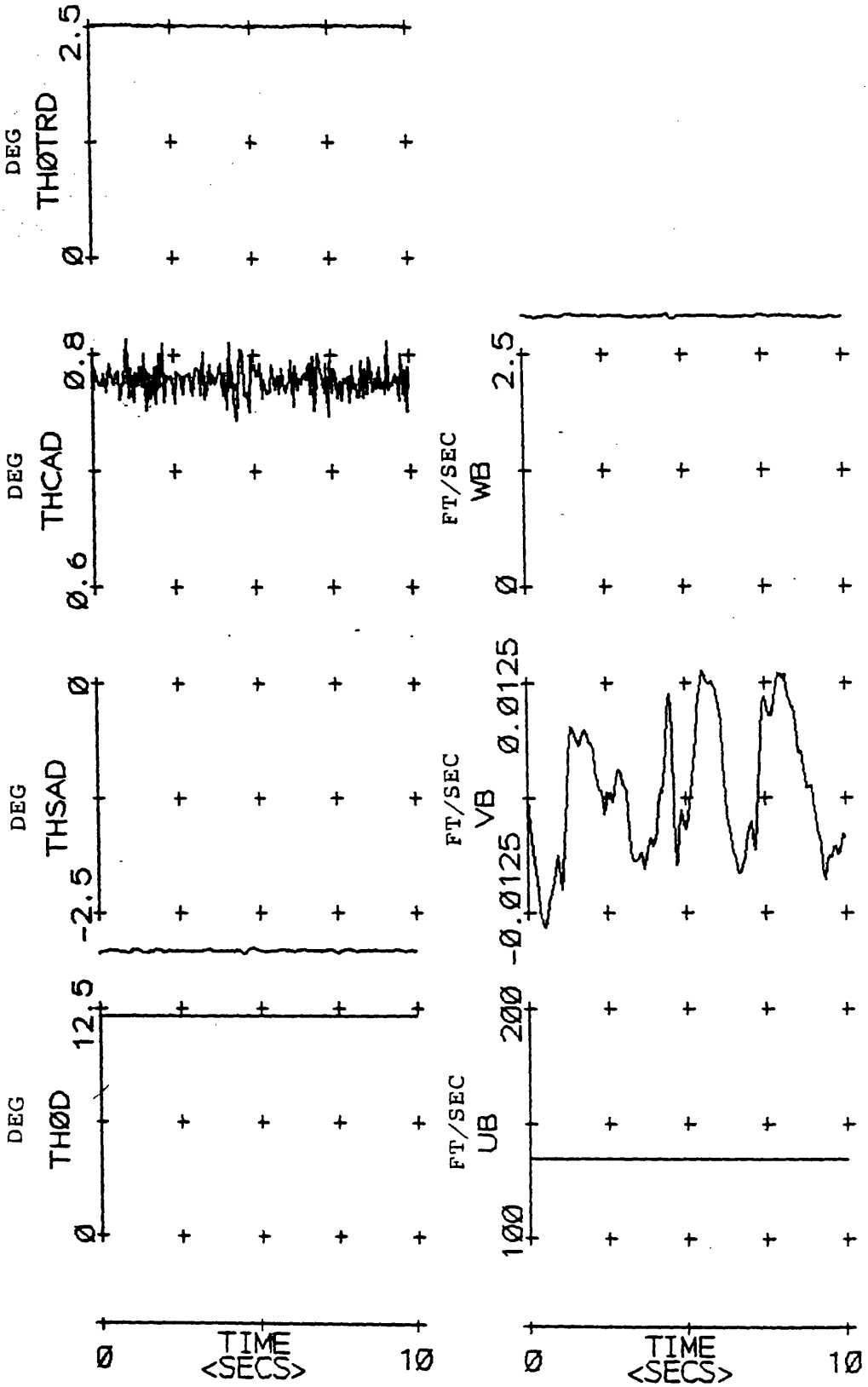
DEG
THØTRD
2.5
Ø
DEG
THCAD
Ø.8
Ø.6
FT/SEC
WB
2.5
Ø
DEG
THSAD
Ø
-2.5
FT/SEC
VB
Ø.Ø125
-Ø.Ø125
DEG
THØD
12.5
Ø
FT/SEC
UB
2ØØ
1ØØ
Ø
TIME
<SECS>
1Ø
Ø
TIME
<SECS>
1Ø

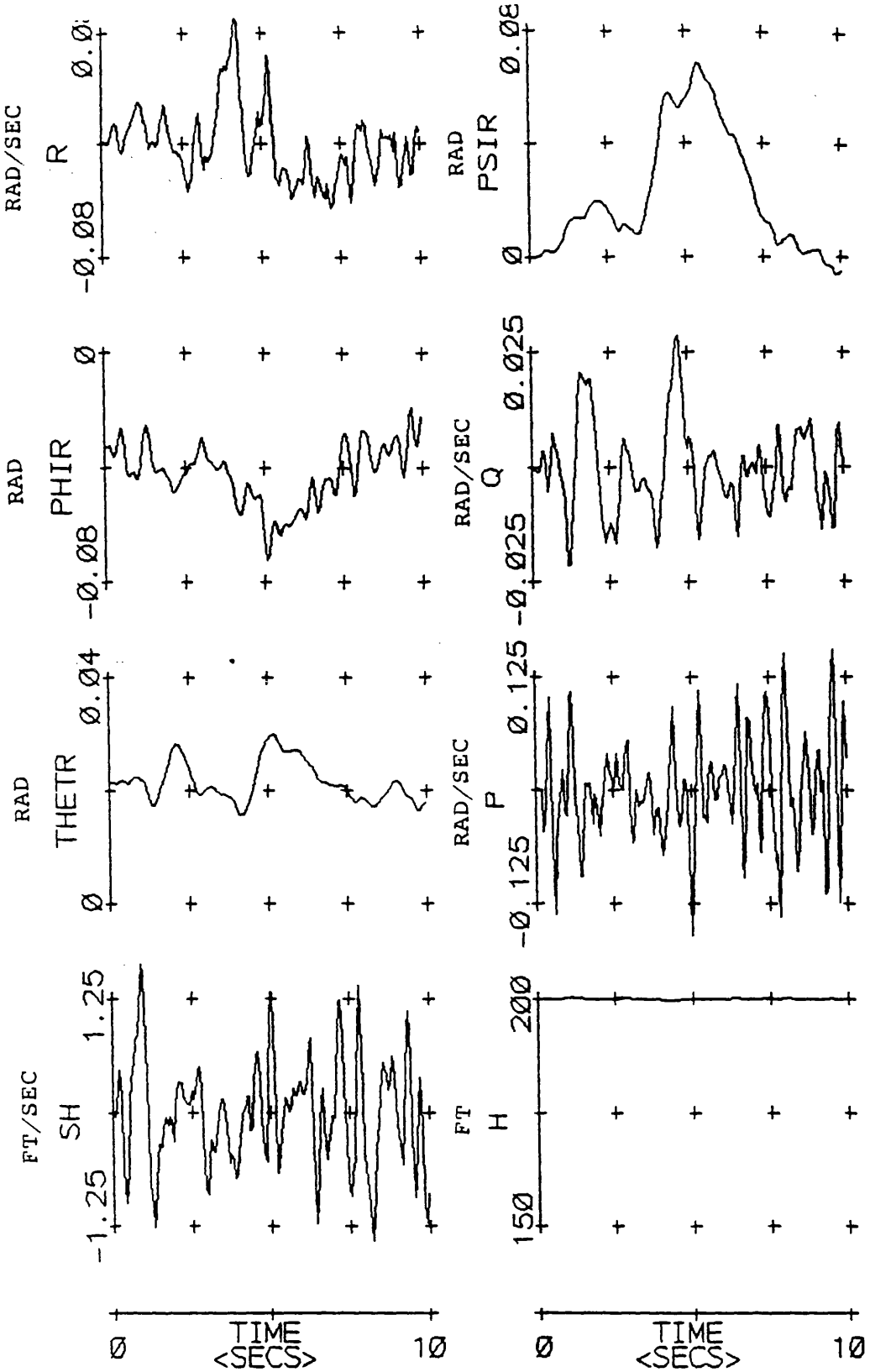

Figure 6.17 Helisim Model With Turbulence And Noise

Trim Condition

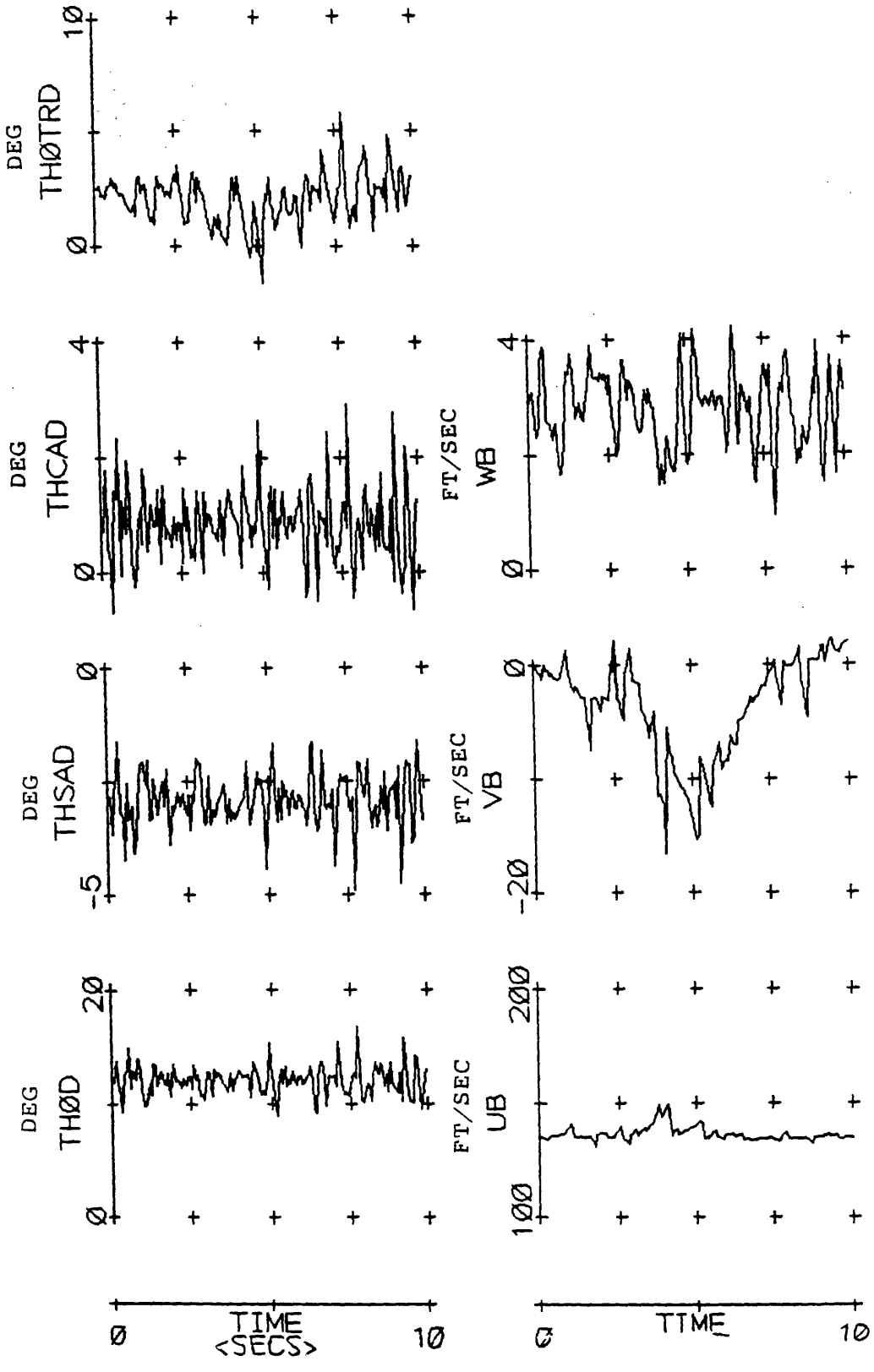
DEG
THØTRD
1Ø
Ø
DEG
THCAD
4
Ø
FT/SEC
WB
4
Ø
DEG
THSAD
Ø
-5
FT/SEC
VB
Ø
-2Ø
DEG
THØD
2Ø
Ø
FT/SEC
UB
2ØØ
1ØØ
Ø
TIME
<SECS>
1Ø
Ø
TTME
1Ø

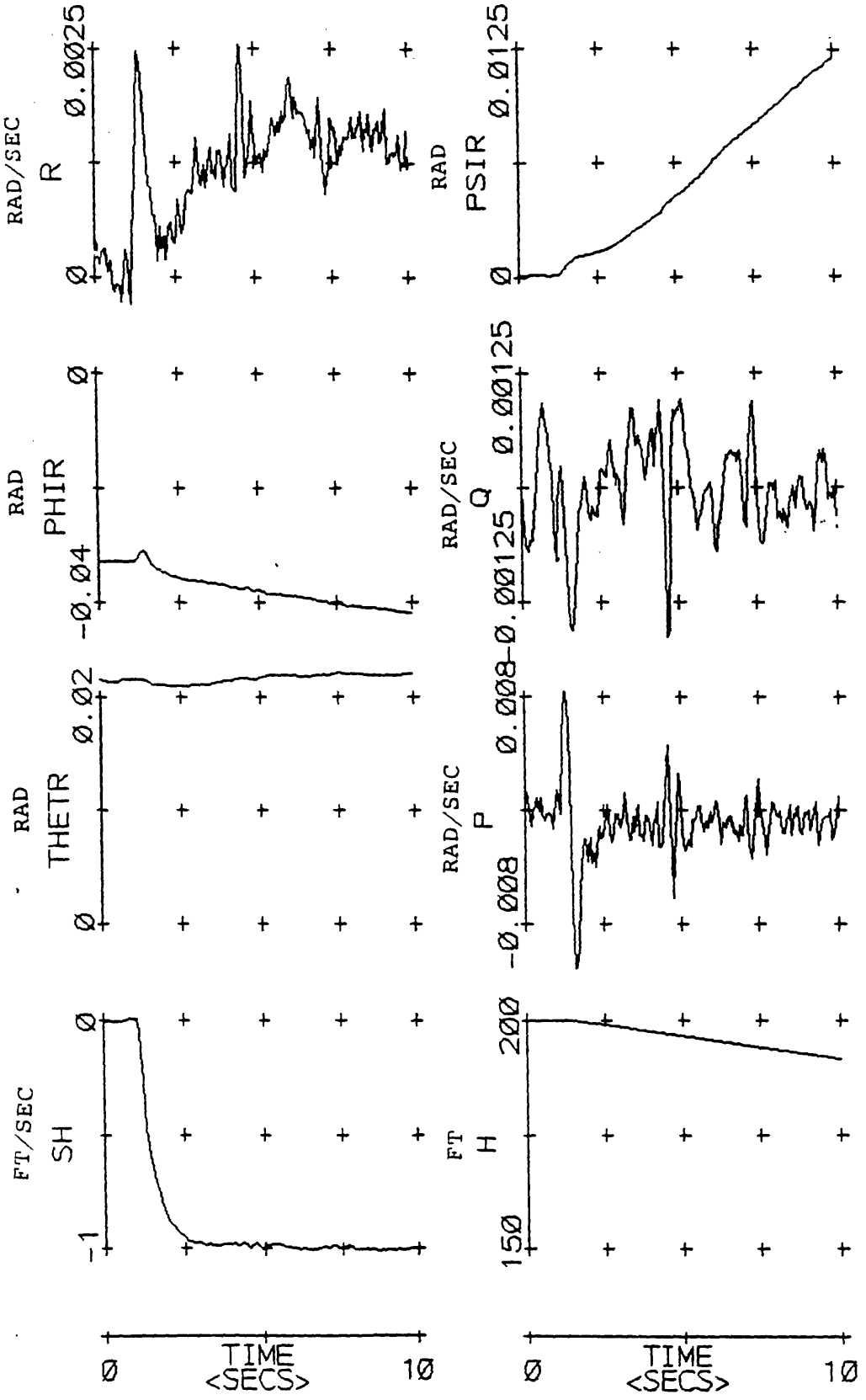

Figure 6.18 Helisim Model Without Turbulence But With Noise

Step Input Of Amplitude -1.0 Applied To First Inceptor

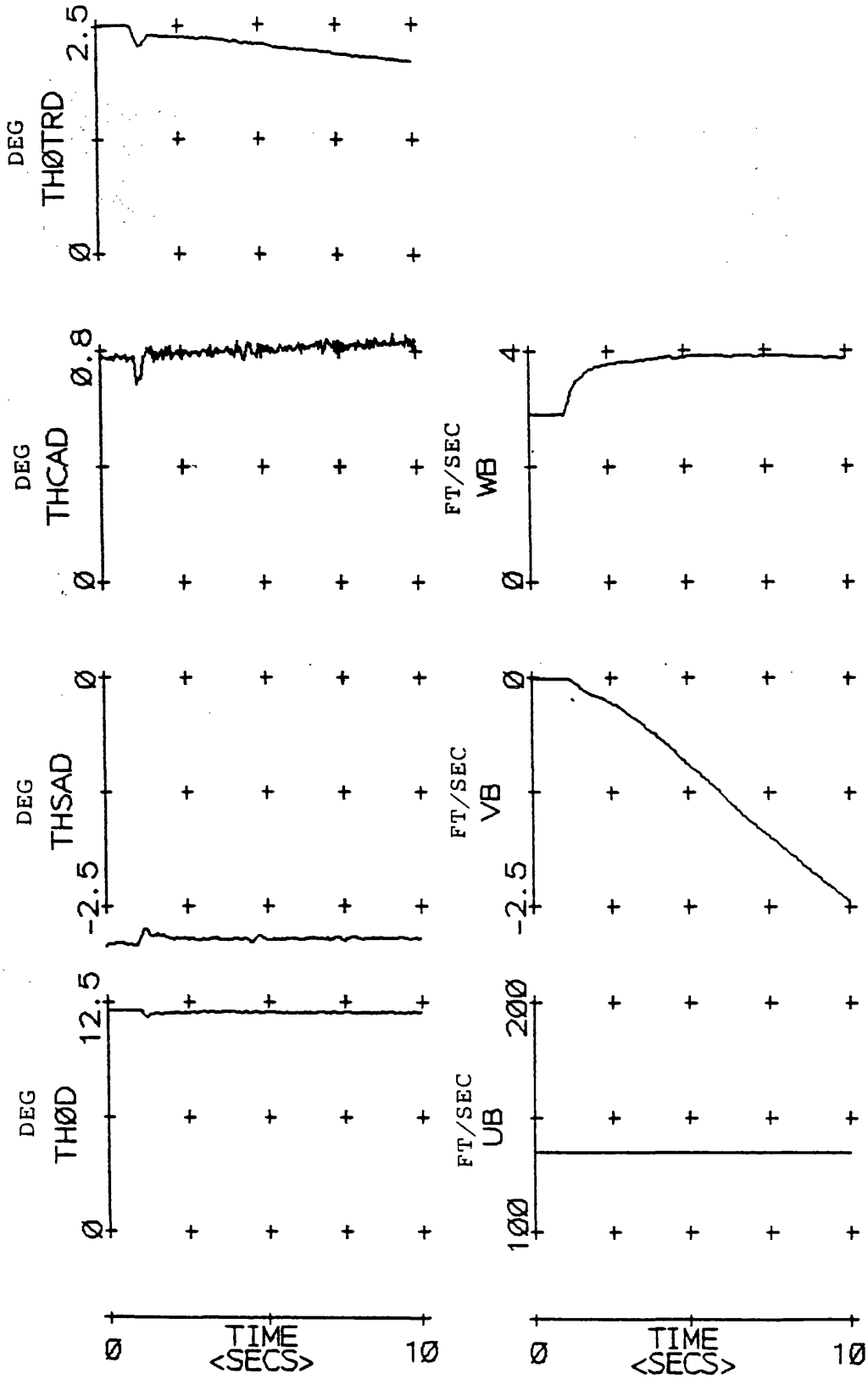
DEG
THØTRD
2.5
Ø
DEG
THCAD
Ø.8
Ø
FT/SEC
WB
4
Ø
DEG
THSAD
Ø
-2.5
FT/SEC
VB
Ø
-2.5
DEG
THØD
12.5
Ø
FT/SEC
UB
2ØØ
1ØØ
Ø
TIME
<SECS>
1Ø
Ø
TIME
<SECS>
1Ø

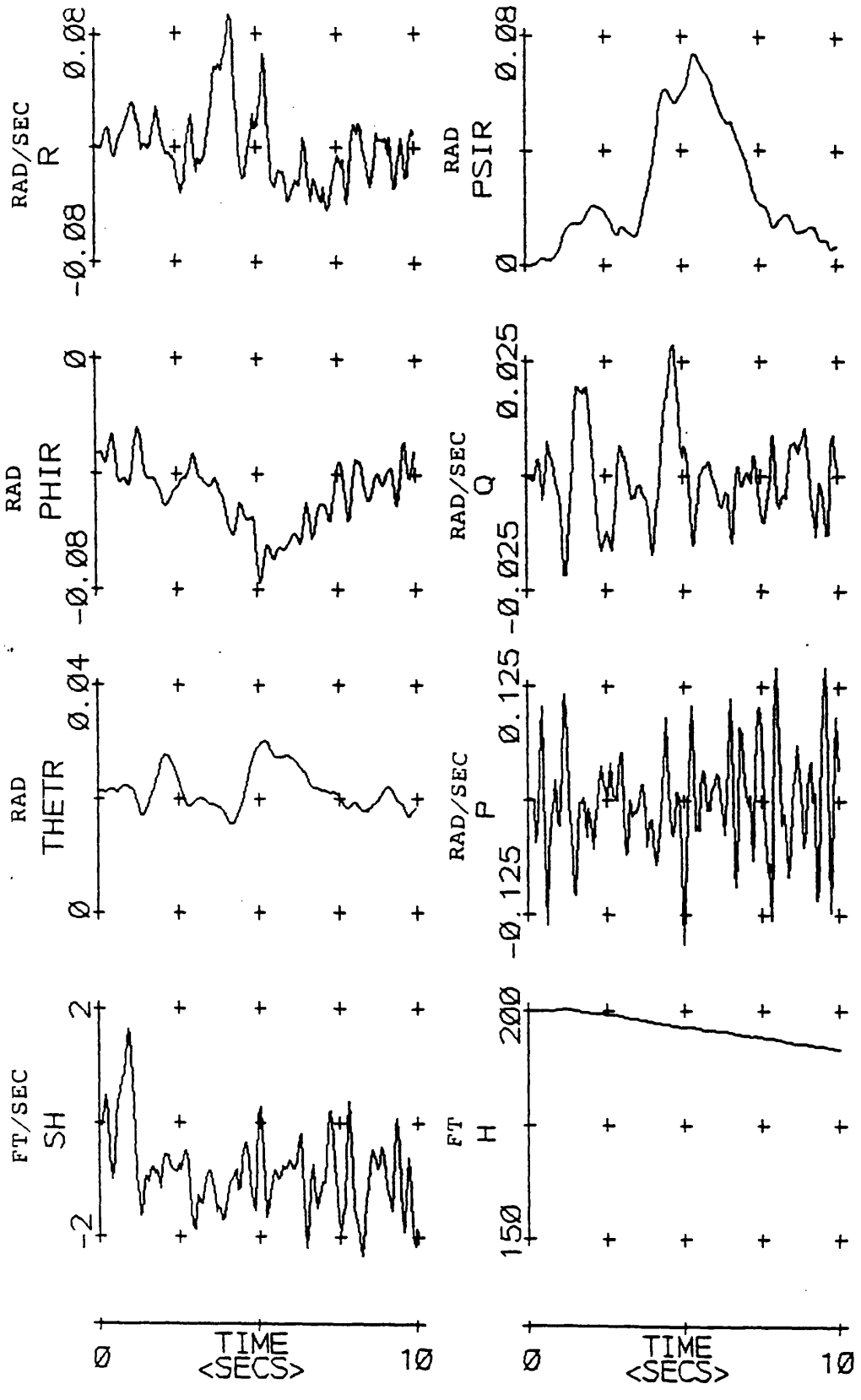

Figure 6.19 Helisim Model With Turbulence And Noise

Step Input Of Amplitude -1.0 Applied To First Inceptor

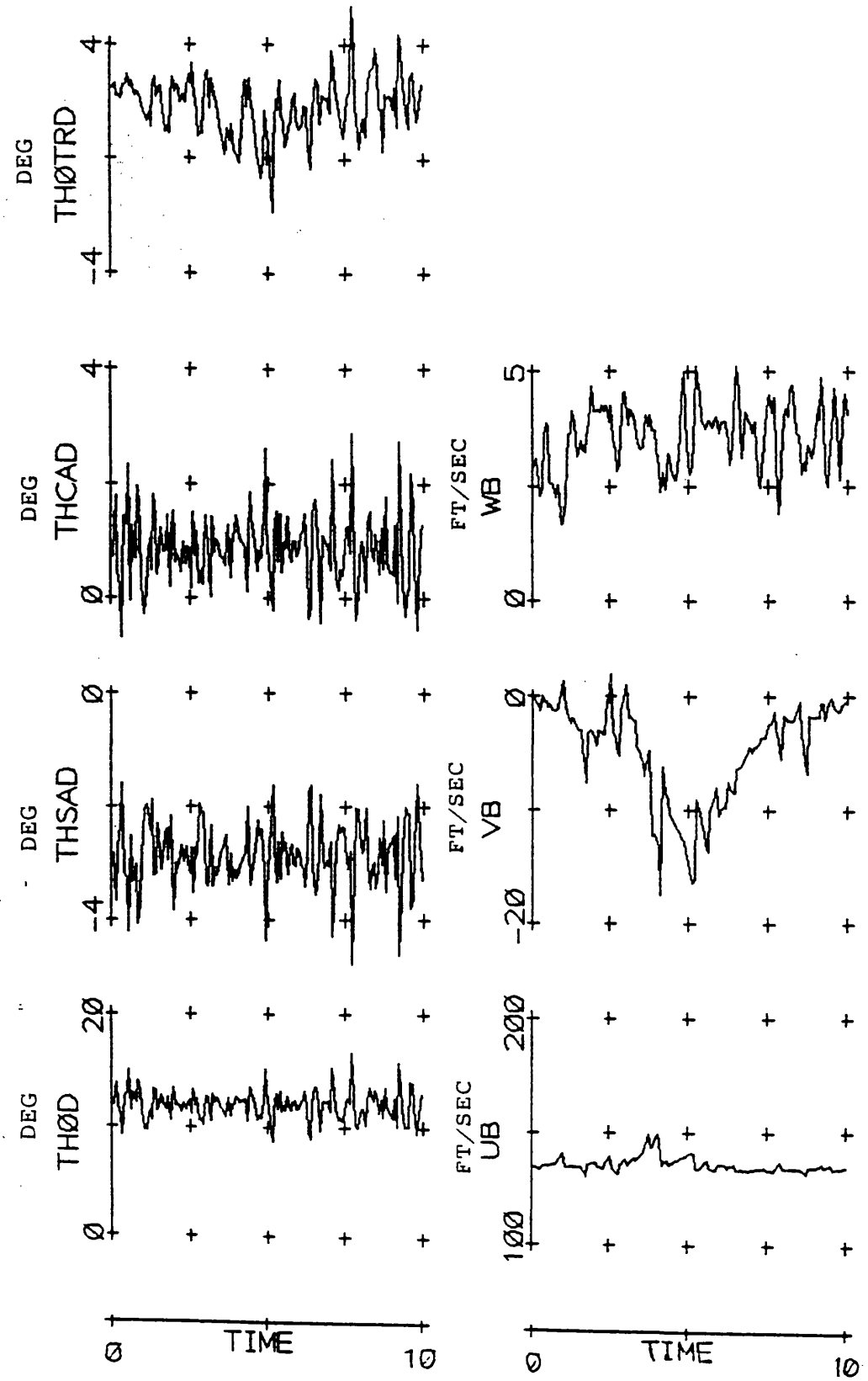
DEG
THØTRD
4
-4
DEG
THCAD
4
Ø
FT/SEC
WB
5
Ø
DEG
THSAD
Ø
-4
FT/SEC
VB
Ø
-2Ø
DEG
THØD
2Ø
Ø
FT/SEC
UB
2ØØ
1ØØ
Ø
TIME
10
Ø
TIME
10

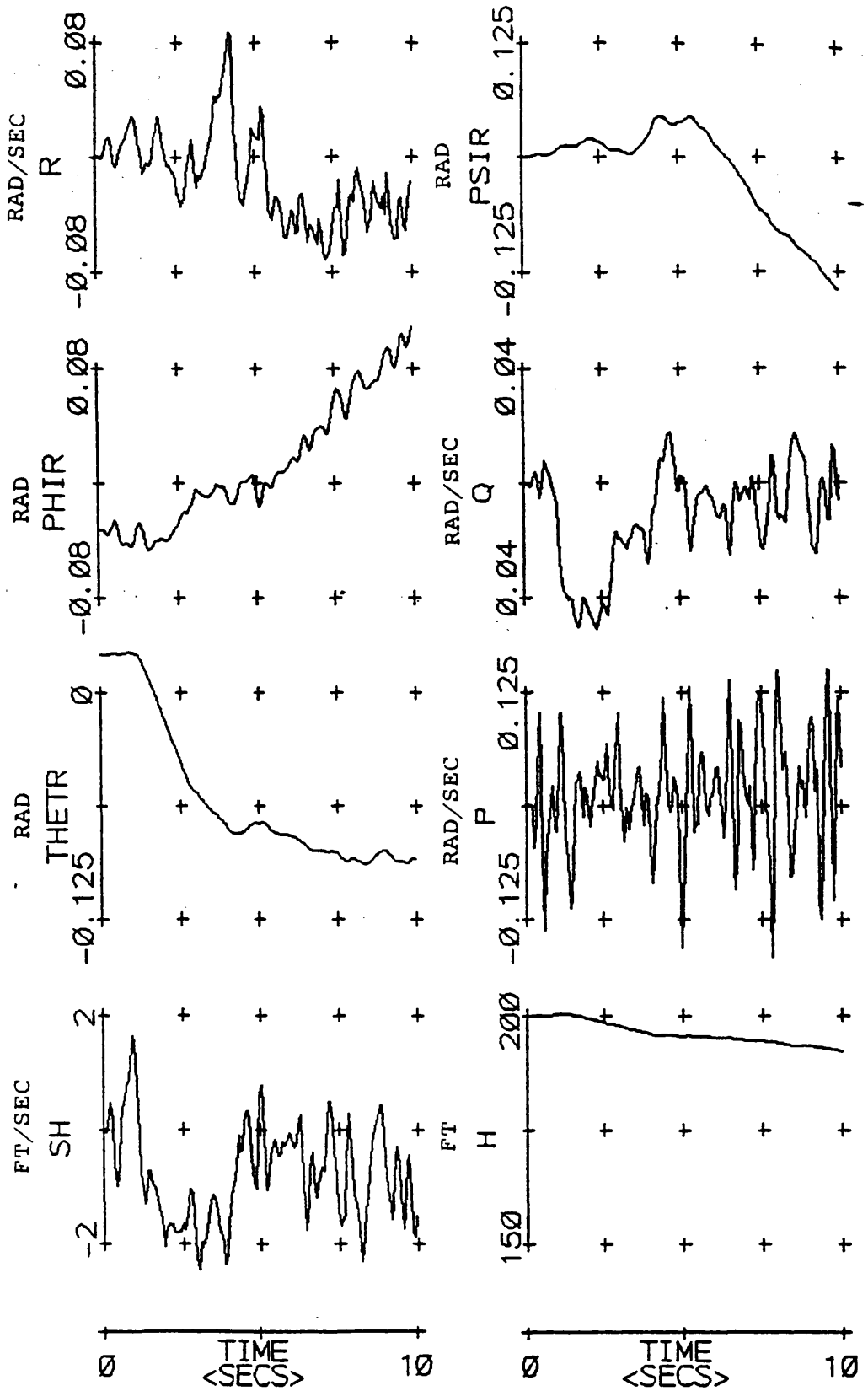

Figure 6.20 Helisim Model With Turbulence And Noise

Step Input Of Amplitude -0.1 Applied To Second Inceptor

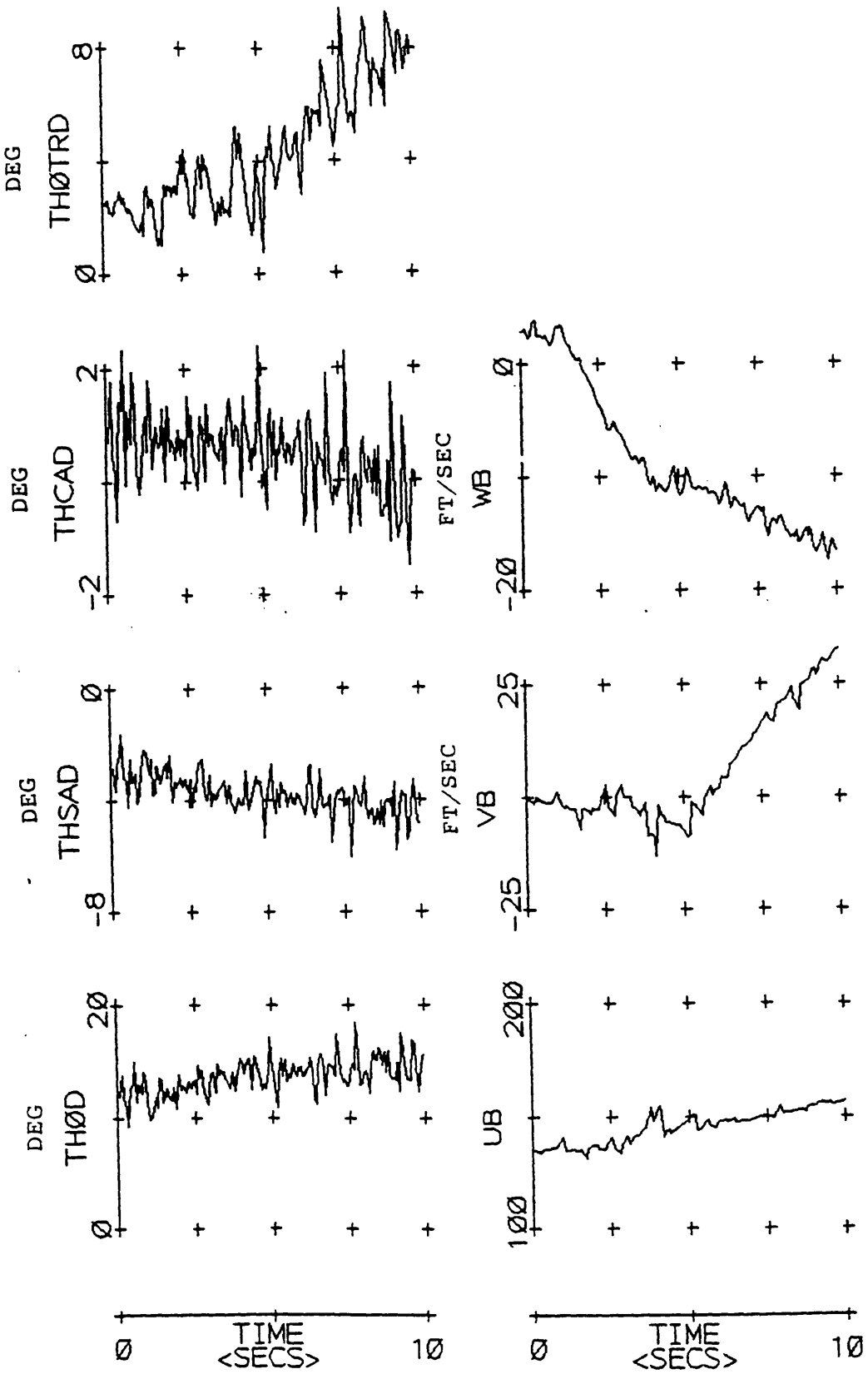
DEG
THØTRD
8
Ø
DEG
THCAD
2
-2
FT/SEC
WB
Ø
-2Ø
DEG
THSAD
Ø
-8
FT/SEC
VB
25
-25
DEG
THØD
2Ø
Ø
UB
2ØØ
1ØØ
TIME
<SECS>
Ø
1Ø
TIME
<SECS>
Ø
1Ø

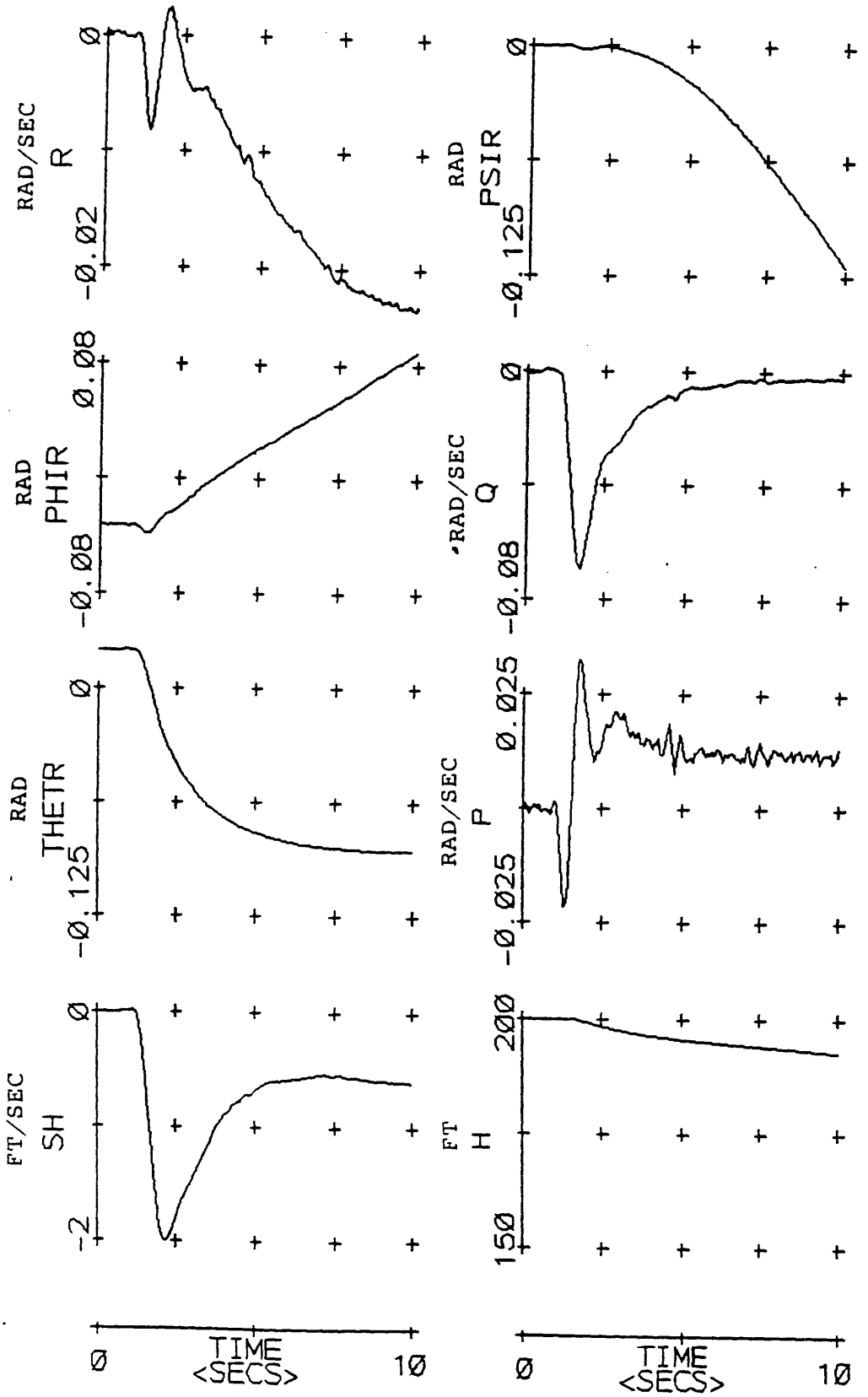

Figure 6.21 Helisim Model Without Turbulence But With Noise

Step Input Of Amplitude -0.1 Applied To Second Inceptor

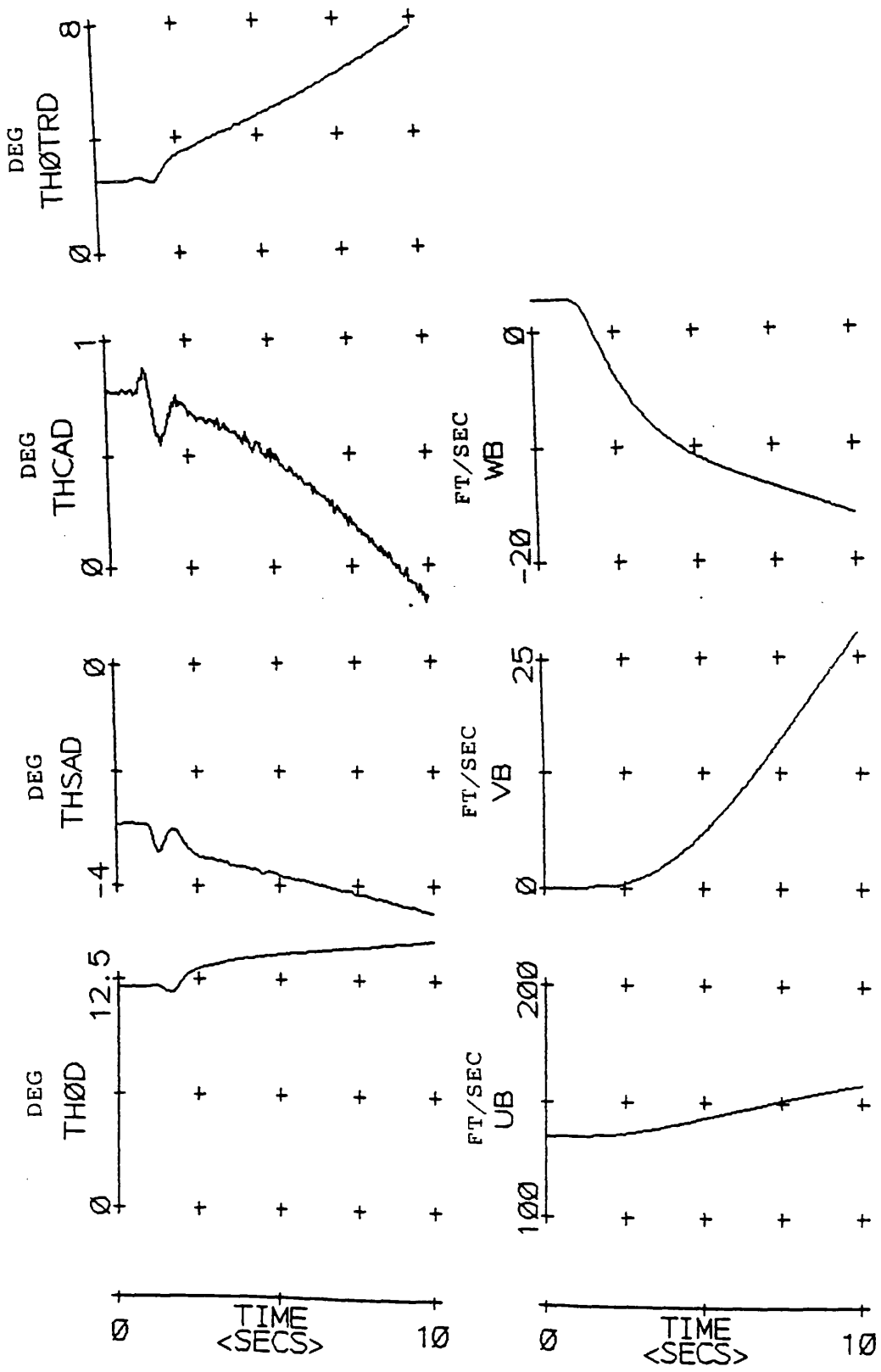
DEG
THØTRD
8
Ø
DEG
THCAD
1
Ø
DEG
THSAD
Ø
-4
DEG
THØD
12.5
Ø
TIME
<SECS>
Ø
1Ø
FT/SEC
WB
Ø
-2Ø
FT/SEC
VB
25
Ø
FT/SEC
UB
2ØØ
1ØØ
TIME
<SECS>
Ø
1Ø

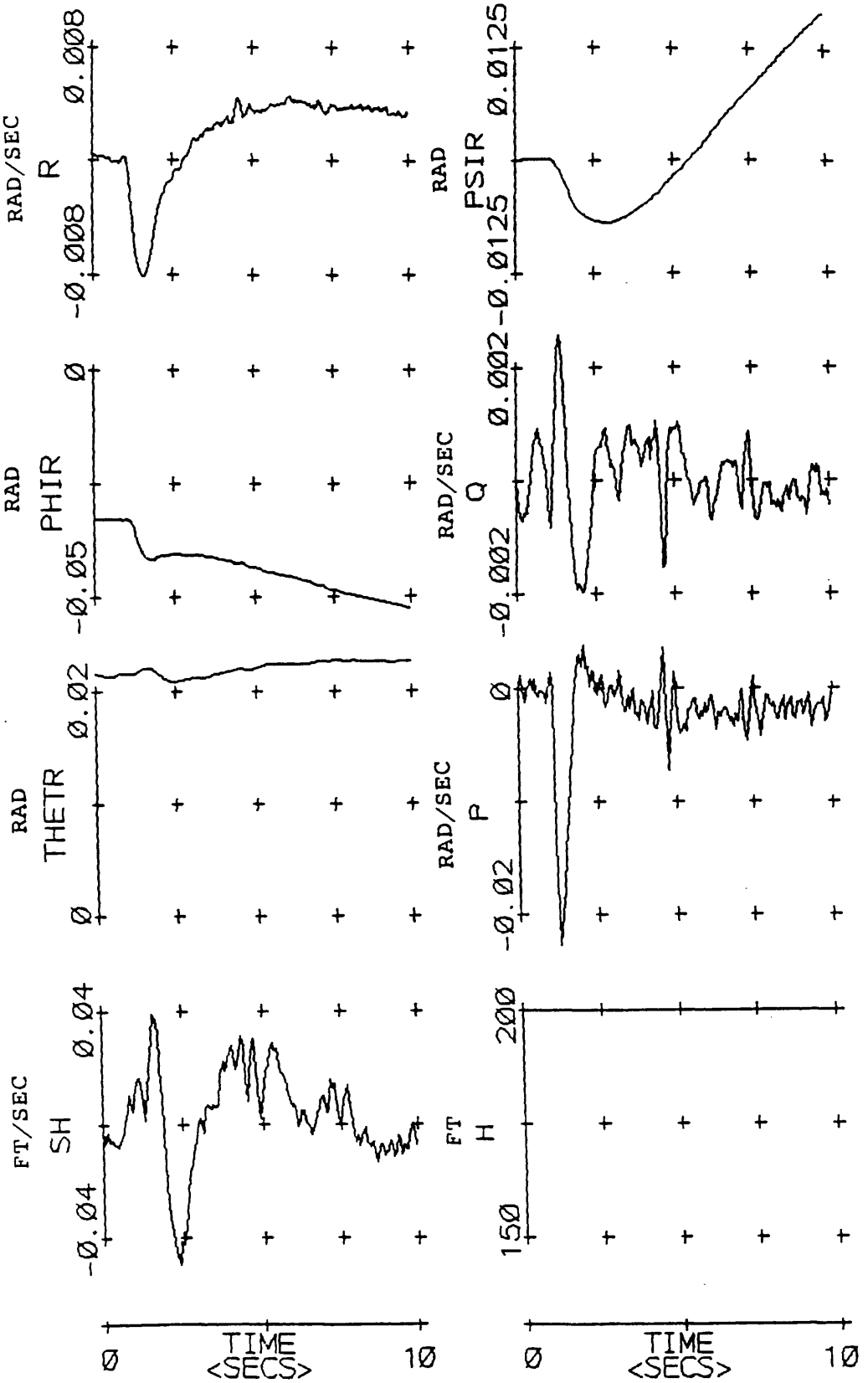

Figure 6.22 Helisim Model Without Turbulence But With Noise Step Input Of Amplitude -0.1 Applied To Third Inceptor

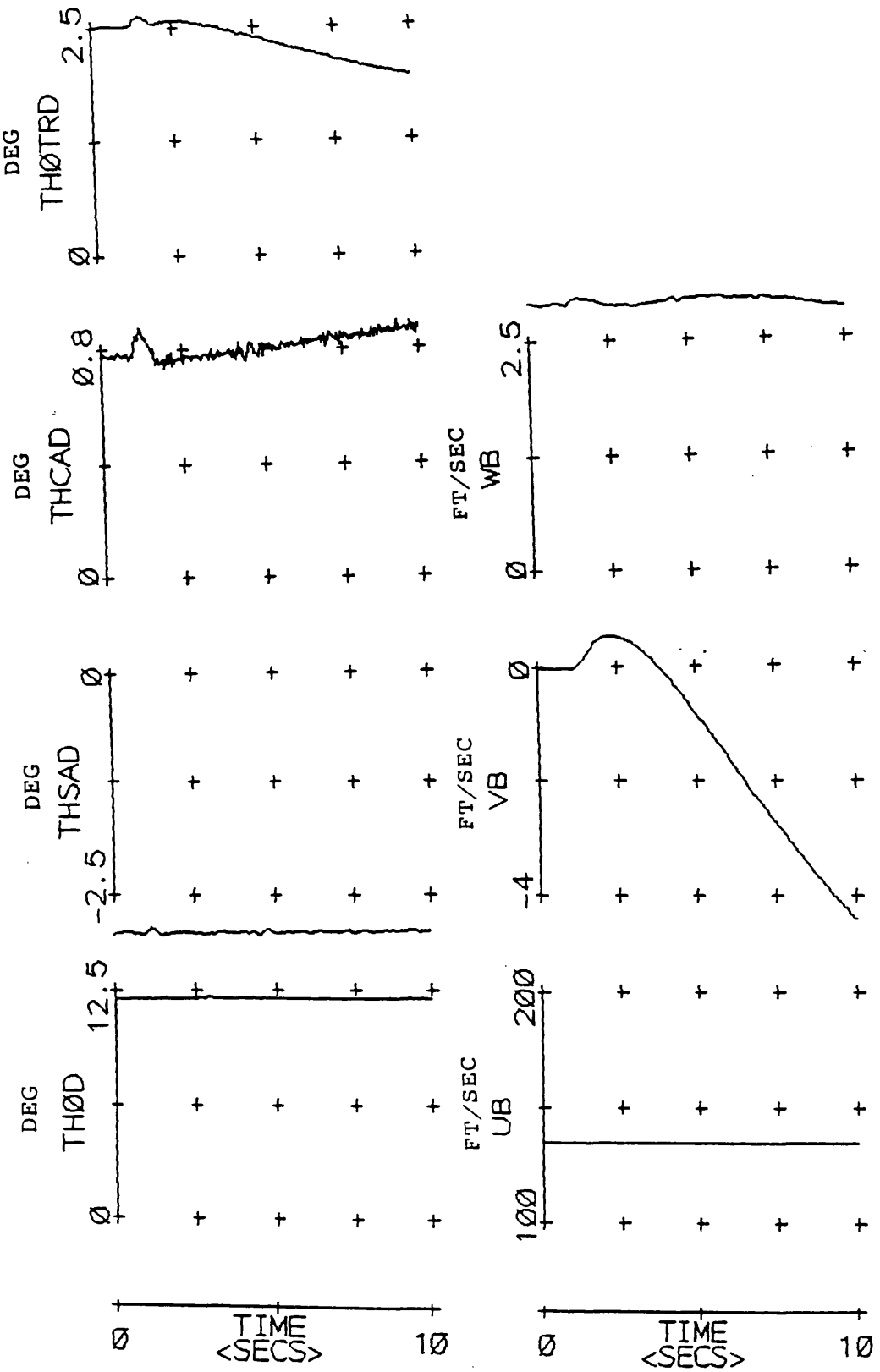
DEG
THØTRD
2.5
Ø
DEG
THCAD
Ø.8
Ø
FT/SEC
WB
2.5
Ø
DEG
THSAD
Ø
-2.5
FT/SEC
VB
Ø
-4
DEG
THØD
12.5
Ø
FT/SEC
UB
200
100
Ø
TIME
<SECS>
10
Ø
TIME
<SECS>
10

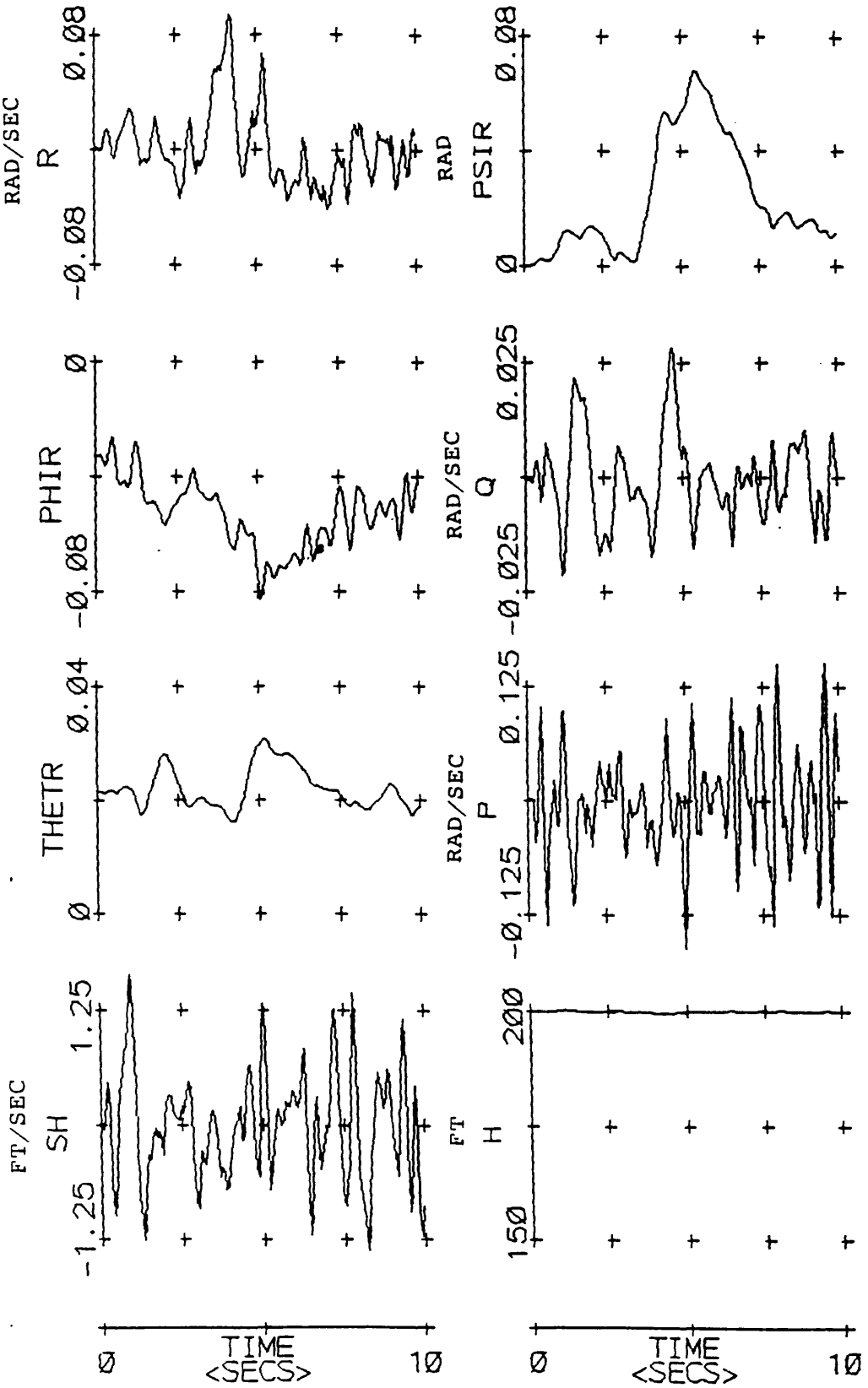

Figure 6.23 Helisim Model With Turbulence And Noise

Step Input Of Amplitude -0.1 Applied To Third Inceptor

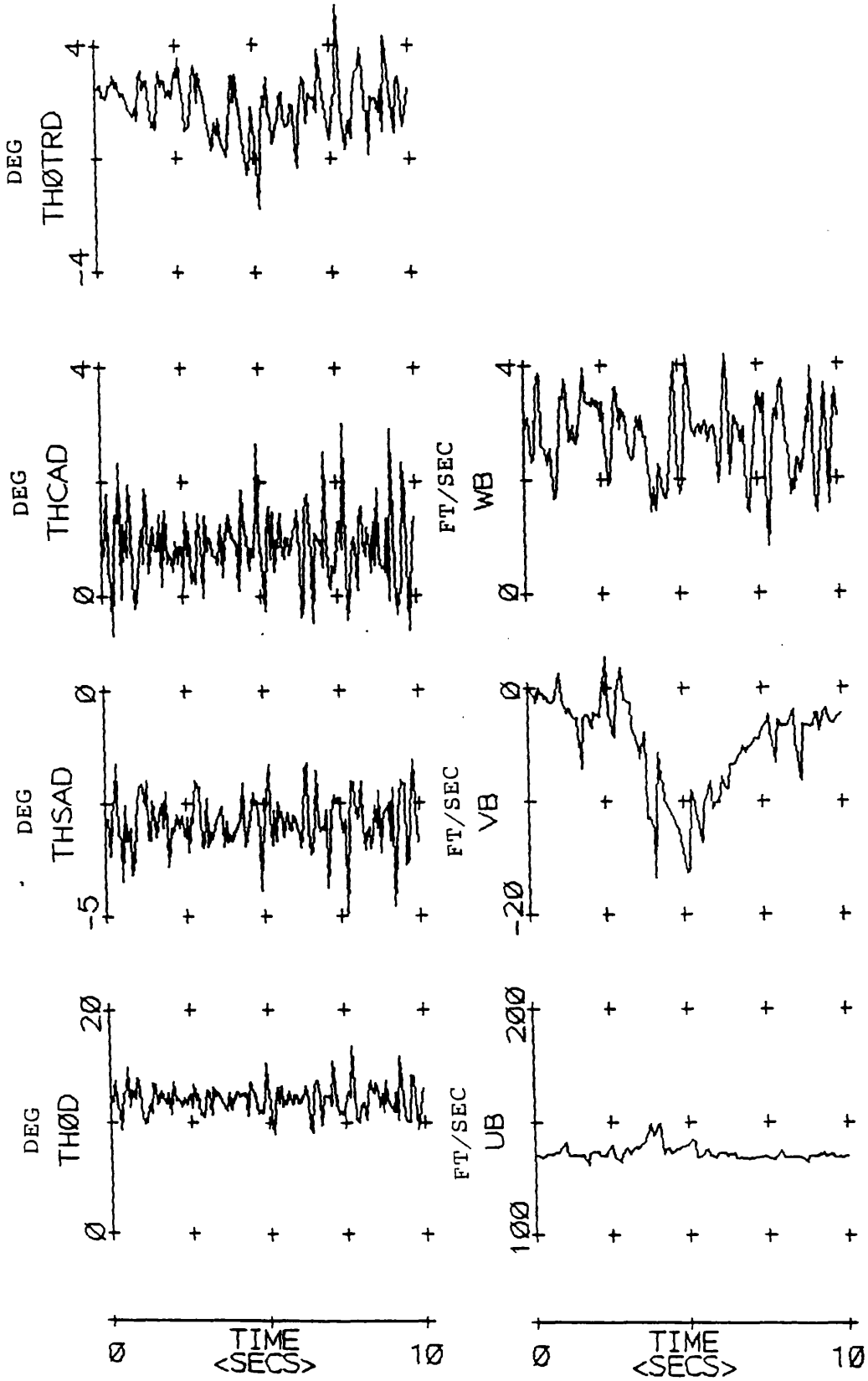
DEG
THØTRD
4
-4
DEG
THCAD
4
Ø
FT/SEC
WB
4
Ø
DEG
THSAD
Ø
-5
FT/SEC
VB
Ø
-2Ø
DEG
THØD
2Ø
Ø
FT/SEC
UB
2ØØ
1ØØ
Ø
TIME
<SECS>
1Ø
Ø
TIME
<SECS>
1Ø

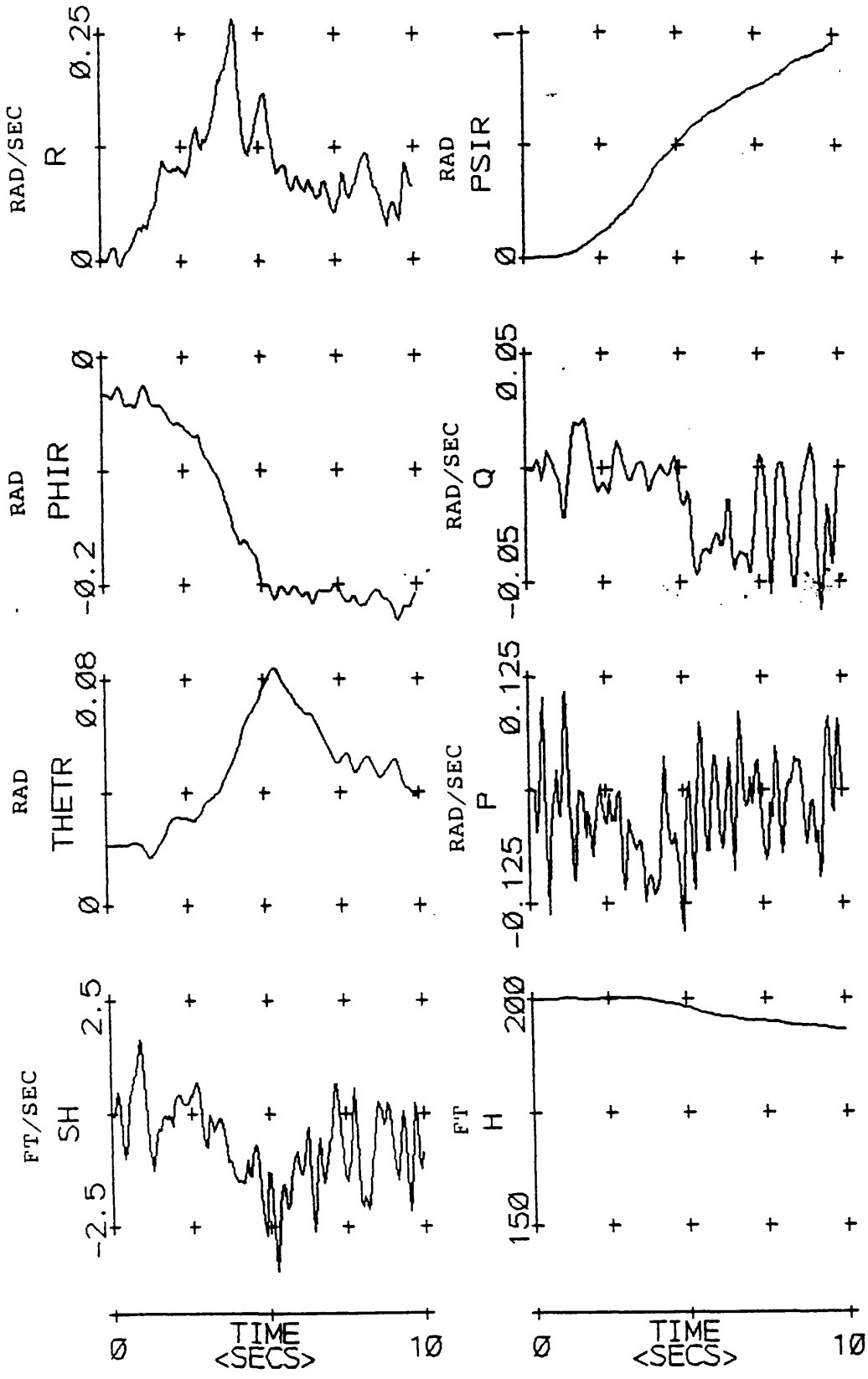

Figure 6.24 Helisim Model With Turbulence And Noise

Step Input Of Amplitude 0.06 Applied To Fourth Inceptor

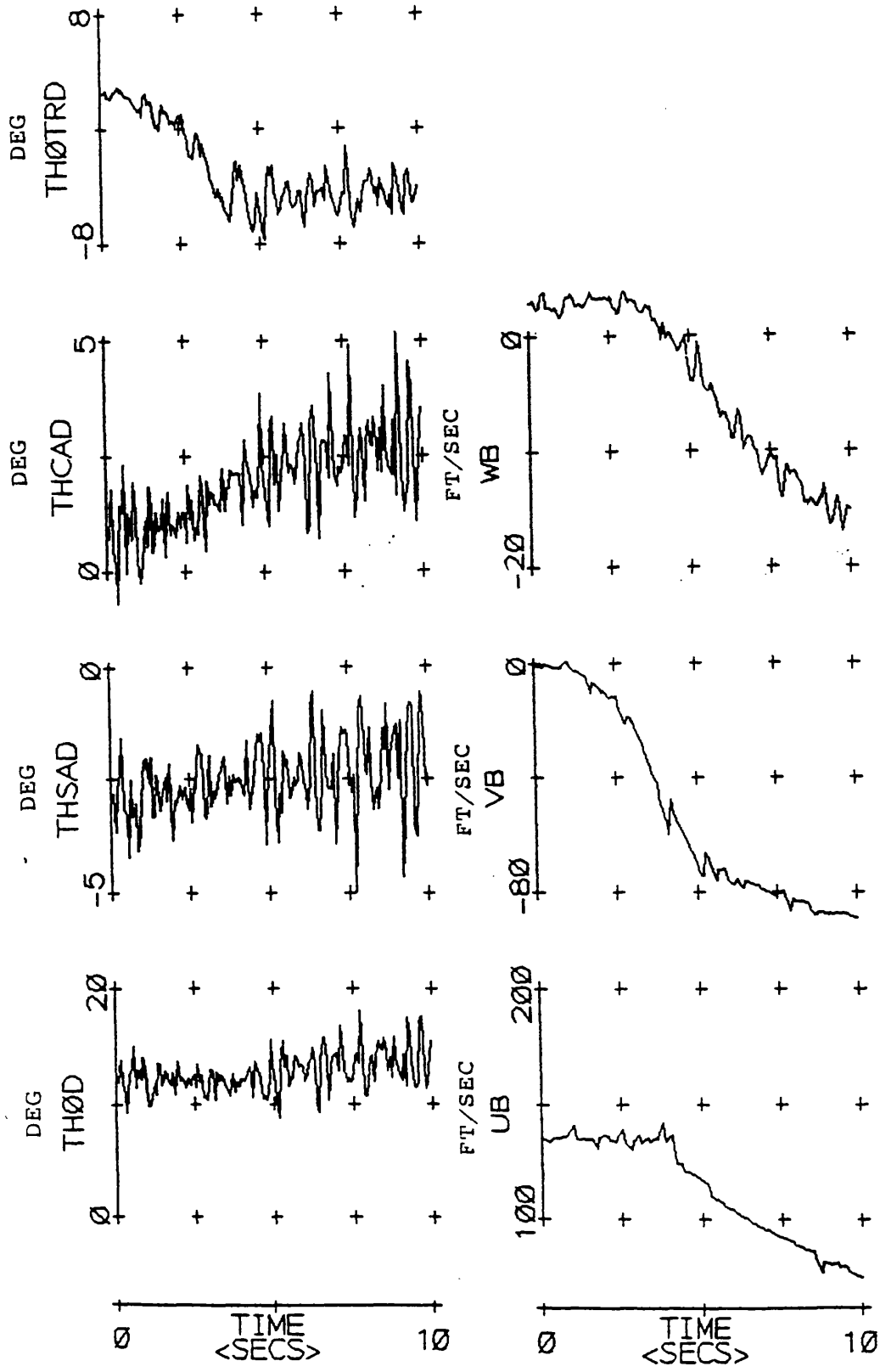
DEG
THØTRD
8
-8
DEG
THCAD
5
Ø
FT/SEC
WB
Ø
-2Ø
DEG
THSAD
Ø
-5
FT/SEC
VB
Ø
-8Ø
DEG
THØD
2Ø
Ø
FT/SEC
UB
2ØØ
1ØØ
Ø
TIME
<SECS>
1Ø
Ø
TIME
<SECS>
1Ø

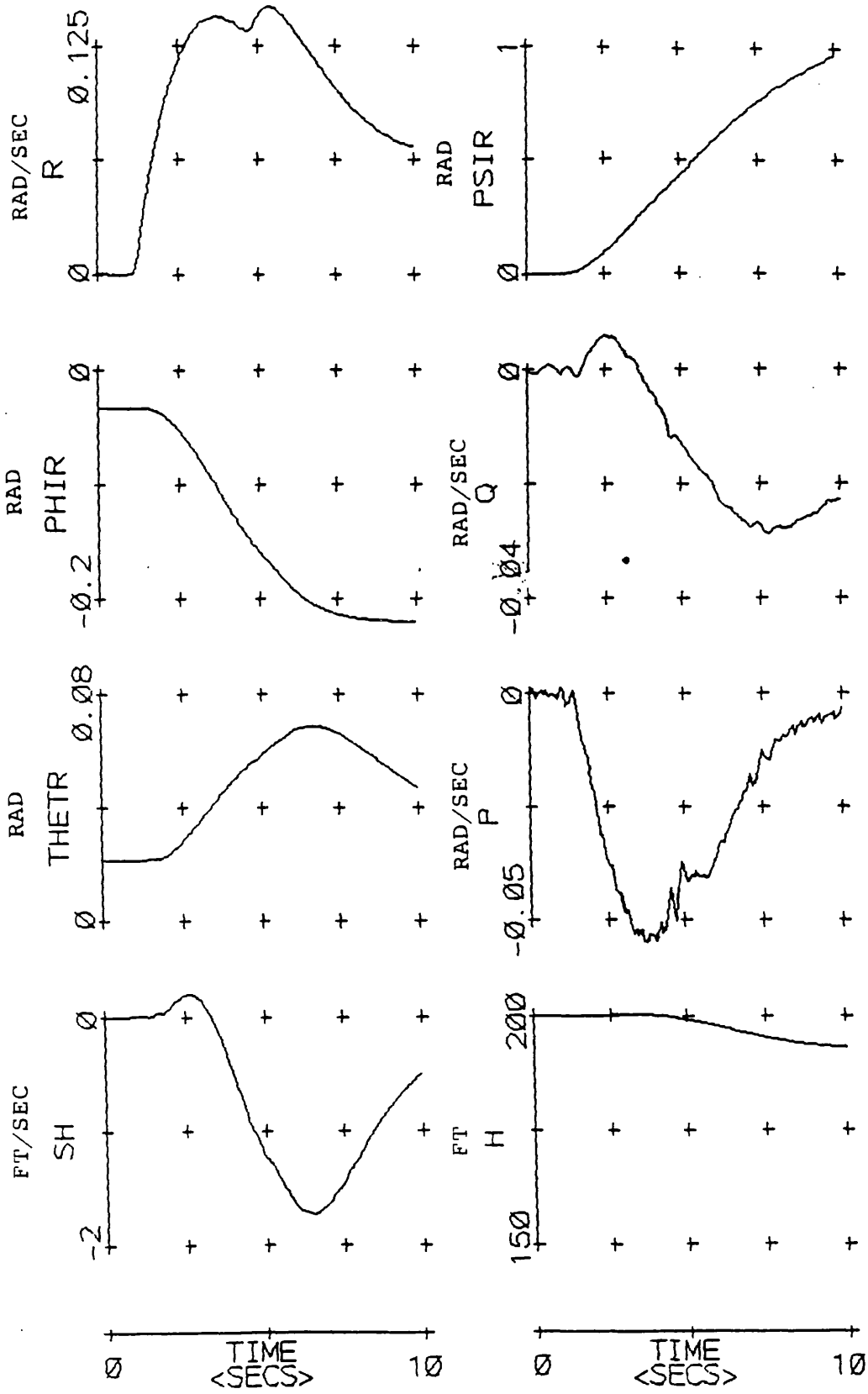

Figure 6.25 Helisim Model Without Turbulence But With Noise

Step Input Of Amplitude 0.06 Applied To Fourth Inceptor

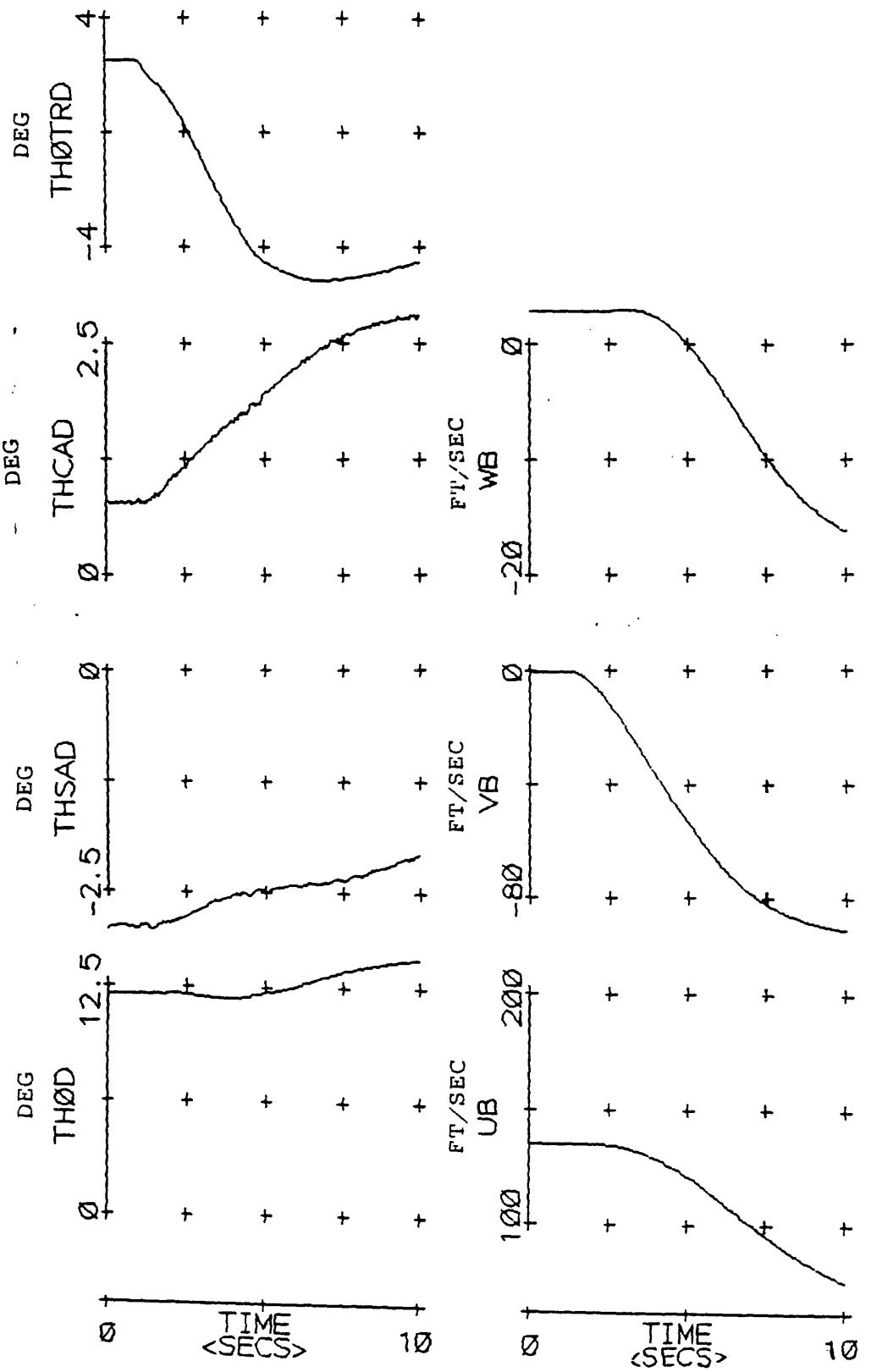
DEG
THØTRD
4
-4
DEG
THCAD
2.5
Ø
FT/SEC
WB
Ø
-2Ø
DEG
THSAD
Ø
-2.5
FT/SEC
VB
Ø
-8Ø
DEG
THØD
12.5
Ø
FT/SEC
UB
2ØØ
1ØØ
Ø
TIME
<SECS>
1Ø
Ø
TIME
<SECS>
1Ø

CHAPTER 7 CONCLUSIONS AND RECOMMENDATIONS FOR FUTURE WORK

Eigenstructure assignment techniques are useful because of the degree of visibility associated with them. Results from eigenstructure assignment methods can be easily interpretted in terms of stability and speed of response. In chapter 4 it was shown that eigenstructure assignment techniques do not always produce a well-conditioned solution. The difficulty that is often associated with placing closed loop poles in areas of the complex plane to give the required transient performance was also demonstrated. In the case of the Lynx helicopter the handling qualities documentation gives information that restricts the areas in which poles can be placed but due to the complex nature of the system it is possible that all poles may lie in appropriate areas but the desired transient response is not achieved.

It was shown in chapter 5 that by using eigenstructure assignment techniques the problems associated with helicopter's dynamics could be addressed. The method adopted in that chapter allowed zeros and their directions to be cancelled. This was useful on two accounts: it effectively reduced the order of the system and eliminated the effects of the system's zeros. This method also decreased the level of coupling present in the helicopter. There was a fixed number of assignable modes some of which were used to cancel the zeros associated with the system. The remaining assignable modes were to be distributed across the four output channels. For the case of the Lynx at 80 knots forward flight it was found that the best results were obtained by assigning one mode each to the first and fourth outputs and two modes each to the second and third outputs. The next task was to decide on the best position for each of the assignable modes. This was achieved partly through the requirements of stability, eigenstructure assignment restrictions and handling qualities criteria.

The controlled helicopter system was shown to meet helicopter handling qualities requirements in terms of bandwidth and phase delay measurements. The controller was robust to the addition of dynamics which were not included in the model at the design condition. The controller (which was designed at 80 knots forward flight condition)

maintained stability when used at flight conditions of 50 & 120 knots. However, by scheduling the controller, the performance at all flight conditions between 50 & 120 knots was found to be much closer to that of the original design at 80 knots. The feedback and feedforward controllers formed an inner loop while an outer loop was added which contained a P+I controller. It was noted that the position of the assigned eigenvalues in the inner/outer loop structure followed the movement of the zeros much more closely as flight condition was changed than those with only the inner loop control. This suggested that there may be benefits in adopting an inner/outer loop structure where the inner loop provides stability and decouples the dynamics and the outer loop augments the performance of the inner loop.

When implemented on a non-linear helicopter model the controller maintained stability across the range of forward flight conditions 50 - 120 knots. The responses of the non-linear controlled system for small inputs were similar in character to those of the linear controlled system.

In chapter 6 noise and turbulence were added to the controlled helicopter simulation. Again, stability was maintained. There was an increase in the activity of the actuators but at no point were actuator rate or authority limits exceeded.

It can be concluded from the results that the eigenstructure assignment method for decoupled tracking has proved to be effective in providing a controller which improves the handling qualities of a helicopter. The method has produced a controller which was designed on an 8th order linear helicopter model but still gave good performance on higher order linear helicopter models and a non-linear helicopter model. The improvement in the controlled helicopter system was also maintained across a wide range of operating conditions (even when sensor noise and atmospheric turbulence were added).

The eigenstructure assignment method used here has therefore been shown to produce a robust controller which improves handling qualities, decreasing the pilot's workload and thus potentially increasing safety and mission effectiveness.

One area which could provide future work is in the scheduling of the controller. In this case the controller was scheduled at 16 points equally spaced (about every 4 knots) between 50 and 120 knots. It may prove to be the case that fewer points could provide as good a performance. It may also be the case that an optimium performance could be achieved from the minimum number of scheduling points by not having the scheduled controllers evenly spaced across the range (by finding the areas within the range where more or fewer points would be required).

Another area for further study is concerned with the inner and outer loop control structure. More work requires to be done on this to establish why the two loop structure gives a better performance generally and why, according to the findings of this research, cancelling eigenvalues continue to cancel the zeros as the zeros move with changes in flight condition.

Limited authority actuators usually interface the mechanical flight controls of the helicopter with the automatic flight control system (AFCS). By replacing the mechanical controls by computers a fly-by-wire system can be created that will permit the use of active control technology.

The use of active control technology (ACT) may result in an improvement in handling qualities because it allows greater use of the usable flight envelope. In the case of fixed-wing aircraft ACT has included safety boundaries in the flight control computer. This has meant that pilots need not worry about losing control by crossing limits and this has introduced carefree manoeuvring. Helicopters require much more complex control laws than fixed wing aircraft due to their complex cross-coupled dynamics. Because of this the advantages in weight and cost are less to helicopters than fixed-wing aircraft. Nevertheless it is still hoped that the introduction of ACT will reduce pilot workload and allow the helicopter pilot to use the agility of the helicopter to its best advantage without exceeding safety limits. In order to achieve this it will be necessary to develop a design procedure that is able to handle all conditions that could be encountered during operation. This task

would be far from trivial given the non-linearities, instability and cross-coupled dynamics that are inherent to the helicopter's dynamics. The availability of helicopter states (sensed or estimated), actuation dynamics and the changing nature of the helicopter with flight condition would also have to be taken into account. Other implementation issues are sensor redundancy, level of on-board vibration and computing delays. With a view to creating a successful ACT system perhaps the most useful area for future work would be in the development of a model of a high specification on which control law design could be more accurately performed.

APPENDIX 1 EQUATIONS OF MOTION

Fundamentals of Helicopter Flight Mechanics

During steady flight there are 4 forces acting on an aircraft: lift, drag, gravity & thrust. Gravity is counteracted by lift and drag by thrust.

In forward flight advancing blades will experience faster air flow than retreating blades, causing the advancing blades to generate greater lift than the retreating blades. The variation in lift is reduced through changes in the angle of attack of the blades - advancing blade angle reaching a maximum at the front of the helicopter and a minimum at the back. This is called flapping.

Feathering can also be used. This is where the pitch of the blades is altered sinusoidally in keeping with the sinusoidal airflow changes.

Two sets of axes can be defined: earth-fixed and body-fixed. Earth-fixed axes are fixed relative to the earth (which is assumed to be flat and non-rotating). The origin of body-fixed axes is located at the aircraft's centre of gravity, with the x-axis pointing to the front of the aircraft, the y-axis starboard and the z-axis downwards.

The body-fixed axes system can be related to the earth-fixed axes system by a series of rotations through angles known as Euler angles. The axes system from earth-fixed is rotated around the z-axis by angle ψ, then around y-axis by angle θ and finally around x-axis by angle φ. The resultant axis system is coincident with the body-fixed system. see fig.2.1

By considering these rotations separately, a transformation matrix can be derived which can transform components from body to earth axes.

There is the disadvantage with the body-fixed axes that equations for translational accelerations (e.g. u, v, w) contain angular velocity components. For this reason, earth-fixed axes are often used to solve translational equations of motion but body-fixed axes are generally used for solving rotational equations of motion because they have constant moments of inertia in body-fixed axes.

Other axes systems are also employed to facilitate main rotor analysis: hub/wind system, blade system and hub system. The hub/wind system has the hub's x-axis aligned with the

resultant aircraft velocity in the hub x-y plane, the blade system is fixed in the flapping blade and the hub system is aligned along the shaft and centred at the rotor hub.

The model outlined in this chapter has rigid blades of constant chord and a centre spring model representing flap. Blade pitch can be altered once per revolution. Lag is not included in the model. Forces and moments are referred to a body-fixed axes system. These forces and moments are shown in Table 1 (system of axes). Flapping angles are assumed to be small, fuselage acceleration and blade weight effects are neglected and yaw rate and sideslip rates are also assumed to be small compared to the angular rate Ω.

Dynamical equations for a free turbine engine controlled by a rotorspeed governor are based on a simple model consisting of a first order lag giving the relationship between rotorspeed error and fuel flow rate and another first order lag, supplemented by a lead term, relating fuel flow to engine torque.

Mathematical Model

(Padfield, 1981)

TABLE 1

System Of Axes and Associated Notation

	longitudinal	lateral	normal
Force	X	Y	Z
Moment	L	M	N
	(rolling)	(pitching)	(yawing)
Angle Of Rotation	φ	θ	ψ
Velocity	u	v	w
Rate of Turn	p	q	r

Forces & Moments

The external forces and moments are considered to be the sum of contributions from all dynamic and aerodynamic sources.

Using the notation of table 1 equations of external forces can be expressed in component form. The following equations express the external forces in terms of five components.

$$X = X_R + X_T + X_{TP} + X_{FN} + X_F$$

$$Y = Y_R + Y_T + Y_{TP} + Y_{FN} + Y_F$$

$$Z = Z_R + Z_T + Z_{TP} + Z_{FN} + Z_F$$

where subscripts are R main rotor FN fin

T tail rotor F fuselage

TP tail plane

These components must now be considered individually. In order to work out rotor forces and moments some assumptions are made. These are that a constant, two-dimensional lift curve slope is assumed, compressibility effects are ignored, unsteady aerodynamic effects are ignored, as are stall and reverse flow effects. It is also assumed that the induced velocity distribution, normal to the rotor disc, includes linear longitudinal and lateral variations, the value at the centre satisfying simple momentum considerations.

Other assumptions are that the flapping behaviour of hingeless rotors and of small offset articulated rotors is adequately represented by the centre spring model.An implication of this is that the effect on stability and control of the higher blade flapping modes is negligible. Couplings from blade pitch and lag dynamics into flapping motion are ignored.

It is possible to show that

$$\begin{bmatrix} X_R \\ Y_R \\ Z_R \end{bmatrix} = \begin{bmatrix} \cos\gamma_S & 0 & -\sin\gamma_S \\ 0 & 1 & 0 \\ \sin\gamma_S & 0 & \cos\gamma_S \end{bmatrix} \begin{bmatrix} X_H \\ Y_H \\ Z_H \end{bmatrix}$$

where X_R, Y_R and Z_R are rotor hub forces in body reference axes and the rotor hub forces in the shaft axes are denoted by X_H, Y_H and Z_H while γ_S is the forward inclination of the shaft relative to the fuselage z axis.

The tail rotor produces a relatively small thrust compared with the main rotor. The assumption is therefore made that the tail rotor drag and sideforce can be neglected.

Flapping is ignored when equations are derived for tail rotor thrust. A mechanical link is incorporated between tail rotor blade coning and pitch angle. Also, a fin blockage factor reduces the achieved thrust.

The tail rotor contribution is limited to Y_T. Therefore $X_T = Z_T = 0$. The resulting equation for the tail rotor has the form

$$Y_T = \rho(\Omega_T R_T)^2 \, s_T a_{0T} \, (\pi R_T)^2 \, (C_{TT}/(a_{0T} s_T)) \, F_T$$

where ρ air density

Y_T lateral tail rotor thrust

Ω_T tail rotor speed

R_T radius of tail rotor

s_T tail rotor solidity

a_{0T} lift curve slope of tail rotor blades

C_{TT} tail rotor thrust coefficient

F_T fin blockage factor

Another assumption is that the tailplane and fin contribute normal forces along the body Z and Y axes respectively.

The tailplane contribution is limited to Z_{TP}. Therefore $X_{TP} = Y_{TP} = 0$. The tailplane force is described by the equation

$$Z_{TP} = \tfrac{1}{2}\rho(\Omega R)^2 \, V_T^2 \, S_{TP} \, C_{ZTP}(\alpha_{TP})$$

where V_T tailplane total velocity

Ω rotor speed

S_{TP} tailplane area

C_{ZTP} tailplane force coefficient

α_{TP} tailplane incidence angle

The fin contribution is limited to Y_{FN}. Therefore $X_{FN} = Z_{FN} = 0$.

The fin sideforce, Y_{FN}, can be written as

$$Y_{FN} = \tfrac{1}{2}\rho(\Omega R)^2 \, V_{FN}^2 \, S_{FN} \, C_{YFN}(\beta_{FN})$$

where V_{FN} fin total velocity

C_{YFN} fin sideforce function

β_{FN} fin sideslip angle

Within the Helistab model the force and moment contributions from the fuselage were synthesised from wind tunnel data. Wind tunnel results were used to produce piece-wise linear variations with body incidence angles of force and moments contributions from

fuselage and empennage. The reason for adopting this rather than an analytical derivation is that the main rotor wake interacts with the fuselage, fin and tailplane in forward flight creating difficulties in the mathematical formulation. The effect of rotor downwash on the fuselage is accounted for approximately. The equations for the fuselage forces take the following form

$$X_F = \tfrac{1}{2}\rho(\Omega R)^2 \, S_P \, V_F^2 \, C_{XF}(\alpha_F)$$

$$Y_F = \tfrac{1}{2}\rho(\Omega R)^2 \, V_F^2 \, S_S \, C_{YS}(v_A/V_F)$$

$$Z_F = \tfrac{1}{2}\rho(\Omega R)^2 \, S_P \, V_F^2 \, C_{ZF}(\alpha_F)$$

where S_S fuselage side area

S_p fuselage plan area

V_F fuselage total velocity

v_A lateral aerodynamic velocity at centre of gravity

C_{XF} fuselage force function

C_{YS} fuselage sideforce function

C_{ZF} fuselage force function

α_F fuselage incidence angle

Moments can also be expressed in component form as follows:

$$L = L_R + L_T + L_{TP} + L_{FN} + L_F$$

$$M = M_R + M_T + M_{TP} + M_{FN} + M_F$$

$$N = N_R + N_T + N_{TP} + N_{FN} + N_F$$

The components of the moment equations are examined in more detail below.The rotor moments can be written as follows:

$$L_R = L_H + h_R \, Y_R$$

$$M_R = M_H - h_R \, X_R + x_{CG} \, Z_R$$

$$N_R = N_H - x_{CG} \, Y_R$$

where h_R negative z coordinate of rotor hub

x_{CG} centre of gravity location forward of fuselage ref. point

The rotor hub pitching and rolling moments are approximately proportional to quasi-steady blade flapping and can be written in terms of the spring

stiffness, K_β. The equations are as follows:

$$L_H = -b/2\ K_\beta\ \beta_{1s}$$

$$M_H = -b/2\ K_\beta\ \beta_{1c}$$

$$\frac{N_H}{\frac{1}{2}\rho\ (\Omega R)^2\ \pi R^3\ s a_0} = \frac{2C_Q}{a_0 s} + 2\left[\frac{I_R}{b I_\beta}\right]\ \frac{1}{\gamma}\ \Omega'$$

where $\Omega' = \Omega/\Omega^2$

γ	(Lock number) , $\gamma = \rho c a_0 R^4 / I_\beta$
s	rotor solidity , $s = bc/\pi R$
a_0	(lift curve slope)
C_Q	main rotor torque coefficient
b	number of main rotor blades
I_β	blade moment of inertia
c	(chord)
β_{1s}, β_{1c}	harmonics of flapping

I_R is the moment of inertia of the rotor blades about the shaft axis plus the appropriate moment of inertia of any other directly coupled rotating part such as the transmission.

Moments of other elements are given by the product of the moment arm with the force on that element. Hence we obtain the equations

$$L_T = h_T\ Y_T$$

$$M_T = 0$$

$$N_T = -(l_T + x_{CG}) Y_T$$

where h_T negative z coordinate of hub

l_T tail rotor location aft of fuselage ref. point

Similarly,

$$L_{TP} = N_{TP} = 0$$

$$M_{TP} = (l_{TP} + x_{CG})\ Z_{TP}$$

where l_{TP} location aft of fuselage reference point

$$L_{FN} = h_{FN}\ Y_{FN}$$

$$M_{FN} = 0$$

$$N_{FN} = -(l_{FN} + x_{CG})\ Y_{FN}$$

where l_{FN} location aft of fuselage reference point

h_{FN} negative z component of fin centre of pressure

The fuselage rolling moment, L_F, is assumed to be zero. The remaining fuselage

components are

$$M_F = \tfrac{1}{2}\rho(\Omega R)^2 S_p l_F V_F^2 C_{MF}(\alpha_F)$$

$$N_F = \tfrac{1}{2}\rho(\Omega R)^2 V_F^2 S_s l_F C_{NF}(\beta_F)$$

where S_p fuselage plan area

S_s fuselage side area

l_F reference length

C_{MF} fuselage pitching moment function

C_{NF} fuselage yawing moment function

Equations Of Motion

Let I_{xx}, I_{yy} and I_{zz} be the moments of inertia about the x, y and z axes respectively and I_{xz} the product of inertia about the x and z axes. Assuming a choice of axes such that I_{xy} and I_{yz} are negligible, the equations of motion can be written as follows :

$$I_{xx}p = (I_{yy} - I_{zz})qr + I_{xz}(r + pq) + L$$

$$I_{yy}q = (I_{zz} - I_{xx})rp + I_{xz}(r^2 - p^2) + M$$

$$I_{zz}r = (I_{xx} - I_{yy})pq + I_{xz}(p - qr) + N$$

Let u, v, w and p, q, r be the vehicle translational and rotational components about the x, y, z axes respectively. In the transformation from earth to body axes, let ψ, θ, φ be the Euler angles, m the vehicle mass and g the gravitational constant.

$$u = -(wq - vr) + x/m - g\sin\theta$$

$$v = -(ur - wp) + y/m + g\cos\theta\sin\theta$$

$$w = -(vp - uq) + z/m + g\cos\theta\cos\theta$$

Wind and turbulence components, u_{wg}, v_{wg}, w_{wg}, can be added to u, v, w to produce aerodynamic velocities at the centre of gravity.

$$u_A = u + u_{wg}$$

$$v_A = v + v_{wg}$$

$$w_A = w + w_{wg}$$

Euler angles can be determined from the equations which relate them to body angular components.

$$\dot{\varphi} = p + q \sin\theta \tan\theta + r \cos\varphi \tan\theta$$

$$\dot{\theta} = q \cos\varphi - r \sin\varphi$$

$$\dot{\psi} = q \sin\varphi \sec\theta + r \cos\varphi \sec\theta$$

Rotor Hub Forces In Shaft Axes (X_H, Y_H, Z_H)

The relationship between vector components in an axes system (X_H, Y_H, Z_H) aligned along the shaft and centred at the hub of the rotor sytem and an axes system (X_B, Y_B, Z_B) fixed in a centrally hinged rigid blade, free to flap, is one which requires two transformations. The first, angle ψ, is due to the rotation of the shaft with angular velocity, Ω, and the second is due to the flapping angle, β.

For an anti-clockwise rotating rotor, with ψ=0 at the back of the disc and β positive up, the transformation can be written in terms of unit vectors in the above two systems.

$$\begin{bmatrix} i_H \\ j_H \\ k_H \end{bmatrix} = \begin{bmatrix} -\cos\psi & -\sin\psi & 0 \\ \sin\psi & -\cos\psi & 0 \\ 0 & 0 & 1 \end{bmatrix} \begin{bmatrix} \cos\beta & 0 & \sin\beta \\ 0 & 1 & 0 \\ -\sin\beta & 0 & \cos\beta \end{bmatrix} \begin{bmatrix} i_B \\ j_B \\ k_B \end{bmatrix}$$

which becomes

$$\begin{bmatrix} i_H \\ j_H \\ k_H \end{bmatrix} = \begin{bmatrix} -\cos\psi\cos\beta & -\sin\psi & -\cos\psi\sin\beta \\ \sin\psi\cos\beta & -\cos\psi & \sin\psi\sin\beta \\ -\sin\beta & 0 & \cos\beta \end{bmatrix} \begin{bmatrix} i_B \\ j_B \\ k_B \end{bmatrix}$$

The hub x axis can be aligned with the resultant aircraft velocity in the hub xy plane. This means that there will be no y velocity component in this system and the angular velocity will have an additional contribution produced by the rate of change of sideslip. This axes system is referred to as the hub/wind system and is denoted by the subscript Hw.

Rotor Blade Flapping

Equations of flapping motion are derived here for a centrally sprung hinged, rigid blade model with spring stiffness K_β.

The rotor moments L_H, M_H, N_H were described above by the harmonics of flapping (β_{1s}, β_{1c}). Here the individual blade flapping angles are transformed into multi-blade coordinates which include a differential coning variable for a four blade rotor.

For a b-bladed rotor,

coning

$$\beta_0 = 1/b \sum_{i=1}^{b} \beta_i$$

differential coning (even-bladed rotors, b>2)

$$\beta_d = 1/b \sum_{i=1}^{b} \beta_i (-1)^i$$

cyclic flapping

$$\beta_{jc} = 2/b \sum_{i=1}^{b} \beta_i \cos j\psi_i$$

$$\beta_{js} = 2/b \sum_{i=1}^{b} \beta_i \cos j\psi_i$$

With four blades the transformation can be written,

$$\beta_I = L_\beta \beta_M$$

where $\beta_I = [\beta_1, \beta_2, \beta_3, \beta_4]^T$

$\beta_M = [\beta_0, \beta_d, \beta_{1c}, \beta_{1s}]^T$

$$L_\beta = \begin{bmatrix} 1 & -1 & \cos\psi & \sin\psi \\ 1 & 1 & \sin\psi & -\cos\psi \\ 1 & -1 & -\cos\psi & -\sin\psi \\ 1 & 1 & -\sin\psi & \cos\psi \end{bmatrix}$$

Induced Flow through the Rotor

The normal induced flow field of the rotor is approximated by a simple, uniform distribution with a longitudinal variations produced by the rotor wake.

Downwash distribution can be written,

$$V_i/\Omega R = \lambda_i = \lambda_0 + r_B/R(\lambda_{1cw}\cos\psi + \lambda_{1sw}\sin\psi)$$

The uniform component, normal to the rotor disc, can be derived from momentum theory,

$$\lambda_0 = \frac{C_T}{2(\mu^2 + (\mu_z - \lambda_0)^2)^{\frac{1}{2}}}$$

where μ in-plane velocity component

μ_z normal velocity component

λ_0 downwash at the rotor centre

C_T main rotor thrust coefficient

μ normalised rotor velocity in xy plane

μ_z normalised rotor velocity component

$$\lambda_{1cw} = \lambda_0 \tan(\chi/2) \qquad \chi < \pi/2$$

$$\lambda_{1cw} = \lambda_0 \cot(\chi/2) \qquad \chi > \pi/2$$

$$\chi = \tan^{-1}(\mu/(\lambda_0 - \mu_z))$$

$$\lambda_{1sw} = 0$$

where λ_{sw}, λ_{cw} harmonic downwash components in hub wind axes

X wake angle

Simplified Free Turbine Engine

The dynamic equation of the rotating rotor and transmission system can be written as follows,

$$\Omega = \frac{(Q_E - Q_R - G_{TR}Q_{TR} - Q_{ACC})}{I_R} + r$$

where Q_E engine torque

Q_R main rotor torque

Q_{TR} tail rotor torque

Q_{ACC} accessories torques

G_{TR} tail rotor gear ratio

Ω main rotor speed relative to the fuselage

A governor system which senses a change in rotor speed and demands a fuel flow (ω_f) change automatically controls the engine torque. This governor is represented by a first order lag of the form

$$\frac{\Delta\omega f}{\Delta\Omega} = \frac{K_{e1}}{1 + \tau_{e1}s}$$

where τ_{e1}, τ_{e2}, τ_{e3} engine time lags

The engine response to change in fuel flow can be represented by

$$\frac{\Delta Q_E}{\Delta \omega_f} = K_{e2}\left[\frac{1 + \tau_{e2}s}{1 + \tau_{e3}s}\right]$$

where ω_f is the fuel flow rate

$$Q_E = 1/(\tau_{e1}\tau_{e3})\ (-(\tau_{e1} + \tau_{e3})Q_E - Q_E + K_3(\Omega - \Omega_i + \tau_{e2}\Omega\ )$$

where $\tau_{e2} = \tau_{20} + \tau_{21}Q_E$

$\tau_{e3} = \tau_{30} + \tau_{31}Q_E$

Q_E engine torque

$K_3 = K_{e1}K_{e2} = -\ \ Q_{E_{max}}/\Omega_i(1 - \Omega_{mi})$

where $\Omega_{mi} = \Omega_m/\Omega_i$

Ω_m rotor speed at maximum contingency

Ω_i rotor speed at flight idle

K_3 overall engine torque

Flight Control System

A contribution to cyclic pitch from the autostabiliser, θ_{1sa}^* & θ_{1ca}^*, is passed through limited authority series actuators and are given by

$$\theta_{1sa}^* = k_\theta\theta + k_q q + k_{1s}(\eta_{1s} - \eta_{1s0})$$

$$\theta_{1ca}^* = k_\varphi\varphi + k_p p + k_{1c}(\eta_{1c} - \eta_{1c0})$$

where k_θ, k_φ, k_p, k_q feedback gains

k_{1c}, k_{1s} feedforward gains

η_{1s0}, η_{1c0} constants, adjustable by the pilot

η_{1c}, η_{1s} lateral and longitudinal cyclic stick variables

The basic longitudinal stick gearing is a function of collective lever setting. Assuming straight line approximation, the pitch contribution to cyclic pitch, θ_{1sp}^* for longitudinal and θ_{1cp}^* for lateral,

$$\theta_{1cp}^* = g_{1c0} + g_{1c1}\eta_{1c}$$

$$\theta_{1sp}^* = g_{1s0} + g_{1s1}\eta_{1s} + (g_{sc0} + g_{sc1}\eta_{1s})\eta_c$$

where η_c $\qquad 0 \leqslant \eta_c \leqslant 1$

$\qquad\qquad 0 \leqslant \eta_{1s} \leqslant 1$

$g_{1s0} = \theta_{1s0}$

$g_{1s1} = \theta_{1s1} - \theta_{1s0}$

$g_{sc0} = \theta_{1s2} - \theta_{1s0}$

$g_{sc1} = (\theta_{1s3} - \theta_{1s2}) - (\theta_{1s1} - \theta_{1s0})$

θ_{1s0} pitch at zero cyclic stick and collective lever

θ_{1s1} pitch at maximum cyclic stick and zero collective lever

θ_{1s2} pitch at zero cyclic stick andn maximum collective lever

θ_{1s3} pitch at maximum cyclic stick and maximum collective lever

At control extremities there may be non-linearities which may not make these the best points to measure.

Before phasing, dressed signals, θ_{1s}^* & θ_{1c}^*, are produced from the servo driven by the pilot and autostabiliser inputs.

$$\theta_{1s}^* = \frac{\theta_{1sp}^* + \theta_{1sa}}{1 + \tau_{c1}s}$$

$$\theta_{1c}^* = \frac{\theta_{1cp}^* + \theta_{1sa}}{1 + \tau_{c2}s}$$

where θ_{1s}^*, θ_{1c}^* blade cyclic pitch components before phasing

τ_{c1} time constant

τ_{c2} time constant

The bar denotes the Laplace transform of a variable.

Cyclic mixing is as follows,

$$\theta_{1s} = \theta_{1s}^* \cos \psi_F + \theta_{1c}^* \sin \psi_F$$

$$\theta_{1c} = \theta_{1c}^* \cos \psi_F - \theta_{1s}^* \sin \psi_F$$

References

Padfield, G D

A Theoretical Model of Helicopter Flight Mechanics for Application to Piloted Simulation

RAE Technical Report 81048

April 1981

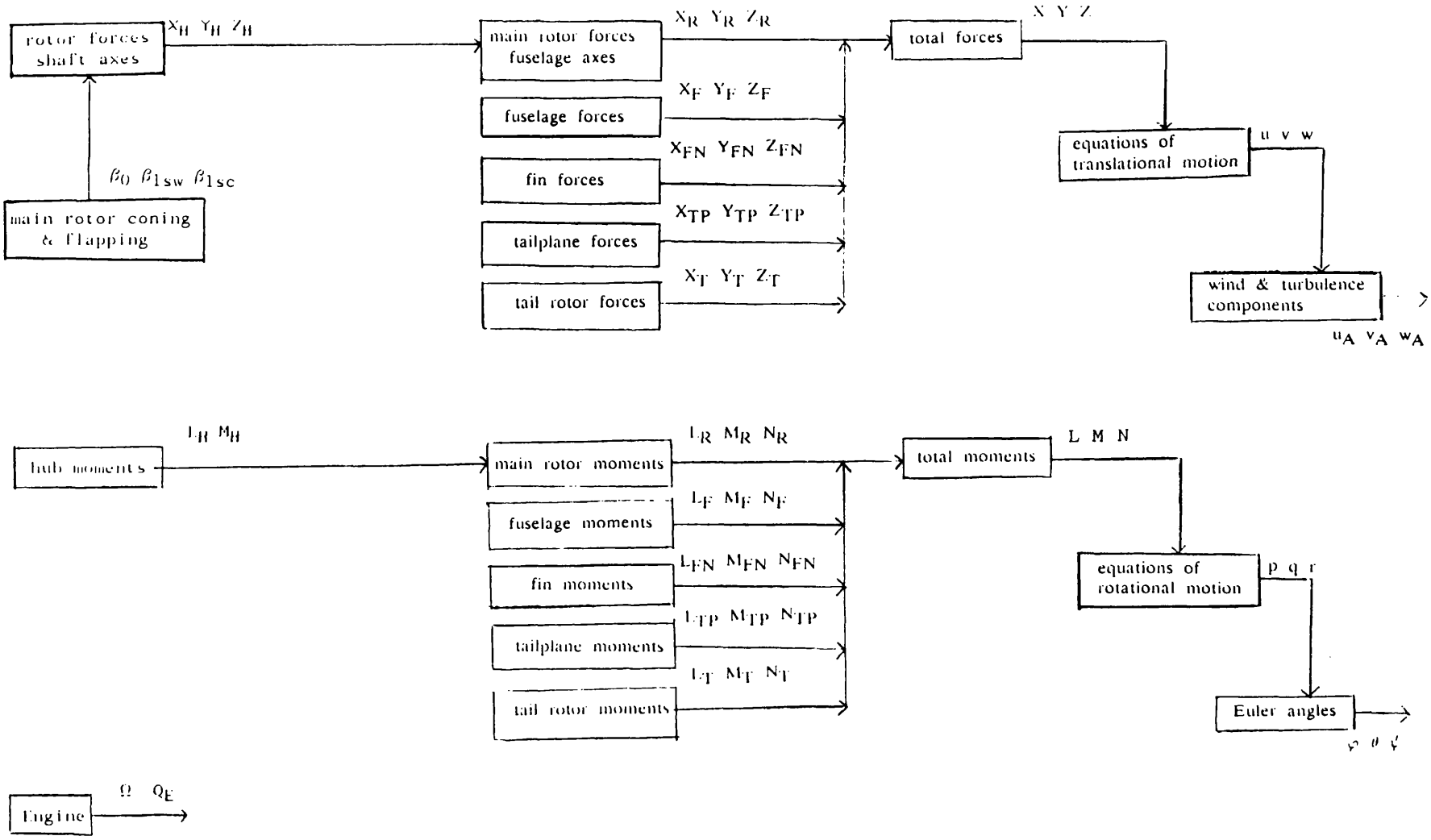

Figure A1.1 Block Diagram of Helicopter Model

APPENDIX 2 Zero Structure for Combinations of Outputs

For each combination of outputs the zero structure is different.

This table shows possible output sets and gives an indication of the zero structure of each set.

KEY

* - satisfactory zero positions

h - high frequency invariant zeros in left half plane

+ - invariant zeros in the right half plane

0 - zero at the origin

Chosen set of outputs				Outcome of zero structure
h	θ	Ω	β	*
h	θ	Ω	r	+
h	θ	Ω	vb	*
h	θ	φ	β	h
h	θ	φ	r	*
h	θ	φ	vb	h
h	θ	p	β	+ h
h	θ	p	r	0
h	θ	p	vb	+ h
h	θ	vb	β	h
h	θ	vb	r	*
h	θ	vb	vb	+ h
h	q	Ω	β	0
h	q	Ω	r	0
h	q	Ω	vb	0
h	q	φ	β	h
h	q	φ	r	0 h
h	q	φ	vb	h
h	q	p	β	+ 0
h	q	p	r	0 h
h	q	p	vb	0 h

h	q	vb	β	h
h	q	vb	r	0
h	q	vb	vb	+
h	vt	Ω	β	*
h	vt	Ω	r	0
h	vt	Ω	vb	*
h	vt	φ	β	h
h	vt	φ	r	*
h	vt	φ	vb	h
h	vt	p	β	h
h	vt	p	r	0
h	vt	p	vb	h
h	vt	vb	β	h
h	vt	vb	r	*
h	vt	vb	vb	+
h	ub	Ω	β	*
h	ub	Ω	r	0
h	ub	Ω	vb	*
h	ub	φ	β	h
h	ub	φ	r	*
h	ub	φ	vb	h
h	ub	p	β	h
h	ub	p	r	0
h	ub	p	vb	h
h	ub	vb	β	h
h	ub	vb	r	*
h	ub	vb	vb	+
γ	θ	Ω	β	*
γ	θ	Ω	r	+
γ	θ	Ω	vb	*
γ	θ	φ	β	h
γ	θ	φ	r	*
γ	θ	φ	vb	h
γ	θ	p	β	h
γ	θ	p	r	0
γ	θ	p	vb	h
γ	θ	vb	β	h
γ	θ	vb	r	*
γ	θ	vb	vb	h

γ	q	Ω	β	0
γ	q	Ω	r	0
γ	q	Ω	vb	0
γ	q	φ	β	h
γ	q	φ	r	0
γ	q	φ	vb	h
γ	q	p	β	0 h
γ	q	p	r	0
γ	q	p	vb	0 + h
γ	q	vb	β	0 h
γ	q	vb	r	0
γ	q	vb	vb	*
γ	vt	Ω	β	*
γ	vt	Ω	r	0
γ	vt	Ω	vb	*
γ	vt	φ	β	h
γ	vt	φ	r	*
γ	vt	φ	vb	h
γ	vt	p	β	h
γ	vt	p	r	0
γ	vt	p	vb	+ h
γ	vt	vb	β	+ h
γ	vt	vb	r	*
γ	vt	vb	vb	+
γ	ub	Ω	β	*
γ	ub	Ω	r	+ 0
γ	ub	Ω	vb	*
γ	ub	φ	β	h
γ	ub	φ	r	*
γ	ub	φ	vb	h
γ	ub	p	β	h+
γ	ub	p	r	0
γ	ub	p	vb	h+
γ	ub	vb	β	h
γ	ub	vb	r	*
γ	ub	vb	vb	+
wb	θ	Ω	β	*
wb	θ	Ω	r	+
wb	θ	Ω	vb	*

wb	θ	φ	β	h
wb	θ	φ	r	*
wb	θ	φ	vb	h
wb	θ	p	β	h +
wb	θ	p	r	0
wb	θ	p	vb	h +
wb	θ	vb	β	0 h +
wb	θ	vb	r	*
wb	θ	vb	vb	+ h
wb	q	Ω	β	0
wb	q	Ω	r	+ 0
wb	q	Ω	vb	0
wb	q	φ	β	h
wb	q	φ	r	0
wb	q	φ	vb	h
wb	q	p	β	h 0
wb	q	p	r	+ 0
wb	q	p	vb	h 0
wb	q	vb	β	0 h
wb	q	vb	r	+ 0
wb	q	vb	vb	+
wb	vt	Ω	β	+
wb	vt	Ω	r	h 0
wb	vt	Ω	vb	+
wb	vt	φ	β	+ h
wb	vt	φ	r	+
wb	vt	φ	vb	+ h
wb	vt	p	β	+ h
wb	vt	p	r	+ 0
wb	vt	p	vb	+ h
wb	vt	vb	β	+ h
wb	vt	vb	r	+
wb	vt	vb	vb	+
wb	ub	Ω	β	+
wb	ub	Ω	r	h 0
wb	ub	Ω	vb	+
wb	ub	φ	β	+ h
wb	ub	φ	r	+
wb	ub	φ	vb	+ h

wb	ub	p	β	+ h
wb	ub	p	r	+ 0
wb	ub	p	vb	h + 0
wb	ub	vb	β	+ h
wb	ub	vb	r	+
wb	ub	vb	vb	+

APPENDIX 3 Eigenstructure Assignment Method Software

APPENDIX 4 Helicopter Handling Qualities

The purpose of designing a flight control system for a helicopter is to provide improved safety, to improve the performance of the vehicle in terms of agility and manoeuvrability and to reduce pilot workload. To achieve these aims we are required to design control laws to produce a controlled helicopter which has good handling qualities in terms of response to pilot input and thus provides the required agility and manoeuvrability for its intended role. The designer of a control law must take into account not only the dynamics of the helicopter but also the pilot since it is the helicopter-plus-pilot system which must perform well.Pilots can assign a rating of how well a controlled helicopter handles according to the Cooper-Harper scale (fig. 18)(Cooper & Harper, 1969).

Handling qualities specifications can be used to facilitate decisions involved in producing control laws. They can help to provide design criteria which aim to define dynamics requirements which give good handling qualities. In this way they can influence choices of eigenvalues and eigenvectors during the design process. Handling qualities specifications are deficient in the sense that compliance does not guarantee that the helicopter will achieve the desired performance. Other factors must be taken into account.

In recent years handling qualities information has been well documented. (MIL–STD–1797 USAF & Hoh, Mitchell & Aponso) The following is a summary of that information.

Since different tasks will require different handling qualities, a representative set of tasks is defined, known as mission task elements (MTE). The dynamic response of the helicopter can be categorised by 3 regions: hover (< 15 knots), low speed (15 - 45 knots) and forward flight (> 45 knots). MTEs for these flight regions are shown in fig. 1 & 2.

The quality of handling of the same helicopter will vary with environmental conditions. Because environmental conditions have an effect on handling, atmospheric conditions and the useable cue environment are taken into consideration. The useable cue environment (UCE) is a parameter which alters the stringency of the requirement to be met according to the visual cues available to the pilot (e.g. view through the window, visual aids, poor weather & night vision). (Hoh, Mitchell & Aponso, 1988). UCE is defined by three levels (fig. 3). Level 1 is the best and allows aggressive manoeuvring whereas level 3 is the worst and permits only gentle manoeuvres.

Another factor which affects handling qualities performance is pilot attention. Clearly, the pilot's ability to respond to changes occurring during flight will be reduced due to increased workload if flying without a copilot. As an indication of this, two states are defined: fully attended and partially attended. It would be reasonable to expect that during a partialiy attended manoeuvre, the handling qualities rating would be lower than for the same task when fully attended. To accommodate this difference, specifications for partially attended flight can be lowered (fig. 4).

In fig. 1 & 2 a number of different response types are referred to. These are rate, attitude command (AC), attitude hold (AH), translational rate command (TRC), position hold (PH), turn coordination (TC) and height hold (HH). (Hoh, 1988). They are defined as follows:

Rate: Attitude diverges from trim for at least 4 secs following a step change applied to the cockpit controller.

AH & HH: Pitch attitude shall return to within 10% of peak excursion in <20 secs following a pulse cockpit controller input when UCE=1 and in <10 secs when UCE>1.

Roll attitude and heading return to within 10% in <10 secs.

Attitude or heading will remain within 10% for at least 30 secs.

AC: Constant cockpit controller force input shall produce proportional angular displacement. A separate trim control must be supplied.

TR: Constant pitch & roll controller force and deflection inputs shall produce a proportional steady translational rate in appropriate direction.

PH: Must hold position if the force on the cockpit controller is zero.

TC: For low speed flight, during banked turns with any available heading hold modes disengaged, the heading response to lateral controller inputs shall remain sufficiently aligned with the direction of flight so as not to be objectionable to the pilot.

Dynamic requirements can be divided into 3 categories: small, moderate and large amplitude responses. Controllers used in conjunction with linear models can be tested with small amplitude inputs only because the linear model is valid for small excursions. Criteria for small amplitude manoeuvring can be given in terms of bandwidth. Bandwidth is measured from a frequency response plot of angular attitude response to cockpit controller force (fig. 5). Two bandwidths are measured: one for 6dB of gain margin, ω_{BWgain}, and the other for 45 degrees of phase margin, $\omega_{BWphase}$, which describe the margin above the vehicle's response in which the pilot can double his gain or add a time delay or phase lag without causing an instability. $\omega_{BWphase}$ is the frequency at which the phase margin is 45 degrees. However, pilots are also sensitive to the shape of the phase curve at

frequencies beyond the bandwidth frequency. Phase delay, τ_p, gives an indication of the shape of the curve beyond the bandwidth frequency. It is a measure of how rapidly the phase curve drops after -180 degrees and therefore gives an indication of how the helicopter behaves as the pilot increases his crossover frequency. Large phase delay indicates that the helicopter could be PIO (pilot induced oscillation) prone because of the short frequency range between normal tracking at 45 degrees and instability. Low gain margin can also be an indication of a PIO prone system. This is because small changes in gain can result in a rapid reduction in phase margin. A system is said to be gain limited when $\omega_{BWgain} < \omega_{BWphase}$.

Hover and Low Speed Flight

Small amplitude responses are assumed to be concerned with the accuracy of closed loop tracking tasks and can be characterised by bandwidth frequency. Inputs should be large enough to produce attitude changes of 5 degrees in pitch and 10 degrees in roll. In the case of small amplitude responses, bandwidth and phase delay measurements are made from the frequency response according to fig. 5. These can then be plotted on two parameter graphs (fig. 6 & 7) which give an indication of the level of handling qualities we can expect from the helicopter.

For moderate amplitude responses (concerned with rapid but less accurate responses), the peak angular rate to change in angular attitude ($q_{pk}/\Delta\theta_{pk}$ or $p_{pk}/\Delta\varphi_{pk}$) shall exceed limits given in fig. 8 & 9.

For large amplitude responses, the minimum achievable angular rate (for rate response types) or attitude change from trim (for attitude response types) shall be no less than the values in fig.10.

Forward Flight

The small amplitude response criteria are divided into two categories: high

frequency and mid-low frequency. The short term (high frequency) criteria are specified in terms of bandwidth parameters. The mid-term response is specified in terms of frequency and damping of oscillations.

Short Term Response

The pitch attitude response to the longitudinal cockpit control force shall meet the limits in fig. 11. The size of the inputs shall be large enough to produce change in pitch attitude of up to 5 degrees or to produce normal load factors that represent the limits of the OFE, whichever is less.

Mid Term Response

In steady turning flight and in pullups and pushovers at constant speed, for levels 1 & 2 there shall be no tendency for the helicopter pitch attitude or angle of attack to diverge aperiodically with controls fixed of controls free. The variations in longitudinal cockpit control force with steady state normal acceleration shall have no objectionable non-linearities throughout the OFE.

Flight Path Control

Vertical rate response following a step collective input shall have a qualitative first order appearance (fig. 12).

Collective to Attitude Coupling

For small collective inputs (< 20% of full control), the peak change in pitch attitude occurring within the first 3 seconds following an abrupt change in collective shall be such that $|\theta_{pk}/n_{zpk}|$ is no greater than 0.1 deg/ft/sec^2, where n_{zpk} is peak normal acceleration.

For large collective inputs ($\geq$ 20% of full control), the peak change in pitch attitude occurring within the first 3 seconds following a step change in collective shall be such that $|\theta_{pk}/n_{zpk}|$ is no greater than 0.5 deg/ft/sec^2 in the up direction

and is no greater than 0.25 deg/ft/sec^2 in the down direction.

Pitch-to-Roll & Roll-to-Pitch Coupling During Aggressive Manoeuvres

q_{pk}/p and p_{pk}/q for rate response types or θ_{pk}/φ and φ_{pk}/θ for attitude response types following an abrupt cyclic step input shall not exceed the limits given in fig. 13 for at least 5 seconds after the input is initiated.

Roll Attitude Response to Lateral Controller

Small Amplitude Roll Attitude Response to Control Inputs

The roll attitude response to lateral cockpit control force shall meet with fig. 14. Inputs shall be large enough to produce roll attitude changes of 10 degrees.

Moderate Amplitude Attitude Changes

$p_{pk}/\Delta\varphi_{pk}$ shall exceed the limits given in fig. 14. The required attitude changes shall be made as rapidly as possible starting from zero angular rate.

Large Amplitude Roll Attitude Changes

The minimum achievable roll rate or bank angle from a trimmed zero roll rate condition shall meet or exceed the values given in fig. 15.

Turn Coordination

$|\Delta\beta/\varphi_1|$ (where φ_1 is initial peak magnitude of roll response) for an abrupt lateral control pulse command for rate response types or step command for attitude response types shall not exceed limits of fig. 16. In addition, $|\Delta\beta/\varphi_1| \times |\varphi/\beta|_d$ shall not exceed limits given in fig. 16.

Yaw Response to Yaw Controller

Small Amplitude Yaw Response for Air Combat

The heading response to cockpit yaw control force or position inputs shall meet fig 17. The size of the inputs shall be large enough to produce heading changes of 10 degrees.

Large Amplitude Heading Changes

Folowing an abrupt step displacement of the yaw control with all other cockpit controls fixed,the change in heading shall be not less than:

Level 1: the lesser of 16 degrees or β_L

Level 2: the lesser of 8 degrees or 1/2 β_L

Level 3: the lesser of 4 degrees or 1/4 β_L

where β_L is the sideslip limit of the OFE in degrees.

The above specifications are a subset of those available for helicopters. As well as defining quantities and qualities for different MTEs on all axes and taking the UCE and pilot workload into account, handling qualities specifications can perform another role - since handling qualities provide a measure of how well a controlled helicopter can be expected to perform, these measures can be used to provide a comparison between different control law design methods and between different designs created by use of one design method. The same approach allows the designer to monitor the effect on handling qualities when dynamics, unmodelled at the design condition, are added to the controlled helicopter or when the flight condition of the helicopter is changed. The obvious benefit of this is that development time will be greatly reduced because deficiencies occurring at any stage will be highlighted by poor handling qualities performance and can be dealt with at that point rather than continuing the design and development process only to find a deficient controller at the end.

During the design process in chapter 5, handling qualities information will be referred to in order to decide whether the controller in question is good enough to pass to the next stage of development.

References

Cooper, G E & Harper, R P

The Use of Pilot Ratings in the Evaluation of Aircraft Handling Qualities

NASA TN D-5153 1969.

Hoh, R H, Mitchell, D G & Aponso, B L

Proposed Specification for Handling Qualities of Military Rotorcraft

Vol. 1 - Requirements, Draft, NASA Technical Memorandum, USAAVSCOM Technical Report 87-A-4, May 1988

Hoh, R H

Dynamic Requirements in the New Handling Qualities Specification for US Military Rotorcraft

Proc. Helicopter Handling Qualities and Control Conference, Royal Aeronautical Society, London, Paper No. 4, November 1988.

	UCE-1		UCE-2		UCE-3	
	LEVEL 1	LEVEL 2	LEVEL 1	LEVEL 2	LEVEL 1	LEVEL 2
Stationary MTEs						
precision hover (4.1.1, 4.1.2.)* suspended load pickup and delivery rapid vertical landing (4.1.5) shipboard landing RAST recovery vertical takeoff slope landing (4.1.6) rapid hovering turn sonar dunking	Rate	Rate	ACAH + RCDH + RCHH	Rate + RCDH	NA	ACAH + RCDH + RCHH
bob up/down (4.2.3)			ACAH + RCDH + PH + RCHH			Rate + RCDH + RCHH + PH
hovering tasks involving divided attention operation (see 1.4.5.2)**	Rate + RCDH + RCHH + PH		ACAH + RCDH + PH + RCHH			
Translating MTEs						
mine sweeping	ACAH + RCDH		TRC + PH + RCDH + RCHH			
approach to hover shipboard stationkeeping target acquisition and tracking assault landing evasive action lateral sidestep (4.2.2) rapid accel/decel (4.2.1) slalom (4.2.5) dolphin (4.2.4)	Rate					

*Numbers in parentheses refer to maneuvers in Section 4 which represent a flight test version of these Mission Elements

**Important consideration for single pilot

Notes:

1. A requirement for RCHH may be deleted if the Vertical Translational Rate visual cue rating is 2 or better, and divided attention operation is not required. If RCHH is not specified, an Altitude-Rate Response-Type is required (Paragraph 3.2.9).

2. Turn Coordination (TC) is always required as an available Response-Type for the slalom MTE in the Low Speed flight range as defined in Paragraph 1.4.6.2. However, TC is not required at airspeeds less than 15 knots.

3. A specified Response-Type may be replaced with a higher level of stabilization providing that the moderate and large amplitude maneuvering requirements may still be met.

   The rank-ordering of Combinations of Response-Types from least to most stabilization is defined as:.

   1. Rate
   2. ACAH + RCDH
   3. ACAH + RCDH + RCHH
   4. Rate + RCDH + RCHH + PH
   5. ACAH + RCDH + RCHH + PH
   6. TRC + RCDH + RCHH + PH

Definitions:

Rate => Rate or Rate Command Attitude Hold (RCAH) Response-Type (Paragraphs 3.2.5, and 3.2.6).

TC => Turn Coordination (Paragraph 3.2.10).

ACAH => Attitude Command Attitude Hold Response-Type (Paragraphs 3.2.6 and 3.2.7).

RCHH => Vertical Rate Command with Altitude (Height) Hold Response-Type (Paragraph 3.2.9.1).

PH => Position Hold Response-Type (Paragraph 3.3.11).

TRC => Translational Rate Command Response-Type (Paragraph 3.2.8).

Figure A4.1 Required Response Type for Hover and Low Speed Near Earth

Pitch and Roll Attitude	
RATE	PITCH - RATE OR ATTITUDE, ATTITUDE HOLD REQUIRED (RCAH OR ACAH) ROLL - RATE WITH ATTITUDE HOLD (RCAH)
ground attack slalom (4.2.5) dolphin (4.2.4) assault landing mine sweeping sonobuoy deploy VMC cruise/climb/ descent air-to-air combat Mission-Task-Elements (4.2.6, 4.2.7)	IMC cruise/climb/descent IMC departure IMC autorotation IMC approach (constant speed) IMC decelerating approach - 3-Cue flight director required (4.3) air-to-air refuel mid air retrieval weapons delivery requiring a stable platform
Heading -- All Require Turn Coordination (Paragraph 3.4.6.2)	
Height -- No Specific Response-Type (see Paragraph 3.4.3)	

Figure A4.2 Required Response Types in Forward Flight

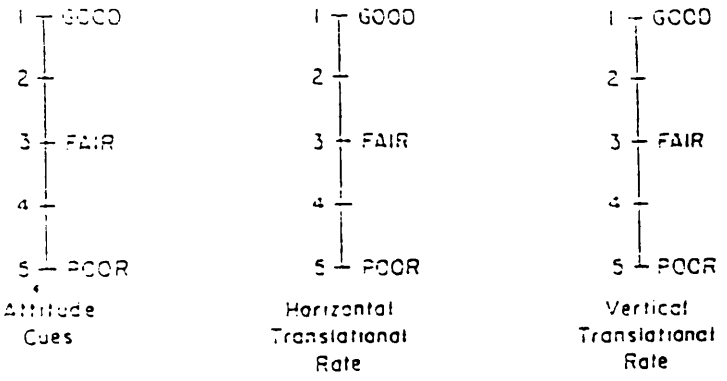

Definitions of Cues

X = Pitch or roll attitude and lateral longitudinal, or vertical translational rate.

Good X Cues: Can make aggressive and precise X corrections with confidence and precision is good.

Fair X Cues: Can make only moderate X corrections with confidence and precision is only fair.

Poor X Cues: Only small and gentle corrections in X are possible, and consistent precision is not attainable.

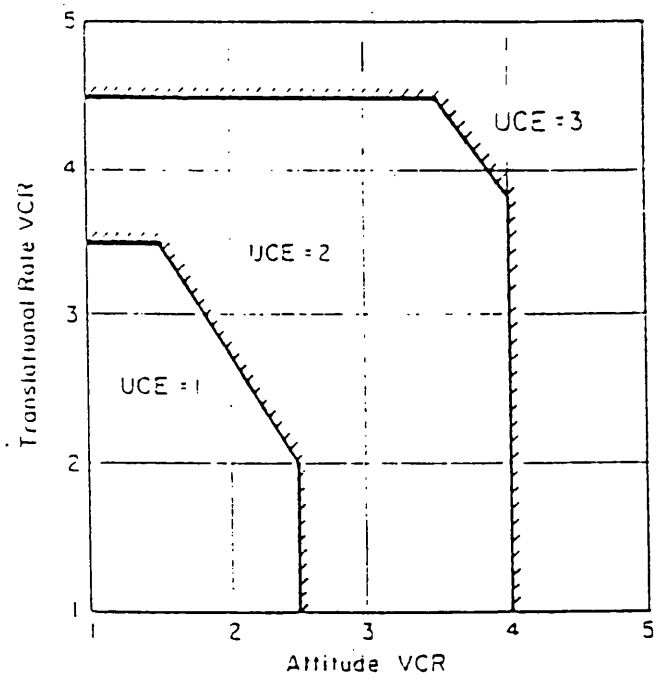

Figure A4.3 Definition of Usable Cue Environments

UCE	LEVEL FOR RESPONSE-TYPE (TABLE 1(3.2))	LEVEL FOR DYNAMICS (SECTION 3.3)	OVERALL LEVEL
2	1	2	2
2	2	1	2
2	2	2	3
3	1	2	3
3	2	1	2
3	2	2	3

Figure A4.4 Levels for Combinations of Degraded Response Type Dynamics

Phase Delay:

$$\tau_p = \frac{\Delta\Phi 2\omega_{180}}{57.3(2\omega_{180})}$$

Notes: 1) if phase is nonlinear between ω_{180} and $2\omega_{180}$, τ_e shall be determined from a linear least squares fit to phase curve between ω_{180} and $2\omega_{180}$

CAUTION:
For ACAH, if $\omega_{BW_{gain}} < \omega_{BW_{phase}}$, or if $\omega_{BW_{gain}}$ is indeterminate, the rotorcraft may be PIO prone for super-precision tasks or aggressive pilot technique.

Rate Response-Types:

ω_{BW} is lesser of $\omega_{BW_{gain}}$ and $\omega_{BW_{phase}}$

Attitude Command/Attitude Hold Response-Types (ACAH):

$\omega_{BW} \equiv \omega_{BW_{phase}}$

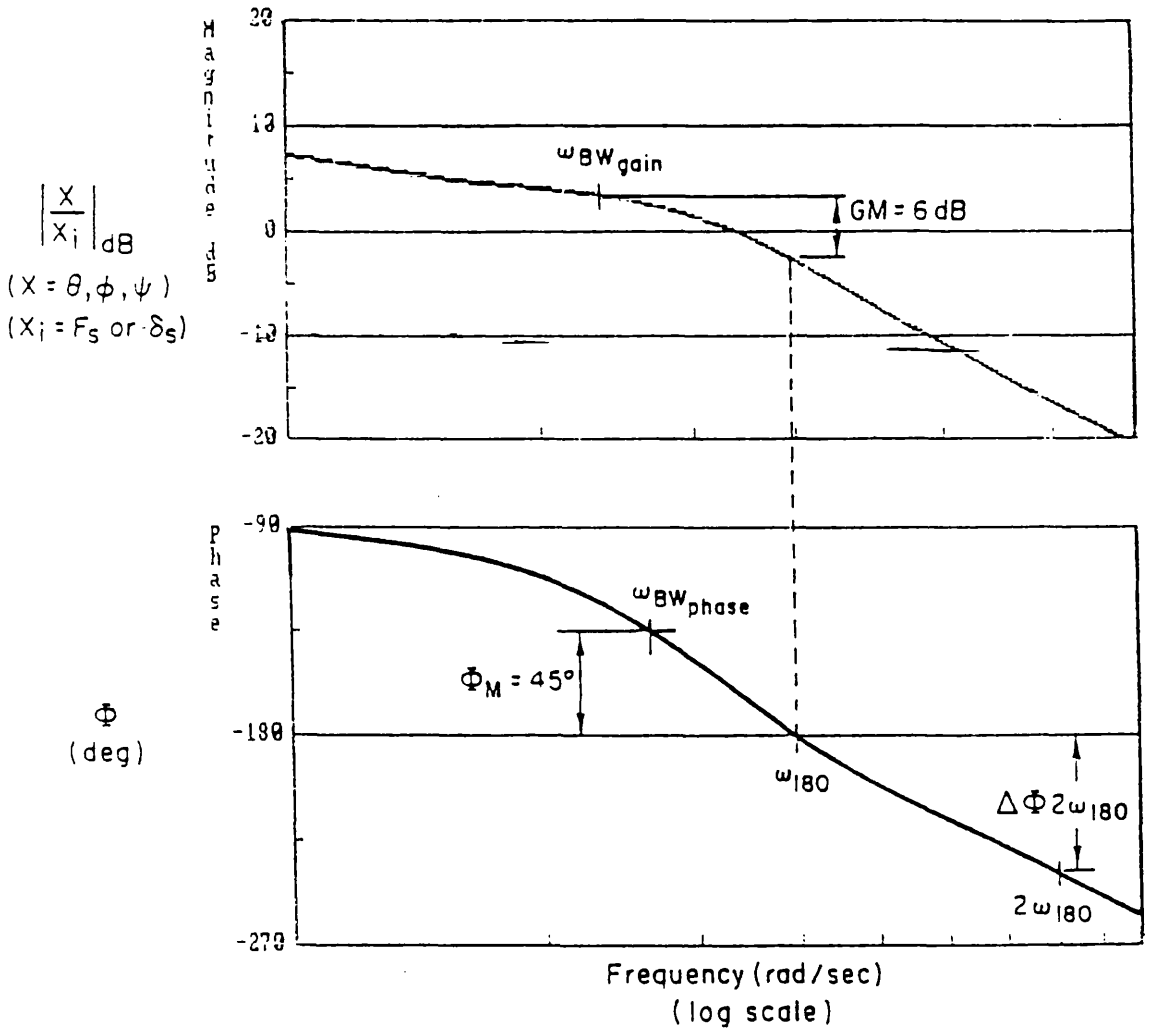

Figure A4.5 Definitions of Bandwidth and Phase Delay

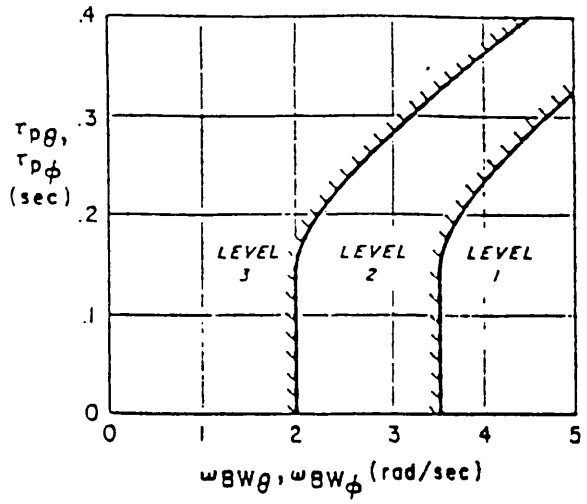

a) Target Acquisition and Tracking (pitch and roll)

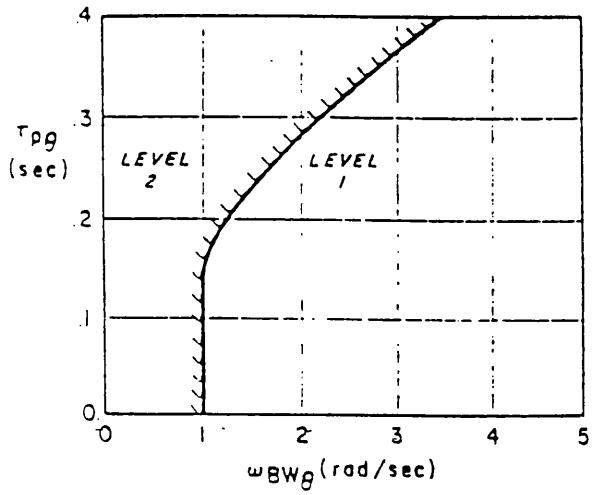

b) All Other MTES – UCE = 1 and Fully Attended Operation (pitch)

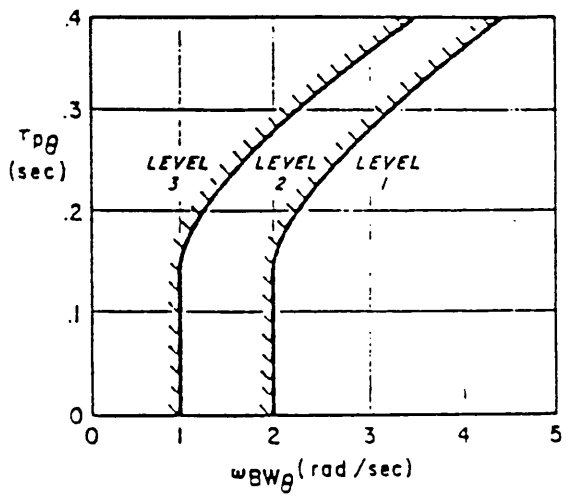

c) All Other MTES – UCE > 1 and/or Divided Attention Operations (pitch)

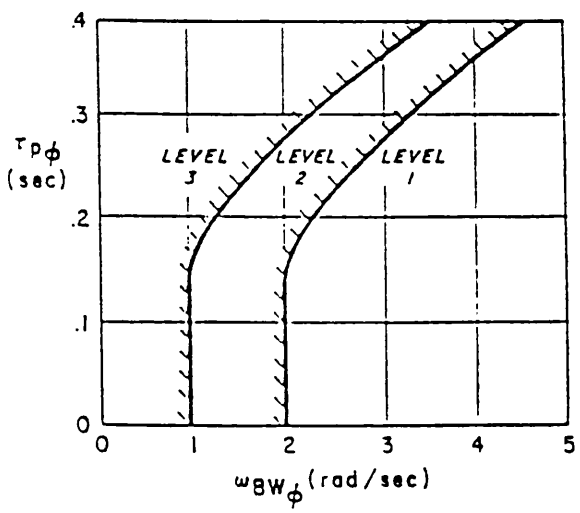

d) All Other MTES – All UCE (roll)

Figure A4.6 Requirements for Small Amplitude Pitch (Roll) Attitude Changes, Hover and Low Speed

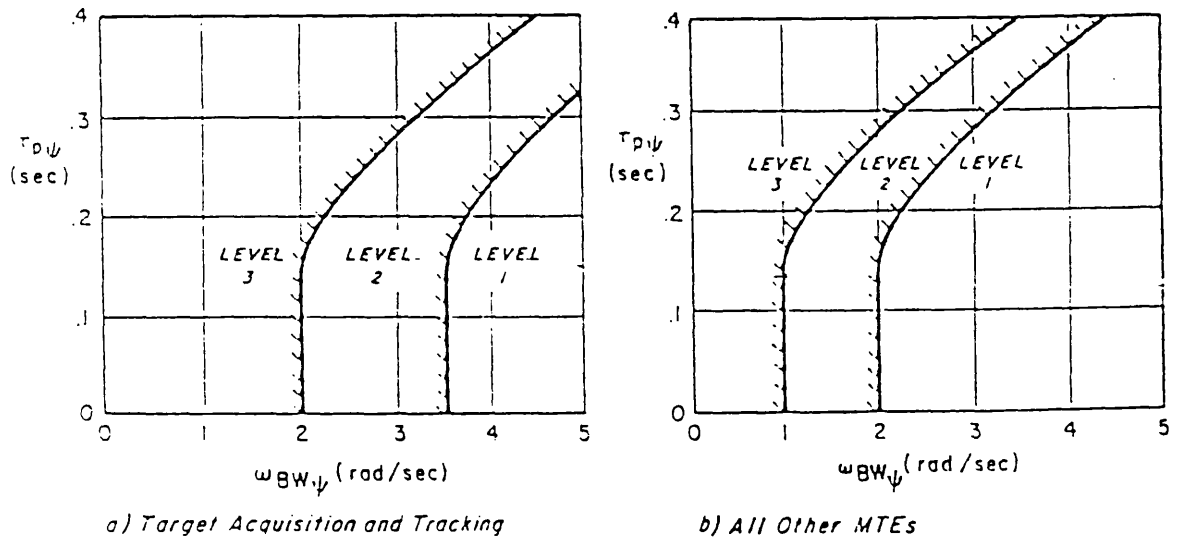

Figure A4.7 Requirements for Small Amplitude Heading Changes, Hover and Low Speed

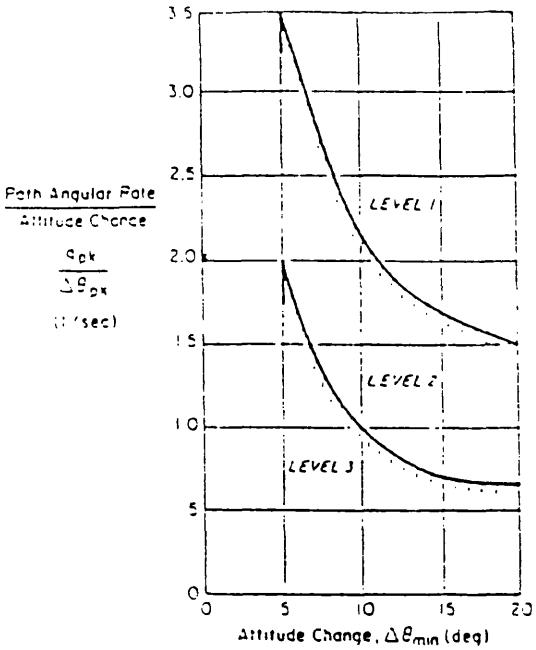

a) Target Acquisition and Tracking (pitch)

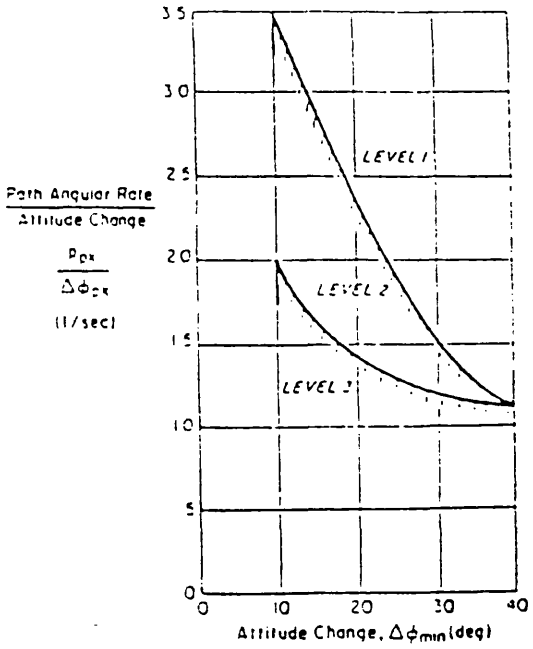

b) Target Acquisition and Tracking (roll)

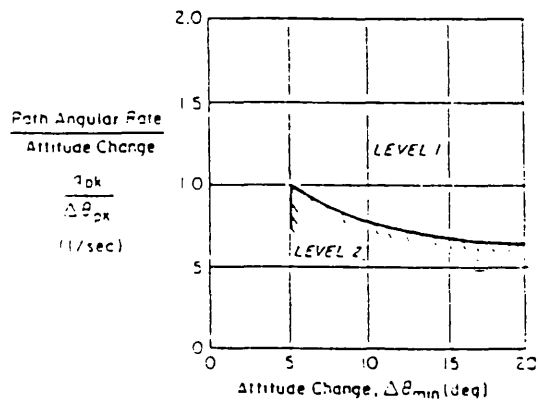

c) All Other MTEs -- UCE = 1 (and Fully Attended Operations (pitch)

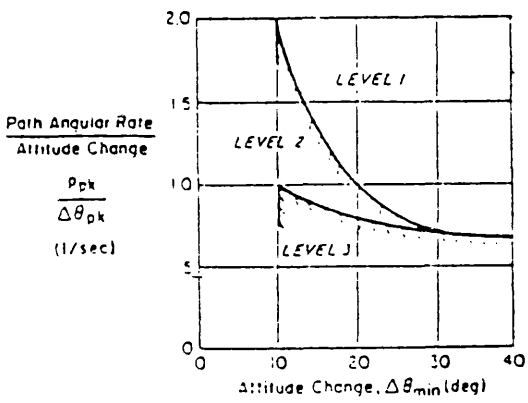

d) All Other MTEs -- UCE 1 and/or Divided Attention Operations (pitch)

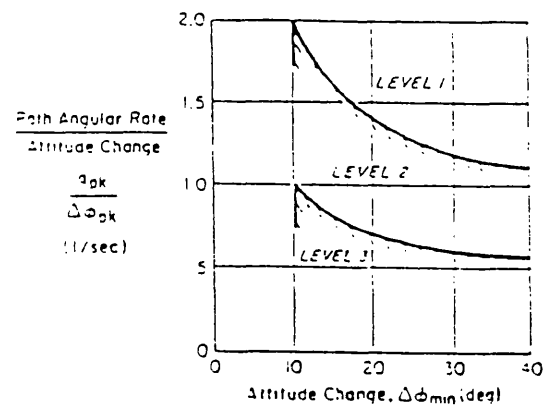

e) All Other MTEs -- All UCE (roll)

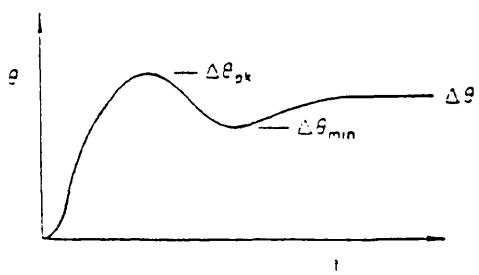

f) Definition of Moderate Amplitude Criterion Parameters

Figure A4.8 Requirements for Moderate Amplitude Pitch (Roll) Attitude Changes, Hover and Low Speed

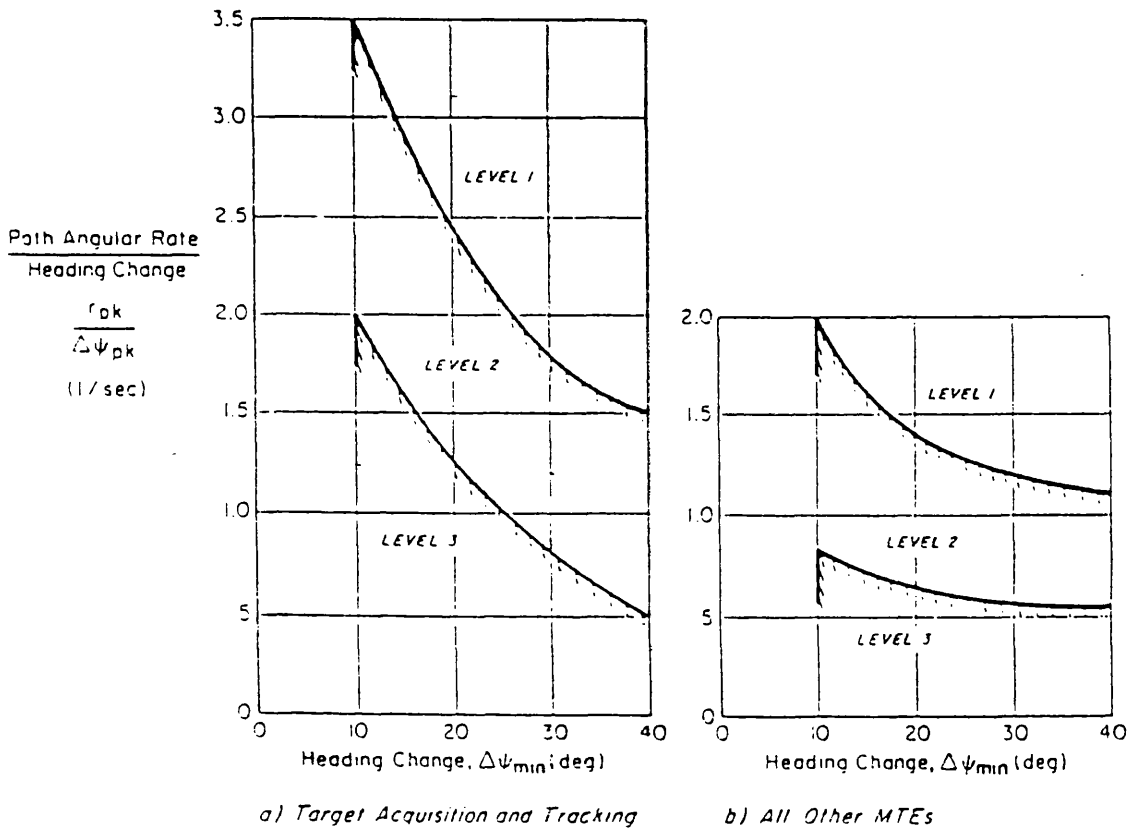

Figure A4.9 Requirements for Moderate Amplitude Heading Changes, Hover and Low Speed

MISSION-TASK ELEMENT	RATE RESPONSE-TYPES						ATTITUDE RESPONSE-TYPES			
	MINIMUM ACHIEVABLE ANGULAR RATE (deg/sec)						MINIMUM ACHIEVABLE ANGLE (deg)			
	LEVEL 1			LEVELS 2 AND 3			LEVEL 1		LEVELS 2 AND 3	
	q	p	r	q	p	r	θ	ϕ	θ	ϕ
Limited Maneuvering All MTEs not otherwise specified	±6	±21	±9.5	±3	±15	±5	±13	±13	±6	±6
Moderate Maneuvering Evasive Action Assault Landing Shipboard Landing	±13	±50	±22	±6	±21	±9.5	+20 -30	±60	±13	±30
Aggressive Maneuvering Rapid Accel/Decel Lateral Sidestep Rapid Hovering Turn Dolphin Slalom	±30	±50	±60	±13	±50	±22	±30	±60	+20 -30	±30

Note: Letters in parentheses denote subparagraphs in Supporting Data where the limits are discussed.

Figure A4.10 Requirements for Large Amplitude Attitude Changes

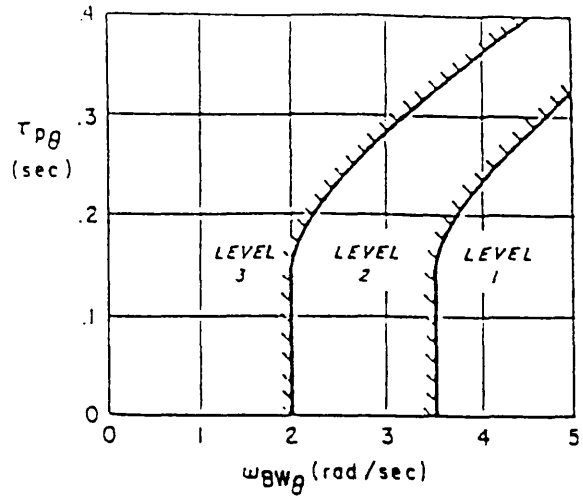

a) Air Combat

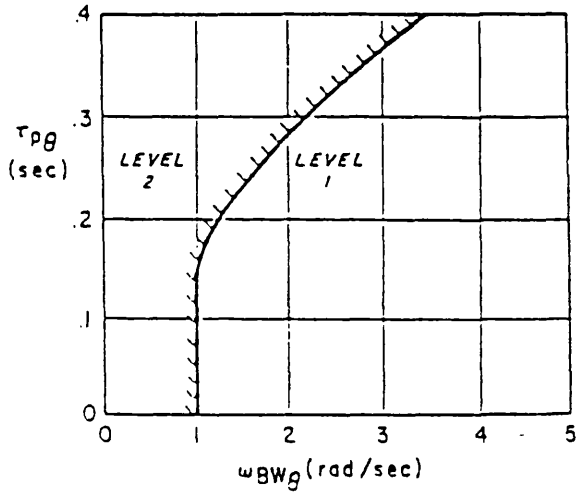

b) All Other MTES - VMC and Fully Attended Operations

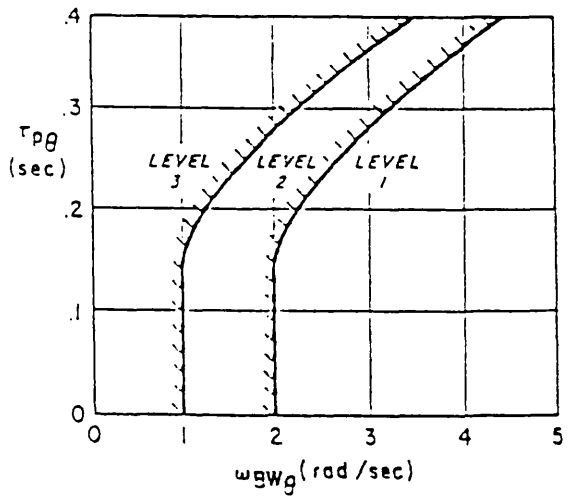

c) All Other MTES - IMC and/or Divided Attention Operations

Figure A4.11 Bandwidth Requirements for Pitch Rate and Attitude Response Types, Forward Flight

LEVEL	$T_{\dot{h}_{eq}}$ sec	$\tau_{\dot{h}_{eq}}$ sec
1	5.0	0.2
2	∞	0.3

$$\frac{\dot{h}}{\delta_c} = \frac{K\, e^{-\tau_{\dot{h}_{eq}} s}}{T_{\dot{h}_{eq}} s + 1}$$

Figure A4.12 Maximum Values for Height Response to Collective Controller

PARAMETER		LEVEL 1	LEVEL 2
RATE RESPONSE-TYPES	ATTITUDE RESPONSE-TYPES		
$(q_{pk}/p)_{\delta_A}$ or $(p_{pk}/q)_{\delta_B}$	$(\theta_{pk}/\phi)_{\delta_A}$ or $(\phi_{pk}/\theta)_{\delta_B}$	±0.25	±0.60

Figure A4.13 Limiting Values for Pitch-to-|Roll and Roll-to-Pitch Coupling

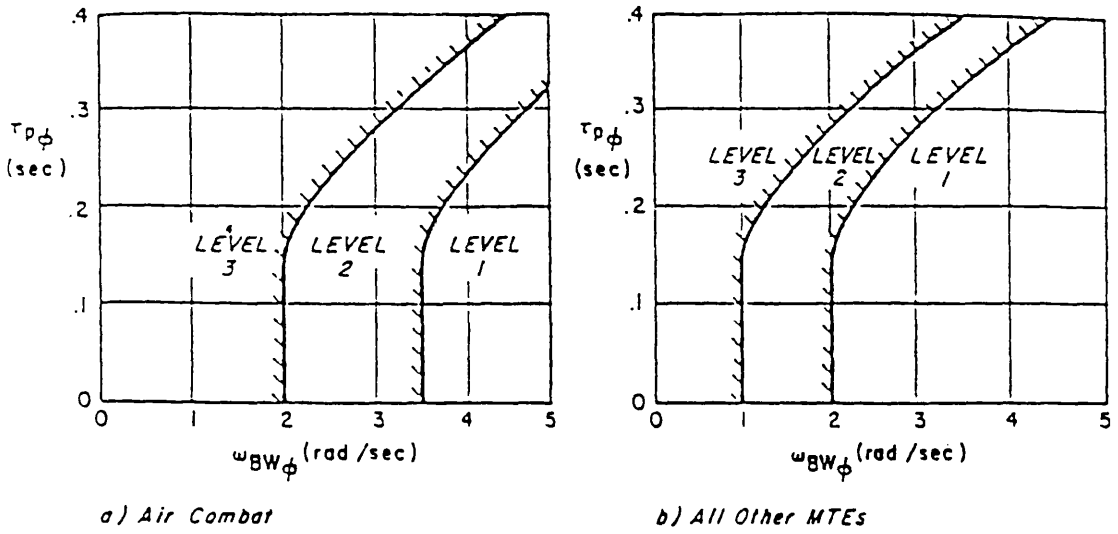

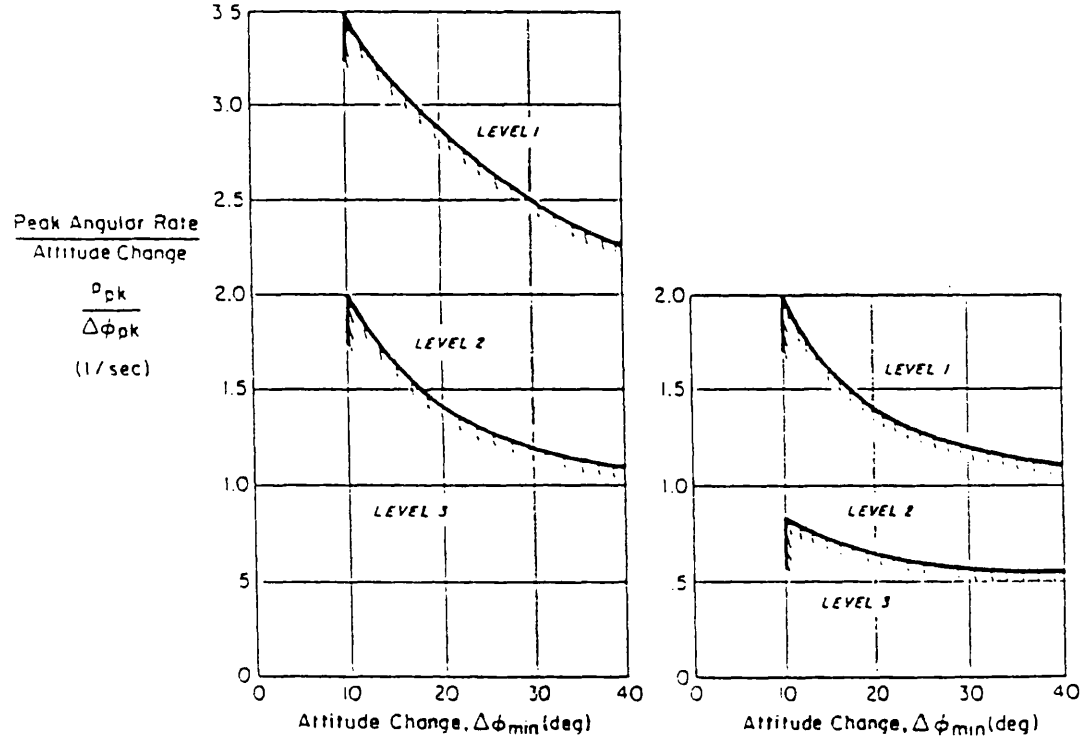

Figure A4.14 Roll Response Limits for Moderate Amplitude Roll Attitude Changes, Forward Flight

MISSION-TASK-ELEMENT (MTE).	RATE RESPONSE-TYPES		ATTITUDE RESPONSE-TYPES	
	MINIMUM ACHIEVABLE ROLL RATE (deg/sec)		MINIMUM ACHIEVABLE BANK ANGLE (deg)	
	LEVEL 1	LEVEL 2	LEVEL 1	LEVEL 2
Limited Maneuvering				
All MTEs not otherwise specified	30	15	25	15
IMC MTEs	15	12	25	15
Aggressive Maneuvering				
Ground Attack Dolphin Slalom Assault Landing	50	21	90	30
Air Combat	90	50	Unlimited	60

Figure A4.15 Requirements for Large Amplitude Roll Attitude Changes

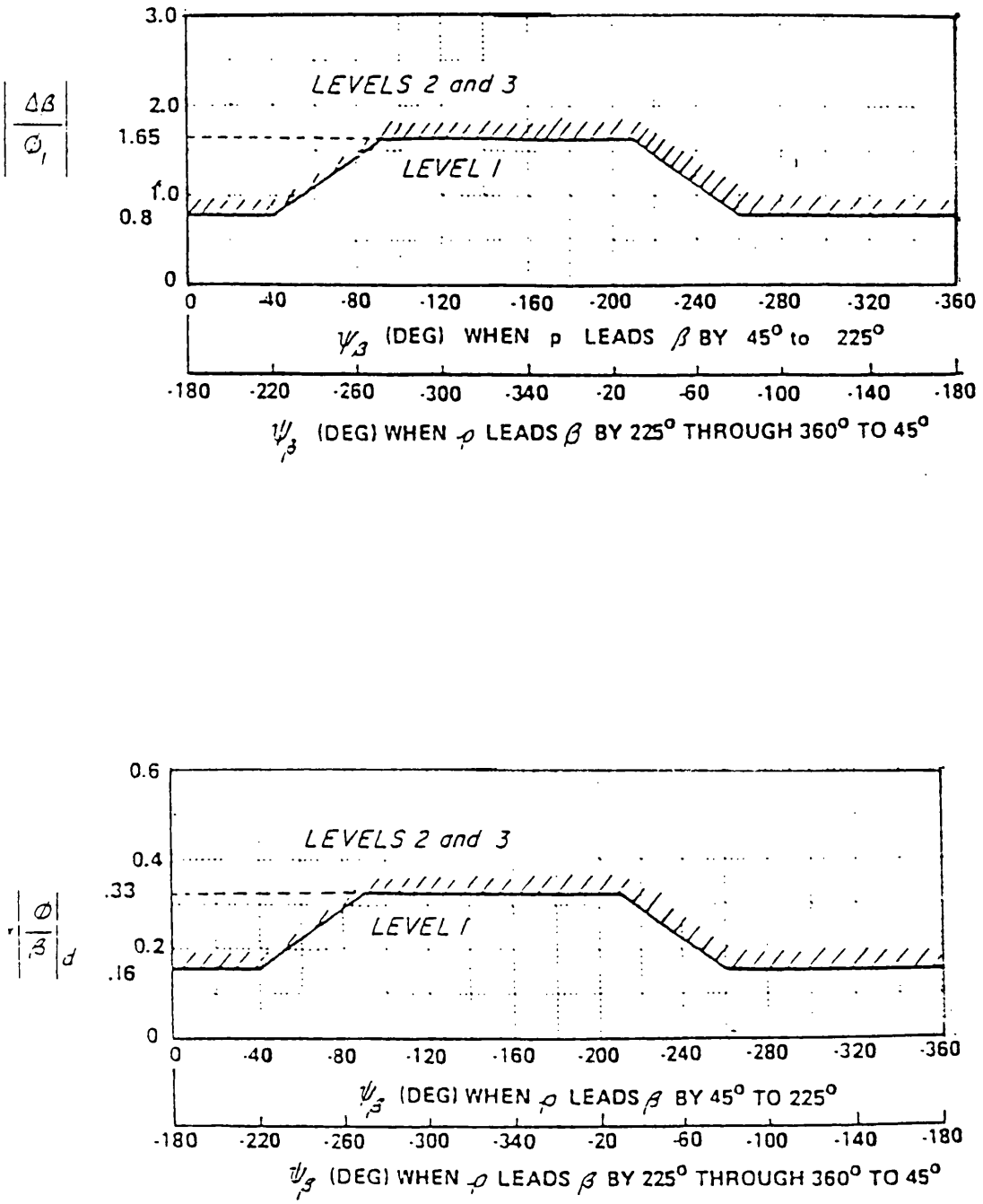

Figure A4.16 Sideslip Excursion Limitations

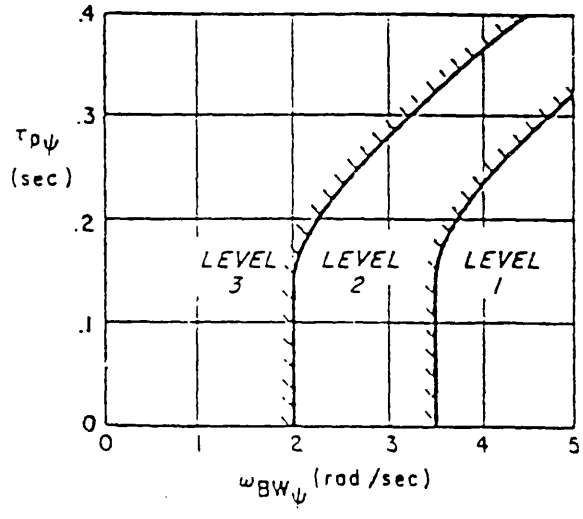

Figure A4.17 Requirements for Small Amplitude Heading Changes, Forward Flight

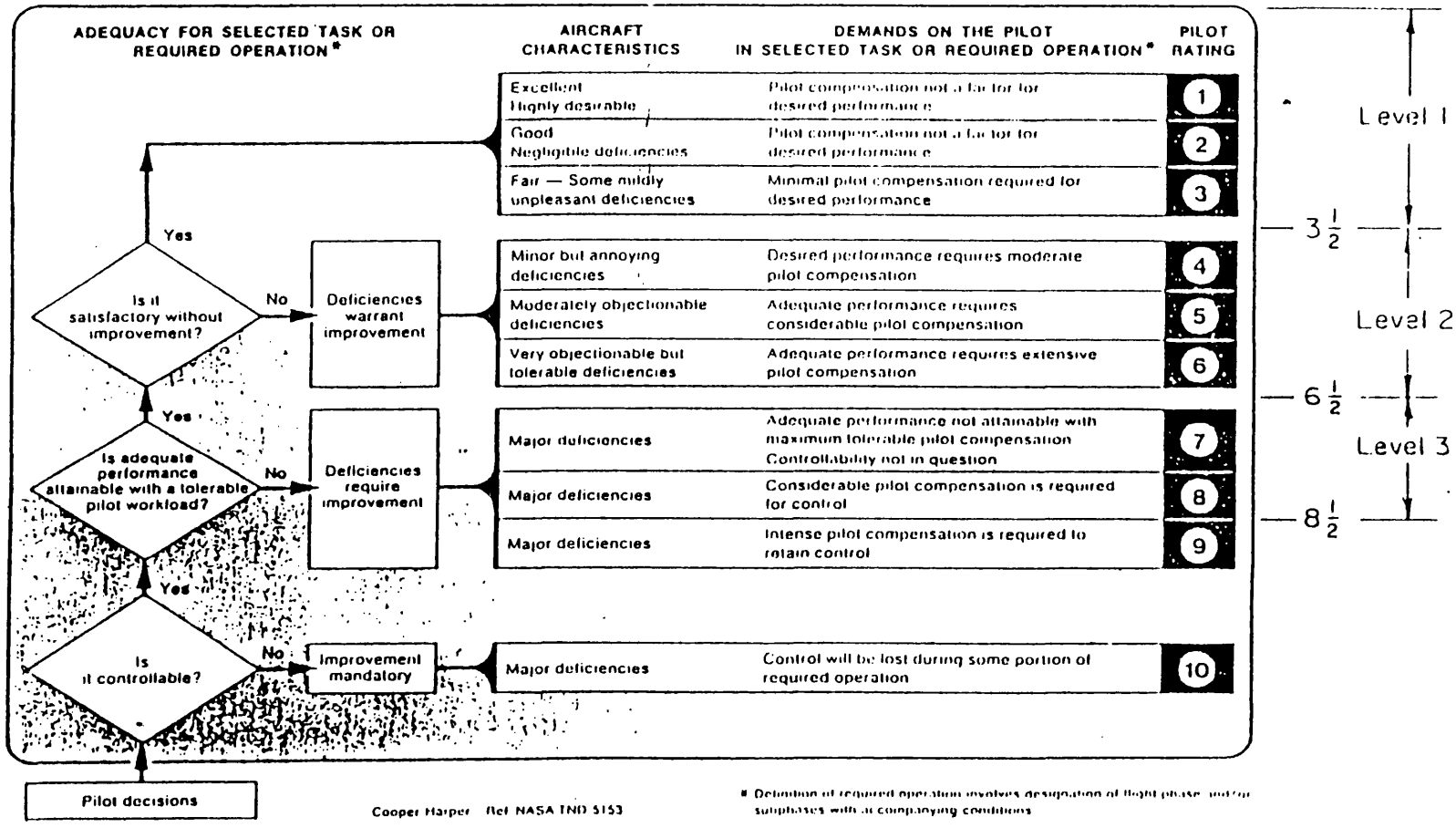

Figure A4.18 Cooper-Harper Scale

APPENDIX 5 HELISIM Software Functions

SESSIMB2 sets up tsim body axes equations and calls the active control laws (ACTLAW), turbulence (TWIND), user input (USERCMI) and user output (USERCMO) routines.

USERCMI sets up user input to the model.

USERCMO communicates information back from the model to the user.

ACTLAW contains a user-defined active control law. This subroutine is listed in Appendix 3.

SESAME is a System of Equations for the Simulation of Aircraft in a Modular Environment. It calls CONTROLS, TOTF and TOTM.

TOTF calls other subroutines which calculate forces and moments for the model generally, main rotor, tail rotor, fuselage, fin, tailplane and undercarriage.

TOTM sums the moments generated in these subroutine calls.

CONTROLS calls subroutines which perform control functions.

CIN takes pilot inputs, scales controls to ±1 and applies a shaping function to each input in turn.

FCS provides a basic autostab

ENG calculates engine torque and power.

CMX applies control mixing (usually done mechanically in the helicopter) to the pilot inputs. It converts the ±1 values into blade angles and sums them with autostab outputs. These final outputs are then fed to the actuator model. This subroutine is not called if active control is being used.

ATR equates active control inputs with actuator outputs bypassing blade limits and actuators.

SHP shapes raw pilot inputs.